Effects of dietary and pharmacological interventions on pancreatic β-cell compensation in Nile rats: a model for spontaneous type 2 diabetes

by

Hui Huang

A thesis submitted in partial fulfillment of the requirements for the degree of

Doctor of Philosophy

Department of Physiology
University of Alberta

Abstract

Insulin-secreting pancreatic β-cells adapt to obesity-related insulin resistance via increases in insulin secretion and β-cell mass, which is referred to as β-cell compensation. Failed β-cell compensation predicts the onset of type 2 diabetes (T2D). However, the mechanisms underlying β-cell compensation are not fully understood. The previous study reported changes in β-cell mass during the progression of T2D in the Nile rat (NR), a model developing T2D naturally when fed with a standard lab chow diet (Chow). In the present study, I hypothesized that in addition to cell mass adaption, NR is an animal model that demonstrates β-cell functional compensation and decompensation during the development of T2D. The results showed that, compared to healthy NRs fed with a fiber-rich diet (Hfib), young Chow-fed NRs exhibited enhanced β-cell insulin secretion in response to insulin resistance that failed with aging, along with the onset of prediabetes and eventually T2D. I further hypothesized that the β-cell adaptive response is associated with increased insulin processing and β-cell replication. While both compensatory processes existed at 13 weeks of age, I observed increased proinsulin secretion in the transition from compensation to decompensation at 25 weeks, indicative of impaired insulin processing. Meanwhile, finding of correlations of ER chaperones with plasma insulin and glucose concentration demonstrated a positive role of ER chaperones in insulin secretion. Moreover, restricted β-cell proliferation and an increase in insulin-positive duct-associated β-cells were observed at the compensation stage, indicating a neogenic mechanism of β-cell mass adaptation. β-cells at decompensation stage showed less neogenic cell structures with evidence of dedifferentiation. In contrast, the pathophysiological abnormalities of β-cells were prevented by Hfib diet. Besides diet modification, I also proposed that the β-cell decompensation in NRs could be alleviated by pharmacological intervention. Metformin is a first line antidiabetic medication

which is also effective in preventing T2D. I treated Chow NRs during the compensation stage with a relatively low dose of metformin (20mg/kg body weight). The results showed an improvement in glucose tolerance and insulin secretion after 7 weeks of treatment, while the impaired glucose tolerance and insulin sensitivity seen in Chow NRs at 25 weeks (6 months) were alleviated with metformin. The activation of AMPK and downregulated hepatic gluconeogenic pathway indicated suppression of glucose production by metformin. Additionally, due to increased glucose-stimulated insulin secretion *in vivo*, I further hypothesized that metformin affects β-cell function. β-cell secretion capacity was preserved in the metformin group, which was correlated with changes in glucose sensing genes, indicating a protective role for metformin in β-cell function. However, *in vitro* metformin treatment of islets failed to exert change in insulin secretion, suggesting an indirect mechanism underlying β-cell preservation *in vivo*.

In summary, results of this study demonstrate a model of T2D showing β-cell compensation in insulin secretion and cell expansion, which is accompanied by adaptive changes in ER chaperones and β-cell neogenesis. Failure of β-cell compensation leads to diabetes progression. The disease progression and β-cell decompensation can be prevented by Hfib diet and delayed by early treatment with metformin.

Preface

This thesis is an original work by Hui Huang. All animal work received research ethics approval from the University of Alberta Animal Care and Use Committee (Animal use protocol #00000328) and were conducted in accordance with Canadian Council on Animal Care Guidelines.

A version of Chapter 3 has been accepted for publication (May2, 2019) in Applied Physiology, Nutrition and Metabolism with authorship of Hui Huang, Kaiyuan Yang, Rennian Wang, Woo Hyun Han, Sharee Kuny, Paula Horn Zelmanovitz, Yves Sauvé and Catherine B Chan. **β-cell compensation concomitant with adaptive ER stress and β-cell neogenesis in a diet-induced type 2 diabetes model.** I was responsible for experimental design, performing experiments, analyzing results, and drafting the manuscript. K Y, W H H and S K assisted with tissue collection. R W performed the staining of PDX1 at Western University (Ontario). P H Z analyzed data. All authors revised the manuscript and approved the final version. Y S and C B C provided funding. C B C is the guarantor of this publication and takes full responsibility for the work. A copy of this manuscript is attached in Appendix A.

Chapter 4 is presented in manuscript format and will be prepared for submission to a relevant journal. I was responsible for performing experiments, analyzing the data and drafting the manuscript. Bradi Lorenz contributed to data collection and analysis. Paula Horn Zelmanovitz contributed to data analysis. Kaiyuan Yang and Andrew Forgie from Dr. Benjamin Willing's lab performed the analysis of microbial composition. Yves Sauvé and Catherine B Chan provided funding.

Acknowledgment

First and foremost, I would like to express my sincere gratitude to my supervisor Dr. Cathy Chan for her support, guidance, and encouragement of my Ph.D. work. I have been fortunate to have Cathy as my supervisor who motivated me, who cared about my work, and whose office door was always open whenever I had a question or needed help. Without her patience and guidance, I would not have been able to complete the thesis. I also appreciated the trust and understanding I received from her, which gave me the courage to overcome the hurdles encountered in the study. Thank you, Cathy, for all the support and opportunities you offered me over the past five years.

I would also like to thank the current and previous members of my supervisory committee, Dr. Yves Sauvé, Dr. Patrick MacDonald and Dr. Jessica Yue for their valuable time, generous support and suggestion during my studies.

I would also like to acknowledge the contributions from all the collaborators. I am very grateful to Dr. Yves Sauvé, Sharee Kuny and Ted Han in Sauvé lab, and Zhining Zhu in HSLAS for the effort they put into the Nile rat project and their assistance in the animal care and handling. I thank Dr. Ben Willing and his student Andrew Forgiea for the excellent work in the microbiota analysis; Dr. Rennian Wang at Western University for her expertise and contributions to this work.

I would like to give a big thanks to the current and former members of the Chan lab for all the laugh, joy and company! I thank Dr. Kaiyuan Yang for the assistance and teaching when I first came to the lab. She is thoughtful and supportive, and I have enjoyed the time working with her. Dr. Zohre Hashemi has been a great friend to me, and I appreciate the encouragement and suggestions I got from her, especially in the last two years and during my thesis preparation. Dr.

Xiaofeng Wang, Dr. Fatheema Subhan, Stepheny Zani, Carolina Archundia Herrera, Carla Sosa Alvarad, Bradi Rai Lorenz and Paula Horn Zelmanovitz: the time here in the lab would have been much more difficult for me without all your guys! A huge thanks also goes to Nichole Coursen for the technical assistance with the animal work, and Dr. Kunimasa Suzuki for his excellent expertise and help with techniques in molecular biology.

I would also like to acknowledge the financial support from the China Scholarship Council and my supervisor Dr. Cathy Chan; and the travel awards from the Faculty of Graduate Studies and Research, Graduate Students' Association, and Department of Physiology.

Finally, I would like to express my utmost gratitude to my parents for their support and unconditional love. Thank you to my dear Michael, who has experienced this Ph.D. journey with me for his love, patience, understanding, and company!

Table of Contents

Appendix

Appendix A: Applied Physiology, Nutrition and Metabolism manuscript

Appendix B: Data extraction table for the animal model review in Chapter 1.3

List of Tables

List of Figures

List of Abbreviations

4-PBA	4-phenyl butyric acid
AC	adenylyl cyclase
ACC	Acetyl-CoA carboxylase
ADP	adenosine diphosphate
AMPK	AMP-activated protein kinase
ATF6	transcription factor 6
ATP	adenosine triphosphate
Bax	Bcl-2-associated X protein
Bcl2	B-cell lymphoma 2
Bip	immunoglobulin binding protein
BMI	body mass index
cAMP	cyclic adenosine monophosphate
CHOP	C/EBP homologous protein
CRCT2	CREB co-activator 2
CREB	cAMP response element-binding protein
DPP	Diabetes Prevention Program
ER	endoplasmic reticulum
ERp44	ER chaperones
FBG	fasting blood glucose
FoxO1	forkhead box protein O1
G6Pase	glucose-6 phosphatase
GCK	glucokinase
GDM	gestational diabetes mellites

GLP-1	glucagon-like-peptide 1
GLUT	glucose transporters
GRP94	glucose-regulated protein 94
GSIS	glucose-stimulated insulin secretion
GWAS	genome-wide association studies
HFD	High-fat diet
Hfib	low-energy, fiber-rich diet
HGP	hepatic glucose production
HOMA-B	homeostatic model assessment of β-cell function
HOMA-IR	homeostatic model assessment of insulin resistance
IAPP	islet amyloid polypeptide
IFG	impaired fasting glucose
IGF1	insulin-like growth factor 1
IGT	impaired glucose tolerance
ipGTT	intraperitoneal glucose tolerance
IR	insulin receptor
IRE1	inositol-requiring enzyme 1
IRS	insulin receptor substrate
ISI	insulin sensitivity
ISI	insulin sensitivity index
ITT	insulin tolerance tests
K_{ATP} channel	ATP-sensitive potassium channel
LKB1	liver kinase B1
MafA	musculoaponeurotic fibrosarcoma oncogene family A
mGPDH	mitochondrial glycerol phosphate dehydrogenase

NGT	normal glucose tolerance
NR	Nile rat
PC1/3	prohormone convertase 1/3
PDI	protein disulfide isomerase
Pdx-1	pancreatic duodenal homeobox-1
PEPCK	phosphoenolpyruvate carboxykinase
PERK	protein kinase RNA-activated-like ER kinase
PGC-1α	PPARγ coactivator 1-alpha
PPARγ	peroxisome proliferator-activated receptor γ
PTT	pyruvate tolerance test
Px	pancreatectomy
RIA	insulin radioimmunoassay
ROS	reactive oxygen species
RRP	readily releasable pool
STZ	streptozotocin
SGLT1	sodium glucose cotransporter-1
T1D	type 1 diabetes
T2D	type 2 diabetes
Tcf7l2	transcription factor 7-like 2
TUDAC	tauroursodeoxycholic acid
UPR	unfolded protein response
VGCC	voltage-gated Ca^{2+} channel
Xbp1	X-box binding protein 1
ZDF	Zucker diabetic fatty

Chapter 1. Introduction

1.1 Introduction to diabetes mellitus

Diabetes mellitus is a group of metabolic diseases marked by hyperglycemia and insulin deficiency (American Diabetes Association 2014). Long-term hyperglycemia can give rise to chronic organ damage, leading to severe complications including neuropathy, retinopathy, cardiovascular disease and renal failure (American Diabetes Association 2014). Diabetes is one of the top five life-threatening illnesses in the world (Cho et al. 2018). The number of adults with diabetes increased from 171 million in 2000 (Wild et al. 2004) to 425 million in 2017 (Cho et al. 2018), accounting for 8.8% of the global population. In 2018, diabetes was diagnosed in over 3.5 million Canadians accounting for 9% of the people in Canada (Cho et al. 2018). The Canadian diagnostic criteria for diabetes are shown in Table 1.

The majority of the cases of diabetes fall into three categories, type 1 diabetes (T1D), type 2 diabetes (T2D), and gestational diabetes mellites (GDM). T1D, also referred to as insulin-dependent diabetes, is an autoimmune disease characterized by hyperglycemia and severe insulin deficiency due to the loss of insulin-secreting pancreatic β-cell cells. T2D, on the other hand, is a chronic metabolic disorder as a result of decreased insulin sensitivity and inadequate insulin production. Over 90% of the diabetic population was diagnosed with T2D (Cho et al. 2018). GDM is a temporary condition with hyperglycemia during pregnancy. One significant contributor to the personal and societal costs of diabetes is that over 48% of the estimated diabetic population, especially with T2D, goes undiagnosed until the presence of irreversible complications (Beagley et al. 2014), which increases the risk of morbidity and the financial burden (Cho et al. 2018). This highlights the importance of early diagnosis in the treatment of

T2D as well as understanding critical events in disease progression when intervention may be particularly beneficial.

1.1.1 Natural history of type 2 diabetes

Under normal physiological conditions, the concentration of circulating blood glucose is under the tight control of pancreatic hormones in order to maintain homeostasis. In the fed state, pancreatic β-cells sense the rise of blood glucose following food ingestion and release insulin, a peptide hormone that acts on adipose tissue and skeletal muscle to stimulate glucose uptake from the blood to the cells and suppresses glucose output from liver, leading to reduced blood glucose. Insulin also inhibits glycogenolysis, gluconeogenesis, lipolysis and protein breakdown. On the contrary, in the fasting state, pancreatic α-cells secrete a counter-regulatory hormone of insulin, glucagon, to suppress glucose utilization and promote glycogenolysis and gluconeogenesis to increase glucose production (Saltiel and Kahn 2001; Moore et al. 2003).

As a result of sedentary lifestyle, western diet and obesity, insulin resistance manifests; this is a state in which the body cannot respond efficiently to insulin to lower blood glucose (Iozzo et al. 1999; Neeland et al. 2012). The pancreas releases more insulin to compensate for the insulin resistance (Festa et al. 2006). As the acute glucose-stimulated insulin secretion (GSIS) declines, glucose begins to rise, resulting in impaired glucose tolerance (IGT, Table 1) or impaired fasting glucose (IFG, Table 1) (Weyer et al. 1999; Abdul-Ghani et al. 2006). This moderate increase in glucose is referred to as prediabetes (Tabák et al. 2012). Prediabetes is a high-risk state for T2D; it can progress to overt diabetes if not diagnosed and treated in time (Table 1) (Meigs et al. 2003). However, although there is substantial heterogeneity between ethnic groups (Hulman et

al. 2017), this abnormality in glucose homeostasis can generally be controlled within the normal range for many years, thanks to a sustained elevated plasma insulin concentration (Tabák et al. 2012). The glycemic trajectory reported in longitudinal studies shows a steeper rise in blood glucose in later stages of prediabetes (2 years before diagnosis of T2D) that is tightly associated with a decrease in β-cell function (Tabák et al. 2009). This highlights the crucial role of maintaining β-cell function in preventing T2D development (Seino et al. 2011).

Table 1-1 Diabetes diagnostic criteria (Punthakee et al. 2018)

	Prediabetes		Diabetes*
	IGT	IFG#	
Fasting plasma glucose (mmol/L)		6.1-6.9	≥7.0
2-hour plasma glucose in a 75 g oral glucose tolerance test (mmol/L)	7.8-11.1		≥11.1
Glycated hemoglobin A1C (%)	6.0-6.4		≥6.5

* If two of the test results are above the diagnostic threshold, the diagnosis of diabetes is confirmed. # The cut point for IFG defined by American Diabetes Association is 5.6 mmol/L (American Diabetes Association 2014).

1.1.2 Hallmarks of T2D

Insulin resistance and β-cell dysfunction are two hallmarks of the pathophysiology of T2D. The traditional perspective regarding these two determinants of T2D is that insulin resistance is the primary abnormality, which places a high demand for insulin production in β-cells, whereas the β-cell dysfunction is a later event that occurs with the onset of hyperglycemia (Kruszynska and Olefsky 1996). However, when comparing insulin sensitivity and GSIS between normal glucose tolerant (NGT) with IGT subjects, decreased insulin sensitivity does not always lead to IGT. Instead, diminished GSIS is associated with the conversion of NGT to IGT (Weyer et al. 1999; Kahn 2003). It suggests that impaired β-cell insulin secretion happens before hyperglycemia and is the most important prerequisite for T2D development.

Genome-wide association studies (GWAS) have identified numerous diabetes susceptibility loci (Florez 2008). The majority of risk genes initially associated with insulin resistance are proven to regulate β-cell mass and function (Brown and Walker 2016). The most studied risk variants, including transcription factor 7-like 2 (*Tcf7l2*), peroxisome proliferator-activated receptor γ (PPARγ) and insulin-like growth factor 1 (IGF1) are found to play roles in regulating β-cell mass and function (Okada et al. 2007; Medina-Gomez et al. 2009; Takamoto et al. 2014). Therefore, interacting with insulin resistance, it may be argued that β-cell function/dysfunction is the primary determinant of T2D progression.

1.1.3 β-cell compensation and dysfunction

Weir (Weir and Bonner-Weir 2004) characterized β-cell dysfunction into multiple stages that correspond to T2D development in rodent models and humans. β-cells compensate for insulin

resistance in the first stage by enhancing GSIS, which is associated with expanded β-cell mass and intact β-cell integrity. The compensatory β-cell response can be seen in obese patients. Studies have shown a 20-50% increase in β-cell mass from obese nondiabetic subjects compared to lean controls (Butler et al. 2003a; Rahier et al. 2008; Hanley et al. 2010). The second stage describes the transition from compensation to mild decompensation of β-cells accompanied by diminished GSIS, leading to IGT and IFG. However, in line with the fact that prediabetes can be maintained for years, the second stage is considered as a stable stage of adaptation because of the partially preserved insulin secretion. Evidence suggests that β-cell mass is reduced in IFG subjects at this stage (Butler et al. 2003a), but whether losing β-cells is also a cause of IGT and IFG is unknown. Stage 3 is transient as the blood glucose rises rapidly reaching the clinical threshold of hyperglycemia, which indicates the onset of T2D seen in stage 4. Stage 3 corresponds to a steep rise of blood glucose and pronounced decline in insulin secretion in the glycemia and insulin trajectories of T2D patients as mentioned above (Tabák et al. 2009). In the later stages, β-cells decompensate with reduced β-cell mass and a profound loss of insulin secretion. Moreover, loss of β-cell differentiation, at least in rodent models, further reduces the capacity for insulin secretion capacity per unit of β-cell mass, resulting in a roughly 50% reduction in functioning β-cell mass (Weir and Bonner-Weir 2004; Talchai et al. 2012). Overall, the progressive nature of β-cell dysfunction, as well as the natural history of T2D, calls attention to the changes in β-cell mass and function underlying compensatory GSIS that is critical in delaying T2D progression.

1.2 Pathophysiology of β-cell compensation in human T2D

1.2.1 β-cell functional compensation

Clinically, systemic insulin secretion capacity is determined by acute GSIS during a glucose tolerance test. However, it remains unclear whether the enhanced GSIS comes from the increase in β-cell mass or whether the insulin secretion per cell mass changes as well. A study measured the 24-hour profile of insulin secretion in obese, non-diabetic subjects and found a 100% increase compared with lean controls (Camastra et al. 2005). As mentioned above, a 20-50% increase in β-cell mass was reported in human obesity (Butler et al. 2003a; Rahier et al. 2008; Hanley et al. 2010). Thus, to account for 100% insulin secretion compensation not only the increased cell mass but also enhanced insulin output per β-cell must be considered. In line with this theory, a higher insulin secretory capacity has been observed in human islets isolated from obese donors (Mezghenna et al. 2011). Given that GSIS plays a critical role in β-cell compensation, it is important to understand the physiology of β-cells GSIS as well as the pathophysiological changes in the context of insulin compensation.

1.2.1.1 Glucose sensing

Stimulated insulin secretion from β-cells is tightly regulated by intracellular glucose metabolism (Figure 1-1). Plasma glucose elevates after food ingestion and enters β-cells through glucose transporters (GLUT). GLUT 1 and GLUT3, low K_m isoforms of GLUT, act as the primary glucose sensors and transporters in human pancreatic β-cells, whereas rodent β-cells express mainly GLUT2 (De Vos et al. 1995; McCulloch et al. 2011). However, inactivating mutations of GLUT2 have been reported as a rare cause of neonatal diabetes, suggesting a

unique role of GLUT2 in humans (Sansbury et al. 2012). Moreover, islets isolated from T2D donors have low expression and activity of both GLUT1 and GLUT2 (Ohtsubo et al. 2011); the endogenous expression of either isoform is sufficient to maintain GSIS (Thorens et al. 2000). This implies that the presence of different isoforms of GLUT in β-cells ensures the efficiency of glucose uptake for the next rate-limiting step of GSIS.

After transport into β-cells, glucose is sensed and phosphorylated by glucokinase (GCK) (De Vos et al. 1995). Serving as an intracellular sensor of glucose, GCK plays a critical role in insulin secretion through initiation of glycolysis. *In vitro* studies have demonstrated that activation of GCK lowers the glucose threshold for insulin secretion in normal human islets and can restore insulin secretion in islets isolated from T2D patients (Doliba et al. 2012; Henquin et al. 2017). Mutations of GCK gene have been identified in families with persistent hyperinsulinemic hypoglycemia (activating mutation) or GCK-linked maturity-onset of diabetes of the young (MODY-2) (inactive mutation) (Froguel et al. 1993; Glaser et al. 1998; Seino et al. 2011). Although GCK activity has been linked to hyperinsulinemia in rodents (Chan 1993), an understanding of the dynamics of GCK in human T2D compensation is elusive.

1.2.1.2 Mitochondrial oxidation

Glycolysis generates nicotinamide adenine dinucleotide (NADH), adenosine triphosphate (ATP) and pyruvate. Cytosolic NADH and pyruvate are transported into mitochondria. Pyruvate is then decarboxylated to acetyl-CoA, which is a substrate in the tricarboxylic acid cycle (TCA). Driven by the NADH and flavin adenine dinucleotide ($FADH_2$) released from glycolysis and TCA cycle, adenosine diphosphate (ADP) is phosphorylated into ATP through the respiratory chain, increasing the ratio of ATP to ADP in the cytoplasm (MacDonald et al. 2005).

Mitochondrial oxidation and signaling are central to GSIS (Jitrapakdee et al. 2010). Decreased expression of the key enzymes glycerol phosphate dehydrogenase (mGPDH), pyruvate carboxylase (PC) and succinyl-CoA:3-ketoacid-CoA transferase (SCOT) have been found in islets isolated from patients with T2D (MacDonald et al. 2009). Conversely, increases in these enzyme activities have been demonstrated in animal models with hyperinsulinemia (Liu et al. 2002).

In addition to changes in capacity for glucose oxidation, changes in morphology of mitochondria have been identified in islets from T2D subjects (Anello et al. 2005). Chronic exposure of β-cell to high glucose leads to excessive mitochondrial glucose oxidation and generation of reactive oxygen species (ROS), which induces oxidative stress and mitochondrial damage (Robertson et al. 2004). Mitochondria undergo fission and selective fusion and autophagy of fragments, which serves as quality control to prevent accumulation of damaged mitochondria and maintain function (Twig et al. 2008; Molina et al. 2009; Stiles and Shirihai 2012). Autophagy of mitochondria, also known as mitophagy, has been proposed as a protective mechanism in β-cells (Youle and Narendra 2011; Sarparanta et al. 2017). Recent clinical studies showed that nondiabetic obese and prediabetic subjects displayed higher markers of mitophagy and lower oxidative stress compared with diabetic subjects (Bhansali et al. 2017a, 2017b), indicating a possible role of mitophagy in β-cell compensation.

1.2.1.3 Post-mitochondrial steps in insulin secretion

Mitochondrial metabolism of glucose leads to a rise in intracellular ATP/ADP which closes the ATP-sensitive potassium channel (K_{ATP} channel) on the cell membrane (Straub et al. 1998), depolarizing the plasma membrane, which triggers the opening of the voltage-gated Ca^{2+} channel

(VGCC) and Na^+ channels in human β-cells, generating action potentials (Braun et al. 2008). The influx of Ca^{2+} increases cytosolic Ca^{2+} concentration and stimulates the exocytosis of insulin granules (Braun et al. 2008, 2009). β-cells are then repolarized to resting membrane potential by the opening of voltage-gated potassium (K_v) channels and inactivation of VGCC, limiting Ca^{2+} entry and insulin secretion (MacDonald and Wheeler 2003). Increase in intracellular Ca^{2+} triggers the exocytosis of insulin granule (Graves and Hinkle 2003). In addition to primary stimulation by glucose, β-cell insulin secretion can be amplified or regulated via a wide range of nutrients and hormones (Itoh et al. 2003; Doyle and Egan 2007).

Similar to rodents, insulin secretion in human β-cells follows a biphasic time course, a first-phase peak generated by the prompt action potentials mentioned above and a flat second-phase in response to prolonged stimulus (Henquin et al. 2006). The decline of first-phase insulin secretion is due to the depletion of the readily releasable pool (RRP) of insulin granules as well as the closing of VGCC (Michael et al. 2007; Braun et al. 2008, 2009). Not all features of rodent insulin secretion can be observed in human islets. A left-shifted glucose-insulin response curve is documented in human islets, with a detectable GSIS at glucose as low as 3 mmol/L (Henquin et al. 2006), which corresponds to the lower physiological plasma glucose seen in humans (King 2012).

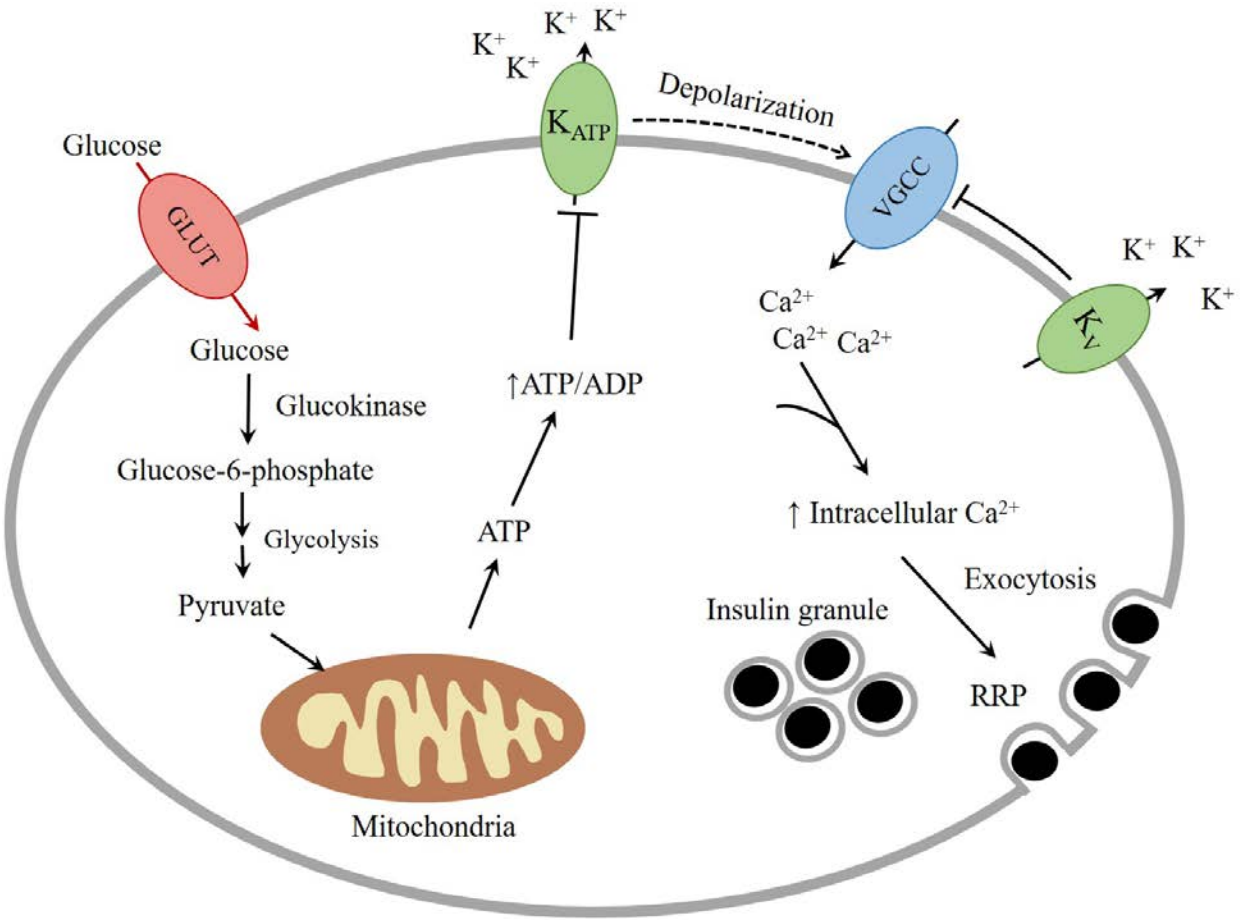

Figure 1-1. Glucose-stimulated insulin secretion. Plasma glucose enters β-cells through GLUT1 and 3 (in humans) and is then phosphorylated into glucose-6-phosphate by glucokinase. Glucose-6-phosphate is further metabolized via glycolysis, producing ATP and pyruvate. Cytosolic pyruvate is transported into mitochondria and enters the TCA cycle, which generates more ATP, leading to an increased ratio of ATP and ADP. The rise of ATP/ADP in cytoplasm closes the K_{ATP} channel on the cell membrane, resulting in membrane depolarization and the opening of the VGCC and Na^+ channels. The influx of Ca^{2+} increases cytosolic Ca^{2+} concentration, together with intracellular Ca^{2+} release, stimulating the exocytosis of insulin granules. β-cell action potentials are then repolarized to resting potentials by the opening of K_v channels and inactivation of VGCC, limiting the Ca^{2+} entry and insulin secretion.

1.2.2 Insulin biosynthesis and endoplasmic reticulum stress

1.2.2.1 Overview of insulin biosynthesis

Secreted insulin is a 51-amino-acid peptide, consisting of a 21-residue A chain and a 30-residue B chain linked by disulfide bonds. It is derived from the pre-hormone preproinsulin, encoded by *Ins* gene (*Ins1* and *Ins2* in rodents) located on the short arm of chromosome 11 in humans. Preproinsulin is composed of an N-terminal signal peptide (SP) and A and B chains joined by a 31-residue C-peptide. After translation, preproinsulin is translocated into the rough endoplasmic reticulum (ER) lumen by interaction of the N-terminal signal peptide with a signal recognizing receptor in the ER membrane. The signal peptide is then cleaved from preproinsulin, generating proinsulin (Weiss et al. 2000). In the ER lumen, proinsulin undergoes serial post-translational modifications including folding and formation of disulfide bonds between A and B chains for the correct cleavage of proinsulin. This process requires a variety of different ER chaperones (Feige and Hendershot 2011). The folded proinsulin is then transported to the Golgi apparatus where it is packaged into early secretory granules, during which the proinsulin is converted into insulin and C-peptide by prohormone convertases 1/3, 2 and carboxypeptidase E (Davidson et al. 1988; Song and Fricker 1995). Insulin and proinsulin intermediates bind to zinc, forming insulin-zinc hexamers that are stored as a dense core in mature secretory granules together with free C-peptide (Weiss et al. 2000; Jones and Persaud 2010). Insulin biosynthesis is summarized in Figure 1-2.

Glucose is the primary regulator of insulin biosynthesis (Andrali et al. 2008). Glucose increases the cyclic adenosine monophosphate (cAMP) concentration and promotes the binding of β-cell specific transcriptional factors including pancreatic duodenal homeobox-1 (Pdx-1) and musculoaponeurotic fibrosarcoma oncogene family A (MafA) to the insulin promoter,

stimulating *Ins* expression (Inagaki et al. 1992; Zhao et al. 2005; Iype et al. 2005). The glucose concentration required for insulin biosynthesis is lower than the glucose threshold for insulin secretion to maintain insulin stores (Boland et al. 2017).

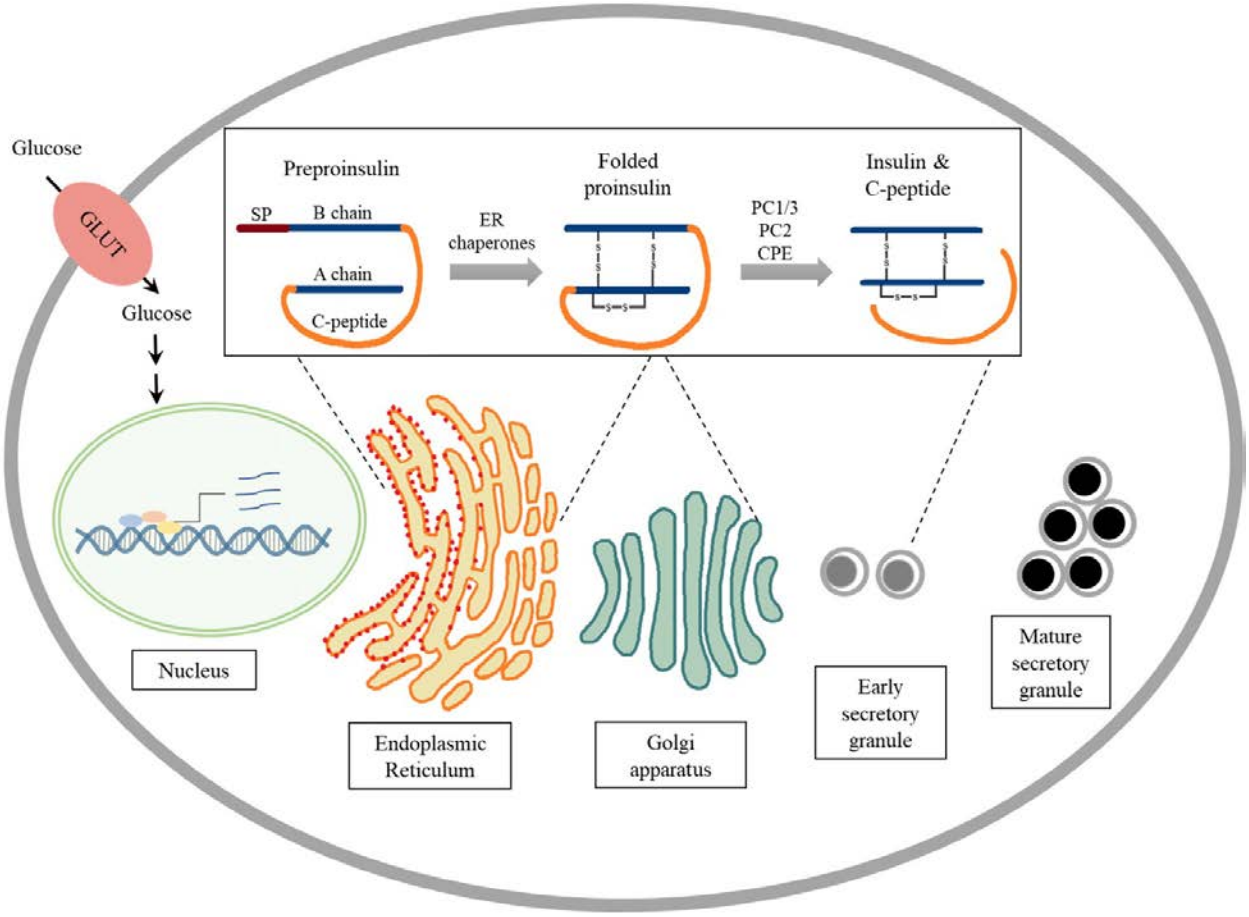

Figure 1-2 Insulin biosynthesis. Encoded by the *Ins* gene, preproinsulin mRNA is expressed under the regulation of glucose. After translation on the rough ER, preproinsulin is translocated into the ER lumen by interactions of the N-terminal signal peptide (SP) with signal recognizing receptor in the ER membrane. The SP is then cleaved from preproinsulin, generating proinsulin. In the ER lumen, proinsulin undergoes folding and formation of disulfide bonds between A and B chain to allow for the correct cleavage. Folded proinsulin is then transported to Golgi apparatus where it is packed into an early secretory granule, during which the proinsulin is converted into insulin and C-peptide by convertases (PC) 1/3, 2 and carboxypeptidase E (CPE). Insulin binds to zinc, forming insulin-zinc hexamers which are stored as a crystalized dense core in mature secretory granule together with C-peptide.

1.2.2.2 ER and unfolded protein response

ER is a membranous cell organelle consisting of cisternae as part of the intracellular membrane system. Protein translation initially takes place on the ribosome attached in the rough ER, and then the newly synthesized protein is translocated into the ER lumen for further assembly (Price 1992). Protein folding/assembly in the ER is the rate-limiting step in protein trafficking (Lodish 1988). Aberrantly folded proinsulin accumulates in the ER, resulting in impaired proinsulin trafficking and defective insulin secretion (Gupta et al. 2010). Whereas proper folding of proinsulin is correlated with protein exit from the ER and most importantly increased insulin secretion (Rajpal et al. 2012). If misfolded protein is retained in the ER at a steady rate, as assumed, proinsulin accumulation should be observed in ER, which, however, is not seen under normal conditions (Haataja et al. 2013). This reflects the presence of a system of alleviating the accumulated proinsulin pressure in the ER, which is referred to as the unfolded protein response (UPR) (Rasheva and Domingos 2009).

1.2.2.3 Adaptive UPR and ER chaperones

Figure 1-3 is a simplified summary of adaptive UPR. When there is unfolded protein in the ER lumen, immunoglobulin binding protein (Bip) senses the perturbation and dissociates from three downstream sensors: transcription factor 6 (ATF6), inositol-requiring enzyme 1 (IRE1) and protein kinase RNA-activated-like ER kinase (PERK), activating all 3 arms of the UPR (Oyadomari et al. 2002; Marchetti et al. 2007). First, after dissociating from Bip, ATF6 translocates to the Golgi apparatus and is cleaved by site 1 and site 2 proteases. Cleaved ATF6 enters the nucleus and acts as a transcriptional factor of ER chaperones, folding enzymes and the ER-associated degradation machinery (Haze et al. 1999; Shen et al. 2002; Nadanaka et al. 2007).

Secondly, free IRE1 is an active serine/threonine kinase, activated by conformational changes and autophosphorylation (Chen and Brandizzi 2013). Active IRE1 cleaves the mRNA of X-box binding protein 1 (Xbp1), altering the open reading frame of the mRNA. Expressed XBP1 is another transcriptional factor of ER chaperones (Sriburi et al. 2004; Uemura et al. 2009). Also, the IRE1 acts as an RNase to cleave mRNA of secretory proteins (such as preproinsulin) to reduce overall protein translation (Hollien et al. 2009). Lastly, similar to IRE1, PERK is activated by oligomerization. PERK dimer phosphorylates eukaryotic initiation factor-2α (eIF-2α) which attenuates translation initiation and selectively induces ATF4, a transcriptional factor initiating transcriptions of adaptive UPR components (Harding et al. 1999, 2000; Sonenberg and Hinnebusch 2009). Of note, when β-cells are exposed to chronic perturbations such as hyperglycemia, UPR induces pro-apoptotic factors such as C/EBP homologous protein (CHOP) mainly by the PERK arm of ER stress, leading to cell death (Laybutt et al. 2007; Brewer 2014).

As mentioned above, proinsulin folding by ER chaperones plays a prominent role in insulin biosynthesis. One of the most studied ER chaperones is protein disulfide isomerase (PDI). PDI is a thio-oxidoreductase that catalyzes disulfide bond formation (Ellgaard and Ruddock 2005). PDI donates a disulfide bond to proinsulin and then is re-oxidized by ER oxidoreductin-1 (Ero1) (Zito et al. 2010). This chaperone also works as a reductase, breaking disulfide bonds on misfolded proteins to ameliorate insulin secretion (Rajpal et al. 2012; He et al. 2015; Gorasia et al. 2016), suggesting a protective role of PDI in insulin secretion. There is lack of evidence of a role of ER chaperones in human islet compensation; however, clinical studies reported beneficial effects of chemical chaperones on patients with insulin resistance (Kars et al. 2010; Xiao et al. 2011). Islets isolated from diabetic donors, on the other hand, have decreased adaptive UPR and increased

pro-apoptotic UPR markers (Laybutt et al. 2007; Engin et al. 2014), but the full range of islet compensation through to decompensation has not yet been examined in human islets.

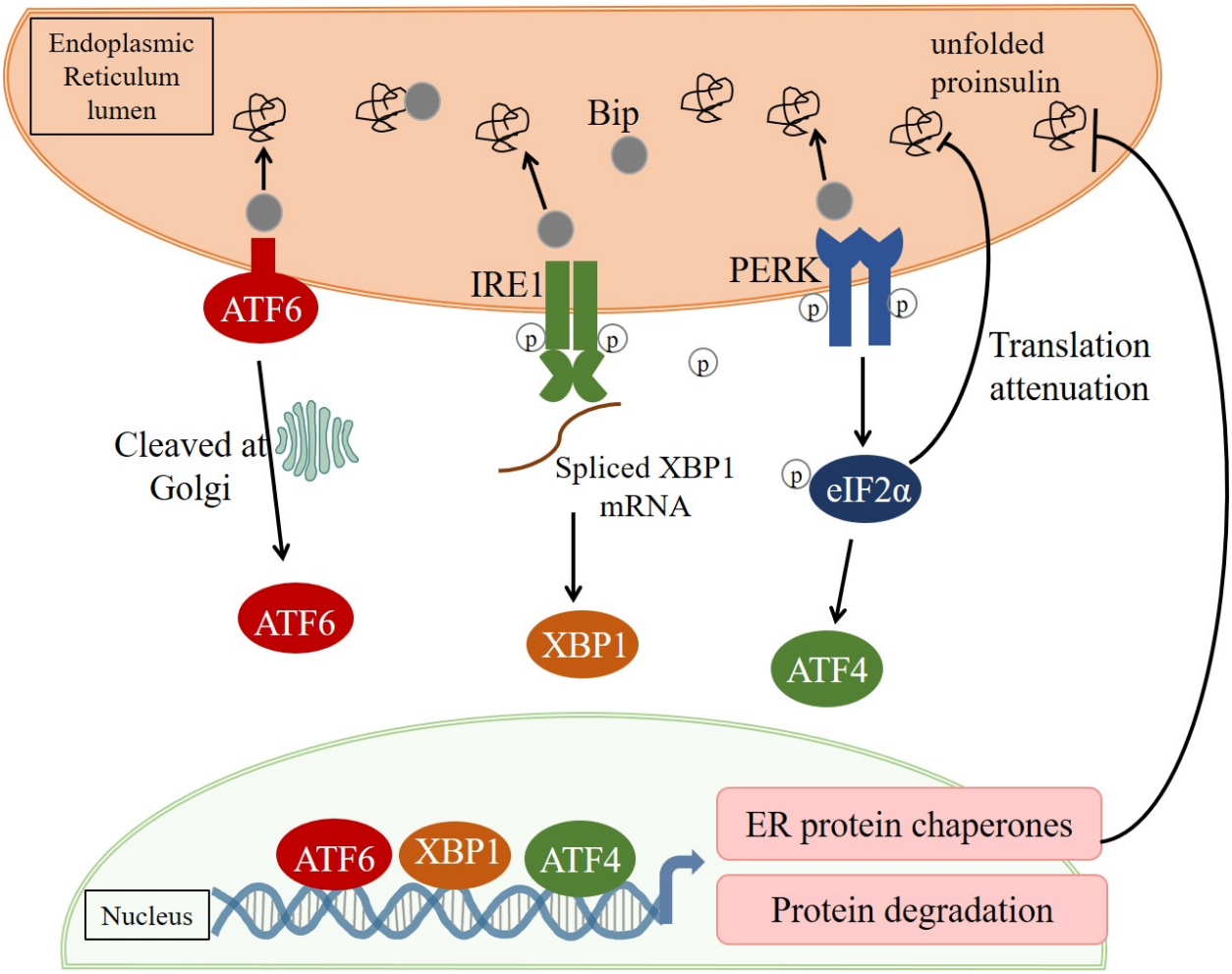

Figure 1-3 Adaptive UPR. When unfolded protein is accumulated in the ER lumen, Bip (solid grey circle) senses the perturbation and dissociates from membrane proteins ATF6 (in red), IRE1 (in green) and PERK (in blue), activating all 3 arms of UPR. 1) ATF6 translocates to the Golgi apparatus and is cleaved into active ATF6; 2) IRE1α cleaves the mRNA of XBP1, altering the open reading frame of the mRNA, which is expressed as XBP1; 3) PERK is activated by oligomerization and then phosphorylates eIF-2α which attenuates translation initiation and selectively induces ATF4. The transcriptional factors ATF4, XBP1, and ATF4 enter the nucleus and induce the transcription of ER chaperones, folding enzymes and the machinery of ER-associated degradation, alleviating the unfolded protein stress in the ER.

1.2.3 β-cell proliferation and neogenesis

It is well accepted that β-cell mass expands under conditions of insulin resistance. Of note, although β-cell proliferation has been proposed as a major contributor to β-cell expansion in rodents (Skau et al. 2001; Bock et al. 2003), the rate of β-cell replication rarely increases and is difficult to detect in nondiabetic obese adults or patients with T2D (Butler et al. 2003a; Hanley et al. 2010). In fact, it has been reported that proliferation serves as an essential mechanism in β-cell expansion during infancy, but declines in adolescence, after which islets grow more in size (hypertrophy) than number (hyperplasia) (Meier et al. 2008). However, the inability to detect proliferation in obese/insulin-resistant human samples could be due to a preceding β-cell replication, which leads to an enlarged β-cell mass later on. Lastly, in spite of the low replication rate in adult human pancreas, β-cells do have replication potential when treated with pharmaceutical stressors *in vitro* (Aguayo-Mazzucato and Bonner-Weir 2018), indicating another therapeutic target.

Instead of β-cell self-replication, neogenesis promotes formation of new islets originating from progenitor cells (Xu et al. 2008). Increases in cell neogenesis have been reported in different cohorts of nondiabetic obese subjects, indicating neogenesis as a mechanism of compensation of β-cell mass (Meier et al. 2008; Hanley et al. 2010). Also, taking advantage of single-cell transcriptomics and specific cell surface markers, studies have confirmed that the long-speculated heterogeneity seen in rodents does exist in human β-cells (Dorrell et al. 2016; Segerstolpe et al. 2016; Lawlor et al. 2017), which could be a result of immature cells newly formed from neogenesis. It is worth noting that β-cell neogenesis discussed here is not confirmed by lineage tracing but estimated by quantifying small clusters of insulin-positive cells that are associated with ductal or acinar cells. Although a multipotent stem cell has been found in adult

human pancreas (Smukler et al. 2011), it remains elusive as to how and to what extent these progenitor cells contribute to β-cell mass adaptation.

In addition, a growing body of evidence supports that ductal, acinar and non-β islet cells can act as β-cell precursors and be reprogrammed to β-cells, which is defined as trans-differentiation (Cigliola et al. 2016). Mezza et al. reported an inverse correlation between insulin sensitivity and islet size with an increased number of insulin-glucagon double positive cells in insulin-resistant nondiabetic subjects (Mezza et al. 2014), suggesting trans-differentiation of α-cells as a contributor in β-cell adaptation. Moreover, human pancreatic ductal cells can also be reprogrammed into insulin-secreting cells *in vitro* (Lee et al. 2013). Therefore, trans-differentiation may be a strategy in expanding or restoring β-cell mass.

In addition to β-cell replenishment, β-cell demise is another factor altering β-cell turnover and cell mass (Donath and Halban 2004). Loss of β-cell mass in T2D has been described and reviewed by different authors (Butler et al. 2003a; Weir and Bonner-Weir 2004; Rahier et al. 2008). Butler reported that patients with T2D had comparable β-cell replication but increased β-cell apoptosis compared to nondiabetic subjects, indicating that apoptosis is the primary pathophysiology of β-cell mass loss in the context of T2D (Butler et al. 2003a). Whereas in the obese or prediabetic cohort, β-cell apoptosis rate is usually low and not different from nondiabetic controls (Butler et al. 2003a; Meier et al. 2008; Hanley et al. 2010). The evidence so far favors the notion that the primary mechanism underlying β-cell mass compensation is increased β-cell replenishment with low rate of apoptosis. Figure 1-4 shows the possible sources of β-cell mass compensation.

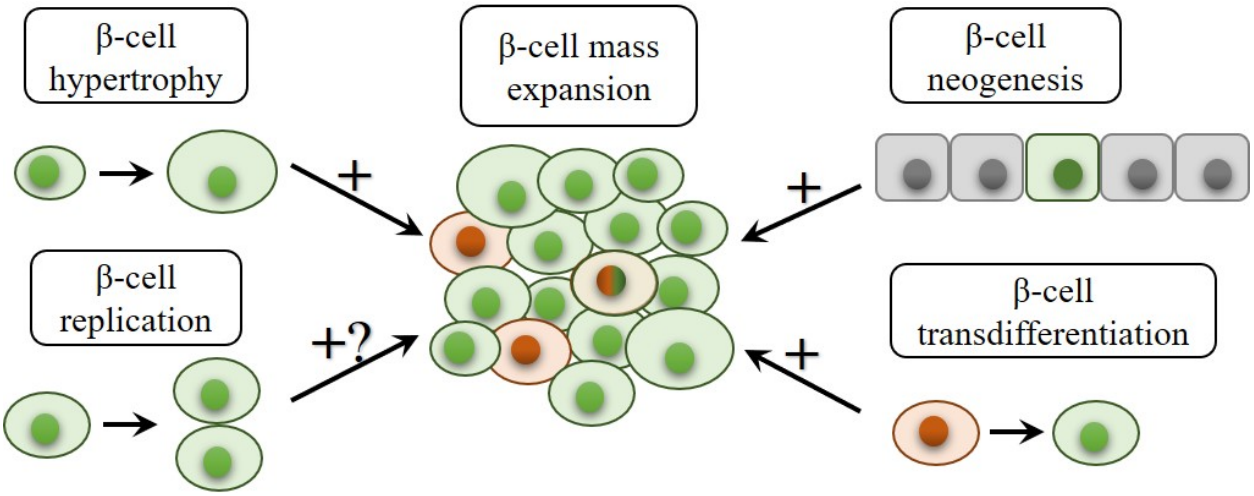

Figure 1-4 Proposed mechanisms of β-cell compensation. In human T2D, β-cell hypertrophy, neogenesis and trans-differentiation are speculated to be major mechanisms underlying β-cell expansion; whereas β-cell replication is rare in adult humans.

In summary, human studies have demonstrated that β-cell compensation is essential to maintain NGT, compensate for decreased insulin sensitivity (IS), lower hepatic glucose output by inhibiting glucagon action, and therefore keeping prediabetes from progressing (Festa et al. 2006; Ferrannini et al. 2011). In spite of β-cell compensation playing a critical role, the cellular origins and mechanisms are not yet clear. A significant challenge for studying β-cells in human is the restricted source of islets and limited interventions allowed in human research. To elucidate the cellular basis of β-cell adaptation in T2D progression as well as assess novel therapeutic interventions that target early-on β-cell abnormalities, animal models that resemble human T2D history are required.

1.3 Animal models for studying β-cell compensation

Since Banting and Best discovered insulin in dog pancreas extracts in 1921, animal models have been an indispensable tool and led to important breakthroughs in diabetes (Karamanou et al. 2016). Transgenic animals carrying various gene variants have been studied to shed light on the genetic basis of diabetes (Takamoto et al. 2014; da Silva Xavier et al. 2017); however, T2D is not a monogenic disease. Genetics, environmental factors, lifestyle, and diet are all interrelated and contribute to diabetes progression (Fletcher et al. 2002). Animal models with specific causes and pathogenesis may emphasize only particular aspects of the diabetic phenotype but not resemble the pathophysiology or disease development observed in human subjects. Therefore, a better understanding of animal models regarding their genetic background, pathogenesis, and pathophysiology is necessary to choose the right model for β cell compensation and to interpret results from animal studies correctly.

In this section, animal models commonly used in studies of β-cell adaptation are discussed and compared with the current knowledge gained from human studies, in terms of the genetic background, cause of diabetes, metabolic characteristics, β-cell dynamics, and the mechanism implied. Animal models evaluated were classified into four different types by the origin of T2D. Table 1-2 summarizes the β-cell compensatory response and the mechanisms identified in the models discussed in this overview. A summary of data extracted from included studies is provided in appendix B.

1.3.1 Monogenic models

Monogenic obese models are widely used in obesity-induced T2D research. The most common are *ob/ob (Lep$^{ob/ob}$)* mouse, *db/db* (*Lepr$^{db/db}$*) mouse and Zucker Fatty *fa/fa* (ZF) rat.

Metabolic abnormalities in these models are a result of a homozygous, autosomal recessive mutations on gene leptin (*Lep*$^{ob/ob}$) or leptin receptor (*Lepr*$^{db/db}$, *fa/fa*), which can lead to hyperphagia, impaired lipid metabolism and severe obesity or/and diabetes in a relatively short period. Models with homozygous *lep* or *lepr*-mutant are usually infertile.

1.3.1.1 *ob/ob* and *db/db* mice

The phenotype of the *ob* mutation was first discovered at Jackson Laboratory in 1949 and then backcrossed onto the C57BL/6J strain. Later in 1994, Friedman's group mapped the mutation to human chromosome 4 and identified the product as leptin (Zhang et al. 1994; Halaas et al. 1995). *ob/ob* mice are characterized by hyperphagia, obesity and insulin resistance. Robust hyperinsulinemia develops in *ob/ob* mice as early as 4 weeks of age and is sustained thereafter with enhanced GSIS and increased β-cell mass, whereas plasma glucose is stable for most of the time (Medina-Gomez et al. 2007; Chan et al. 2013; Engin et al. 2014). These features mimic the compensation stages 1 and 2 in human T2D. However, while GSIS is enhanced, *ob/ob* mice do exhibit IGT and transient hyperglycemia (Chan et al. 2013). It is possible that the unchecked glycemia results from a prompt but inadequate β-cell functional response to compensate for the massive obesity driven by lack of leptin. Thus, there must be a mechanism further exerting β-cell adaptations to keep up with the insulin demand and prevent diabetes in *ob/ob* mice.

One possibility is that adaptive UPR promotes β-cell functional capacity in compensation. Chan et al. (Chan et al. 2013) showed that β-cell GSIS increases at 6 weeks, accompanied by upregulated ER chaperones, but fails to further increase with time in spite of the sustained adaptive UPR. Of note, expression of key transcriptional factors for β-cell function and anti-inflammation markers is maintained, indicating the importance of staying differentiated in β-cell

compensation (Chan et al. 2013). However, enhancing adaptive UPR *in vitro* does not improve β-cell function and identity (Chan et al. 2013), demonstrating a supportive but not deterministic role of UPR in β-cell compensation. On the other hand, β-cell mass significantly increases in *ob/ob* mice compared with age-matched lean controls, with evident β-cell proliferation as indicated by increased proliferation markers ki67 and cyclinD1 (Medina-Gomez et al. 2009). It may not be the case in human tissue, but β-cell replication does occur in *ob/ob* mice and contributes to the β-cell adaptation, especially at late stages when β-cells reach their maximal functional capacity. Also, *ob/ob* mice lacking peroxisome proliferator-activated receptor γ2 (PPAR-γ2) lose the adaptive responses in GSIS and proliferation, indicating a role of PPAR-γ2 in β-cell compensation (Medina-Gomez et al. 2009).

The *db/db* (*Lepr*$^{db/db}$) mouse is another obesity-induced diabetes model discovered at Jackson Laboratory with homozygous mutation of the leptin receptor (Chen et al. 1996). In contrast to *ob/ob* mice, *db/db* mice on C57BL/KsJ background exhibit a short compensation stage with hyperinsulinemia at 2-4 weeks of age followed by an early onset of hyperglycemia at 6-8 weeks (Kanda et al. 2009; Chan et al. 2013; Burke et al. 2017). Although hyperinsulinemia is maintained in diabetic *db/db* mice, β-cells display diminished GSIS and reduced insulin content after 8 weeks (Kanda et al. 2009; Chan et al. 2013). Marked β-cell dedifferentiation and stress-related apoptosis also suggest evident β-cell decompensation in *db/db* mice, albeit with increased β-cell mass (Kanda et al. 2009; Chan et al. 2013; Burke et al. 2017). Thus, the *db/db* mouse is not a model for β-cell compensation but rather for β-cell dysfunction.

Interestingly, *db/db* mice bred onto the C57BL/6J strain are resistant to obesity-induced diabetes (Chan et al. 2013). β-cell gene expression in C57BL/6J *db/db* mice is broadly consistent with the findings in *ob/ob* mice, indicating that different backgrounds affect metabolic phenotype

and β-cells adaptive response more than *db/db* mutation (Chan et al. 2013). Moreover, it is surprising that, compared with wild-type, C57BL/KsJ mice with heterozygous *db/m* mutation can resist high-fat diet (HFD)-induced IGT with elevated GSIS and β-cell mass (Kanda et al. 2009). It would be interesting to look at how the presence of *db* mutation exerts a greater β-cell compensatory response.

1.3.1.2 Zucker Fatty *fa/fa* rat

Zucker Fatty *fa/fa* (ZF) rats harbor a homozygous mutation (*fatty, fa)* on leptin receptor gene (*Lepr*$^{fa/fa}$). This strain is characterized by obesity, insulin resistance, hyperinsulinemia and euglycemia (Jones et al. 2010). Similar to *ob/ob* mice, ZF rats exhibit a long-lasting compensation stage with hyperinsulinemia starting at 3-6 weeks of age (Aleixandre de Artiñano and Miguel Castro 2009; Jones et al. 2010; Omikorede et al. 2013). Obese ZF islets at 6 weeks have intact structure and comparable size to lean controls, whereas islets at 14 weeks are significantly larger, which is a consequence of increased β-cell proliferation and neogenesis as well as substantial β-cell hypertrophy and vascularization. There is also a marked increase in gene expression regarding ER stress, β-cell function and growth, and metabolism in islets from 14-week ZF rats. In spite of the mild degenerative changes, β-cells in ZF rats are well-adapted to obesity-related insulin resistance (Jones et al. 2010).

In contrast, Zucker diabetic fatty (ZDF) rats, derived from selective inbreeding of ZF rats with IGT, display initial hyperinsulinemia followed by an early onset of hyperglycemia and a decline in plasma insulin over time (Jones et al. 2010). Pathological changes in β-cells from ZDF at the compensation stage are similar to the findings in ZF rats at 14 weeks but much more severe (Jones et al. 2010). Diabetic ZDF islets have significantly fewer β-cells compared to lean and ZF

rats (Jones et al. 2010). One interesting finding of the ZDF strain is that female ZDF rats are resistant to *fa/fa* induced hyperglycemia because of β-cell compensation but susceptible to HFD-diabetes, which is proposed as a model of diet-induced β-cell dysfunction (Omikorede et al. 2013).

In summary, obese models with defective leptin signaling are widely used and well characterized in terms of the time course, metabolic features, and β-cell phenotype. *ob/ob* and *db/db* mice allow studies to target β-cell pathophysiology at different stages of β-cell compensation. However, monogenic T2D is distinct from the polygenic nature of human T2D. Also, as mentioned previously, the genetic background markedly affects an animal's phenotype. Therefore, scientists need to be cautious when comparing animals with different backgrounds. Obese ZF and ZDF rats, on the other hand, are found less commonly than *ob/ob* and *db/db* mice in recent studies related to β-cell function. It may be due to increased usage of readily available transgenic models, but they are still powerful tools in metabolic syndrome research (Aleixandre de Artiñano and Miguel Castro 2009).

1.3.2 Transgenic models

Transgenic models have been used in elucidating the molecular basis of diabetes by genetically modifying specific genes. The technological revolution in gene-editing allows precise point mutation, inducible and tissue-specific gene modifications in rodents. Models carrying genetic defects that cause human T2D symptoms provide novel insight into disease pathogenesis and pathophysiology.

1.3.2.1 Islet amyloid polypeptide (IAPP)

IAPP is a 37-residue protein that is co-secreted with insulin by β-cells. Fibrils derived from human IAPP (hIAPP) are present in islets from subjects with T2D (Cooper et al. 1987), and are linked to loss of β-cells in human T2D (Lorenzo et al. 1994). However, rodent IAPP does not have the propensity for aggregation in islets. Therefore, the hIAPP knock-in animal is a useful tool for investigating the relationship between hIAPP and β-cell expansion (Matveyenko and Butler 2006). Butler et al. (Butler et al. 2003b; Matveyenko et al. 2009) have demonstrated that the induction of *hIAPP* abolishes the adaptational increases in both β-cell function and mass in insulin-resistant models. Instead of activating adaptive UPR to enhance insulin secretion, β-cells expressing hIAPP manifest defective GSIS and ER stress-related apoptosis, resulting in IGT and hyperglycemia. It is worth noting that increased β-cell apoptosis is found preceding formation of visible islet amyloid fibrils in hIAPP models, suggesting that intermediate-sized IAPP oligomers rather than IAPP deposits are cytotoxic to β-cells (Butler et al. 2003b). This confirmed by a separate study showing that hIAPP caused deterioration of insulin secretion and IGT of HFD mice without the presence of intraislet amyloid formation (Hiddinga et al. 2012).

1.3.2.2 Insulin receptor/Insulin receptor substrate

Impaired autocrine insulin action is the initial pathogenesis of β-cell compensation. Insulin signaling pathways affect not only peripheral glucose metabolism but also β-cell function and proliferation (Accili 2004). Homozygous knockout of insulin receptor substrate 2 ($Irs2^{-/-}$) crossed with a heterozygous deficient insulin receptor ($IR^{+/-}$) generates a phenotype displaying hyperinsulinemia at 8 weeks and hyperglycemia at 12 weeks of age due to the loss of downstream IR/Irs signaling (Kim et al. 2007). Despite increased fasting insulin, the double

knock-out mice have impaired GSIS, substantial loss of β-cell mass and growth retardation (Kim et al. 2007). Therefore, the tissue-specific knockout strategy was applied (Kadowaki 2000; Okada et al. 2007; Escribano et al. 2009). The tissue-specific $IR^{-/-}$study suggests that liver $IR^{-/-}$ is responsible for the insulin-resistant phenotype which leads to β-cell compensation (Okada et al. 2007; Escribano et al. 2009); whereas β-cell specific $IR^{-/-}$ alone does not induce IGT or T2D but disables the ability of β-cell to proliferate or secrete more insulin in response to HFD (Okada et al. 2007). This inhibitory effect of IR on β-cell compensatory capacity is suggested to occur via FoxO1 activity (Okada et al. 2007), which has led to the creation of *FoxO1* transgenic mice.

1.3.2.3 Forkhead box protein O1

Forkhead box protein O1 (FoxO1) belongs to the forkhead family of transcription factors characterized by a conserved forkhead-box DNA binding domain. FoxO1 regulates diverse cell functions, including metabolism, differentiation, and proliferation, which is controlled by insulin/IGF-1 signaling via phosphorylation-mediated nuclear exclusion (Accili and Arden 2004; Okada et al. 2007). In order to examine the effect of FoxO1 activation in β-cell adaptation, Okamoto et al. (Okamoto et al. 2006) introduced a constitutively nuclear-expressed *FoxO1* mutant into pancreatic ductal and β-cells in muscle-specific $IR^{-/-}$ mice. As a result, the adaptational expansion of β-cells in response to $IR^{-/-}$ was lost entirely in mutant *FoxO1* mice, with totally absent cell proliferation and reduced periductal β-cells (Okamoto et al. 2006). However, an unexpected increase in insulin secretion was found, indicating nuclear FoxO1 suppresses β-cell proliferation but enhances β-cell function (Okamoto et al. 2006). β-cell specific overexpression of wild-type *FoxO1* in mice revealed enhances GSIS and glucose sensing by FoxO1 nuclear translocation, as well as a protective effect on oxidative stress via nuclear

retention (Zhang et al. 2016). Although the actual effect of FoxO1 in β-cell GSIS is still controversial, these findings underline the importance of FoxO1 in regulating both β-cell function and mass.

1.3.3 Experimentally induced models

Human T2D has two major pathogenic hallmarks, insulin resistance and β-cell dysfunction. These features can be induced by approaches like dietary manipulation, β-cell toxins, surgery, or their combinations. Models generated can resemble different aspects or stages of human T2D based on the purpose of the study. Thus they are widely used in T2D research.

1.3.3.1 High-fat diet

High-fat diet (HFD) models are typically generated by utilizing diets containing 40-60% of calories from fat, which is 4-6 times higher than that of standard chow diet. HFD is often used as an extra metabolic pressure on transgenic models to induce T2D. In fact, HFD feeding alone can elicit major pathogenic features of T2D, including IGT, hyperinsulinemia, obesity, and moderate hyperglycemia depending on the animal's age, strain and duration of HFD (Ellenbroek et al. 2013; Stamateris et al. 2013; Maschio et al. 2016; Gupta et al. 2017). Within 1 week of HFD, young adult C57BL/6 mice develop IGT and a responsive increase in β-cell proliferation and GSIS (Stamateris et al. 2013; Gupta et al. 2017). After that, continued HFD exposure worsens the IGT, which stimulates β-cell GSIS and mass expansion through 16 weeks, resulting in a stable prediabetic state (Ellenbroek et al. 2013; Gupta et al. 2017). In contrast, older C57BL/6 mice develop hyperglycemia after 8 weeks of HFD, albeit with increased β-cell mass (Maschio

et al. 2016). β-cell proliferation has been suggested as the primary mechanism of β-cell mass adaptation in response to overnutrition (Ellenbroek et al. 2013; Stamateris et al. 2013; Maschio et al. 2016) but a longitudinal study showed an increasing number of small islets along with β-cell mass expansion in an HFD-fed cohort, indicating a non-proliferative mechanism was involved in β-cell adaptation (Gupta et al. 2017). Furthermore, as suggested in *ob/ob* mice, PPAR-γ is associated with β-cell compensation, as a link to downstream adaptive UPR, glycolysis, mitochondrial function, and survival (Gupta et al. 2017). Of note, as opposed to obese monogenic and polygenic strains, the HFD-induced early β-cell compensation is not related to the loss of insulin sensitivity as suggested by the normal ITT but is mainly driven by deteriorated glucose tolerance. And last but not least, varying the fat source alters the metabolic phenotype of HFD-induced models (Buettner et al. 2006).

1.3.3.2 Chemical toxins

Streptozotocin (STZ) is a natural antibiotic that selectively destroys pancreatic β-cells in a dose-dependent manner (Szkudelski 2001). Single high-dose STZ (100-200 mg/kg BW for mice) leads to massive loss of β-cells and rapid hyperglycemia, which are characteristics of T1D, whereas single intermediate-dose (45-90 mg/kg BW) or multiple low-dose (20-40 mg/kg) of STZ reduces β-cell volume and insulin secretion as seen in T2D (Tschen et al. 2009; Meier et al. 2011). Alloxan, although less used in recent studies, is another β-cell toxin that induces β-cell destruction at a dose of 40-200 mg/kg (Szkudelski 2001). The inducible β-cell loss by STZ and alloxan, combined with HFD-induced insulin resistance, creates an excellent model for studying the mechanisms of β-cell mass renewal in the context of T2D (Tschen et al. 2009; Shu et al. 2012; Jiang et al. 2015). Evidence from the STZ or alloxan models confirms that both

proliferation and neogenesis are involved in β-cell mass adaptation/restoration, which is associated with transcription factor TCF7L2, and that the capacity of β-cell proliferation is restricted in older mice (Tschen et al. 2009; Shu et al. 2012; Song et al. 2015).

1.3.3.3 Pancreatectomy

Pancreatectomy (Px) has been used to create produce diabetes in mice since 1949. To study the consequence of reduced β-cell mass on β-cell function, Bonner-Weir et al. (Bonner-Weir et al. 1983) performed 90% partial Px on mice and found that Px mice displayed an evident β-cell regeneration but with diminished GSIS per β-cell mass, leading to IGT. This study suggests that loss of β-cells induces susceptibility of β-cells to lose function with chronic stimulation. Since that time, the Px model has been widely used in β-cell regeneration and compensation research (Delghingaro-Augusto et al. 2009; Rankin and Kushner 2009; Téllez et al. 2016). To examine the capacity of β-cell compensation in the context of obesity, 60% Px was performed on Zucker fatty rats (Delghingaro-Augusto et al. 2009). In contrast with lean-Px rats, ZF-Px rats display hypoinsulinemia and hyperglycemia, accompanied by blunted β-cell GSIS, marked depletion of insulin content and β-cell dedifferentiation (Delghingaro-Augusto et al. 2009), which implies that metabolic stress impairs β-cell compensation in response to reduction of β-cell mass. Moreover, the age-related restriction of β-cell proliferation is confirmed in Px models (Rankin and Kushner 2009; Téllez et al. 2016). Therefore, strategies aiming to promote β-cell compensation may require prevention of β-cell exhaustion, dedifferentiation or stimulation of β-cell neogenesis.

The disadvantage of using STZ and Px models is the absence of functional adaptation. β-cell insulin content is depleted to compensate for the sudden loss of functional mass, leading to β-cell

dysfunction. Nevertheless, STZ and Px models are useful for evaluating interventions targeting on β-cell regeneration. It has been reported that epidermal growth factor (EGF), gastrin and GLP-1 analog exendin-4 promote β-cell restoration in the STZ and Px models (Delghingaro-Augusto et al. 2009; Shu et al. 2012; Song et al. 2015).

1.3.4 Polygenic models

Although monogenic and transgenic models demonstrate a direct link between genetic mutations and metabolic phenotypes, the clinical heterogeneity of T2D cannot be explained by a single genetic cause. In general, polygenic models may provide a more accurate platform to better study T2D as a complex genetic disease.

1.3.4.1 Goto-Kakizaki rat

Although it is less common, people can develop T2D without being obese (Taylor and Holman 2015). The Goto-Kakizaki (GK) rat is a well-known animal model for non-obese T2D derived from inbred Wistar rats selected by animals with poor glucose tolerance and characterized by the absence of obesity, IGT, and early onset of hyperglycemia (Portha 2005; Portha et al. 2009). There is a short period of euglycemia in young GK rats that is considered as a prediabetes stage, ranging from birth to weaning at 4 weeks. Unlike obese models showing early onset of hyperinsulinemia produced by compensating β-cells, prediabetic GK rats exhibit initial loss of β-cell population and defective β-cell function followed by insulin deficiency (Portha et al. 2001; Movassat et al. 2008). This early β-cell growth retardation is linked to defective expression of embryonic insulin-like growth factor (IGF) and reduced capacity for β-

cell neogenesis (Plachot et al. 2001; Portha et al. 2001; Calderari et al. 2007). Although there is an increase in basal plasma insulin in adult diabetic GK rats, it is more age-related (Movassat et al. 2008). Therefore, GK rats serve as a significant model for β-cell failure (Lacraz et al. 2010), but not for β-cell adaptation due to lack of β-cell compensatory response.

1.3.4.2 Obese strains

The New Zealand Obese (NZO) mouse is one of the most well-characterized polygenic models for T2D, created by selective inbreeding of agouti-colored mice (Kluge et al. 2012). The metabolic phenotype of NZO described in different colonies varies due to the use of different diets and sub-strains of NZO (Kluge et al. 2012), but the majority of studies on NZO mice report an obesity-induced T2D. NZO mice develop obesity and insulin resistance at 1-3 months and about 50% of them progress to chronic hyperglycemia by the age of 4-5 months (Lange et al. 2006; Kluge et al. 2012). Compared with diabetic NZO mice, non-diabetic mice exhibit higher plasma insulin concentrations and larger β-cell areas (Cameron et al. 1974; Lange et al. 2006), indicating β-cell adaption in NZO mice. A positive correlation of β-cell proliferation and basal insulin secretion is found in non-diabetic mice. However, its overall proliferation rate is lower compared with diabetic NZO mice (Lange et al. 2006). Thus, the difference in cell mass may result from β-cell apoptosis in diabetic mice or other mechanisms like neogenesis in non-diabetic NZO mice.

The Otsuka Long-Evans Tokushima Fat (OLETF) rat is derived from Long-Evans rats. Similar to the phenotype of NZO mice, OLETF rats display an early onset of obesity and IGT and a late onset of hyperglycemia (Kawano et al. 1994). The prediabetes stage can be maintained for over 30 weeks with progressive increases in fasting insulin, postprandial GSIS, and β-cell

mass (Kawano et al. 1994; Huang et al. 2007). Increased insulin content in OLETF rats indicates a more active insulin biosynthesis during β-cell compensation (Huang et al. 2007). However, the mechanism of compensation in OLETE rats is not fully explored.

To preserve fertility in the monogenic obese strains, lean ZDF rats are crossbred with obese Sprague-Dawley rats to produce a fertile polygenic obese model, named UC Davis type 2 diabetes mellitus (UCD-T2DM) rat (Cummings et al. 2008). In comparison with ZDF rats, this strain develops adult-onset obesity and prediabetes and later T2D at 6-9 months of age in both male and female animals (Cummings et al. 2008). Similar to OLETF rats, evidence so far suggests β-cell mass and insulin content are critical in prediabetic UCD-T2DM rats (Cummings et al. 2008).

1.3.4.3 Spontaneous T2D models

Although rodents are quite resistant to developing diabetes, some can develop T2D naturally. The sand rat (*Psammomys obesus*) is from the arid regions of North Africa and the Eastern Mediterranean. Wild sand rats do not exhibit symptoms of T2D, but animals in captivity fed on chow diet display obesity and insulin resistance (Shafrir et al. 2006; Khalkhal et al. 2012). It is important to emphasize the heterogeneity in T2D development of sand rats. At the age of 12 months, sand rats can be divided into four subtypes based on their glycemia: euglycemic-euinsulinemic, euglycemic-hyperinsulinemic, hyperglycemic-hyperinsulinemic, and hyperglycemic-hypoinsulinemic (Shafrir et al. 2006). The differences between euglycemic and hyperglycemic groups are mainly attributed to β-cell activity and fat metabolism (Shafrir et al. 2006). The euglycemic phenotypes have elevated β-cell GSIS, high insulin content and relatively low triglyceride and cholesterol in plasma (Kaiser et al. 2005; Khalkhal et al. 2012), whereas

diabetic rats show a gradual loss of β-cell insulin content, glucokinase, and glucose transporter 2, which results in impaired GSIS (Jorns et al. 2002; Kaiser et al. 2005). Also, a transient increase in β-cell proliferation is observed in sand rats newly placed on a chow diet, but β-cell mass is not altered (Kaiser et al. 2005). Evidence so far suggests a critical role of β-cell function in keeping normal blood glucose in sand rats.

Nile rats, also known as Africa grass rat (*Arvicanthis niloticus*), respond similarly to sand rats when kept in the laboratory and fed on chow diet (Chaabo et al. 2010). This model displays an age-related T2D development, with an early onset of insulin resistance and hyperinsulinemia at 2 months, a mild rise of glucose at 6 months, and overt hyperglycemia at 12 months (Noda et al. 2010; Yang et al. 2016). Nile rats with chronic diabetes also manifest T2D complications in liver, kidney, and retina (Subramaniam et al. 2018). Pathogenesis of the prolonged prediabetes stage in Nile rats is not clear, but a negative correlation between β-cell area and blood glucose is reported, indicating β-cell mass adaptation in euglycemic Nile rats (Yang et al. 2016). Besides, islets from diabetic Nile rats have impaired GSIS, defective insulin synthesis and increased ER stress (Yang et al. 2016), which implies a potential change of β-cell function in T2D development of Nile rats.

It is worth noting that the diet of sand rats and Nile rats has a substantial influence on the evolution of T2D. Animals fed with a low-calorie diet that is similar to their natural food do not exhibit obese or diabetic phenotypes (Kaiser et al. 2005; Yang et al. 2016). Indeed, diet intervention can reverse the early symptoms of diabetes in sand rats (Shafrir et al. 2006). A high-fat diet, on the other hand, accelerates T2D progression in Nile rats (Chaabo et al. 2010). Thus, the T2D in spontaneously obese animals is a result of genetic predisposition interacting with environmental changes.

1.3.5 A summary of the current understanding of β-cell compensation

β-cell compensation in nature is a complex cell response stimulated by chronic metabolic pressure (Figure 1-5). This pressure mainly comes from an unbalanced glucose metabolism that can be affected by both the metabolic environment and genetics. In humans, β-cell compensation occurs in obesity-induced prediabetes and appears to be caused by multiple factors. Among all the models reviewed here, while the phenotypes of monogenic models (*ob/ob* mouse*,* ZF rat) are different from human T2D and largely dependent on genetic background, obese polygenic models represent not only the polygenic causation but also the similar disease progression to human T2D. However, this type of model is less favored by researchers, probably due to the high cost of colony maintenance and phenotype heterogeneity. In fact, heterogeneity is a major characteristic of human T2D, as indicated by the different susceptibility to obesity and diabetes between ethnic groups. Therefore, with different metabolic traits or rates of T2D progression, sub-strains of polygenic models can be used in the identification of susceptibility genes, supplementary to GWAS (Kluge et al. 2012; Bihoreau et al. 2017)

In response to metabolic stress, β-cells compensate to meet the increased insulin demand by altering β-cell function and mass. Increased β-cell mass is a hallmark of β-cell compensation. A 50-100% increase in β-cell mass was reported in HFD models. Of note, the β-cell mass expansion may contribute but not determine insulin compensation, seeing that increased insulin output precedes the onset of mass adaption and the β-cell decompensation can occur when cell mass is still adapting. Thus, the processes of GSIS in individual β-cells, such as glucose sensing, insulin biosynthesis and exocytosis seem to be the major mechanism of β-cell compensation.

Chen et al. established a novel model for monitoring β-cell compensation *in vivo* by transplantation of fluorescent protein-tagged islets into the eyes of HFD mice, which allows *in vivo* measurement of β-cell calcium dynamics and β-cell volume (Chen et al. 2016). Their observations about the trajectories of insulin secretion, calcium dynamics and β-cell mass during prediabetes reflect that calcium-triggered GSIS is associated with insulin compensation rather than β-cell volume (Chen et al. 2016). Therefore, the regulation of β-cell secretory function should be a primary approach to maintain β-cell compensation.

Regarding the mechanisms underlying β-cell mass adaption, current evidence favors the notion that β-cell function primarily responds to the insulin resistance, and the corresponding increase in glucose metabolism initiates β-cell regeneration (Prentki and Nolan 2006; Mezza et al. 2014). It has been established in glucose infusion models that exogenous glucose triggers β-cell proliferation. Results derived from β-cell-specific IR/IGF knockout models reveal that insulin receptor signaling is also critical for β-cell compensatory proliferation (Shirakawa et al. 2017). In addition to glucose and insulin, GLP-1, growth factors and hormones are also linked to β-cell proliferation (Bernal-Mizrachi et al. 2014).

Moreover, neogenesis and re-differentiation have been proposed as mechanisms in human β-cell compensation (Butler et al. 2003a). In adult mouse models, genetic lineage tracing results indicate that multipotent progenitor cells associated with ductal cells can be differentiated into β-cells after pancreatic injury (Xu et al. 2008). Neogenesis can also be achieved through intra-islet or acinar to β-cell trans-differentiation in response to severe loss of β-cells or stimulation by GLP-1 (Thorel et al. 2010; Ye et al. 2015; Lee et al. 2018). However, whether the neogenesis/trans-differentiation truly occurs in obesity and prediabetes requires validation in β-cell compensation models.

Lastly, β-cell dedifferentiation is proposed as a link between proliferation and dysfunction. Recent evidence from single-cell sequencing revealed an inverse correlation between β-cell function and the potential for proliferation (Xin et al. 2018). Combined with the fact that transcription factors like FoxO1 have opposite effects on β-cell function and proliferation, dedifferentiation may be an indicator of transition from compensation to decompensation, leading to increased number of β-cells but decreased functional mass.

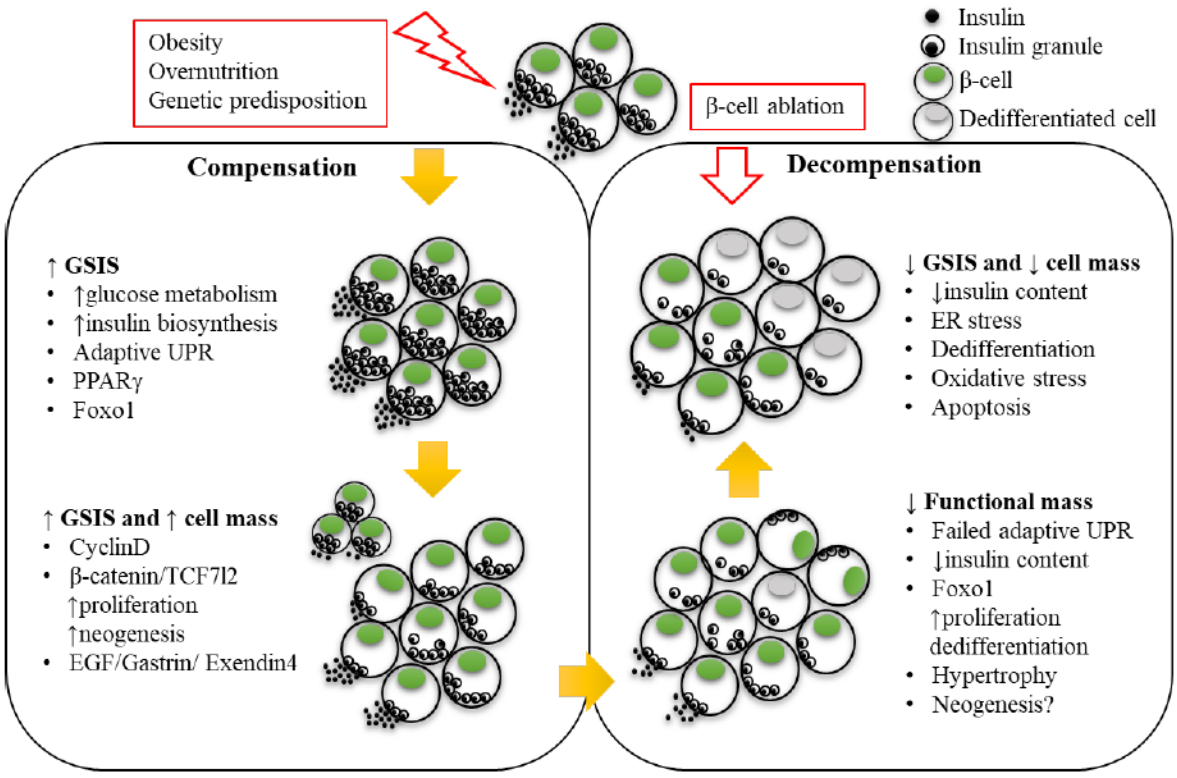

Figure 1-5 Proposed mechanisms of β-cell compensation in early type 2 diabetes. A summary of events that occur during the progression of β-cell compensation to decompensation is presented, see the text for a more detailed description; ↑, increased; ↓, decreased.

Table 1-2. Summary of rodent models for β-cell compensation

Induction Mechanism	Model	Metabolic Features	β-cell Compensation		Possible Mechanism
			Function	Mass	
Obese Monogenic Model	*ob/ob* mice ZF rat	Obesity, ↑insulin, euglycemia	Yes	Yes	Adaptive UPR, PPARγ2, ↑proliferation
	db/db mice ZDF rat	Obesity, ↑insulin, IGT, hyperglycemia	No	↓β-cell/islet ratio	↑glucose metabolism, oxidative stress, dedifferentiation, apoptosis
Transgenic Model	hIAPP knock-in	↑body weight, insulin resistance, ↓insulin, hyperglycemia		No	ER stress, ↑↑apoptosis, ↑proliferation/neogenesis
	$IR^{-/-}$	(liver/muscle) insulin resistance, IGT, ↑insulin	Yes	Yes	Irs-FoxO1 related proliferation
		(β-cell) mild IGT; ↓insulin	No	No	
	FoxO1 overexpression	↑ glucose tolerance	Yes	Yes	↑proliferation, ↑antioxidative function
Experimentally Induced Model	HFD	↑body weight, ↑caloric intake, IGT, ↑insulin, insulin resistance	Yes	Yes	Adaptive UPR, ↑proliferation, ↑neogenesis, ↑PPARγ, ↑CyclinD1/2, ↑β-catenin/TCF7L2
	STZ/Alloxan HFD	IGT, insulin resistance, ↓insulin, hyperglycemia		β-cell mass restoration	(EGF, gastrin and exendin-4) ↑proliferation, ↑neogenesis, ↑re-differentiation

	Pancreatectomy	↓insulin, hyperglycemia (old or obese mice/rats)	No	β-cell mass restoration	↑cell dedifferentiation, ↑proliferation (not in old animals), ↓insulin content and biosynthesis
Polygenic Model	GK rat	↓body weight, ↓insulin, hyperglycemia	No	No	β-cell growth retardation, oxidative stress
	NZO mice OLETF rat UCD-T2DM rat	Obese, ↑insulin, IGT, late onset of hyperglycemia	Yes	Yes	↑insulin content, ↑proliferation
	Sand rat Nile rat	Obese, ↑insulin, IGT, late onset of hyperglycemia	Yes	Yes	(Diabetic β-cells) ↓GCK, ↓GLUT2, ER stress, β-cell hypertrophy

↑, increased; ↓, decreased; ZF, Zucker fatty; ZDF, Zucker diabetic fatty; IGT, impaired glucose tolerance; UPR, unfolded protein response; PPARγ, peroxisome proliferator-activated receptor gamma; hIAPP, human islet amyloid polypeptide; IR, insulin receptor; Irs, insulin receptor substrate; FoxO1, forkhead box protein O1; HFD, high-fat diet; STZ, streptozotocin; EGF, epidermal growth factor; GK, Goto-Kakizaki; NZO, New Zealand obese; OLETF, Otsuka Long-Evans Tokushima Fat; UCD-T2DM, UC Davis type 2 diabetes mellitus; GCK, glucokinase; GLUT2, glucose transporter 2.

1.4 Metformin and T2D prevention

Metformin is a biguanide anti-diabetic drug that has been used as first-line pharmacological therapy for type 2 diabetes for decades (Bailey 1992; Bailey and Turner 1996). The beneficial clinical effects of metformin on glucose control are associated with less weight gain and fewer hypoglycemic cases compared to insulin (UKPDS 1998).

1.4.1 Metformin in T2D prevention

As a high-risk state and an early stage of T2D, prediabetes was suggested to be preventable with lifestyle modification and drug treatment enacted in clinical trials (Knowler et al. 1995). However, the results of early intervention trials were inconsistent due to small sample sizes and poor study designs. In 2002, a large randomized trial of diabetes prevention was conducted in the US. The Diabetes Prevention Program (DPP) enrolled 3234 participants with prediabetes (see diagnostic criteria in Table 1-1) and randomized them into 3 groups: lifestyle modification with a target of 7% weight loss and active physical activity, metformin treatment or placebo. After 2.8-year follow-up, although the adherence to lifestyle intervention was lower than the other two groups, the lifestyle change and metformin reduced the incidence of T2D by 58% and 31%, respectively (Knowler et al. 2002). With similar calorie intake and physical activity levels, participants taking metformin showed a modest weight loss compared with the placebo group, indicating metformin is effective in preventing in T2D, although less so than intensive lifestyle intervention (Knowler et al. 2002). In the 10-year follow-up of the DPP, the reduced body weight and cumulative incidence of T2D were sustained in the metformin group (Knowler et al. 2009). At 15 years after randomization, the cumulative incidence of diabetes in placebo, lifestyle and metformin groups were 62%, 55% and 56%, respectively. Over the entire study, the incidence

rates were 27% and 18% lower for lifestyle and metformin compared with placebo, respectively (Diabetes Prevention Program Research Group 2015). Although metformin is recommended for people with prediabetes, particularly those with HbA1C higher than 6.1% (Nathan et al. 2007), the use of metformin is low due to the concerns of side-effects and a reluctance to use drugs in prediabetes management (Tseng et al. 2017). The data collected from the DPP indicates that metformin can delay or possibly prevent the progression of T2D in the long term when added to lifestyle modification (Aroda et al. 2017). Therefore, metformin treatment can be a cost-effective option for second-line treatment for prediabetes when intensive lifestyle change is not feasible, or the adherence to such interventions is low.

1.4.2 Actions of metformin in liver

The glucose-lowering effect of metformin is thought to be through decreasing endogenous hepatic glucose output by suppression of hepatic glucose production (Hundal et al. 2000). Metformin is not metabolized in the liver. Uptake of metformin from the circulation into hepatocytes is through organic cation transporter 1 (OCT1) (Koepsell et al. 2007). Although in the 1970s it was speculated that the glucose-lowering effect of metformin was related to mitochondrial respiration, it was not until 2000 that two studies reported direct evidence of metformin inhibiting the mitochondrial respiratory chain complex, which leads to a reduction of ATP and increases in the AMP/ATP ratio (El-Mir et al. 2000; Owen et al. 2000). The 5' AMP-activated protein kinase (AMPK) is a sensor of the cellular energy state, and phosphorylated AMPK can activate a serial of downstream actions (Zhou et al. 2001). Acetyl-CoA carboxylase (ACC) is a well-known target of AMPK. Phosphorylated ACC inhibits the generation of malonyl-CoA, which is a precursor in fatty acid synthesis as well as an inhibitor of the

transporter for mitochondrial oxidation, by which metformin promotes fatty acid oxidation and suppresses lipid synthesis (McGarry et al. 1978; Zhou et al. 2001). AMPK is also found to regulate expression of phosphoenolpyruvate carboxykinase (PEPCK) and glucose-6 phosphatase (G6Pase), critical genes in hepatic glucose production (Shaw et al. 2005). Expression of PEPCK and G6Pase is under control of cAMP response element-binding protein (CREB), CREB co-activator 2 (CRCT2) and formation of CREB-CRCT2-CBP complex. The complex binds on the cAMP element site and increases transcription of the PPARγ coactivator 1-alpha (PGC-1α), a transcription factor of PEPCK and G6pase (Koo et al. 2005; Ravnskjaer et al. 2007). In the fasting state, glucagon promotes liver glucose production by activating adenylyl cyclase (AC), which triggers cAMP-protein kinase (PKA) signaling pathway and stimulating CREB-coactivator regulated PGC1α expression leading to PEPCK and G6Pase transcription (Dentin et al. 2008). Insulin, under postprandial conditions, switches off the gluconeogenesis mode by inhibiting these transcriptional factors via Akt signaling (Cho 2001; He et al. 2009). AMPK has demonstrated the same inhibitory effect on gluconeogenesis via decreasing CRCT2 and PGC1α (Zhou et al. 2001; He et al. 2009).

In addition, metformin is reported to act independently of AMPK (Foretz et al. 2010). In mice lacking AMPK, metformin still exerts comparable glucose-lowering effects to wild-type controls, and AMPK knockout hepatocytes exhibit a robust counteractive response to increased cAMP (Foretz et al. 2010). Moreover, 5- aminoimidazole-4-carboxamide-1-β-D-ribofuranoside (AICAR), an analog of AMP showed potent inhibitory effect on glucose production in hepatocytes (Foretz et al. 2010). The results reflect that metformin-induced AMPK activation is secondary to inhibition of mitochondrial respiration. AMP *per se* is essential in reducing hepatic glucose output, which is thought to be by inhibition of AC and cAMP production (Miller et al.

2013). Furthermore, a recent study suggested that metformin targets and inhibits mitochondrial glycerol phosphate dehydrogenase (mGPDH), resulting in changed redox state and reduced glucose production (EGP) (Madiraju et al. 2014). Figure 1-6 shows the proposed mechanism of metformin actions on liver cells.

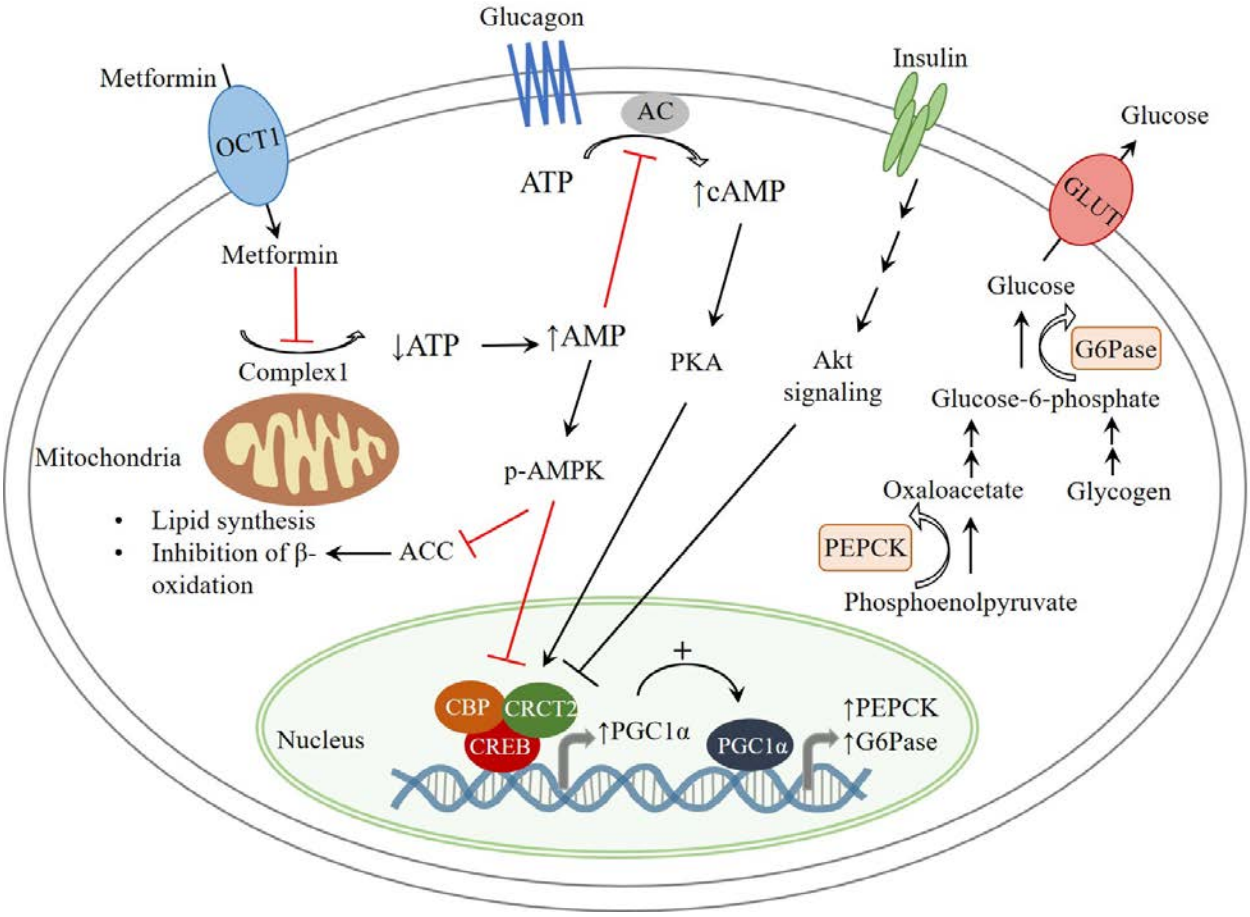

Figure 1-6 Mechanism of metformin actions in liver. Metformin is transported into liver cells through OCT1. Metformin alters the cell energy state (AMP/ATP) by inhibiting mitochondrial respiratory chain complex I, resulting in suppression of hepatic glucose production and lipid synthesis. The metformin action is partially through the AMPK pathway, including inhibition of ACC and transcription coactivators of gluconeogenic genes. Besides, increased AMP counteracts glucagon effect on gluconeogenesis from the upstream. Recent evidence attributes the glucose-lowering effect of metformin to both the AMPK-dependent and independent pathways in the liver.

1.4.3 Effects of metformin on β-cells

Some studies reveal that metformin treatment *in vitro* protects β-cells from glucolipotoxicity by reducing basal insulin secretion while restoring stimulated GSIS (Lupi et al. 1999; Patanè et al. 2000; Marchetti et al. 2004; Piro et al. 2012). Concomitantly with enhanced GSIS, metformin exposure also increases β-cell insulin content and the number of mature insulin granules, and alleviates oxidative stress induced by lipotoxicity (Marchetti et al. 2004; Piro et al. 2012). On the other hand, there is contrary evidence suggesting an inhibitory effect of metformin on β-cell insulin secretion (Leclerc et al. 2004; Lamontagne et al. 2009, 2017). Metformin *in vitro* is shown to cause metabolic deceleration in β-cells with reduced glucose oxidation and ATP production, which then activates AMPK and attenuates insulin secretion especially at half-maximal glucose concentrations (Leclerc et al. 2004; Lamontagne et al. 2009; Gelin et al. 2018). AMPK, being the sensor of cellular energy state, is thought to be the mediator of metformin action (Leclerc et al. 2004); however, pharmacological activation of AMPK does not always lead to suppression of GSIS (Langelueddecke et al. 2012; Fu et al. 2013). Therefore, the impact of metformin on β-cell GSIS remains controversial.

Other than GSIS, metformin has been reported to regulate β-cell mass. Tajima et al. reported that, in the HFD-induced prediabetic mouse model, metformin treatment suppressed the HFD-induced β-cell mass compensation with a lower incidence of cell proliferation (Tajima et al. 2017). Moreover, the *in vitro* experiments in the study link the inhibition of glucose-induced proliferation to AMPK activation (Tajima et al. 2017). Conversely, it has been shown that loss of liver kinase B1 (LKB1), a direct activator of AMPK, in β-cells decreases p-AMPK and upregulates mammalian target of rapamycin (mTOR), leading to β-cell mass expansion *in vivo* (Fu et al. 2009; Granot et al. 2009). Despite that, the question remains as to whether the reduced

proliferation is attributable to the improved overall glucose regulation with metformin or occurs as a result of direct effect of preventing the compensatory β-cell responses.

1.4.4 Effects of metformin on the gastrointestinal tract

A recent study identified a metformin-activated gut-brain-liver axis that regulates hepatic glucose production (Duca et al. 2015). Intraduodenal infusion of metformin, which bypassed the portal vein, activated duodenal AMPK and lowered hepatic glucose production, which was completely reversed by co-infusion with GLP-1 receptor antagonist or PKA inhibitor (Duca et al. 2015). The findings suggest that metformin reduces hepatic glucose production via activation of AMPK, GLP-1 receptor and PKA in the intestine. Also, blocking afferent vagal signaling attenuated the effect of metformin infusion (Duca et al. 2015). This classic study reveals the duodenal-neuronal network-mediated action of metformin.

Besides GLP-1 receptor activation, metformin treatment has been documented to increase plasma GLP-1 concentration (Maida et al. 2011; Bahne et al. 2018). The elevated plasma GLP-1 with metformin is associated with enhanced GLP-1 secretion from intestinal L postprandial cells *in vivo* (Mulherin et al. 2011; Kim et al. 2014; Bahne et al. 2018), which is linked to increased β-cell GSIS and growth of β-cell mass (Tourrel et al. 2001; Shigeto et al. 2015).

Lastly, a growing body of evidence suggests that metformin treatment alters the gut microbiota in T2D patients (Forslund et al. 2015; Wu et al. 2017). By shifting the microbiota structure through the enrichment of short-chain fatty acid (SCFA)-producing bacteria, e.g. *Escherichia* and *Bifidobacterium bifidum* (de la Cuesta-Zuluaga et al. 2017), metformin treatment promotes SCFA production, contributing to gut barrier function and glucose regulation (Forslund et al. 2015; Chambers et al. 2018). Besides, Bauer et al. showed that, in accompanied

with increased abundance of microbiota *Lactobacillus*, metformin increased the expression of sodium-glucose cotransporter-1(SGLT1) and GLP-1 receptor in the small intestine and, improving intestinal glucose sensing and reducing glucose production (Bauer et al. 2018). Moreover, bile acid and the farnesoid X receptor (FXR) signaling have been reported to mediate gut microbiota-related metabolic benefits of metformin (Lien et al. 2014; Sun et al. 2018). Taken together, the gastrointestinal tract serves as an essential target of metformin.

Chapter 2. General hypothesis and objectives

2.1 Rationale

T2D is a chronic metabolic disease characterized by high blood glucose resulting from insulin resistance and β-cell dysfunction. As reviewed in chapter 1.1, the natural history of T2D consists of a euglycemic phase with reduced insulin sensitivity, a prediabetic stage with a moderate rise of glucose, followed by a hyperglycemic phase, which is overt T2D (Weyer et al. 1999). Studies have demonstrated that β-cells compensate for insulin resistance by enhancing insulin secretion in the first stage. Impairment of compensatory secretion leads to progression of T2D (Meigs et al. 2003). It is well accepted that enlarged β-cell mass and improved secretory function contribute to the β-cell compensation, but the mechanisms governing these adaptations are not clear. Because of limited interventions allowed in human research and the restricted sources of islet samples, especially islets from prediabetic donors, animal models for prediabetes are an indispensable tool for investigation of the mechanisms underlying β-cell compensation.

In an attempt to better integrate and interpret the information obtained from different models with distinct causes of T2D, I reviewed models commonly used in studies of β-cell compensation and compared with results from human studies (chapter 1.3). Among those, a polygenic model for spontaneous T2D, the Nile rat stands out for the prolonged disease progression and similar causes of T2D to humans. Nile rats develop T2D naturally when fed with a standard laboratory diet, which can be prevented or delayed by a low-energy high-fiber diet intervention (Chaabo et al. 2010). Studies have shown that Nile rats recapitulate the development of human T2D with the presence of euglycemia concomitant with hyperinsulinemia at 2 months progressing to IFG at 6 months followed by the onset of overt diabetes at 12 months (Noda et al. 2010; Yang et al. 2016). This age- and diet-related T2D development allows researchers to target specific stages of

T2D and investigate the relevant events that happen during that period. The previous study demonstrates β-cell dysfunction at 12 months concurrently with impaired insulin secretion and biosynthesis (Yang et al. 2016), but less is known about the earlier stages. An increasing trend of β-cell mass is found in Nile rats before the onset of IFG (Yang et al. 2016), indicating β-cell mass adaptation. The pronounced rise in insulin secretion suggests a possible role of β-cell functional compensation in addition to cell mass.

The Diabetes Prevention Program showed that metformin is effective in preventing T2D in addition to lifestyle change (Knowler et al. 2002). Metformin is an antidiabetic drug that improves insulin sensitivity mainly via reducing hepatic glucose production and lipid synthesis. It has been shown in mice that long-term treatment with metformin mimics the benefits of caloric restriction through reducing insulin resistance, oxidative damage and inflammation (Martin-Montalvo et al. 2013). Thus, metformin treatment of Nile rats during the compensation stage may reduce the pressure on β-cells to secrete and thereby stop the conversion from β-cell compensation to dysfunction, preventing the onset of T2D. Thus, metformin treatment may also reveal critical changes in β-cells relevant to compensation, particularly when compared with other interventions such as lower energy, higher fibre diets.

2.2 Hypothesis and objectives

Chapter 3 overall hypothesis: The Nile rat is an animal model that demonstrates β-cell compensation and decompensation during the development of T2D.

To address the hypothesis, I will examine:

i. metabolic characteristics at different ages to confirm the model phenotype;

ii. glucose and insulin tolerance and the *in vivo* insulin response of Nile rats at different disease stages;
iii. β-cell secretory function by measuring GSIS of isolated islets at different stages;

To address potential mechanisms involved in compensation and decompensation, I propose two **specific hypotheses**: **a)** The capacity of ER chaperones to properly transport and fold insulin is increased in compensating β-cells, which contributes to insulin secretion; **b)** β-cell mass compensation is associated with increased cell proliferation and neogenesis. To test these hypotheses, I will investigate:

iv. proinsulin secretion and ER chaperone abundance and colocalization with insulin in β-cells as indicators of β-cell function regarding insulin processing;
v. the effect of *in vitro* chemical chaperones treatment on islet insulin secretion;
vi. the possible mechanisms underlying the change in β-cell mass, including proliferation and neogenesis.

Chapter 4 overall hypothesis: As an alternative to diet intervention, early treatment of Nile rats with metformin during the compensation stage will prevent prediabetes in NRs by improving insulin sensitivity and β-cell insulin secretion.

To test this hypothesis, I will examine:

i. the lowest effective dose of metformin able to alleviate glucose intolerance in Nile rats;
ii. the effect of metformin on systemic glucose tolerance, insulin secretion and insulin sensitivity at 13 and 25 weeks when compensation and decompensation occur in NRs fed with Chow diet;

iii. the actions of metformin in the liver, focusing on the AMPK-dependent pathway and the influence on PKA activation in fasting and refeeding states at 13 and 25 weeks;

Given the documented direct effect of metformin on β-cells and beneficial effect through metformin actions on the intestine, I further **hypothesize that: a)** islets from NRs receiving metformin exhibit improved insulin secretion capacity *in vitro*, which can be achieved by administering metformin to naïve islets in culture; **b)** metformin treatment alters the glucose sensing and metabolism of β-cells; **c)** metformin stimulates GLP-1 secretion and restores the gut microbiota to a phenotype typical of lean NR. To examine these hypotheses, I will assess:

iv. static GSIS from isolated islets and the expression of genes related to islet function at 3 and 6 months in control and metformin-treated Nile rats fed Chow;
v. the effect of physiologically achievable and high doses of metformin treatment *in vitro* on β-cell function;
vi. β-cell mass adaptation including proliferation and neogenesis in response to metformin treatment.
vii. GLP-1 secretion and changes in gut microbiota induced by high-fiber diet and metformin interventions in Nile rats.

Chapter 3. β-cell compensation concomitant with adaptive ER stress and β-cell neogenesis in a diet-induced type 2 diabetes model

The following chapter is adapted from a manuscript accepted for publication as follows: Huang H, Yang K, Wang R, Han WH, Kuny S, Sauve Y, Chan CB. **β-cell compensation concomitant with dynamic adaptive pancreatic islet endoplasmic reticulum stress in type 2 diabetes progression**. *Appl Physiol Nutr Metab*. May 2.

3.1 Introduction

Diabetes is a global public health issue. The adult population affected by diabetes was 425 million worldwide in 2017 and this number is expected to reach 629 million by 2045 (Cho et al. 2018). Over 90% of the diabetic population is diagnosed with type 2 diabetes (T2D), which is a chronic metabolic disorder featuring hyperglycemia resulting from insulin resistance and failure of insulin-producing pancreatic β-cells.

In the natural history of T2D, β-cell adaptation or compensation is a major mechanism in preventing or delaying T2D progression. β-cells are capable of adapting to peripheral insulin resistance, which is associated with obesity and impaired lipid metabolism (Neeland et al. 2012), by producing more insulin (Weyer et al. 1999; Festa et al. 2006). Euglycemia can sometimes be maintained for years until the failure of compensation, leading to an increase in blood glucose and the onset of T2D (Tabák et al. 2009; Hulman et al. 2017). Evidence from human studies shows enhanced insulin secretion and expanded β-cell mass in insulin-resistant, non-diabetic subjects, suggesting that both β-cell function and mass are involved in β-cell adaptation (Camastra et al. 2005; Rahier et al. 2008; Hanley et al. 2010); however, due to the limited approaches feasible in human research, the cellular mechanisms of human β-cell adaptation are not clear.

Despite animal models being an indispensable tool in T2D research, not all T2D models are appropriate for studying β-cell compensation. For instance, the classic T2D *db/db* mouse model, which is has a monogenic defect in the leptin receptor, exhibits only a transient adaptation stage followed by early onset of diabetes (Chan et al. 2013). Age, diet and genetic background of the model also affect β-cell phenotype and plasticity observed in the compensation stage (Tschen et al. 2009; Hanley et al. 2010; Burke et al. 2017). To elucidate the molecular basis of β-cell adaptation, a validated animal model that recapitulates human T2D features is required.

Nile rat (NR), *Arvicanthis niloticus*, is a diurnal rodent model of spontaneous T2D. Compared with genetic or chemical-induced models, the NR exhibits a slower progression of T2D when fed a standard chow diet (Chow), which recapitulates human T2D stages from initial hyperinsulinemia through to late-onset hyperglycemia appearing around 12 months of age (Chaabo et al. 2010; Yang et al. 2016; Subramaniam et al. 2018). This progressive T2D can be prevented in NRs fed on a low-energy, fiber-rich (Hfib) diet (Yang et al. 2016). In Chow-fed NRs, the hyperinsulinemia is sustained for months while maintaining euglycemia (Yang et al. 2016), suggesting β-cell adaptation. Also, I found that β-cell mass trends upward in Chow-fed NR during the stage of the early hyperinsulinemia (Yang et al. 2016); however, the mild changes observed in β-cell mass are inadequate to explain the dramatic increase in plasma insulin. Therefore, I speculate that, in addition to β-cell mass, the β-cell function is enhanced as a mechanism of β-cell compensation in NRs.

Our previous study also suggested that β-cell dysfunction in diabetic NRs at 12 months was associated with compromised insulin processing and endoplasmic reticulum (ER) stress (Yang et al. 2016). ER is a membranous cell organelle consisting of cisternae, where the newly synthesized proinsulin is folded into a three-dimensional structure (Price 1992). Increased insulin demand leads

to an overload of proinsulin relative to ER capacity, resulting in unfolded protein accumulation and activation of the ER stress response, also referred to as unfolded protein response (UPR) (Eizirik et al. 2008; Scheuner and Kaufman 2008). Recent evidence has linked early ER stress to β-cell compensation by showing that UPR improves ER capacity, β-cell function, and proliferation (Omikorede et al. 2013; Chan et al. 2013; Sharma et al. 2015). Therefore, I then postulated that the adaptive UPR, as part of the mechanism of β-cell adaptation, is associated with changes in β-cell function and mass.

To validate the NR as a model for β-cell compensation, I first sought to evaluate β-cell function in the context of T2D progression *in vivo* and *in vitro*. NRs fed with Hfib diet were used as healthy controls. I then examined the adaptive events occurring in β-cells including colocalization of ER chaperones involved in insulin processing with insulin, cell proliferation, and neogenesis in order to understand the mechanism of β-cell adaptation.

3.2 Methods and Materials

3.2.1 Animals

Male NRs used in this study were from a colony established at the University of Alberta. Original breeder animals were graciously provided by Dr. L. Smale (Michigan State University). Animals were housed at 21°C under a 14-hour light, 10-hour dark cycle. After weaning at 3 weeks, animals were fed with either high energy, low fiber Chow (Prolab® RMH 2000, 5P06, LabDiet, Nutrition Intl., Richmond, IN) or low energy, high fiber Hfib diet (Mazuri® Chinchilla Diet, 5M01, Purina Mills, LLC, St. Louis, MO) (Table 3-1) (Yang et al. 2016). Rats were fasted for 16 hours with free access to water prior to blood collection and subsequent euthanasia. All animal

studies were approved by the University of Alberta Animal Care and Use Committee (Animal use protocol #00000328) and were conducted in accordance with Canadian Council on Animal Care Guidelines.

Table 3-1: Diet macronutrient distribution and caloric density

Nutrients	Chow	Hfib
Protein, %	19.9	21
Fat, %	10.4	4.1
Carbohydrate, %	50.8	42.5
Fiber, %	3.2	15
Ash, %	6.5	6.9
Metabolizable Energy, kcal/kg	3520	2910

3.2.2 Glucose and insulin tolerance test

Intraperitoneal glucose tolerance (ipGTT) and insulin tolerance tests (ITT) were performed on animals fasted for 16 h and 4 h, respectively. Due to the feral behavior of NRs, animals were anesthetized with isoflurane (Millipore Sigma) during procedures. Glucose and insulin testing involved i.p. injection per kg body weight of 1 g glucose or 1U insulin. Blood glucose was determined using a CONTOUR NEXT blood glucose monitoring system (Bayer Inc., Mississauga, Canada) before (time 0) and 10, 20, 40, 60, 90, 120 minutes after injection. For ipGTT, 100 μL of blood sample was collected from the tail at time 0, 15, 30, 60, 90 for insulin and proinsulin concentrations which were determined by ELISA (Crystal Chem Inc. Downers Grove, IL, USA; ALPCO Diagnostics Inc., Salem, NH).

3.2.3 Fasting blood glucose, plasma insulin concentration, and body mass index

Fasting blood glucose (FBG) was measured from a 1-2 μL tail blood sample using a CONTOUR NEXT blood glucose monitoring system. Animals with an FBG of 5.6 mmol/L or higher were considered hyperglycemic as previously established (Yang et al. 2016). The heterogeneity index, introduced as an indicator of the diversity of FBG phenotype, was calculated by dividing the standard deviation by the mean. Animals were euthanized by Euthanyl injection. Blood and tissue collections were performed as previously described (Yang et al. 2016). BMI, ISI, HOMA-IR, HOMA-B were calculated using the following equations (Yang et al. 2016):

BMI=body weight (kg)/ length form nose tip to base of tail (m^2)

ISI= 2/(1+ (172.1× fasting insulin (μU/L)) × (fasting glucose (mmol/L)/1000)).

HOMA-B= 20 × fasting insulin (μU/L)/ fasting glucose (mmol/L)

3.2.4 Isolation of pancreatic islets and *in vitro* treatment

Pancreatic islets were isolated by collagenase XI digestion (0.5 mg/mL, Millipore Sigma, St. Louis, USA) and purified as described (Salvalaggio et al. 2002; Yang et al. 2016). Isolated islets were cultured overnight in Dulbecco's modified Eagle's medium (DMEM) (Gibco, N.Y., USA) supplemented with 8.3 mM glucose and 10% fetal bovine serum (FBS, Gibco, N.Y., USA).

After overnight recovery, isolated islets from 12-month chow-fed NRs were randomized into three groups and then cultured in fresh medium or medium supplemented with 4-phenyl butyric acid (4-PBA, 20 mmol/L) or tauroursodeoxycholic acid (TUDAC, 2 mmol/L) for 14 hours (Ozcan

et al. 2006). Chemical chaperones 4-PBA and TUDAC were from Calbiochem, San Diego, USA. Islets used for secretion analysis were then subjected to GSIS assay.

3.2.5 Glucose-stimulated insulin secretion (GSIS)

To assess insulin secretion, three isolated islets were incubated in 1mL of DMEM supplemented with different concentrations of glucose from 2.8-22 mM for 90 minutes and then centrifuged at 1500 rpm for 5 minutes. The supernatant (released insulin) was transferred into new tubes and the pellets were lysed using 1mL of 3% acetic acid. Insulin in the supernatant and the pellet was determined by insulin radioimmunoassay (RIA). Insulin release, when expressed as a percentage, was calculated by dividing released insulin by total insulin content (supernatant + pellet). The stimulation index was calculated as the ratio of insulin release (%) at 16.5 mM versus 2.8 mM glucose. Maximal insulin release and half maximal glucose concentration (EC50) were calculated from a sigmoidal dose-concentration plot using GraphPad Prism version 6.0.

3.2.6 Immunofluorescent microscopy

Pancreatic tissues were fixed with formalin. Sections mounted on glass slides were immunostained for insulin, glucagon, ER proteins, ki67, Pdx1 using species appropriate AlexaFluor or HRP-conjugated secondary antibodies as previously described (Yang et al. 2016). Antibody details and staining conditions are listed in Table 3-1. For ER protein staining, slides were visualized using a Wave FX spinning disk confocal microscope (Quorum Technologies Inc., Guelph, ON, Canada); colocalization and staining intensity were analyzed using Volocity 6.0 (PerkinElmer) as previously described (Yang et al. 2016). For ki67, Pdx1, peroxidase-based staining, images were obtained using a Zeiss Axio Imager Z1 with Axio Vision 4.5 (Carl Zeiss

Micro Imaging GmbH, Germany) and quantified with ImageJ (NIH, Bethesda, MD, USA). In the analysis of β-cell neogenesis, insulin-positive pancreatic duct- or acinar-associated cells or cell clusters that had no more that four cells were classified as "neogenic" β-cells (Okamoto et al. 2006; Hanley et al. 2010). Overall β-cell neogenesis was estimated as the percentage of the neogenic β-cell area to total pancreatic section area.

Table 3-2: Antibodies and dilutions used in immunofluorescent microscopy and western blot

Antibody	Source	Dilution	Incubation Condition
Guinea Pig Anti-Insulin	A0564, Dako, Burlington, ON, Canada	1:200	4°C, overnight
Mouse Anti-Glucagon	ab10842, Abcam, Cambridge, UK	1:200	4°C, overnight
Rabbit Anti-PDI	3501, Cell Signaling Technology, Danvers, MA, USA	1:200	4°C, overnight
Rabbit Anti-ERp44	3798, Cell Signaling Technology, Danvers, MA, USA	1:200	4°C, overnight
Rabbit Anti-ERp72	5033, Cell Signaling Technology, Danvers, MA, USA	1:200	4°C, overnight
Rabbit Anti-Ki67	Ab15580, Abcam, Cambridge, UK	1:150	4°C, overnight

Anti-Pdx-1	Dr. Wright (University of Vanderbilt, Nashville, TN, USA)	1:800	4°C, overnight
Rabbit Anti-caspase3	9665, Cell Signaling Technology, Danvers, MA, USA	1:500	4°C, overnight
Rabbit Anti-caspase12	3282, BioVision, Milpitas, CA, USA	1:200	4°C, overnight
Mouse Anti-CHOP	2895, Cell Signaling Technology, Danvers, MA, USA	1:500	4°C, overnight

3.2.7 Semi-quantitative real-time PCR

Total RNA from isolated islets was extracted with TRIzol reagent (Millipore Sigma) and cDNA was synthesized with a QuantiTect reverse transcription kit (QIAGEN, Mississauga, ON, Canada) according to the manufacturer's specifications. Real-time PCR was performed using an SYBR green qPCR Mastermix (QIAGEN) and Rotor Gene 6000 Real-time PCR machine (Corbett Research). q-PCR data was analyzed using the delta Ct method (Livak and Schmittgen 2001). Target gene expression was normalized to β-actin. Due to unknown sequences of NR, primers listed in Table 3-2 were designed in regions conserved among mammalian species. Primers for detecting Atf4 mRNA in NR were designed in a region 100% conserved between Rat (NM_024403.2) and house mouse (NM_009716.3). Atf6 primers were designed in 100% conserved regions between human (NM_007348.3), House mouse (NM_001081304.1) and Rat (NM_001107196.1). Xbp1 primers were designed in 100% conserved regions between human (NM_005080.3), Rat (NM_001004210.2) and house mouse (NM_013842.3). The forward primer

of spliced Xbp1 spanned the splice site, while forward primer of unspliced Xbp1 lay within the splice site. Both spliced and unspliced isoforms shared the same reverse primer. Specificity of primers were checked with BLASTN 2.5.1+.

Table 3-3: q-PCR primers and annealing temperatures

Gene		Primer*	Annealing Tm (°C)
Atf4	Forward	5'-AACATGACCGAGATGAGCTTCCTG-3'	56
	Reverse	5'-AAGTGCTTGGCCACCTCCA-3'	
Atf6	Forward	5'TGCTCTGGAACAGGGCTC-3'	56
	Reverse	5'ATGGACACCAGGATCCTCCA-3'	
spliced *Xbp1*	Forward	5'-CTGAGTCCGCAGCAGGT-3'	56
	Reverse	5'-GGTCCAACTTGTCCAGAATGCC-3'	
Xbp1	Forward	5'-AGTCCGCAGCACTCAGACTA-3'	56
	Reverse	5'-GGTCCAACTTGTCCAGAATGCC-3'	
β-Actin	Forward	5'-TATCCTGGCCTCACTGTCCA-3'	56
	Reverse	5'-AAGGGTGTAAAACGCAGCTCA-3'	

3.2.8 Western blot analysis

Freshly isolated islets were washed with PBS and then lysed in RIPA buffer (30 µl per 50 islets) supplemented with protease inhibitors. Islets were triturated on ice until well lysed. Protein concentration was measured by bicinchoninic acid assay (BCA). Protein sample was diluted into a final concentration at 2µg/µl with RIPA buffer and SDS loading buffer, boiled at 100°C for 5 minutes, and cooled on ice. About 60µg of protein was loaded for each sample. Proteins were separated on 10% SDS-PAGE gels and transferred to nitrocellulose membrane. Membranes were blocked for 1 hour with 5% skim milk in TBS (20 mM Tris, 137 mM NaCl, pH

7.6) with 0.1% Tween-20 and probed with antibodies for CHOP, caspase 3, caspase 12 and β-actin (see Table 3-1 for antibody details and incubation conditions). Blots were developed using ECL (ThermoFisher Scientific) and imaged with a Bio-Rad ChemiDoc MP imaging system.

3.2.9 Statistical analyses

For all experiments, data were expressed as the mean ± SEM (or mean + SEM as indicated in the captions) and statistically analyzed with GraphPad Prism version 6.0. One-way or two-way analysis of variance was used, followed by post-hoc Bonferroni's multiple comparisons if significance was reached. ipGTT and ITT were analyzed using a repeated measures two-way ANOVA. Differences were considered significant at $p<0.05$.

3.3 Results

3.3.1 Metabolic characteristics of Nile rats at 2, 6 and 12 months

NRs fed Chow diet display fasting euglycemia at 2 months, moderate increases in glucose at 6 months (FBG heterogeneity index illustrates the phenotypic diversity at this age), and significant hyperglycemia appearing at 12 months (Figure 3-1A-B). Fasting blood glucose is changed by diet intervention and Hfib controls maintain stable blood glucose at all ages (overall $p=0.001$, Figure 3-1A). NRs in the Chow group display early onset hyperinsulinemia (Figure 3-1C). In concomitant with the 50% reduction in whole-body insulin sensitivity (Figure 3-1D), β-cell function (HOMA-B) increases (Figure 3-1E) during this compensatory stage. Body weight at 6 and 12 months is significantly higher in Chow NRs in comparison with age-matched Hfib controls (Figure 3-1F). To better describe this model, data from individual animals are plotted in the five stages proposed

for human diabetes based on glucose and insulin concentrations (Figure 3-1G)(Weir and Bonner-Weir 2004).

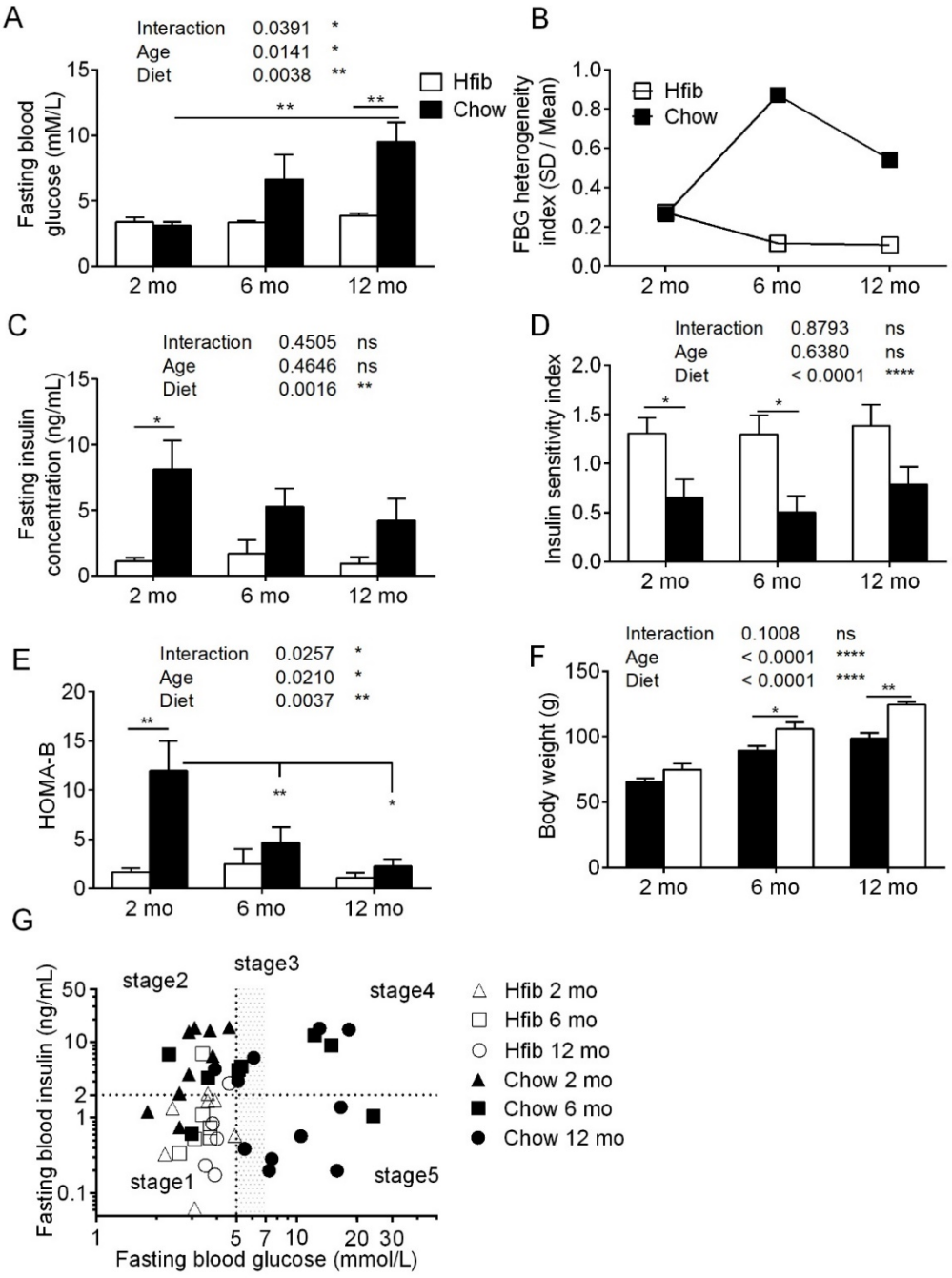

Figure 3-1 Fasting blood glucose and insulin of NR at different T2D stages. A: Fasting blood glucose; B: Heterogeneity index of FBG; C: Fasting plasma insulin; D: Insulin sensitivity index; E: β-cell function index (HOMA-B); F: Body weight; G: Five stages of type 2 diabetes

development in NRs; stage 1=Normal, stage 2=Compensation, stage 3=Decompensation, stage 4= Dysfunction/onset of T2D, stage 5= Overt T2D. Data are presented as mean + SEM. n= 9, 8 and 12 in Chow group at 2, 6 and 12 months, respectively; n= 7 in all Hfib groups. * $p<0.05$ using Bonferroni's multiple comparison test following 2-way ANOVA.

3.3.2 Progression from β-cell compensation to decompensation in NR

To assess β-cell secretory function in NRs, I measured GSIS *in vivo* and *in vitro*. Chow-fed NRs show comparable glucose tolerance compared with Hfib at 2 months (Figure 3-2A), with a 2-fold increase in insulin secretion (overall $p< 0.05$, Figure 3-2B). Plasma proinsulin and the ratio to insulin were measured as an indicator of β-cell function (Mykkänen et al. 1997, 1999). The results show no overall change between Chow and Hfib or timepoints at 2 months (overall $p=0.1$, Figure 3-2C-D). At 6 months, Chow animals present impaired glucose tolerance (overall $p<0.05$, Figure 3-2E), with elevated insulin secretion (overall $p<0.05$, Figure 3-2F). Proinsulin and proinsulin/insulin ratio show marked increases in Chow compared to Hfib group at 6 months (overall diet effect $p<0.001$, Figure 3-2G, H) in Chow NRs, indicating impaired proinsulin processing. Chow-fed animals exhibit impaired insulin tolerance at both 2 and 6 months compared with Hfib (overall $p<0.05$, Figure 3-2I and 2J).

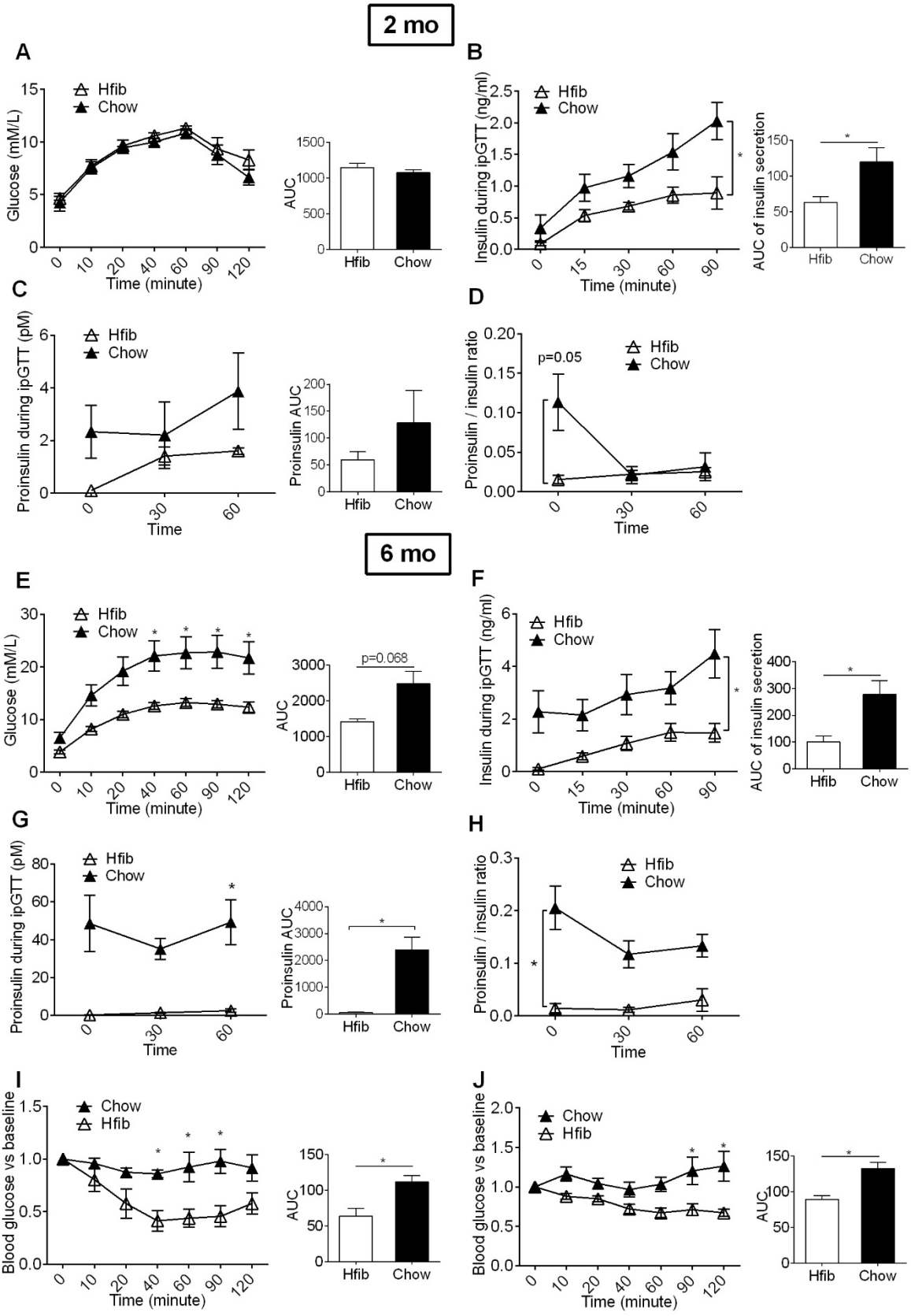
2 mo
A
Hfib
Chow
Glucose (mM/L)
Time (minute)
AUC
B
Insulin during ipGTT (ng/ml)
Time (minute)
AUC of insulin secretion
C
Proinsulin during ipGTT (pM)
Time
Proinsulin AUC
D
Proinsulin / insulin ratio
p=0.05
Time
6 mo
E
Glucose (mM/L)
p=0.068
AUC
F
Insulin during ipGTT (ng/ml)
AUC of insulin secretion
G
Proinsulin during ipGTT (pM)
Proinsulin AUC
H
Proinsulin / insulin ratio
I
Blood glucose vs baseline
AUC
J
Blood glucose vs baseline

Figure 3-2 *In vivo* assessment of glucose homeostasis and β-cell function. A, E: Blood glucose during ipGTT at 2 (A) and 6 (E) months; B and F: Insulin secretion during ipGTT at 2 (B) and 6 (F) months; C,D,G and H: Plasma proinsulin concentrations (C, G) and ratio of proinsulin to insulin concentration (D, H) at 2 (C,D) and 6 (G,H) months; I and J: Percentage change in blood glucose during ITT at 2 (I) and 6 (J) months. AUC data are presented as mean + SEM. n=4, 11 in Chow group at 2 and 6 months, respectively; n= 4-7 in Hfib groups. *$p<0.05$, **$p<0.01$ using Bonferroni's multiple comparison tests following 2-way ANOVA.

In vitro β-cell function was determined by GSIS from intact isolated islets. Although there is no change in the absolute amount of insulin released per islet (Figure 3-3A), at 2 months the insulin release relative to total insulin is augmented particularly at lower glucose concentrations (Figure 3-3B), indicating enhanced responsiveness to physiological concentrations of glucose in Chow islets. This compensation in Chow-fed NRs fails as the animals age, with a significant reduction in insulin secretion (per islet) at 6 and 12 months (Figure 3-3C and 3E) compared to Hfib. The increase in % insulin release in Chow seen at 2 months is diminished at 6 and 12 months (Figure 3-3D and 3F). A 50% decrease in half-maximal glucose concentration in 2-month Chow islets (Figure 3-3G) indicates a left shift of the glucose response. The stimulation index, another indicator of islet function, is slightly decreased in Chow islets (overall $p<0.05$, Figure 3-3H). Total insulin content in islets is markedly reduced with diabetes (12 months, $p< 0.01$, Figure 3-3I).

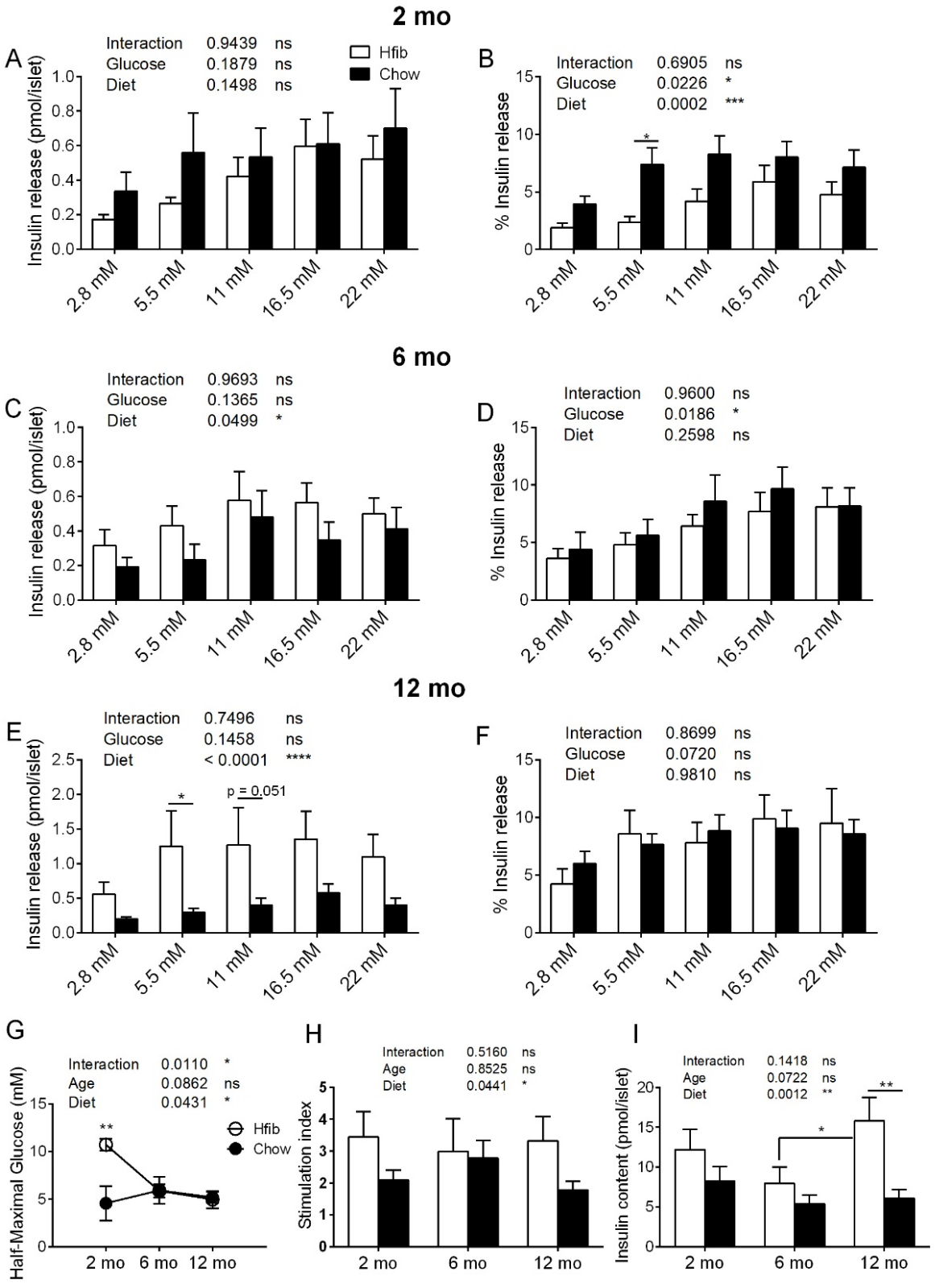
2 mo
A
Interaction 0.9439 ns
Glucose 0.1879 ns
Diet 0.1498 ns
Hfib
Chow
Insulin release (pmol/islet)
2.8 mM
5.5 mM
11 mM
16.5 mM
22 mM
B
Interaction 0.6905 ns
Glucose 0.0226 *
Diet 0.0002 ***
% Insulin release
6 mo
C
Interaction 0.9693 ns
Glucose 0.1365 ns
Diet 0.0499 *
D
Interaction 0.9600 ns
Glucose 0.0186 *
Diet 0.2598 ns
12 mo
E
Interaction 0.7496 ns
Glucose 0.1458 ns
Diet < 0.0001 ****
p = 0.051
F
Interaction 0.8699 ns
Glucose 0.0720 ns
Diet 0.9810 ns
G
Interaction 0.0110 *
Age 0.0862 ns
Diet 0.0431 *
Half-Maximal Glucose (mM)
2 mo
6 mo
12 mo
H
Interaction 0.5160 ns
Age 0.8525 ns
Diet 0.0441 *
Stimulation index
I
Interaction 0.1418 ns
Age 0.0722 ns
Diet 0.0012 **
Insulin content (pmol/islet)

Figure 3-3 *In vitro* islet secretory function analysis. A, C and D: Absolute insulin secreted per islet in GSIS at 2 (A), 6 (C) and 12 (D) months; B, D and F: Glucose-stimulated insulin secretion (GSIS) as percentage of total insulin content; G: Half-maximal glucose (EC_{50}); H: Stimulation index; I: Islet insulin content. Data are presented as mean + SEM. n=9, 8 and 12 in Chow group at 2, 6 and 12 months, respectively; n= 7 in all Hfib groups. *p<0.05, **p<0.01 using Bonferroni's multiple comparison tests following 2-way ANOVA.

3.3.3 ER chaperones in β-cell compensation versus dysfunction

To investigate the role of impaired insulin processing and adaptive ER stress in T2D NRs, I examined three ER chaperones involved in insulin processing: protein disulfide isomerase (PDI), ER resident protein 44 (ERp44) and ER resident protein 72 (ERp72). Increases in PDI are present in β-cells at 2 and 6 months (Figure 3-4A) and demonstrate colocalization with insulin (Figure 3-4B). PDI/insulin colocalization coefficient is proportional to circulating fasting insulin concentration (Figure 3-4E). ERp44 is also upregulated in Chow animals at 2 and 6 months (Figure 3-4A and 4C). ERp72 does not differ between diet groups but significantly declines with age (Figure 3-4A and 4D); however, ERp72 colocalization with insulin is inversely related to fasting blood glucose (12 months, p<0.05, Figure 3-4F). Consistent with the decreased insulin content in diabetic islets (Figure 3-2I), the insulin abundance of β-cells decreases at decompensation stages (Figure 3-4G).

Critical to adaptive UPR, activating transcription factor -4 and -6 (ATF4, ATF6) and XBP1(X-box binding protein, unspliced and spliced) are involved in stimulating expression of ER chaperones, protein foldase and protein degradation machinery (Scheuner and Kaufman 2008). However, mRNA of transcription factors at 2 months are comparable between groups (Figure 3-4H). At 6 months, *Atf4* and *Atf6* show increasing trends between groups (p=0.06 and 0.08 for main effect of diet, respectively, Figure 3-4H). The spliced (s) and unspliced (u) *Xbp1* demonstrate pronounced increases in the Chow group at 6 months (Figure 3-4H).

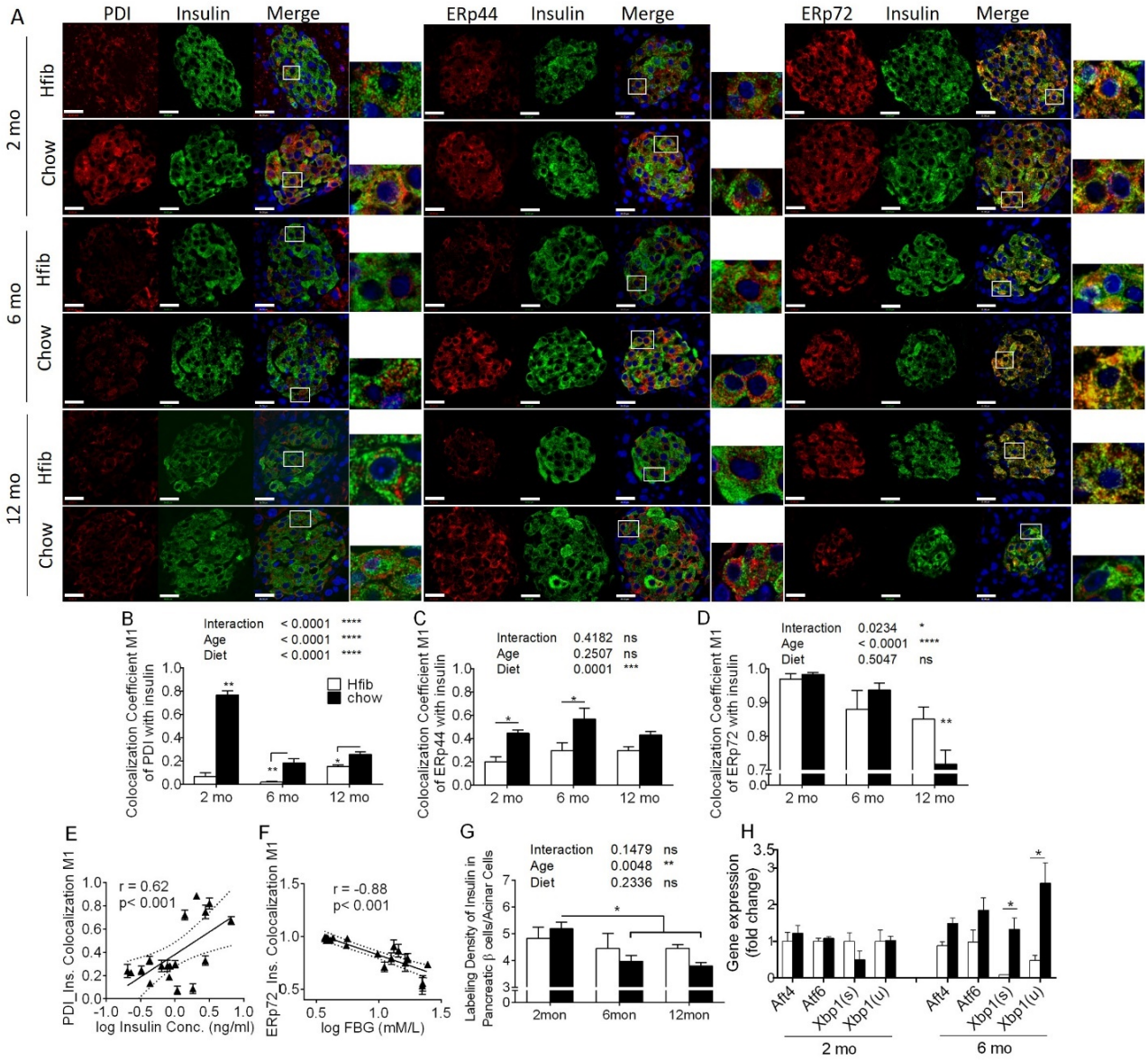

Figure 3-4 Diet and age-related effects on ER chaperones in β-cells. A: Representative images of ER chaperones in islets from 2-12 months; B-D: Colocalization of PDI (B), ERp44 (C) and ERp72 (D) with insulin in β-cells; E: Positive correlation of PDI and blood insulin concentration with dotted lines representing 95% confidence intervals; F: Negative correlation of ERp72 and fasting blood glucose; G: Intensity of insulin in β-cells; H: mRNA expression UPR transcription factors. Data are presented as means + SEM. n=5, 6 and 8 in Chow group at 2, 6 and 12 months, respectively; n=4, 4 and 8 in Hfib group at 2, 6 and 12months. *p<0.05 using Bonferroni's multiple comparison tests following 2-way ANOVA. Scale bar = 20μm.

Chemical chaperones may restore glucose homeostasis by enhancing the adaptive capacity of the ER and reducing ER stress (Ozcan et al. 2006). To examine whether chemical chaperones could restore β-cell function ex vivo, I treated islets from 12-month Chow NRs with 4-PBA and TUDAC. Consistent with data presented in Figure 3-3, Chow islets have defective insulin secretion (Figure 3-5A, B) and reduced insulin content (Figure 3-5C) compared to islets from the age-matched Hfib NRs. 4-PBA and TUDAC treatment do not alleviate the diminished insulin secretion (Figure 3-5A, B) or reduced insulin content (Figure 3-5C) of chow islets.

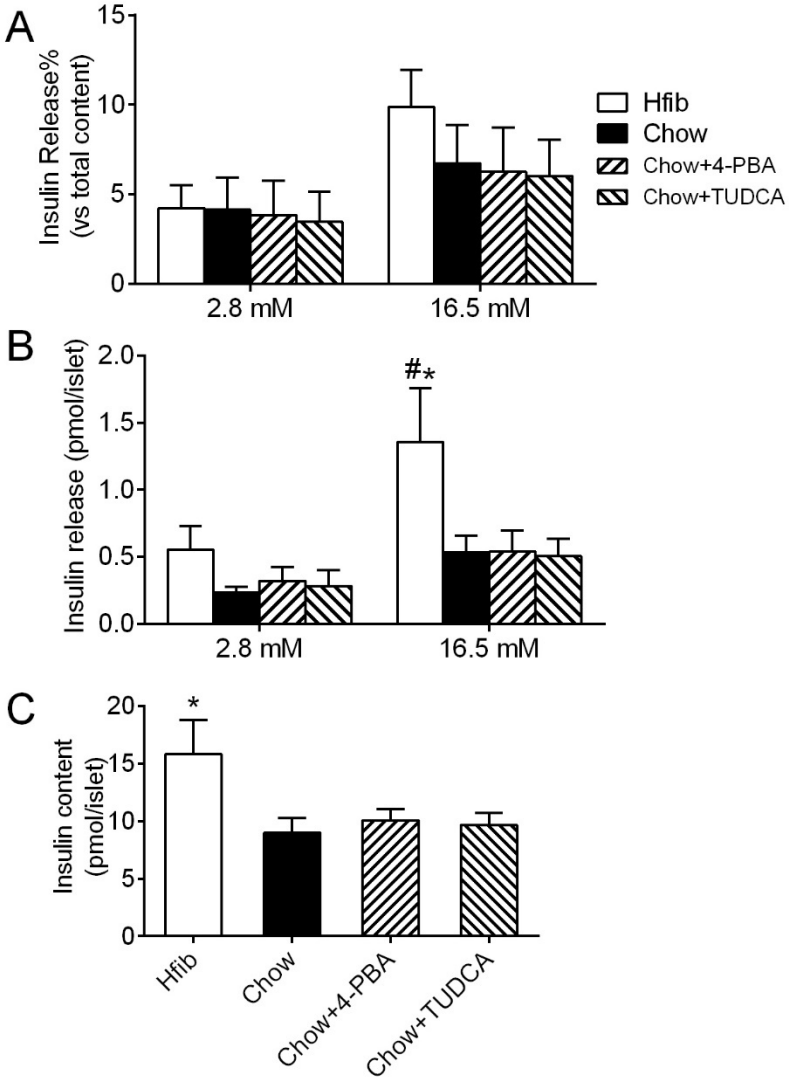

Figure 3-5 *In vitro* treatment of chemical chaperones does not improve islet function. A: Glucose-stimulated insulin secretion (GSIS) as a percentage of total insulin content of islets isolated 12-month NRs; B: Absolute insulin secreted per islet; C: Islet total insulin content. Data are presented as mean + SEM. n=7. #p<0.05 vs 2.8mM, *p<0.05 vs Chow, using Bonferroni's multiple comparison tests following 2-way ANOVA; *p<0.05 using the Kruskal-Wallis test followed by Dunn's multiple comparisons tests.

ER stress can also contribute to β-cell apoptosis and loss of β-cell mass (Eizirik et al. 2008), another feature of human T2D. However, transcription of CHOP, a pro-apoptotic UPR marker, is comparable between groups (Figure 3-6A). The expression of CHOP, active caspase 12 (an ER stress-induced caspase), and caspase 3 (a downstream marker of apoptosis) remain almost undetectable (Figure 3-6B).

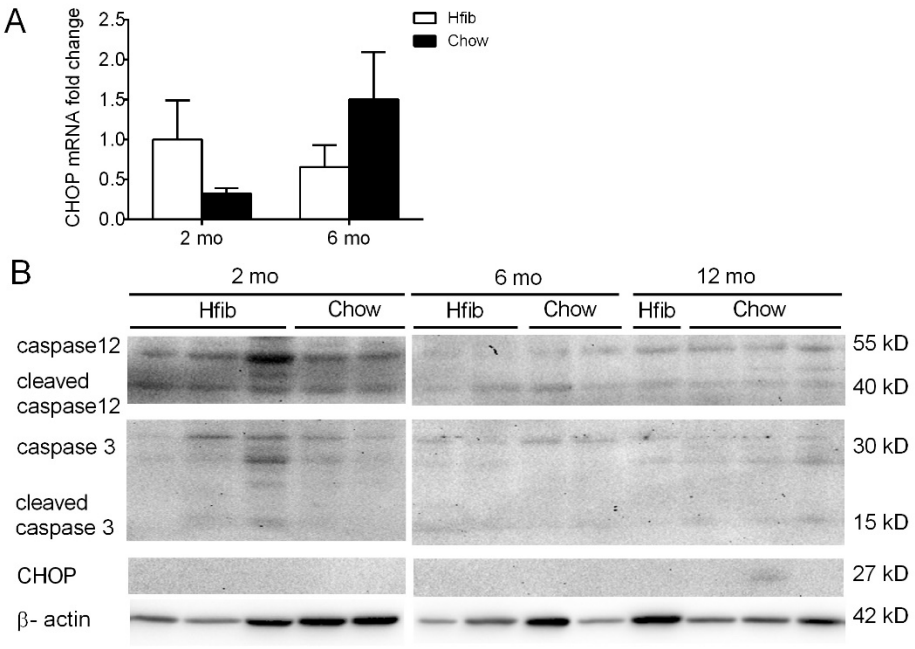

Figure 3-6 CHOP and caspase in islets. A: mRNA expression of CHOP normalized by β-actin; B: caspase3, 12 and CHOP expression in isolated islets. β-actin was used as reference. Data are presented as means + SEM. n=4 for q-PCR. *p<0.05 using Bonferroni's multiple comparison tests following 2-way ANOVA.

3.3.4 β-cell mass compensation by neogenesis but not proliferation

Previous evidence indicated the occurrence of β-cell mass compensation in Chow NRs (Yang et al. 2016), which has been linked to β-cell proliferation and UPR (Sharma et al. 2015). However, using ki67 as a proliferation marker, the occurrence of $ki67^{+}$/$insulin^{+}$ cells in Chow-fed NRs is very low compared with Hfib (overall $p<0.005$, Figure 3-7A, B), indicating a mechanism other than cell replication. Surprisingly, insulin-positive neogenic structures demonstrate a marked increase in chow NRs at the compensation stage (2 mo, $p<0.01$, Figure 3-7A, B), which declined concurrently with the onset of β-cell dysfunction (2 mo vs 12 mo, $p<0.01$, Figure 3-8A, B). Of note, the single β-cells and small β-cell clusters seen in 12-month Chow animals are observed in disrupted islets with α-cells infiltrating the center of the islet (Figure 3-8A), which is consistent with the previous result that α/ β-cells ratio increases with diabetes (Sharma et al. 2015).

A growing body of evidence supports that transdifferentiation occurs in the progression of β-cell dysfunction (Mezza et al. 2014; Cigliola et al. 2016). The existence of cells reacting to both insulin and glucagon (Figure 3-9A), together with co-occurrence of pancreatic and duodenal homeobox 1 (Pdx1), a β-cell-specific transcriptional factor, with glucagon (Figure 3-9B), indicate transdifferentiation in NRs. However, whether it is β-cell dedifferentiation or α-cell-to-β-cell compensatory alteration needs more investigation.

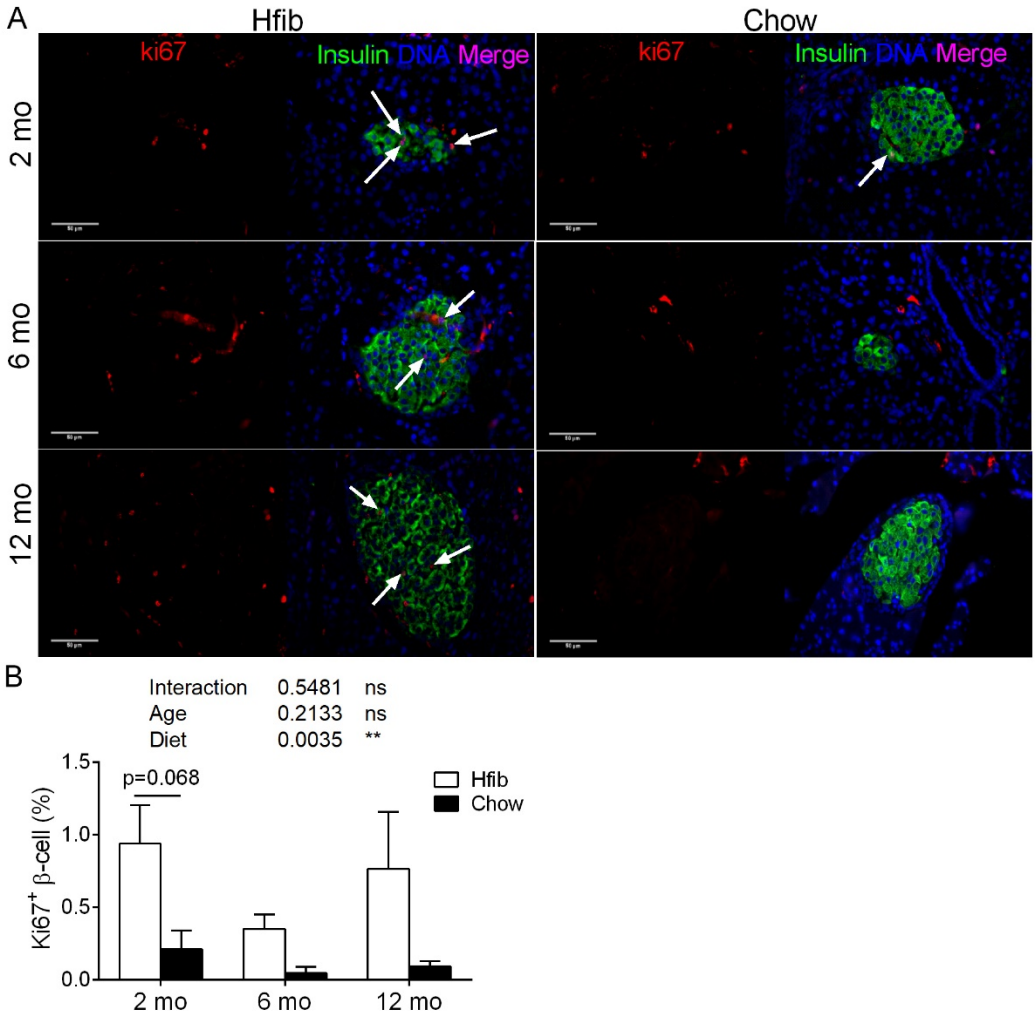

Figure 3-7 β-cell proliferation. A: Representative images of ki67-positive staining in β-cells; B: Quantification of β-cell proliferation as a percentage of all beta-cells. Data are presented as mean + SEM. n=4 in ki67 staining. The analysis was Bonferroni's multiple comparison tests following 2-way ANOVA. Scale bar= 50μm.

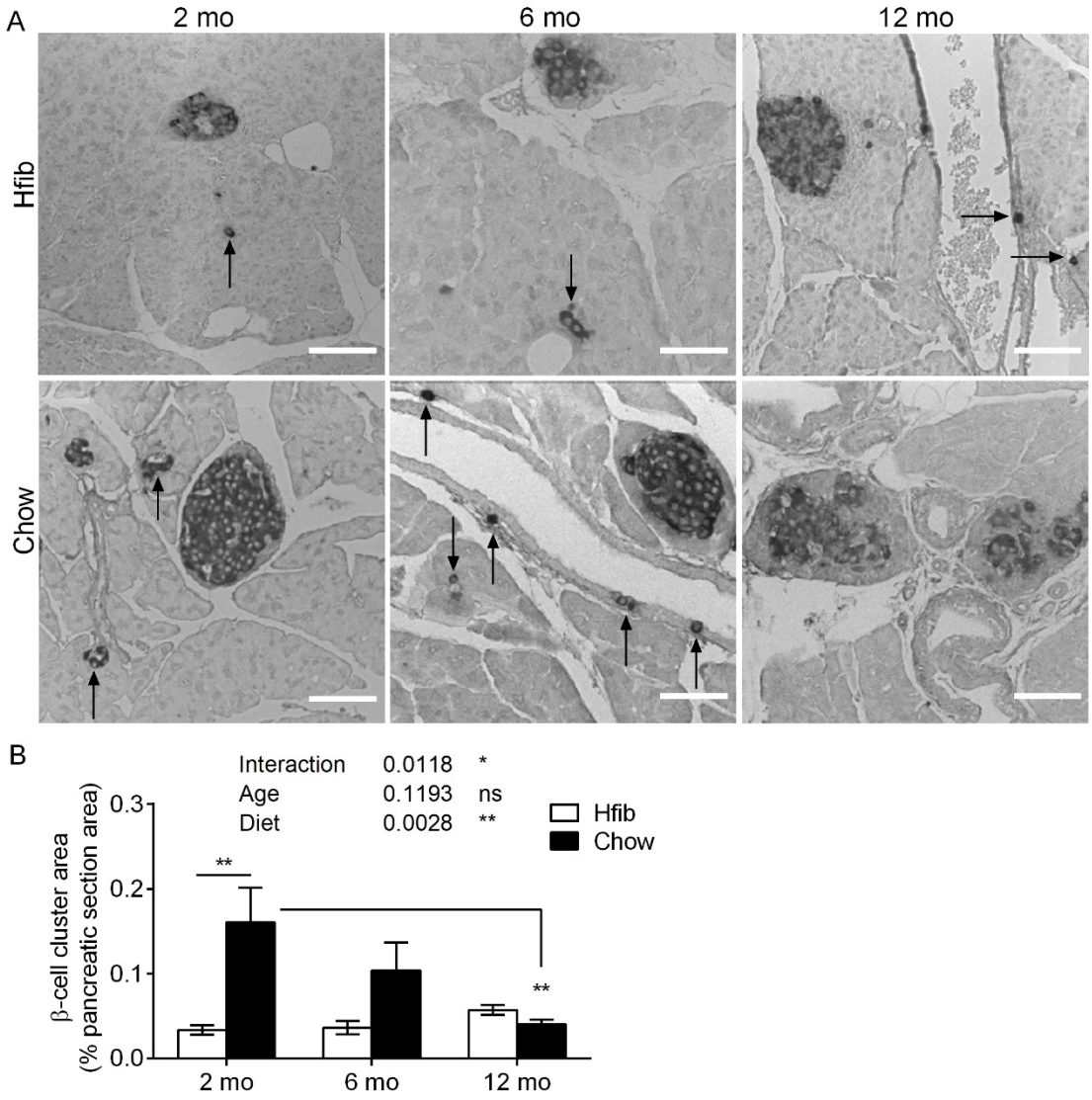

Figure 3-8 Estimate of β-cell neogenesis. A: Representative images of neogenetic β-cell clusters; B: Quantification of neogenic β-cell area. Data are presented as mean + SEM. n=4-6. The analysis was Bonferroni's multiple comparison tests following 2-way ANOVA. Scale bar= 80μm.

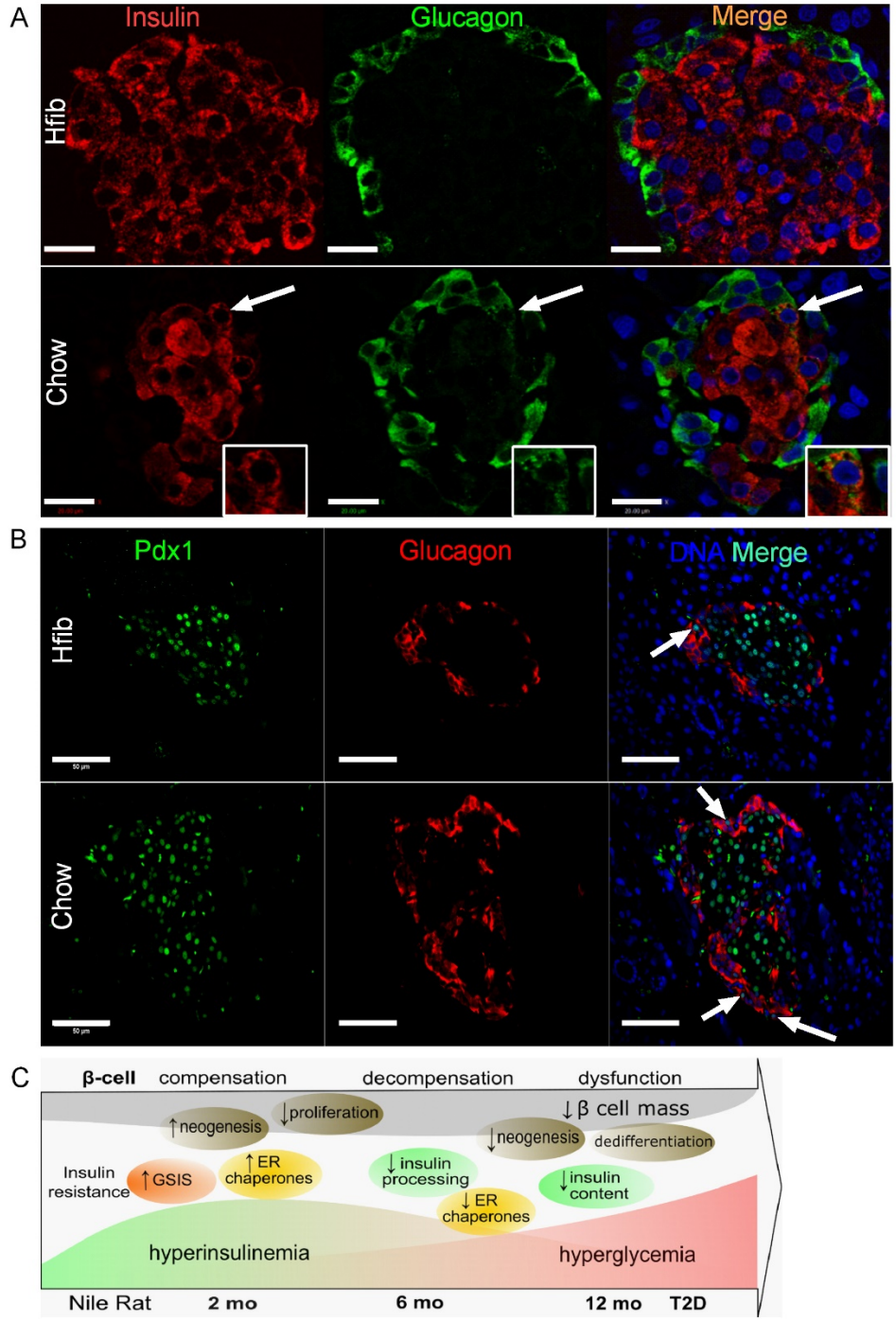

Figure 3-9 Evidence of dedifferentiation after development of diabetes at 12 months. A: Co-occurrence of insulin^{+}/ glucagon^{+} in islet at 12 months; B: Pdx1^{+} /Glucagon^{+} cell at 12 months; C: Summary of events occurring in type 2 diabetes development of NR. Scale bar (A)= 20µm Scale bar (B)= 50µm.

3.4 Discussion

Weir (Weir and Bonner-Weir 2004) characterized the progression of T2D into multiple stages, in which the compensation stage occurs when insulin secretion increases in the face of insulin resistance and blood glucose is kept within the normal range. Animal studies often indicate the stages of T2D models using plasma insulin as the key marker; however, the insulin trajectory in patients with T2D trends upward even after the diagnosis (Tabák et al. 2009; Hulman et al. 2017). Acute GSIS is suggested to be associated with T2D progression regarding glycemic control (Weir and Bonner-Weir 2004; Festa et al. 2006). The present result of elevated GSIS during ipGTT confirms that β-cells from chow-fed NRs at 2 months were compensating for decreased insulin sensitivity while the glucose tolerance was well-maintained. In contrast, glucose tolerance in 6-month NRs was impaired albeit with a pronounced rise in insulin secretion. This phenotype fits the features of the decompensation stage (Weir and Bonner-Weir 2004). The diabetic phenotype is prevented by feeding a high-fiber diet after weaning.

Consistent with insulin secretion *in vivo*, GSIS by isolated islets indicates that Chow β-cells at 2 months were more responsive to glucose than Hfib islets, especially at physiological glucose concentrations (2.8-5.5 mM). However, responsiveness was diminished at 6 months, which together with the disproportional elevation of plasma proinsulin at 6 months demonstrates a functional change in β-cells during the transition from compensation to decompensation stage (Wareham et al. 1999; Pfützner and Forst 2011). Moreover, both islet insulin content and staining intensity *in situ* (Figure 3-2I and Figure 3-4G) began to decline from 6 months, linking the functional change to decreased insulin synthesis or processing.

To meet the increased insulin demand in the context of insulin resistance, β-cells synthesize and process a large amount of proinsulin, which is achieved by a highly active ER (Scheuner and Kaufman 2008). Perturbation in the ER caused by insufficient chaperones can be sensed and corrected by UPR as a protective mechanism of β-cells (Eizirik et al. 2008; Scheuner and Kaufman 2008). In contrast to a recent study showing that UPR is exclusively observed at the decompensation stage (Gupta et al. 2017), the present data suggest adaptive UPR occurs early in the compensation stage. The insulin-colocalized ER resident chaperones showed marked increases in adaptive β-cells (versus Hfib), which then declined concomitant with dysfunction (2 versus 12 months), indicating a positive role of ER chaperones in sustaining β-cell compensation (Omikorede et al. 2013; Chan et al. 2013; Engin et al. 2014; Sharma et al. 2015). Of note, a positive correlation of PDI with circulating insulin concentration was observed in chow-fed NRs. A protective effect of PDI is suggested by a growing number of studies showing PDI overexpression protects β-cell from glucolipotoxicity (Montane et al. 2016), enhances ER-associated degradation (ERAD), and restores insulin production (He et al. 2015; Gorasia et al. 2016). However, no changes were observed regarding transcription factors that are related to ER stress until decompensation at 6 months. A limitation of this study is that nuclear translocation of transcription factors, which could lead to an increase in ER chaperones, could not be directly assessed.

Chemical chaperones are small molecules that stabilize unfolded proteins and prevent aggregation by increasing the interaction of protein and solvent or directly binding to the hydrophobic segment of protein (Welch and Brown 1996). 4-PBA and TUDCA have been shown to alleviate ER stress and restore insulin secretion in prediabetic mice (Ozcan et al. 2006;

Tang et al. 2012) and cell/islets with palmitate-induced defective insulin secretion (Choi et al. 2008; Cadavez et al. 2014). However, I failed to observe any beneficial effect of 4-PBA or TUDCA on islet insulin secretion or content. One explanation is that unlike the insulin inhibition due to acute glucose fusion or palmitate induction, β-cells in T2D islets have already demonstrated severe persistent abnormalities like dedifferentiation, which cannot be alleviated by chemical chaperones treatment alone.

Given that chronic ER stress also induces β-cell apoptosis as part of the pathogenesis of β-cell dysfunction (Negi et al. 2012), the diminished ER chaperones observed at 12 months may imply activation of maladaptive UPR. However, I did not detect any change in CHOP, an apoptotic UPR transcription factor (Rasheva and Domingos 2009), or caspase 12. To better understand ER chaperones and their regulation with diabetes progression, a thorough evaluation of UPR regulators is necessary at different stages.

Our previous study showed an increasing trend in β-cell mass during the compensation stage (Yang et al. 2016), which is another feature of β-cell compensation (Weir and Bonner-Weir 2013). Current evidence favors the concept that β-cells proliferate in response to enhanced glucose metabolism during compensation (Stamateris et al. 2013; Sharma et al. 2015) and UPR is suggested as part of the mechanism (Sharma et al. 2015); however, in this model, β-cell proliferation rate decreased in Chow NRs at all ages. This is supported by single β-cell sequencing results showing that β-cells are less likely to proliferate under the high workload demanded by insulin biosynthesis (Xin et al. 2018). An inverse relationship of β-cell function and proliferation is demonstrated in immortalized β-cell lines (Scharfmann et al. 2014) and validated in animal

models (Szabat et al. 2016). Indeed, β-cell replication is very rare in adult human pancreas (Butler et al. 2003a; Hanley et al. 2010), and the proliferation seen in animal models is restricted with aging (Tschen et al. 2009; Gupta et al. 2017).

As an alternative to proliferation, β-cell neogenesis is speculated to be the main event contributing to human β-cell mass adaptation (Butler et al. 2003a; Meier et al. 2008; Hanley et al. 2010). Neogenesis is defined as formation of β-cells from progenitor cells (Bonner-Weir et al. 2012). In line with that, I showed a 5-fold increase in β-cell area arising from small insulin-positive clusters using a surrogate definition of neogenesis (Hanley et al. 2010) in compensating NRs, which accounts for over 10% of the total β-cell area reported previously (Yang et al. 2016). The change in the number of these small clusters of β-cells induced by diet and age suggests that these are indeed neogenic in origin and not static remnants of embryonic development (Bonner-Weir et al. 2012). Moreover, β-cell dedifferentiation was observed at 12 months, suggesting that in addition to cell growth and death, dedifferentiation is in part related to the disrupted islet structure and failure of β-cell compensation (Talchai et al. 2012).

3.5 Conclusion

I demonstrate a model that recapitulates characteristics of human β-cell compensation to decompensation regarding glucose metabolism, β-cell function, and mass (Figure 3-9C). The enhanced β-cell insulin secretion was detected at 2 months with a surge of upregulated ER chaperones, which decreased with T2D progression. β-cell mass increased during the compensation stage by non-proliferative means. This study highlights the temporal relationship of

adaptive ER capacity with β-cell function in the transition from compensation to decompensation and changes in islet plasticity that play a role in β-cell mass. Furthermore, the ability to prevent all of the stages of diabetes development in this model by increasing fibre content of the diet provides researchers with the ability to manipulate the stages of compensation and decompensation.

Chapter 4. Metformin, as an alternative to diet regimen, delays progression of prediabetes by distinct actions on β-cell function and hepatic gluconeogenesis in Nile rats

4.1 Introduction

Prediabetes is a high-risk condition for T2D and is diagnosed by impaired glucose tolerance (IGT) or impaired fasting glucose (IFG) (Punthakee et al. 2018). According to the IDF, there are over 352 million adults worldwide estimated to have prediabetes in 2017, and up to 70% of the prediabetic population will develop diabetes (Tabák et al. 2012). Much effort has been made to identify effective interventions to prevent or even reverse prediabetes conversion to T2D (Knowler et al. 1995, 2002). The Diabetes Prevention Program (DPP), a large randomized trial, was conducted to evaluate the effect of lifestyle modification and metformin treatment on 3234 participants with prediabetes. After 2.8-years of follow-up, both lifestyle and metformin interventions reduced incident T2D by 58% and 31%, respectively, compared with the placebo group (Knowler et al. 2002). After an average follow-up of 15 years, the reduction of diabetes incidence was 27% and 18% in the lifestyle and metformin groups, respectively (Diabetes Prevention Program Research Group 2015). The data collected from the DPP indicates that metformin can be a cost-effective option to delay or possibly prevent the progression of T2D over the long term (Aroda et al. 2017).

Metformin is a biguanide antidiabetic medication that has been used to treat T2D for decades. It is well-documented that the glucose-lowering effect of metformin is carried out by inhibitory actions on hepatic glucose production and lipid synthesis as reviewed in Chapter 1.4.1 (Hundal et al. 2000). In line with that, metformin treatment in the DPP elicited improvement in glucose tolerance and insulin sensitivity compared with baseline data (Kitabchi et al. 2005). Also, an improvement in insulin secretion relative to insulin sensitivity was observed in the metformin

group, suggesting enhanced β-cell function (Kitabchi et al. 2005). Evidence from *in vitro* studies reveals that metformin restores insulin secretion of β-cells subjected to glucotoxic conditions (Lupi et al. 1999; Patanè et al. 2000; Marchetti et al. 2004; Piro et al. 2012). However, given that metformin inhibits mitochondrial ATP production, which is essential for β-cell insulin secretion, metformin is also proposed to directly inhibit β-cell insulin secretion (Leclerc et al. 2004; Lamontagne et al. 2009, 2017). With little evidence regarding metformin actions on β-cells in prediabetes, the role that metformin could play to advance or prevent the progression of β-cell dysfunction is not clear.

Nile rat (NR, *Arvicanthis niloticus*) is a wild rodent that develops T2D naturally when adapted to a laboratory setting and fed with standard chow diet (Chaabo et al. 2010). My previous study demonstrated that NR is also a model for prediabetes, recapitulating characteristics of human β-cell compensation at age 2 months and decompensation at 6 months in response to insulin resistance (Chapter 3). Similar to the results of the DPP, this progression of T2D in NR, as well as the change in β-cell function, was prevented by administering a diet with lower caloric density (Yang et al. 2016). Taking advantage of the age-related β-cell responses at different stages of T2D, NR could be a useful model to investigate the effect of metformin on β-cells in prediabetes.

In the present study, I treated 6-week-old, hyperinsulinemic NRs with a low dose of metformin and compared the metabolic features, glucose tolerance and β-cell function after 7 weeks of treatment (age 13 weeks) as well as at age 25 weeks when Chow-fed NRs developed β-cell decompensation and prediabetes (as shown in Chapter 3). I hypothesized that, as an alternative to diet regimen, early treatment of Nile rats with metformin during the compensation stage would prevent prediabetes in NRs by improving insulin sensitivity and β-cell insulin secretion.

4.2 Methods and Materials

4.2.1 Animals

Male NRs used in this study were from a colony established at the University of Alberta. Animals were housed at 21°C under a 14-hour light, 10-hour dark cycle. After weaning at 3 weeks, animals were fed with either high energy, low fiber Chow (Prolab® RMH 2000, 5P06, LabDiet, Nutrition Intl., Richmond, IN) or low energy, high fiber Hfib diet (Mazuri® Chinchilla Diet, 5M01, Purina Mills, LLC, St. Louis, MO)(Yang et al. 2016). All animal studies were approved by the University of Alberta Animal Care and Use Committee (Animal use protocol #00000328) and were conducted in accordance with Canadian Council on Animal Care Guidelines.

4.2.2 Study design

The clinically effective dose of metformin for diabetes prevention is 850 mg twice daily, which is equivalent to 20-30 mg/kg body weight (Knowler et al. 2002). In animal studies, metformin dose varies from 50 to 300 mg/kg depending on the species and diabetic condition of the model (Linden et al. 2015; Wang et al. 2016). A recent study revealed that a low dose of metformin (10 mg/kg) mimics the effect of caloric restriction in mice, improving insulin sensitivity with aging and preventing the onset of metabolic syndrome; whereas a higher dose (100 mg/kg) shortens mean lifespan likely due to renal failure (Martin-Montalvo et al. 2013). To determine a safe and effective dose of metformin for alleviating insulin resistance in NR, water consumption was monitored for several days. Then, metformin (Millipore Sigma, St. Louis, USA) was administered at doses approximating 10, 20 or 50 mg/kg body weight/day in drinking

water to 2-month-old chow-fed NRs for 1 week. The animals were then subjected to an intraperitoneal glucose tolerance test (ipGTT). NRs treated with metformin at a dose of 20 mg/kg/day had overall lower glucose vs Chow control (Figure 4-1, Met 20 mg/kg vs chow p=0.034).

A total of 97 NRs (Hfib: n=20; Chow: 77) were used in the main study. To determine baseline metabolic characteristics, ipGTT was performed on half of the NR in Hfib, Chow and Chow-met groups at the age of 6 weeks, an age at which I observed that insulin secretion starts to compensate for insulin resistance (fasting insulin concentration (ng/ml): 1.03± 0.12 vs 0.19± 0.06, Chow vs Hfib, $p<0.01$ by *t*-test). NRs fed with Chow diet were then randomized into Chow or Chow+met groups. Individuals from the same litter were equally assigned into these 2 groups to avoid a litter effect. NRs in the Chow+met group were treated with metformin at 20 mg/kg BW/day in drinking water. Water intake was measured before and during the treatment every week. Metformin concentration in drinking water was adjusted based on animal water intake and body weight if necessary. At age 13 weeks (3 months), sub-groups of NRs (Hfib=11; Chow=21; Chow=24) were subjected to glucose or insulin or pyruvate tolerance test (GTT, ITT, PTT) and then euthanized following overnight fasting or a 16-hour fasting and 4-hour refeeding protocol to allow measurement of the metabolic status and the expression of hepatic gluconeogenic enzymes under fasting and fed conditions, respectively. The remaining 41 NRs (Hfib=9; Chow=16; Chow+met=16) were maintained on their diet or metformin interventions until 25 weeks (6 months). After ipGTT or ITT, animals were euthanized under fasting or refed conditions as mentioned above (Figure 4-2).

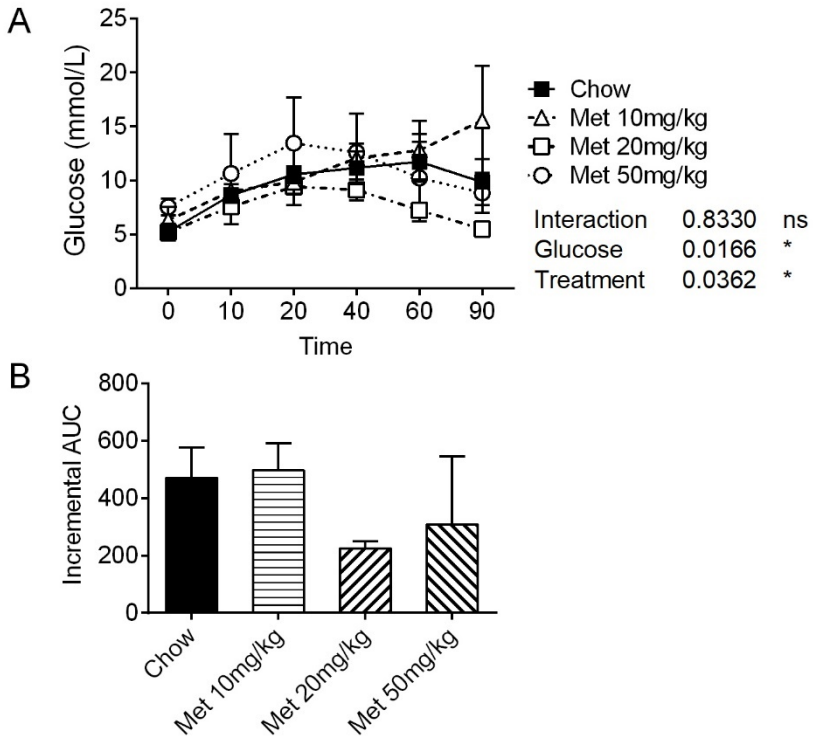

Fig. 4-1 ipGTT for metformin dose pilot study. A: Blood glucose during ipGTT in NR at 2 months after one week of metformin treatment; B: Incremental area under the curve of blood glucose. AUC data are presented as mean + SEM, n=3-4. Data are analyzed by 2-way ANOVA (A) or Kruskal-Wallis test (B).

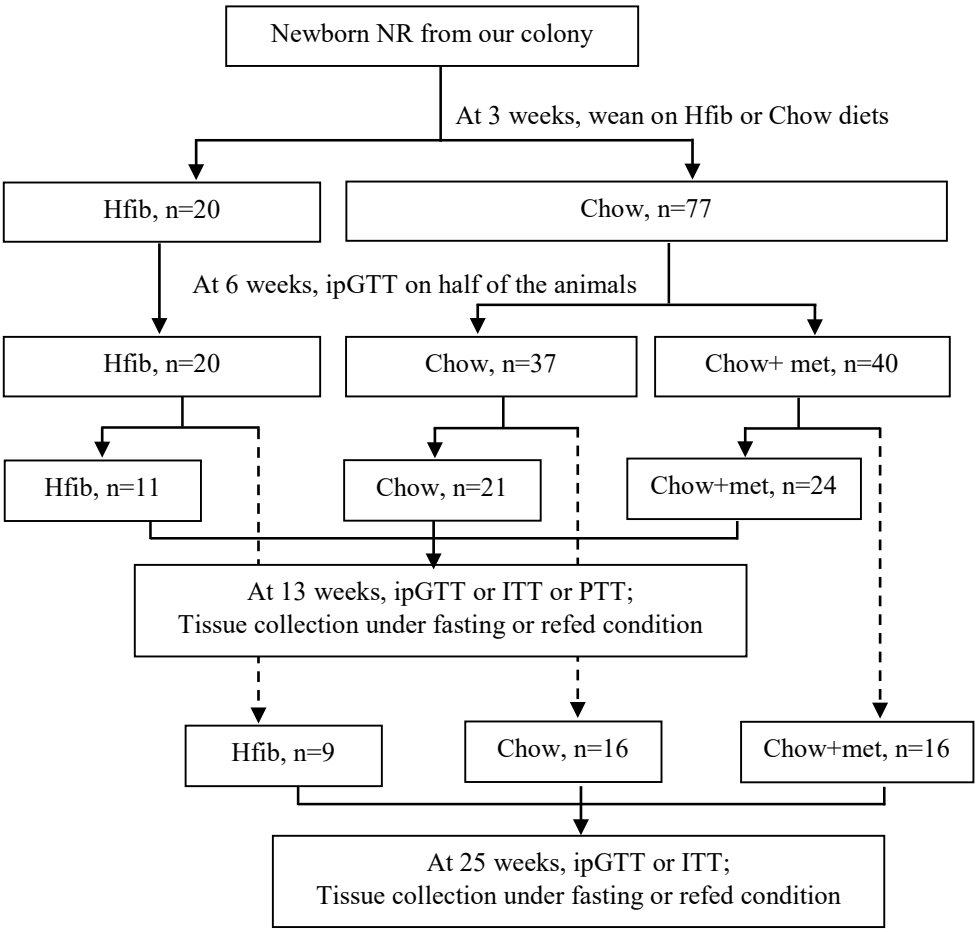

Figure 4-2 Schematic representation of the experimental design.

4.2.3 Glucose, insulin and pyruvate tolerance test

Intraperitoneal GTT and PTT were performed on animal following overnight fasting. ITT required animal fasting for 4 hours. Due to the feral behavior of NRs, animals were anesthetized with isoflurane (Millipore Sigma) during procedures. GTT and ITT were measured by the method described in Chapter 3.2.2. For PTT, pyruvate was intraperitoneally injected at a dose of 2 g/kg body weight. Blood glucose was determined before and 10, 20, 40, 60, 90, 120 minutes after injection using a CONTOUR NEXT blood glucose monitoring system (Bayer Inc.,

Mississauga, Canada). Animals that did not recover from anesthesia in 30 minutes or had blood glucose lower than 2 mmol/L during experiments were excluded from the study.

4.2.4 Tissue collection

After overnight fasting or refeeding, fasting blood glucose (FBG) was measured before administration of Euthanyl. In order to avoid degradation of liver proteins, a lobe of the liver was harvested and snap-frozen immediately after animals achieved a surgical plane of anesthesia without damaging the common bile duct for pancreas perfusion. Blood samples were then collected via cardiac puncture for measurement of insulin, glucagon, and glucagon-like-peptide 1 (GLP-1). DPP-IV inhibitor (10 μmol/L, Millipore, Billerica, MA, USA) was added to blood collected for GLP-1 measurement. Insulin, glucagon and GLP-1 concentrations were determined by ELISA (Insulin, Crystal Chem Inc., Downers Grove, IL, USA; glucagon, ALPCO Diagnostics Inc., Salem, NH; GLP-1, Meso Scale Discovery, Rockville, MD, USA). The pancreas tail was clamped and collected from fasted animals for immunohistochemical (IHC) or immunofluorescent staining (IF) by fixing in formalin. Islets were isolated as previously described (Yang et al. 2016). BMI, ISI, HOMA-IR, HOMA-B were calculated using the following equations (Yang et al. 2016):

BMI=body weight (kg)/ length form nose tip to base of tail (m^2)

ISI= 2/(1+ (172.1× fasting insulin (μU/L)) × (fasting glucose (mmol/L)/1000)).

HOMA-IR=fasting insulin (μU/L) × fasting glucose (mmol/L)/22.5

HOMA-B= 20 × fasting insulin (μU/L)/ fasting glucose (mmol/L)

4.2.5 *In vitro* metformin treatment and glucose-stimulated insulin secretion (GSIS)

To compare the effects of *in vivo* and *in vitro* metformin treatment on islet function, isolated islets from Chow NRs at the age of 13-20 weeks were cultured in Dulbecco's modified Eagle's medium (DMEM) or medium supplemented with 20 μmol/L or 5 mmol/L metformin for 24 hours. Metformin was supplemented in the medium used in the GSIS assay as well.

To assess insulin secretion, three isolated islets were incubated in 1 mL of DMEM supplemented with concentrations of glucose of 2.8, 5.5, 11.0, 16.5 or 22 mM for 90 minutes. The supernatant was transferred into new tubes and the pellets were lysed using 1 mL of 3% acetic acid. Insulin in the supernatant and the pellet was determined by insulin radioimmunoassay (RIA). Absolute insulin secretion indicates the amount of insulin secreted per islet during the 90-minute incubation. Insulin release % was insulin secretion normalized by the corresponding islet insulin content. The stimulation index reflects the ability of islet in insulin secretion at high glucose concentrations and was calculated as the ratio of stimulated to basal secretion at 2.8 mM glucose.

4.2.6 Immunofluorescent microscopy

Formalin-fixed pancreatic tissues were immunostained for insulin, glucagon, ER proteins, and/or ki67 using species appropriate AlexaFluor or HRP-conjugated secondary antibodies as previously described in Chapter 3.2.5 (Table 3-1). For ER protein staining, slides were visualized using a Wave FX spinning disk confocal microscope (Quorum Technologies Inc., Guelph, ON, Canada); colocalization and IF staining intensity were analyzed using Volocity 6.0 (PerkinElmer) as previously described (Yang et al. 2016). For ki67, peroxidase-based IHC, images were obtained using a Zeiss Axio Imager Z1 with Axio Vision 4.5 (Carl Zeiss Micro Imaging GmbH, Germany) and quantified with ImageJ (NIH, Bethesda, MD, USA). The α-/β-cell areas % was calculated by

taking the glucagon- or insulin-positive area divided by total pancreatic section area (excluding large ducts and veins). Duct- or acinar-associated β-cell clusters that had no more that four cells were classified as "neogenic" β-cells (Okamoto et al. 2006; Hanley et al. 2010).

4.2.7 Semi-quantitative real-time PCR

Total RNA was extracted from islets (at least 30 islets) or frozen liver (50-100 mg) using TRIzol reagent (Invitrogen, Carlsbad, CA, USA). 1 μg of RNA was used to synthesize cDNA using QuantiTect reverse transcription kit (QIAGEN, Mississauga, ON, Canada). Because the NR genome has not been sequenced, primers were designed from regions conserved between rat and mouse (Table 4-1). Real-time PCR was performed using an SYBR green qPCR Mastermix (Quanta Biosciences, Gaithersburg, USA) and Rotor Gene 6000 Real-time PCR machine (Corbett Research). The qPCR specificity was confirmed by agarose gel and efficiency of 90-110%. The data were analyzed using the delta Ct method (Livak and Schmittgen 2001). Target gene expression was normalized to β-actin.

Table 4-1: qPCR primers and annealing temperatures

Gene		Primer	Annealing Tm (°C)
Ins	Forward	5'-AAGTGGCACAACTGGAGCTG-3'	58
	Reverse	5'-GATGCTGGTGCAGCACTGA-3'	
IR	Forward	5'-AGACCCGAAGATTTCCGAGAC-3'	58
	Reverse	5'-GAGCCTCGGATGACTGTGAG-3'	
Glut2	Forward	5'- GTCAGAAGACAAGATCACCGGAAC -3'	58
	Reverse	5'- CCTCTTGAGGTGCATTGATCACAC -3'	
	Forward	5'-GAGCTGGTACGACTTGTGCT -3'	58

Gck	Reverse	5’-AACCGCTCCTTGAAGCTCG -3’	
Pdx1	Forward	5’-GCTGGAGCTGGAGAAGGAATTC-3’	58
	Reverse	5’-CTTCATGCGACGGTTTTGGAACC-3’	
MafaA	Forward	5’-AGTTCGAGGTGAAGAAGGAGCC-3’	58
	Reverse	5’-CGCTCATCCAGTACAGATCCTCC-3’	
Pgc1α	Forward	5’-CCAGCCTCTTTGCCCAGAT-3’	58
	Reverse	5’-AGGGCAATCCGTCTTCATCC-3’	
G6pc	Forward	5’-GTCCACCTTGACACTACACCC-3’	58
	Reverse	5’-GCGGTACATGCTGGAGTTGAG -3’	
Pck1	Forward	5’-GTGCTGGAGTGGATGTTCGG-3’	58
	Reverse	5’-TCTGGCTGATTCTCTGTTTCAGG -3’	
Atf4	Forward	5’-AACATGACCGAGATGAGCTTCCTG-3’	56
	Reverse	5’-AAGTGCTTGGCCACCTCCA-3’	
Atf6	Forward	5’-TGCTCTGGAACAGGGCTC-3’	56
	Reverse	5’-ATGGACACCAGGATCCTCCA-3’	
spliced *Xbp1*	Forward	5’-CTGAGTCCGCAGCAGGT-3’	56
	Reverse	5’-GGTCCAACTTGTCCAGAATGCC-3’	
Xbp1	Forward	5’-AGTCCGCAGCACTCAGACTA-3’	56
	Reverse	5’-GGTCCAACTTGTCCAGAATGCC-3’	
Chop	Forward	5’-GGAGCTGGAAGCCTGGTATGAG-3’	56
	Reverse	5’-TGGTCAGGCGCTCGATTTCC-3’	
Bax	Forward	5’-CAGGGTTTCATCCAGGATCGAGC-3’	56
	Reverse	5’-GCAATCATCCTCTGCAGCTCC -3’	
Bcl-2	Forward	5’-GGATGACTGAGTACCTGAACCGG-3’	56
	Reverse	5’-GTCTTCAGAGACAGCCAGGAG -3’	
β-Actin	Forward	5’-TATCCTGGCCTCACTGTCCA-3’	56
	Reverse	5’-AAGGGTGTAAAACGCAGCTCA-3’	

4.2.8 Western blot analysis

Snap-frozen liver (up to 50 mg) was homogenized in 0.5 mL of RIPA buffer supplemented with proteinase inhibitor cocktail, aprotinin (2 μg/mL), sodium fluoride (5 mmol/L), sodium orthovanadate (1 mmol/L) and PMSF (1 mmol/L). All reagents were from Millipore Sigma (St. Louis, USA). The concentration of protein extracts was determined by bicinchoninic acid assay (BCA) and proteins were diluted to a final concentration of 2 μg/μL with RIPA buffer and SDS loading buffer. About 70 μg of protein was loaded for each sample. Proteins were separated on 10% SDS-PAGE gels and transferred to nitrocellulose membranes. Membranes were blocked for 1 hour with 5% skim milk in TBS (20 mM Tris, 137 mM NaCl, pH 7.6) with 0.1% Tween-20 and probed with antibodies (Table 4-2). Blots were developed using ECL (ThermoFisher Scientific) and imaged with a Bio-Rad ChemiDoc MP imaging system. Antibody detecting phosphorylated protein was stripped to enable detection of the corresponding total protein on the same blot. Three independent experiments were done for each condition. The protocol for immunoblotting of islet samples was described in chapter 3.2.7.

Table 4-2: Antibodies and dilutions used in western blot

Antibody	Source	Dilution
Rabbit Anti-AMPKα	2532, Cell Signaling Technology, Danvers, MA, USA	1:1000
Rabbit Anti-phospho-Thr172-AMPKα	2535, Cell Signaling Technology, Danvers, MA, USA	1:1000
Rabbit Anti- PEPCK	10004943, Cayman Chemical, Ann Arbor, MI, USA	1:200
Rabbit Anti-G6Pase	Sc-25840, Santa Cruz Biotechnology, Dallas, Texas, USA	1:1000

Mouse Anti-Glut2	Sc-518022, Santa Cruz Biotechnology, Dallas, Texas, USA	1:200
Rabbit Anti-IRβ	3025, Cell Signaling Technology, Danvers, MA, USA	1:500
Rabbit Anti-PGC1α	Ab54481, Abcam, Cambridge, UK	1:1000
Rabbit Anti-PKA C	4782, Cell Signaling Technology, Danvers, MA, USA	1:1000
Rabbit Anti-phospho-Thr197-PKA	4781, Cell Signaling Technology, Danvers, MA, USA	1:1000
Rabbit Anti-Akt	9272, Cell Signaling Technology, Danvers, MA, USA	1:1000
Rabbit Anti-phospho-Ser473-Akt	9271, Cell Signaling Technology, Danvers, MA, USA	1:1000
Rabbit Anti-Bip	3177, Cell Signaling Technology, Danvers, MA, USA	1:1000
Rabbit Anti-Grp94	2104, Cell Signaling Technology, Danvers, MA, USA	1:1000
Mouse Anti-CHOP	2895, Cell Signaling Technology, Danvers, MA, USA	1:500

4.2.9 Stool sample collection and microbiota analysis

Fecal samples were collected from 3-month NRs (Hfib=4; Chow=5; Chow+met=5) in a sterile setting. Total DNA was extracted using QIAamp DNA mini stool kit (Qiagen, Mississauga, ON, Canada). The V3-V4 regions of 16S rRNA gene were amplified with primer pairs: Forward: TCGTCGGCAGCGTCAGATGTGTATAAGAGACAGCCTACGGGNGGCWGCAG; Reverse: GTCTCGTGGGCTCGGAGATGTGTATAAGAGACAGGACTACHVGGGTATCTAATCC. Paired-End sequencing was performed using the Illumina MiSeq platform (Illumina Inc., San Diego, CA) as previously described (Forgie et al. 2019). The original reads were trimmed using FASTX-Toolkit, merged using PANDAseq algorithm and mapped to a database to obtain the

operational taxonomic units table using Usearch_global (VSEARCH) and QIIME 1.9.1 (Quantitative Insight into Microbial Ecology) (Edgar et al. 2011; Forgie et al. 2019). The alpha diversity analyses for the microbial community was determined using QIIME and normalized to the lowest number of reads (Forgie et al. 2019).

4.2.10 Statistical analyses

For all experiments (excluding microbiota data, described above), data were expressed as the mean ± SEM (or mean + SEM as indicated in the captions) and statistically analyzed with GraphPad Prism version 6.0. One-way or two-way analysis of variance was used, with repeated measures when appropriate, followed by post-hoc Bonferroni's multiple comparisons if significance was reached. Differences were considered significant at $p<0.05$.

4.3 Results

4.3.1 Body weight, glucose and hormone concentrations

Body weight and body mass index (BMI) are not significantly different between Hfib and Chow NR until 25 weeks (Table 4-3), in accordance with the previous cohort (Chapter 3.3.1). Chow+met NRs show similar body weight and BMI to the age-matched Chow groups (Table 4-3). Weight gain during treatment is not statistically different between groups at both 13 and 25 weeks.

Blood glucose and hormones were measured following overnight fasting or 4-hour refeeding to, in part, assess glucose homeostasis parameters. No significant difference was observed in FBG or random glucose between groups at 13 and 25 weeks (Table 4-3). FBG of 5.6 mmol/L

was defined as the cut point for IFG in NR in our previous study (Yang et al. 2016). At 13 weeks, 1 out of 11 (9%) NRs in Chow group has an FBG over 5.6 mmol/L, whereas no NRs in Hfib and Chow+met exceed 5.6 mmol/L. Non-fasting glucose of NRs (measured in refed animals) at 13 weeks is below 7.8 mmol/L, the clinical threshold for IFG. At 25 weeks, Hfib NRs maintain normal FBG and non-fasting glucose. The incidence of IFG is 8% (1 out 12) for both Chow and Chow+met NRs, and 1 animal exhibits impaired non-fasting glucose (over 7.8 mmol/L) in the Chow group.

Compared to Hfib animals, Chow-fed NRs exhibit a typical insulin resistant phenotype with elevated plasma insulin, reduced insulin sensitivity (ISI, HOMA-IR), elevated β-cell function index (HOMA-B) as well as increased fasting glucagon (Table 4-3) (Ferrannini et al. 2007). No significant difference is observed between Chow and Chow+ met NRs at all ages measured. Despite that, it is noted that NRs treated with metformin have comparable glucose to Chow-fed NR but less significant hyperinsulinemia at 25 weeks (Table 4-3). The ratio of glucagon/insulin reflecting the need for glucose production is significantly reduced in fasted Chow vs Hfib at 25 weeks (Table 4-3). Lastly, the fed plasma GLP-1 is not significantly different between groups (p=0.12 Hfib vs Chow+met, Table 4-3).

Table 4-3: Metabolic profile of NRs treated with metformin at 13 and 25 weeks

Outcome	13 weeks			25 weeks		
	Hfib	**Chow**	**Chow+met**	**Hfib**	**Chow**	**Chow+met**
Body weight (g)	71.5±1.9 n=11	77.0±2.6 n=21	78.8±2.3 n=24	77.3±2.8 n=9	94.7±3.2* n=16	91.4±3.7* n=16
BMI (kg/m^2)	4.6±0.1 n=11	4.8±0.1 n=21	4.8±0.1 n=24	4.5±0.1 n=9	5.4±0.3* n=16	5.1±0.1* n=16
Weight gain (%	46±8	44±5	44 ±5	71±6	65±5	72±5

of baseline)	n=8	n=11	n=11	n=7	n=11	n=11
Fasting state						
FBG (mmol/L)	2.9±0.3 n=5	3.2±0.7 n=11	2.5±0.3 n=11	2.5±0.3 n=7	2.8±0.3 n=12	2.8±0.5 n=12
Insulin (ng/mL)	0.6±0.5 n=5	4.9±1.7* n=11	5.0±1.7* n=11	0.3±0.1 n=7	4.9±1.5* n=12	2.9±0.7 n=12
ISI	1.7±0.2 n=5	1.0±0.2* n=11	1.0±0.2 n=11	1.8±0.1 n=7	0.9±0.2* n=12	1.1±0.2 n=12
HOMA-IR	2.0±1.5 n=5	23.0±11.0* n=11	16.7±6.3 n=11	1.1±0.7 n=7	16.7±7.0* n=12	9.0±2.2 n=12
HOMA-B	0.9±0.7 n=5	7.6±2.7* n=11	9.1±3.0* n=11	0.6±0.2 n=7	9.5±3.3* n=12	5.5±1.7 n=12
Glucagon (pg/mL)	47.8±36.3 n=5	325.7±74.2* n=11	480.6±162.2* n=11	133.7±54.1 n=7	128.4±39.0 n=12	102.0±41.3 n=12
Glucagon /Insulin	0.7±0.5 n=5	0.4±0.2 n=11	0.7±0.4 n=11	2.3±1.7 n=7	0.09±0.05* n=12	0.1±0.05 n=12
Fed state						
Glucose (mmol/L)	3.2±0.2 n=6	3.3±0.2 n=10	3.6±0.2 n=13	3.0 n=2	6.0±6.8 n=4	2.7±0.5 n=4
Insulin (ng/mL)	2.8±0.4 n=6	7.0±1.41 n=10	11.3±2.3* n=13	0.7 n=2	13.2±2.9* n=4	7.4±3.5 n=4
Glucagon (pg/mL)	102.1±30.2 n=6	89.0±33.7 n=4	55.9±23.9 n=7	132.7 n=2	127.9±42.0 n=4	43.0±11.9 n=4
Glucagon /Insulin	0.04±0.01 n=6	0.01±0.004 n=4	0.02±0.01 n=7	0.17 n=2	0.01±0.002 n=4	0.01±0.01 n=4
GLP-1 (pmol/L)	1.2±0.2 n=4	0.7±0.4 n=4	0.4±0.1 n=4			

BMI: body mass index; ISI: insulin sensitivity index; HOMA-IR: homeostatic model assessment of insulin resistance; HOMA-B: homeostatic model assessment of β-cell function.

Data were represented as mean ± SEM (as mean for n=2) and analyzed using the Kruskal-Wallis test and Dunn's multiple comparisons test. *$p<0.05$ vs age-matched Hfib.

4.3.2 *In vivo* assessment of glucose homeostasis and insulin secretion

To assess changes in glucose tolerance and insulin secretion in response to metformin treatment, I performed ipGTT on NRs before (6 weeks) and after treatment (13 or 25 weeks). At 13 weeks, there is no significant difference in glucose tolerance between groups (RM 2-way ANOVA p=0.3, Figure 4-3A). When compared to the baseline data at 6 weeks, Chow+met NRs have a smaller glucose response at 13 weeks, while Chow NRs showed no change (Figure 4-3B). There is a trend to different insulin secretion during the GTT between groups (RM 2-way ANOVA p=0.1) with a borderline significant (p=0.05) increase in incremental insulin secretion (iAUC) in Chow+met NRs vs Hfib (Figure 4-3C). The increase in insulin secretion in Chow-met NRs is more evident when compared to baseline at 6 weeks, while there is no change in the Chow group (Figure 4-3C).

After 25 weeks, Chow-fed NRs exhibit a prominent glycemic excursion during GTT with an evident increase in glucose at t=20, 40, 60 ,90 and 120 min compared to Hfib controls (RM 2-way ANOVA P=0.05, Figure 4-3E), whereas the glucose response of NRs receiving metformin is not significantly different from Hfib (Figure 4-3E). Despite that, both Chow and Chow+met NRs display elevated glucose AUC vs baselines at 6 weeks (Figure 4-3F), indicating deteriorated glucose tolerance. The patterns of insulin secretion between groups are significantly different (RM 2-way ANOVA P=0.01, Figure 4-3G). Chow-fed NRs exhibit a high insulin secretion at t=0 and a flat secretion curve with only 2-fold increase (Ins conc.=2.3, 4.5 ng/mL at t=0, 90 min, Figure 4-3G), whereas metformin-treated NRs show an augmented insulin secretion (iAUC, $p<0.01$ vs Hfib) with higher blood insulin concentrations at t=60 and 90 min (Figure 4-3G). However, no difference was detected before and after treatment (Figure 4-3H).

Additionally, insulin sensitivity was assessed by ITT at 13 and 25 weeks. The percentage change in glucose in response to injected insulin is not significantly different between groups at 13 weeks (RM 2-way ANOVA P=0.3, Figure 4-4A). However, evident differences in glucose between Chow and Hfib group are manifested in the glucose recovery phase of the ITT ($p<0.05$ at t=90 and 120 min, Figure 4-4A), suggesting elevated glucose output in Chow NRs. The glycemic excursion elicited by injecting pyruvate in fasted animals reflects hepatic gluconeogenesis (Hughey et al. 2014; Calabuig-Navarro et al. 2015). Chow+met NRs show a subtle change in glucose in response to pyruvate, that is not significantly lower than the Chow group (Figure 4-4B). The impaired insulin tolerance in Chow NRs is further deteriorated at 25 weeks, as suggested by the flat glycemic excursion curve (RM 2-way ANOVA $P<0.01$) and the increased AUC vs Hfib (Figure 4-4C). The difference in glucose at t=90 and 120 min becomes evident compared to Chow+met (Figure 4-4C).

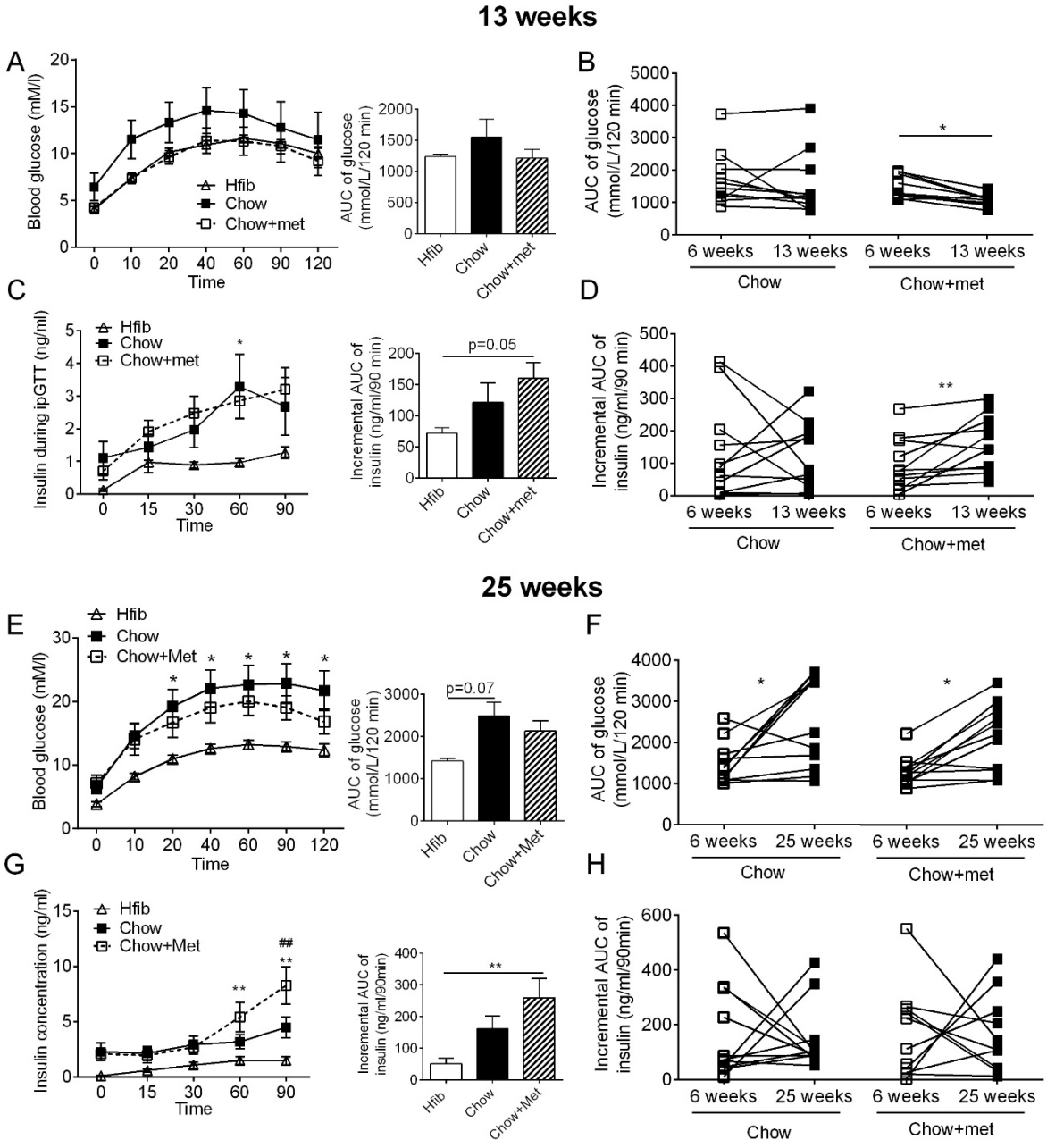

Figure 4-3 Glucose tolerance test. A, C, E and G: Blood glucose (A, E) and insulin secretion (C, G) during ipGTT at 13 (A, C) and 25 (E, G) months; B, D, F and H: Comparisons of total area under the curve of glucose (B, F) or incremental area under the curve of insulin secretion (D, H) during ipGTT between 6 and 13 week (B, D) or 6 and 25 weeks (F, H). AUC data are presented as mean + SEM. n=7-8 in Hfib groups; n=11-12 in Chow, Chow+met groups. For GTT, *p<0.05 vs Hfib, **p<0.01 vs Hfib, #p<0.05 Chow vs Chow+met using Repeated Measure 2-way ANOVA or Kruskal-Wallis test (AUC) followed by Bonferroni's multiple comparison tests. For comparison of AUC before and after treatment, *p<0.05, **p<0.01 using Wilcoxon matched-pairs signed rank test.

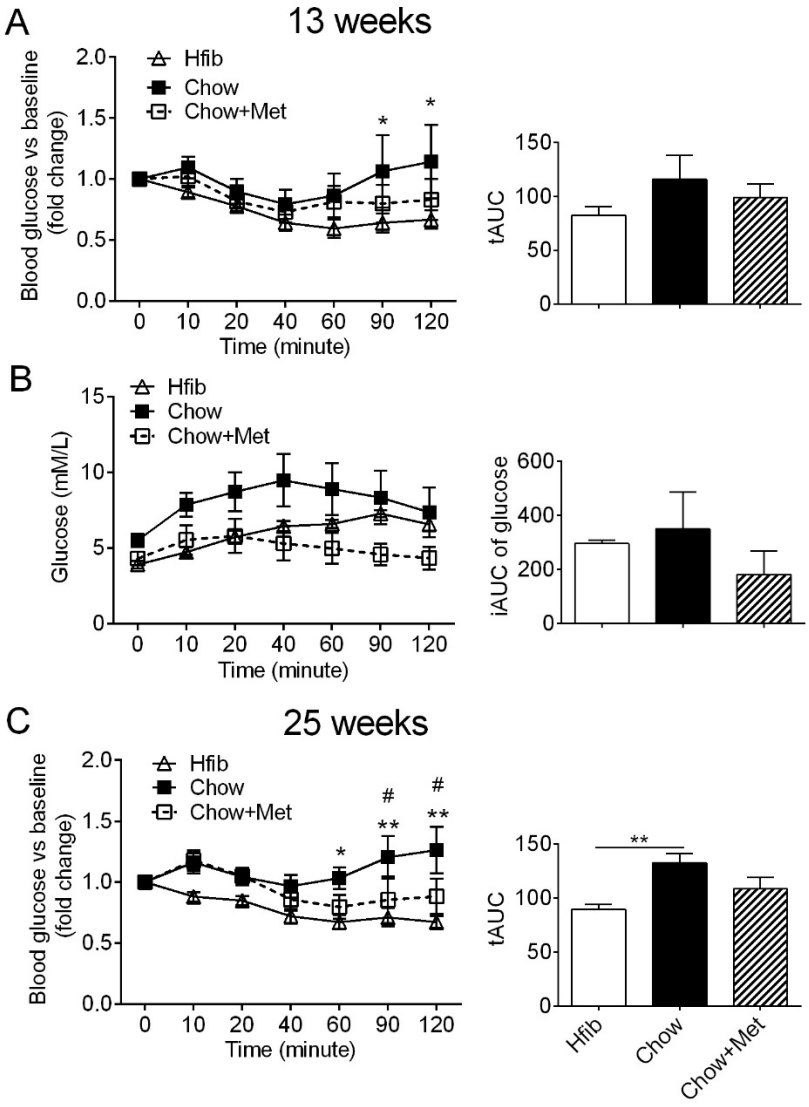

Figure 4-4 Insulin and pyruvate tolerance tests. A, C: Percentage change in blood glucose during ITT at 13 (A) and 25 (B) weeks; B: Glucose response to pyruvate in 13-week NRs. AUC data are presented as mean + SEM for n=7-9 in ITT, n=4-6 in PTT. *p<0.05 vs Hfib, **p<0.01 vs Hfib, #p<0.05 Chow vs Chow+met using Repeated Measure 2-way ANOVA followed by Bonferroni's multiple comparison tests; For AUC, *p<0.05 vs Hfib using Kruskal-Wallis test followed by Dunn's multiple comparisons test.

4.3.3 Hepatic AMPK and gluconeogenic enzymes

To understand the mechanisms by which metformin improved glucose handling as observed in GTT and ITT, I examined the phosphorylation of AMPK, which is known to be induced by metformin and inhibits expression of hepatic gluconeogenic genes such as G6Pase and PEPCK (Zhou et al. 2001; He et al. 2009). In fasted NRs at 13 weeks, hepatic AMPK phosphorylation is significantly downregulated in Chow-fed NRs and partially restored by metformin treatment (Figure 4-5A, F). Liver PKA is activated in NR receiving metformin (Figure 4-5B, F), albeit the comparable plasma glucagon and the ratio of glucagon to insulin between Chow and Chow+met (Table 4-3). Phosphorylated Akt, as an indicator of insulin signaling, shows no change between groups (Figure 4-5C, F). The abundance of G6Pase and PEPCK are comparable between the Chow and Chow+met groups (Figure 4-5D-F).

In the refed state, insulin secretion is stimulated, the act of which modulates transcription of gluconeogenic genes (Cho 2001). Here, I show a significant increase in phosphorylated AMPK in metformin-treated vs untreated Chow NRs (Figure 4-5G, L). Despite the elevated insulin in fed Chow+met group (Table 4-3), Akt phosphorylation is not altered between groups (Figure 4-5H, L). Nevertheless, PGC1α protein abundance and mRNA expression are reduced in Chow+met NRs (Figure 4-5I, L and M). The abundance of hepatic G6Pase protein and transcript is decreased in both Chow and Chow+met NRs compared to Hfib (Figure 4-5J, L, N), whereas reduction of PEPCK is more evident in Chow+met (Figure 4-5K, L, O), which is an indication of reduced gluconeogenesis capacity in NRs receiving metformin.

In fasted NRs at 25 weeks, there is an increasing trend of AMPK phosphorylation in metformin-treated NRs vs Chow controls ($p=0.08$, Figure 4-6A, E). PKA activity exhibits a pattern opposite to that at 13 weeks, showing an evident decrease in phosphorylation in the

metformin group (Figure 4-6B, E). The abundance of G6Pase and PEPCK is downregulated in all Chow-fed NRs (Figure 4-6C-E). Changes of phosphorylation of AMPK and PKA and abundance of PGC1α, G6Pase, and PEPCK protein and transcripts in the refed NRs are consistent with that of the fasted cohort (Figure 4-6 F-N).

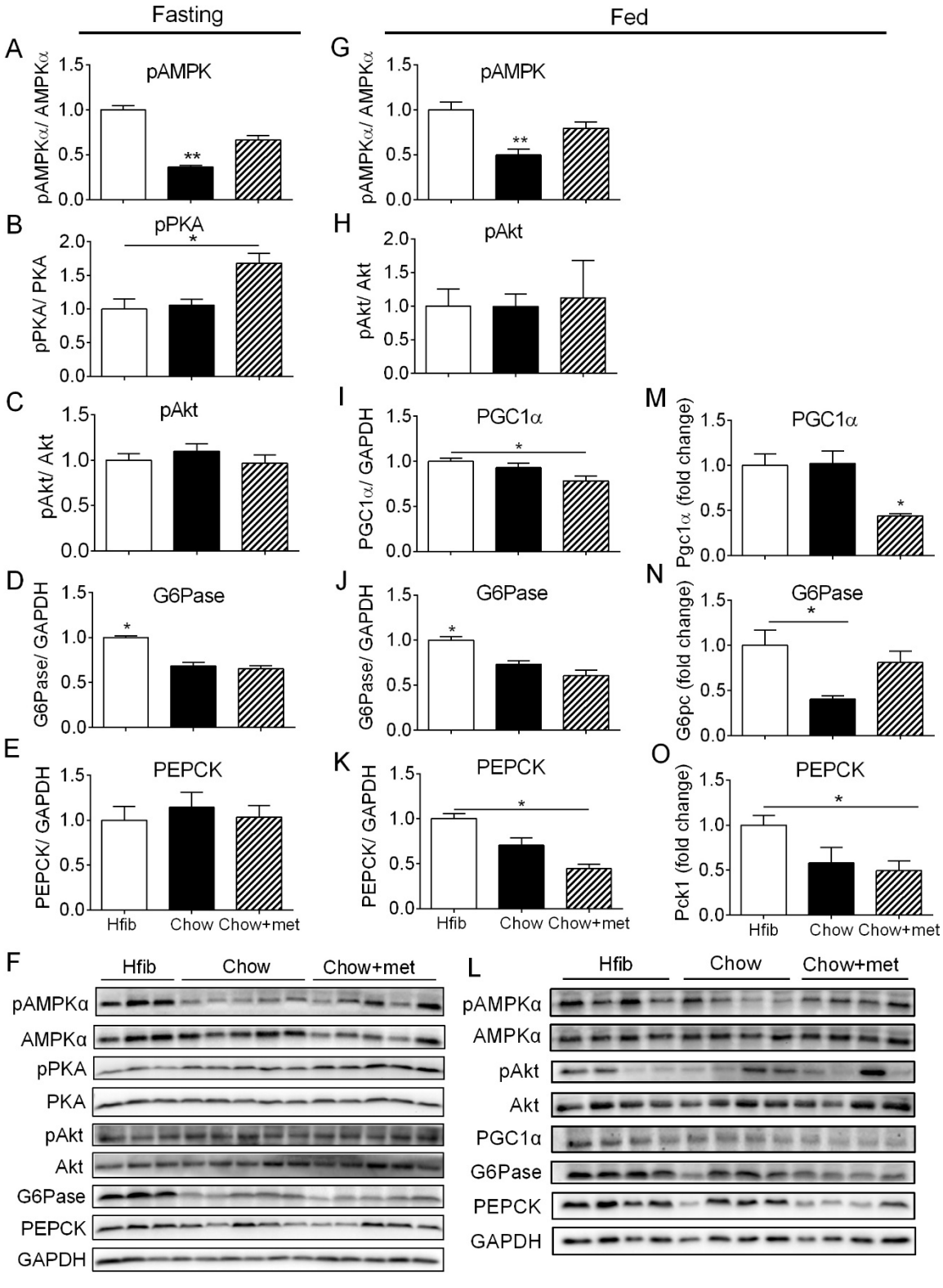

Figure 4-5 Hepatic AMPK activation and glucogenic enzymes at 13 weeks. A-E: Phosphorylation of AMPK (A), PKA (B), Akt (C) and expression of G6Pase (D) and PEPCK (E)

in the fasting state; F: Representative images of liver protein under the fasting state; G-K: Phosphorylation of AMPK (G), Akt (H) and protein abundance of PGC1α (I), G6Pase (J) and PEPCK (K) in the fed state; L: Representative images of liver protein in the refed state; M-O: Gene transcription of PGC1α (M), G6Pase (N) and PEPCK (O) in the refed state. Protein abundance was normalized to GAPGH; gene transcription was normalized to β-actin. Data are presented as mean + SEM. n=5, 11, 11 in fasting Hfib, Chow and Chow+met group, respectively; n=4-6 in refed groups. *p<0.05 using the Kruskal-Wallis test followed by Dunn's multiple comparison test.

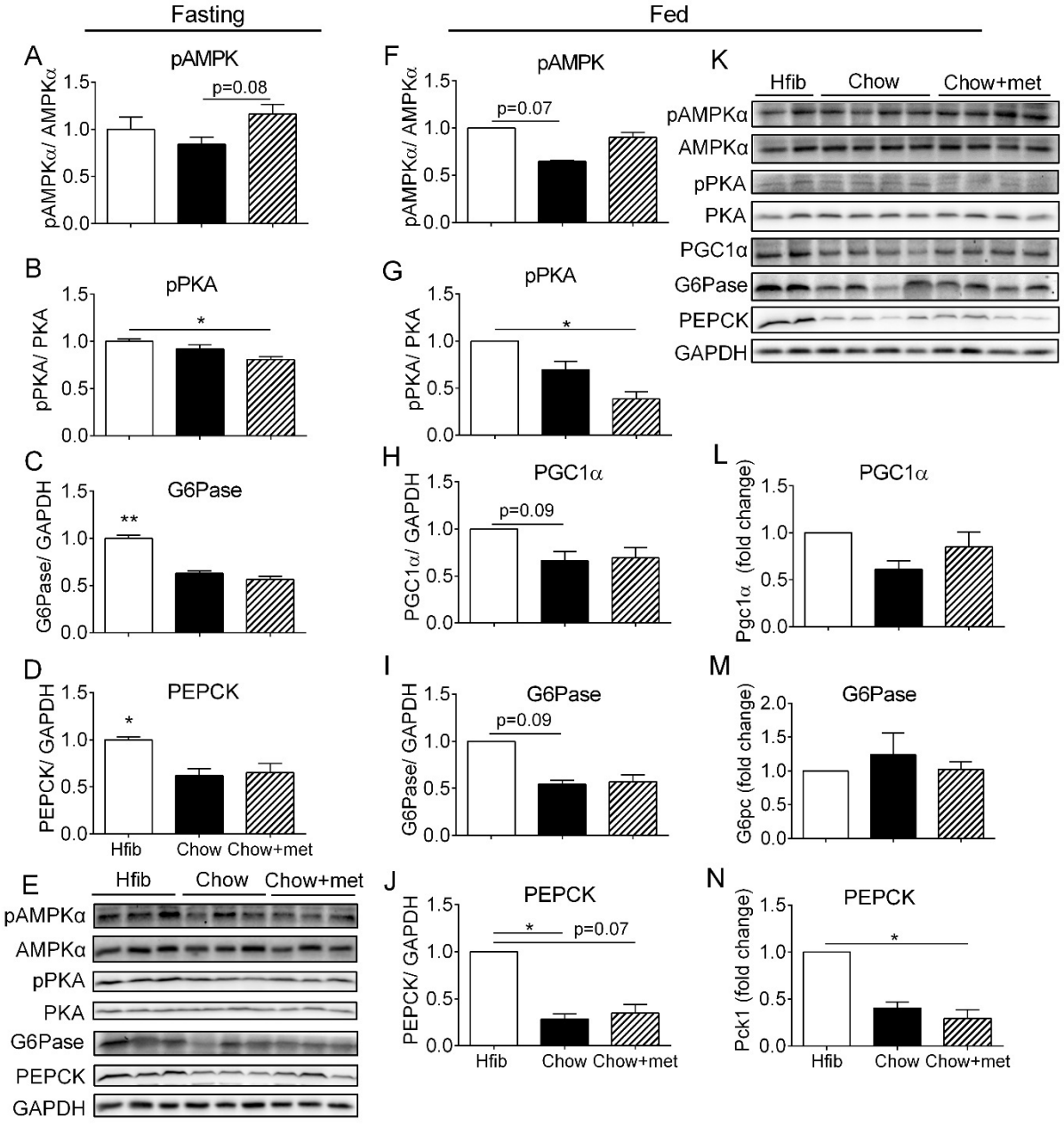

Figure 4-6 Hepatic AMPK activation and glucogenic enzymes at 25 weeks. A-D: Phosphorylation of AMPK (A), PKA (B) and abundance of G6Pase (C) and PEPCK (D) in the fasting state; E: Representative images of liver protein in the fasting state; F-J: Phosphorylation of AMPK (F), PKA (G) and protein abundance of PGC1α (H), G6Pase (I) and PEPCK (J) in the refed state; K: Representative images of liver protein in the refed state; L-N: Gene transcription of PGC1α (L), G6Pase (M) and PEPCK (N) in the refed state. Protein expression was normalized to GAPGH; gene transcription was normalized to β-actin. Data are presented as means + SEM (as mean for n=2). n=7, 12, 12 in fasting Hfib, Chow and Chow+met group, respectively; n=2-4 in refed groups. *$p<0.05$ using the Kruskal-Wallis test followed by Dunn's multiple comparisons tests.

4.3.4 Assessment of islet secretory function

It is well accepted that metformin inhibits ATP synthesis, which could attenuate β-cell GSIS (Leclerc et al. 2004). However, I show enhanced insulin secretion in the late phase of GTT in NRs receiving metformin (Figure 4-3). To explore whether the islet capacity for insulin secretion is altered, GSIS assay was performed on isolated islets cultured in metformin-free medium. At 13 weeks, Chow islets have a greater insulin secretion in response to glucose compared to islets in Hfib and Chow+met groups (overall $p<0.01$, Figure 4-7A), and islet secretion capacities (insulin secretion relative to total insulin content) at basal (2.8-5.5 mM) and stimulated (11-22 mM) glucose. These are significantly augmented compared to Hfib controls as well (Figure 4-7B), which indicates β-cell compensation. Whereas Chow+met islets show a moderate increase in stimulated secretion (16.5 mM, $p<0.05$ vs Hfib) but a marked reduction of basal secretion (5.5 mM) compared to Chow (Figure 4-7B). The stimulation index (stimulated relative to basal secretion at 2.8 mM) of Chow islets is significantly lower than Chow+met islets (Figure 4-7C). There is an increasing trend in insulin content of Hfib islets compared to Chow+met, but no difference is observed between Chow and Chow+met (Figure 4-7D).

Previously, I showed that β-cell decompensation is manifested at 6 months (25 weeks). In this cohort at 25 weeks, the absolute insulin secretion of Chow islets is not decreased vs Hfib (Figure 4-7E); however, the % secretion is diminished compared to other groups (Figure 4-7F). Islets in Chow+met group, on the other hand, exhibit a prominent rise of insulin secretion (Figure 4-7E) and comparable secretion capacity to Hfib islets (Figure 4-7F), which corresponds the profound increase in insulin secretion during GTT at 25 weeks. Despite that, the low stimulation index of Chow and Chow+met islets (Figure 4-7G) reflects an impaired capacity of GSIS. Lastly, insulin content is increased in Chow and Chow+met islets (Figure 4-7H) relative to Hfib, which could be attributed to the increased number of β-cell or/and enhanced insulin synthesis per cell.

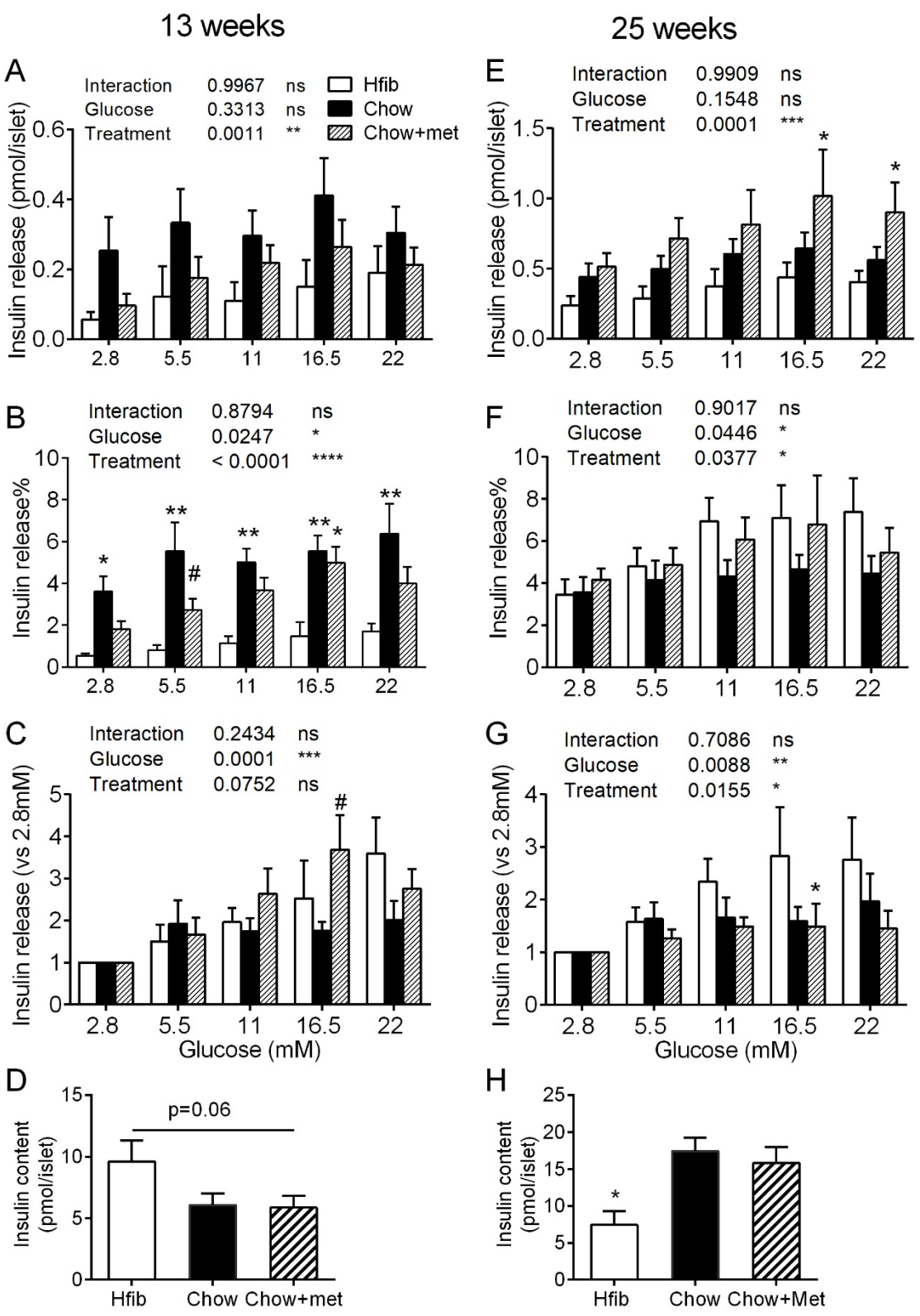
13 weeks
25 weeks
A
Interaction 0.9967 ns
Glucose 0.3313 ns
Treatment 0.0011 **
Hfib
Chow
Chow+met
Insulin release (pmol/islet)
E
Interaction 0.9909 ns
Glucose 0.1548 ns
Treatment 0.0001 ***
B
Interaction 0.8794 ns
Glucose 0.0247 *
Treatment < 0.0001 ****
Insulin release%
F
Interaction 0.9017 ns
Glucose 0.0446 *
Treatment 0.0377 *
C
Interaction 0.2434 ns
Glucose 0.0001 ***
Treatment 0.0752 ns
Insulin release (vs 2.8mM)
Glucose (mM)
G
Interaction 0.7086 ns
Glucose 0.0088 **
Treatment 0.0155 *
D
p=0.06
Insulin content (pmol/islet)
Hfib
Chow
Chow+met
H
Chow+Met

Figure 4-7 Islet glucose-stimulated insulin secretion analysis. A, E: Absolute insulin secreted per islet in GSIS at 13 (A) and 25 (C) weeks; B, F: Percentage insulin release normalized to islet insulin content in GSIS at 13 (B) and 25 (F) weeks; C, G: Ratio of insulin secretion to baseline insulin secretion at 2.8 mM glucose; D, H: Average islet insulin content. Data are presented as mean + SEM. n=6-8 in Hfib group; n= 10-12 in Chow and Chow+met groups. *$p<0.05$ vs Hfib, **$p<0.01$ vs Hfib, #$p<0.05$ vs Chow using ordinary 2-way ANOVA followed by Bonferroni's multiple comparison tests; For insulin content analysis, *$p<0.05$ using the Kruskal-Wallis test followed by Dunn's multiple comparisons tests.

4.3.5 Expression of genes critical to insulin function

To gain insight into the molecular mechanisms that may play a role in altering islet function during diabetes progression and metformin treatment, I analyzed the expression of genes critical to β-cell function and survival (reviewed in Chapter 1.2-1.3). However, no significant change in gene transcription was observed in islets at 13 and 25 weeks (Figure 4-8 A, B). The mGLUT2 (glucose transporter) and mIR (insulin receptor) exhibit a downward trend in Chow islets at 13 weeks, so their protein abundance was examined by western blot. The low expression of GLUT2 in islets from Chow+met NRs (Figure 4-8C) suggests decreased glucose sensing. Insulin signaling is suggested to regulate β-cell insulin secretion (Kim et al. 2007). Total IR slightly increased (Figure 4-8D). However, with limited islet samples, I failed to detect insulin receptor substrate (IRS) or phosphorylated IR. Increased phosphorylated AMPK is observed in Chow+met islets (Figure 4-8E). In islets at 25 weeks, GLUT2 and pAMPK exhibit different trends between groups compared with 13 weeks (Figure 4-8 F-H), corresponding to the enhanced insulin secretion showed in Chow+met at 25 weeks. These experiments were conducted in islets after 24-hour culture without exposure to metformin, indicating that adaptations to *in vivo* metformin were persistent.

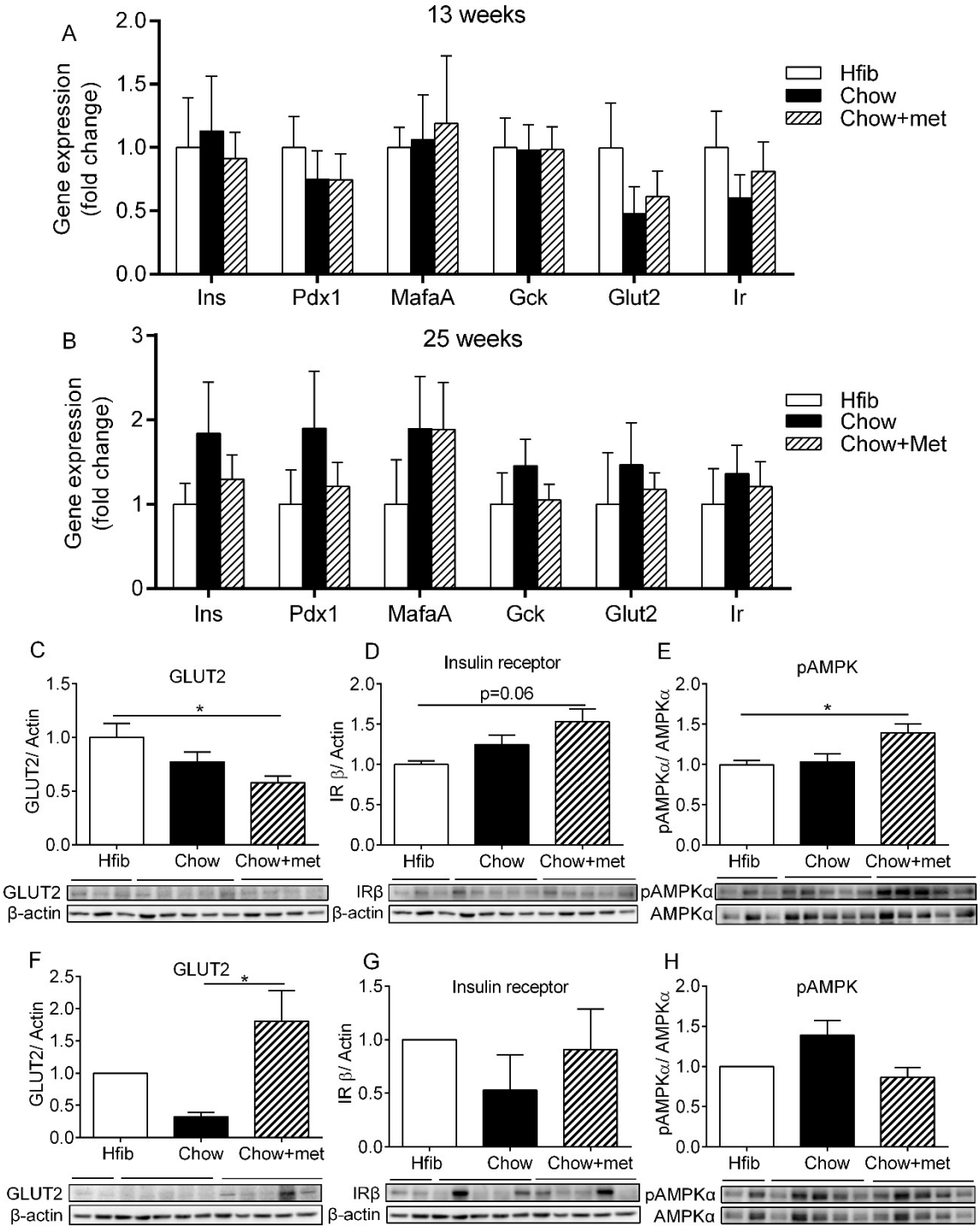

Figure 4-8 Assessment of key factors in regulation of β-cell function. A, B: mRNA of keys genes to β-cell in islets; C-H: Protein abundance of GLUT2 (C, F), IR (D, G) and phosphorylated AMPK (E, H) in islets. Data are presented as means + SEM (as mean for n=2). n=2-3 in Hfib; n=5-8 in Chow and Chow+met groups. *p<0.05 using the Kruskal-Wallis test followed by Dunn's multiple comparison test.

4.3.6 Effects of *in vitro* metformin treatment on islet GSIS

Evidence has suggested that high dose (1-5 mM) of metformin inhibit β-cell insulin secretion in cell lines and isolated islets (Patanè et al. 2000; Leclerc et al. 2004). To examine the direct effects of metformin on islet insulin secretion in NR, I treated islets isolated from Chow-fed NR at 20-25 weeks with metformin at 5 mM or 20 μM, a dose that mimics the plasma concentration of metformin. As shown in Figure 4-9A-C, islets subjected to 24-hour treatment with metformin show no evident change in secretion capacity, stimulation index or islet insulin content, while 5 mM metformin-treated islets demonstrate decreased secretion capacity especially under stimulated glucose conditions (Figure 4-9 D, E). The insulin content of islets shows no change with 5 mM metformin treatment (Figure, 4-9F). It is, therefore, plausible that the changes observed in islets from Chow+met NRs (Figure 4-7) are via indirect actions of metformin.

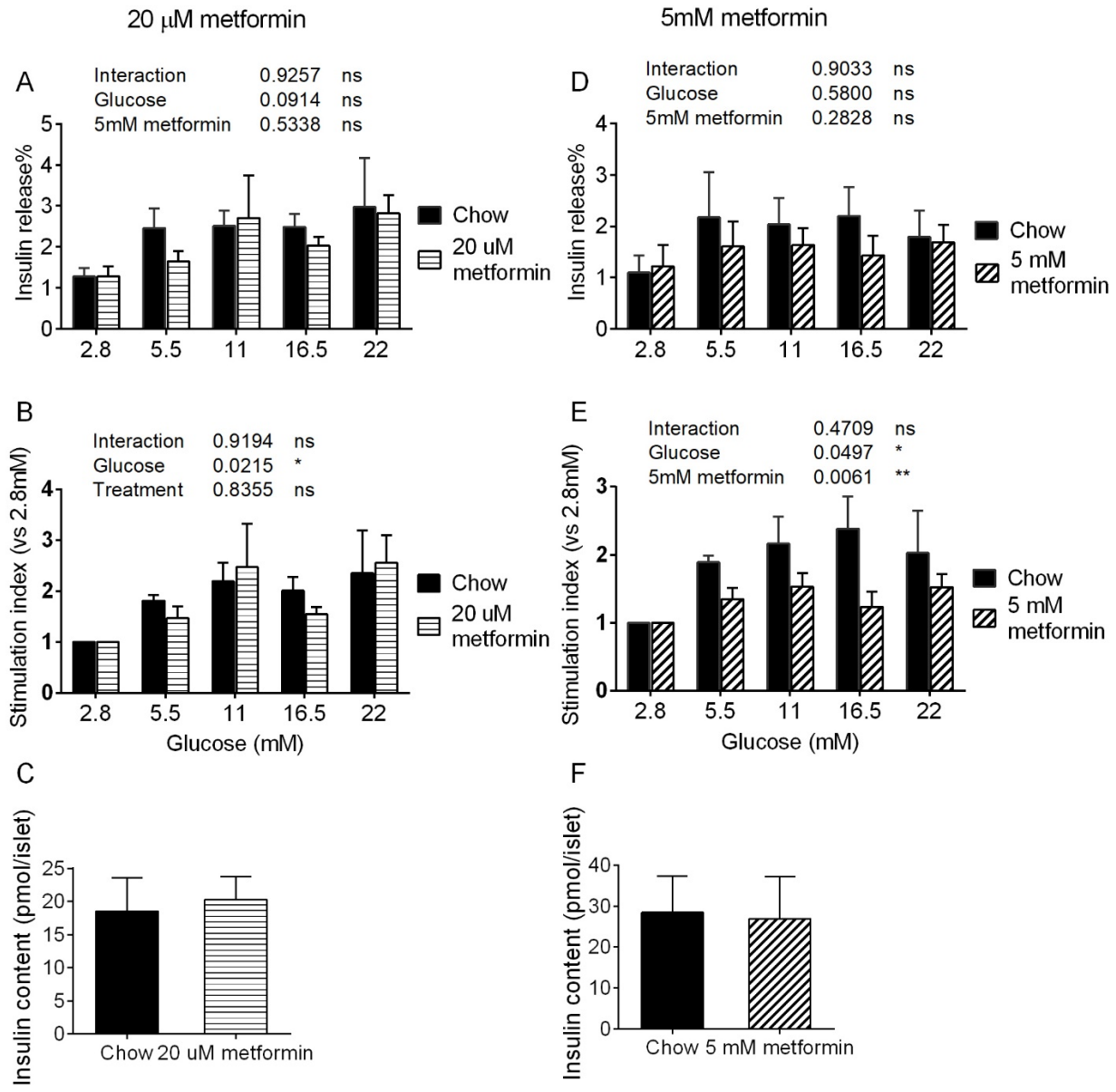

Figure 4-9 GSIS of islet cultured with 20 μM and 5 mM metformin. A, D: Percentage insulin release normalized to islet insulin content in GSIS treated with 20 μM (A) and 5 mM (D) metformin; B, E: Stimulation index calculated as the ratio of insulin secretion to baseline insulin secretion at 2.8 mM glucose; C, F: Islet insulin content. Data are presented as mean + SEM. n=4-5. *$p<0.05$ using ordinary 2-way ANOVA followed by Bonferroni's multiple comparison tests.

4.3.7 ER chaperones and unfolded protein response in β-cells

Our previous study showed that the amount of ER chaperone such as ERp44 and PDI that colocalized with insulin was correlated with insulin secretion (Chapter 3). At 13 weeks, insulin-colocalized ERp44 and PDI in β-cells are significantly increased in Chow and Chow+met NRs (Figure 4-10A, B), and this is accompanied by elevated plasma insulin concentration (Table 4-3). While at 25 weeks, the ERp44 and PDI decrease in Chow+met β-cells (Figure 4-10C, D), along with a decrease in circulating insulin concentration (Table 4-3). As reviewed in Chapter 1.2.2, Bip acts as the sensor of ER stress by binding to the unfolded protein. Glucose-regulated protein 94 (GRP94) is another prominent ER chaperone essential to proinsulin translocation and insulin secretion (Ghiasi et al. 2019); however, the abundance of Bip and GRP94 in islets as determined by immunoblots is comparable between groups (Figure 4-10C, D). In addition to ER chaperones, unfolded protein response (UPR) transcription factors were examined by qPCR. Spliced XBP-1, pro-apoptotic UPR marker CHOP, and Bax (Bcl-2-associated X protein) are upregulated in the Chow group (Figure 4-10I), indicating activation of apoptotic UPR. Whether it leads to β-cell apoptosis requires more investigation. The maladaptive markers show the same trend in Chow islet at 25 weeks (Figure 4-10J).

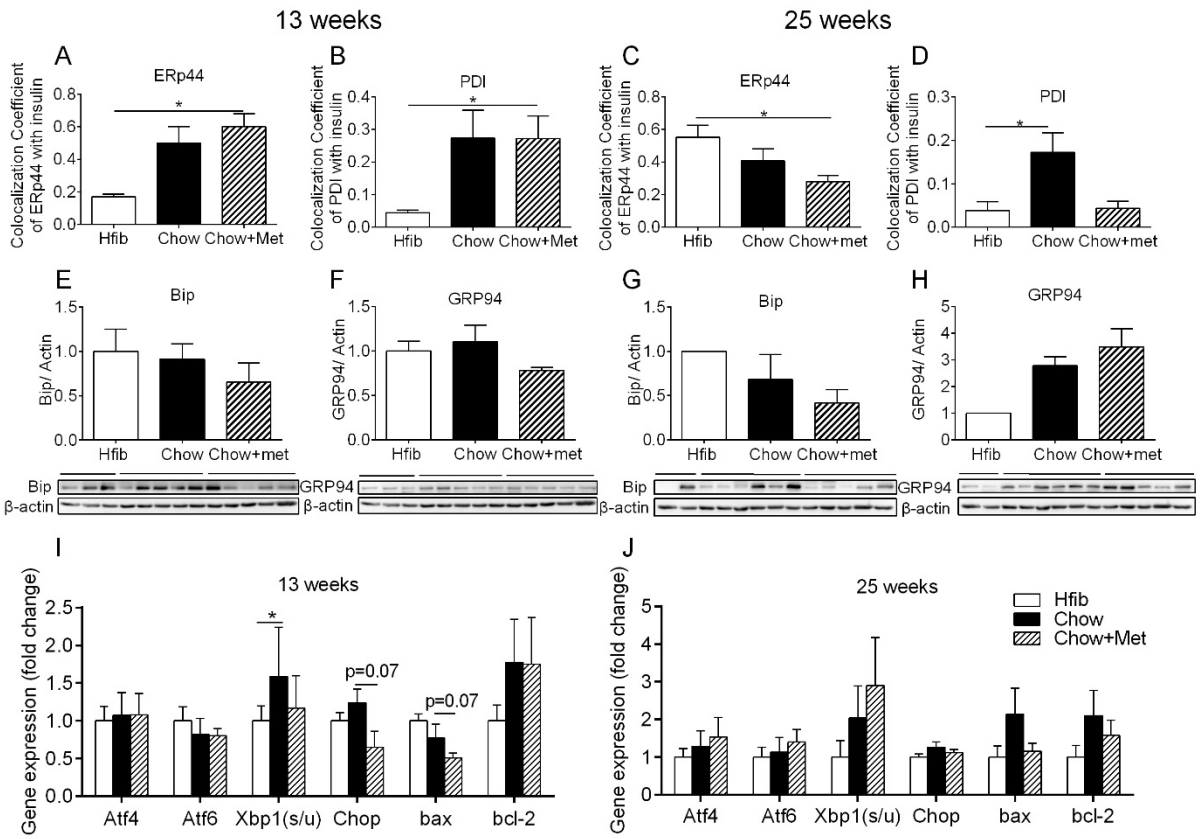

Figure 4-10 ER chaperones and UPR factors in islets. A-D: Colocalization of ERp44 (A, C) and PDI (B, D) with insulin in β-cells at 13 (A, B) and 25 (C, D) weeks; E-H: Protein abundance of Bip (E, G) and GRP 94 (F, H) in islets at 13 (E, F) and 25 (G, H) weeks; I, J: mRNA expression UPR transcription factors. Data are presented as means + SEM (as mean for n=2). n=5-8 at 13 weeks, 2-5 at 25 weeks. *$p<0.05$ using the Kruskal-Wallis test followed by Dunn's multiple comparison test.

4.3.8 Analysis of α-/β-cell area and β-cell proliferation

In addition to its actions on cell function, recent diabetes and cancer research reveal an inhibitory effect of metformin on cell proliferation under physiological conditions (Tajima et al. 2017; Lord et al. 2018). Here, I also evaluated islet morphology and β-cell proliferation in metformin-treated NRs. The β-cell area at 13 weeks shows a 3-fold increase in both Chow and Chow+met NRs compared to Hfib (Figure 4-11A, B); the α-cell area and islet size of Chow-fed NRs is increased as well (Figure 4-11A, C, D). In accordance with the previous results regarding β-cell proliferation, β-cells in Chow NRs demonstrate a lower incidence of proliferation, notwithstanding the larger cell area (Figure 4-11E). There is no difference in individual cell area or proliferation between metformin-treated and untreated groups (Figure 4-11A-E).

At 25 weeks, although less evident, the β-cell area in Chow NRs is still larger than Hfib controls (Figure 4-11F, G). Whereas the α-cell area is identical between three groups at 25 weeks (Figure 4-11F, H), although Hfib NR showing a 2-fold increase in α-cell area at 25 weeks compared to 13 weeks (Figure 4-11C, H). Also, the average size of islets becomes comparable among groups (Figure 4-11F, I). Although decreased with age, the ratio of proliferating β-cells is still higher in Hfib vs Chow independent of metformin treatment (Figure 4-11J). Besides, Chow+met NRs display higher rate of α-cell proliferation compared to Chow controls (Figure 4-11K).

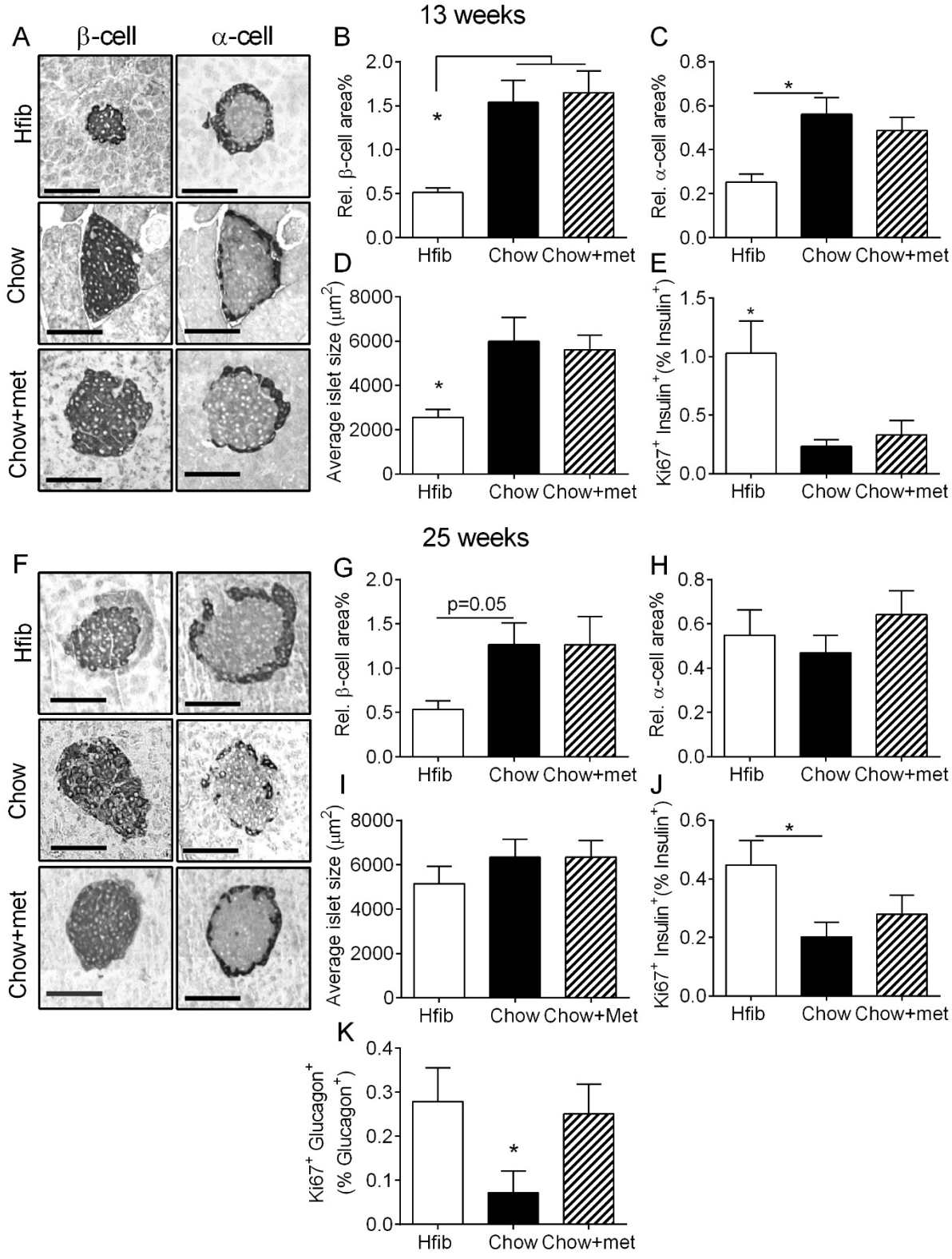
13 weeks
A
β-cell
α-cell
Hfib
Chow
Chow+met
B
Rel. β-cell area%
C
Rel. α-cell area%
D
Average islet size (μm²)
E
Ki67⁺ Insulin⁺(% Insulin⁺)
Hfib
Chow
Chow+met
25 weeks
F
G
p=0.05
H
I
J
K
Ki67⁺ Glucagon⁺ (% Glucagon⁺)
Chow+Met

Figure 4-11 Pancreatic α-/β-cell area and β-cell proliferation. A, F: Representative images of insulin and glucagon staining; B, G: Relative β-cell area to the total pancreas area; C, H: Relative α-cell area to the total pancreas area; D, I: Average β-cell area per islet, calculated by dividing the total β-cell area by the number of islets; E, J: Percentage of the number of proliferating β-cell to the total number of β-cell; K: Percentage of the number of proliferating α-cell to the total number of α-cell. Data are presented as mean + SEM. n=5-7 in Hfib group; n=11-12 in Chow and Chow-met groups. *$p<0.05$ using the Kruskal-Wallis test followed by Dunn's multiple comparisons tests. Scale bar= 100 μm.

4.3.9 Microbiota analysis

It is established that supplementation of dietary fiber protects against diet-induced obesity via restoration of gut microbiota (Chassaing et al. 2015; Zou et al. 2018). Recent evidence indicates that the gut microbiota also responds to metformin treatment for T2D and contributes to the glucose-lowering effect of metformin (Forslund et al. 2015; Wu et al. 2017). A pilot study was performed on 13-week-old NRs to gain insight into whether metformin action on the microbiota could contribute to the metabolic effects. The gut microbial community structure is significantly altered by Hfib diet in NRs as expected ($p=0.008$, Figure 4-12A, B). However, there appears to be no overall difference between the microbial composition of NRs with and without metformin ($p=0.466$, Figure 4-12 C, D).

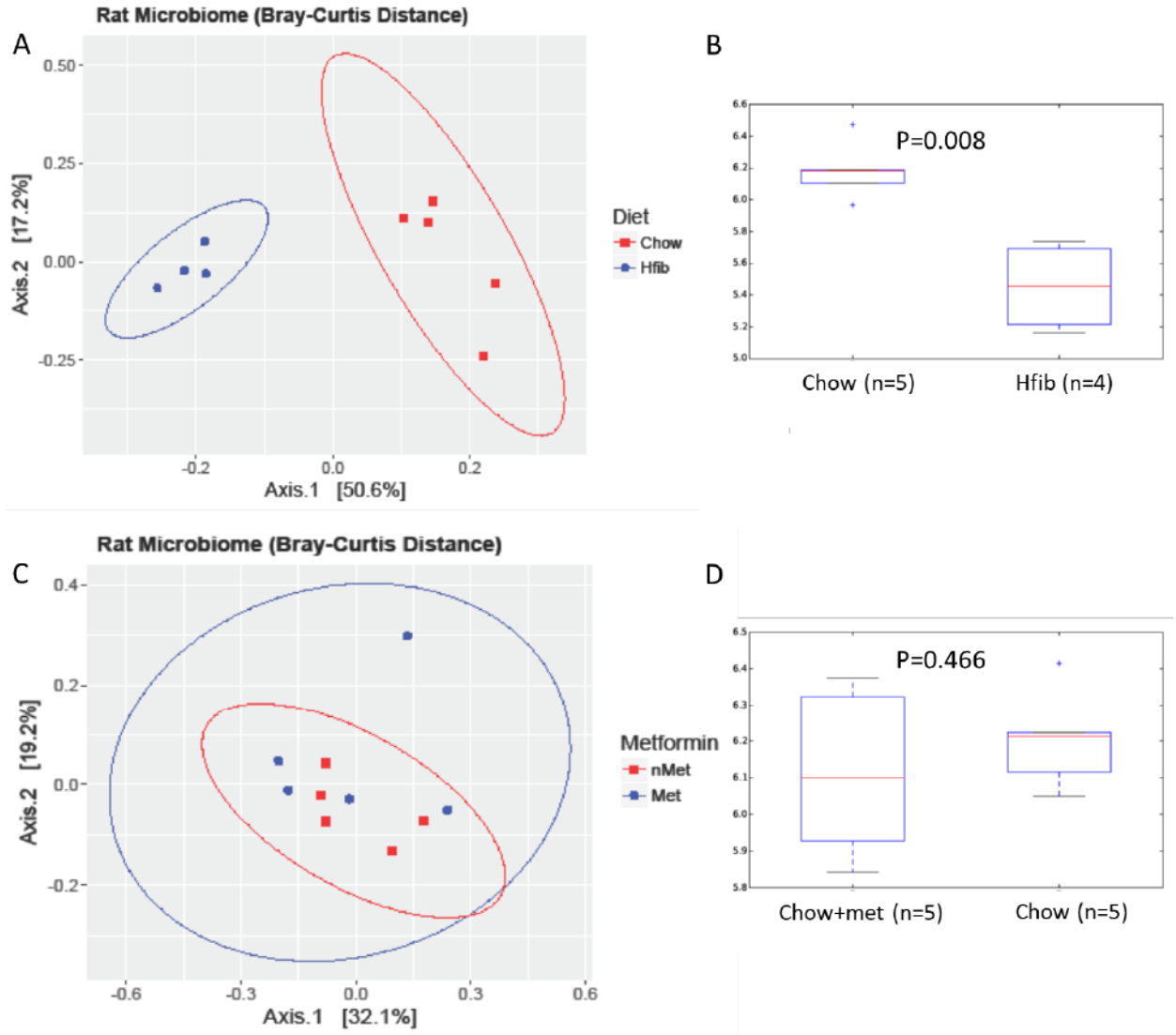

Figure 4-12 Gut microbial community structure affected by diet and metformin. A, C: Principle coordinate analysis (PCoA) plots of bacterial communities from NRs fed Hfib and Chow (A) or Chow NRs treated with metformin or not (C) using Bray-Curtis dissimilarity metrics; B, D: Alpha diversity Shannon's index showing species richness and evenness within the microbial community in Hfib and Chow (B) or Chow+met and Chow (D). $p<0.05$ indicates a significant difference.

4.4 Discussion

Progression of prediabetes depends on the interplay of insulin sensitivity and insulin secretion from β-cells (Meigs et al. 2003; Festa et al. 2006). As reviewed in Chapter 1.1, glucose homeostasis is maintained when β-cells successfully compensate for decreased insulin sensitivity, otherwise, impaired glucose tolerance occurs (Weir and Bonner-Weir 2004). In the present study, the majority of NRs fed with Chow diet demonstrated evident insulin resistance, enhanced insulin secretion and a glucose excursion close to healthy Hfib controls at 13 weeks, suggesting a compensation stage. As animals aged to 25 weeks, Chow NRs displayed the phenotype of decompensation with deteriorated insulin responsiveness and glucose intolerance. In addition to Hfib-diet intervention, metformin also delayed the progression of diabetes. After 7 weeks of treatment, glucose tolerance was improved concomitant with enhanced insulin secretion. At 25 weeks, although metformin did not reverse the prediabetes progression, it prevented the decompensation of Chow NRs by sustaining insulin compensation, ameliorating overall insulin sensitivity.

Metformin has been used to treat prediabetes and insulin resistance in numerous studies (Knowler et al. 2002, 2009; Linden et al. 2015; Wang et al. 2016; Tajima et al. 2017; Lentferink et al. 2018). Interestingly, most animal trials reported complete reversal of insulin resistance; whereas clinical trials showed a far less evident outcome with metformin (Turner et al. 1999; Knowler et al. 2002; Lentferink et al. 2018). Given that the effect of metformin is dose-dependent (Hirst et al. 2012), it is possible that the different efficacy is a result of the 10-fold higher dose used in animal studies, which is not applicable in clinical trials due to consideration of side effects (Flory and Lipska 2019). Herein, the use of metformin at a relatively low dose could represent a more realistic replication of the clinical situation.

Insulin resistance in the liver is a major cause of prediabetes (Escribano et al. 2009; Basu et al. 2013). Dysfunctional mitochondria and disrupted insulin signaling due to extra lipid metabolism lead to uncontrolled hepatic glucose production (Hegarty et al. 2009; Szendroedi et al. 2011); while metformin inhibits mitochondrial function, thereby activating AMPK, which switches off the gluconeogenic pathway (El-Mir et al. 2000; Owen et al. 2000; Zhou et al. 2001). Metformin also improves insulin signaling and counteracting the unopposed action of glucagon on the liver (Miller et al. 2013; An and He 2016). In the current study, the compromised activity of AMPK in Chow NR livers was restored with metformin in the fasting state. PKA was activated, probably in response to the marginal rise in circulating glucagon in 13-week Chow+met NRs, but failed to induce PEPCK and G6Pase, which may be neutralized by AMPK activation. The overall expression of gluconeogenic genes was unchanged, consistent with the similar ratios of glucagon/insulin in the fasting state. In the refed condition, PGC1α, a direct target of AMPK, insulin and glucagon signaling, was significantly downregulated at 13 weeks, accompanied by reduced G6Pase and PEPCK. It was noticed that the reduction of G6Pase and PEPCK in the metformin group was less evident at 25 weeks. In line with the declining glucose tolerance compared with 13 weeks, it implies imminent onset of metformin failure to control glucose at the current dose and the necessity to increase the dose for better glucose control. Of note, healthy NRs fed on Hfib diet demonstrate a high abundance of G6Pase and PEPCK throughout the study, reflecting an overall enhanced hepatic glucose production in NRs which could be a risk factor of glucose intolerance when switching to a high-energy and high refined carbohydrate diet like Chow.

In people, decreased food intake and weight loss are related to the glucose-lowering effect of metformin, the mechanism of which is linked to decreased appetite (Malin and Kashyap 2014). However, low dose metformin did not change the body weight of NRs, which may be attributed

to a lack of suppression of appetite. However, due to the feral behavior of NRs and the way they were fed in the study, I could not track their food intake, which is a limitation of the study.

I also observed preservation of β-cell GSIS in NRs treated with metformin, suggesting a beneficial effect of metformin on β-cell function. Defective β-cell insulin secretion is tightly correlated with the onset of prediabetes (Seino et al. 2011). Considering the increased systemic insulin secretion in GTT with metformin, I initially speculated an increase in β-cell function since I observed β-cell compensation concomitant with increased insulin secretion in the previous cohort (Chapter 3). On the contrary, the islets of Chow+met NRs at 13 weeks showed a decreased basal insulin secretion at 5.5 mM glucose compared to Chow and increased stimulated secretion at 16.5 mM glucose vs Hfib. In fact, this protective effect of metformin on β-cell function has been reported in human and rodent islets. *In vitro* treatment with 15-20 μM metformin, a dose that is close to the plasma metformin concentration in humans, restored a normal secretion pattern and insulin content in islets from T2D subjects or impaired by glucolipotoxicity (Lupi et al. 1999; Patanè et al. 2000; Marchetti et al. 2004). However, I did not detect any change in insulin secretion or content upon 24 h treatment of naïve NR islets with 20 μM metformin. The reason could be related to the initial functionality of the islets before treatment. The beneficial effect of metformin in dysfunctional islets was attributed to increasing insulin gene expression and reducing oxidative stress and apoptosis (Marchetti et al. 2004; Piro et al. 2012; Jiang et al. 2014). Hence, islets showing no apparent functional defects may not benefit from *in vitro* metformin at 20 μM. Indeed, islets and cells with intact function demonstrated a significant reduction of GSIS only when exposed to high doses of metformin at 1-5 mM (Leclerc et al. 2004; Lamontagne et al. 2009; Gelin et al. 2018), which was confirmed in the present study. In addition, the high dose is not achievable in vivo and may induce apoptosis (Choi et al. 2006; Gelin et al. 2018). Furthermore, the onset of

β-cell compensation in Chow+met NRs at 25 weeks suggests that the impact of metformin on β-cell function in vivo depends on the complex interplay of the metabolic profile and insulin demand in addition to any possible direct action on β-cell GSIS per se.

Given the differences observed in β-cell GSIS with *in vivo* metformin treatment, I examined some of the key factors that regulate insulin synthesis and glucose-sensing of β-cells (as reviewed in Chapter 1). Chow+met islets with sustained secretory capacity at 13 weeks demonstrated a low abundance of GLUT2 compared to other groups, indicating decreased glucose sensing. However, it is known that GLUT2 is not the only glucose transporter in β-cells and re-expression of GLUT1 in GLUT-null mice is sufficient to restore insulin secretion (Thorens et al. 2000). Therefore, more evidence is required to support the notion of altered glucose sensing. Also, increased pAMPK was present in β-cells at 13 weeks. It has been documented that upon the same glucose challenge, AMPK activation by the pharmacological inducer AICAR or overexpression leads to reduced insulin secretion (da Silva Xavier et al. 2003; Leclerc et al. 2004). Hence, the AMPK activation in Chow+met islet may mediate the improvement in insulin secretion. In comparison, β-cells at 25 weeks with increased GLUT2 and normal pAMPK exhibit enhanced β-cell insulin secretion in Chow+met islets.

Our previous study revealed that ER chaperones capacity increased concomitant with β-cell compensation (Chapter 3). However, β-cell ER chaperone colocalization with insulin in Chow+met did not change compared with the Chow group, notwithstanding the difference in β-cell function between groups. The comparable ER chaperone capacity is likely due to the elevated systemic insulin profile in Chow and metformin groups. Similarly, at 25 weeks, β-cells in Chow+met animals were compensating, but the plasma insulin decreased, which corresponds to the decreased ER chaperones. The lower plasma insulin could be a result of either β-cell

dysfunction or alleviated insulin demand. Since the β-cell GSIS at 25 weeks were not diminished, the lower value of insulin may indicate a reduction of insulin demand and better glucose control at least compared to Chow control. Moreover, the downregulation of apoptotic UPR factors *Chop* and *Bax* indicates reduced ER stress in β-cells with metformin.

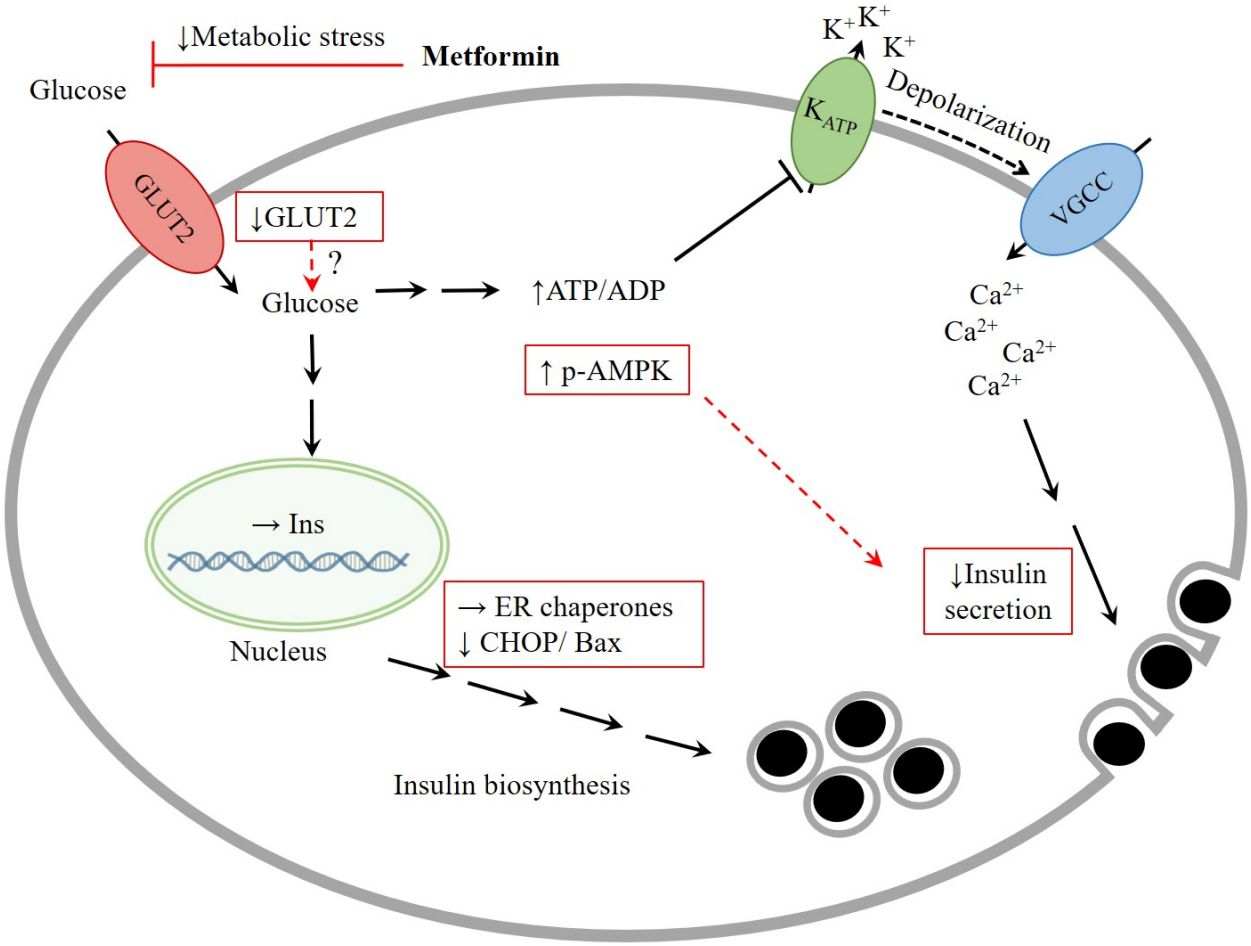

Figure 4-13 Summary of observations in Chow+met islets at 13 weeks. In islets isolated from Chow+met NRs, β-cells secretory capacity is maintained with reduced insulin secretion at basal and intermediate glucose concentrations compared with islets from age-matched Chow NRs. β-cells with restored function show a low abandance of GLUT2 and increased phophorylation of AMPK, suggesting changes in glucose uptake and cellular energy state. Insulin genes transcription and ER chaperone abundance are sustained in Chow+met β-cells, which is accompanied by decreased maladapative UPR markers.

Metformin is an old drug for diabetes but a new drug to treat cancer that was suggested by its ability to inhibit cell proliferation (Kato et al. 2012; Lord et al. 2018). However, the metformin impact on β-cell proliferation is controversial (Tajima et al. 2017; Wyett et al. 2018). In the current study, I did not detect any change in β-cell area between Chow and Chow+met groups. Additionally, β-cell proliferation was not affected by metformin and α-cell proliferation was increased. Evidence from a recent study revealed a relation between α-cell hyperplasia and impaired hepatic glucagon signaling (Dean et al. 2017), but whether metformin is a causal factor in α-cell proliferation requires further investigation.

Last but not least, although not a conventional target of metformin, the gut has been implicated as an important site of metformin actions (McCreight et al. 2016). One of the proposed actions on intestine is stimulation of GLP-1 secretion by direct and indirect means (Mulherin et al. 2011; Lien et al. 2014). However, no change of active plasma GLP-1was found in this study in metformin-treated NR, indicating a limited impact on insulin secretion. Total GLP-1 was not measured in the study; it is, therefore, not a conclusive answer to the question of total GLP-1 secretion. Aside from GLP-1, growing evidence implicates a supportive role for the microbiota in the mediation of therapeutic effects of metformin on diabetes (Forslund et al. 2015; Wu et al. 2017). The result of microbial composition structure was not significant with metformin. The preliminary data suggest that metformin effects on glucose control in this study were not through gut stimulation.

4.5 Conclusion

Overall, the present study demonstrates that metformin treatment of insulin-resistant, prediabetic NRs improves glucose tolerance, insulin secretion and overall insulin sensitivity,

which is accompanied by downregulated expressions of hepatic glucogenic enzymes. The observation of preserved β-cell secretion capacity at 13 weeks and delayed decompensation at 25 weeks in accordance with changes in glucose sensing indicates a protective role for metformin in the β-cell function that helps to delay the onset of overt diabetes. Additionally, metformin does not induce ER chaperone association with insulin granules or affect β-cell proliferation in order to elicit its effects. These observations of metformin effects are less likely to be mediated by actions on GLP-1 or gut microbiota. Taken together, these findings suggest that use of metformin does not exert a negative effect on β-cell function or cell mass, and instead, early metformin treatment may help protect β-cell from exhaustion and decompensation.

Chapter 5. General discussion and Future directions

5.1 Summary of hypotheses and main findings

The purpose of the current research was to understand the β-cell pathophysiology in the development of the naturally occurring T2D in NRs, investigate the impact of metformin intervention compared to low-calorie, high fiber diet on β-cell compensation and explore the possible mechanisms contributing to the preserved β-cell function by metformin. The main findings of the impact of diet and metformin on glucose homeostasis and the β-cell function are summarized as follows (Figure 5-1):

- Male NRs fed on Chow diet demonstrate normal glucose tolerance (NGT) and insulin resistant at 2 months, IGT with sustained insulin secretion at 6 months, and the onset of hyperglycemia at 12 months, concomitantly with development of β-cell compensation, decompensation, and dysfunction, respectively.
- Elevated plasma proinsulin relative to insulin at the decompensation stage indicates impaired insulin processing.
- The temporal correlation of adaptive ER chaperones, critical to insulin processing, with blood insulin suggests upregulated chaperone capacity as an adaptive mechanism in insulin secretion.
- β-cell neogenesis occurs during β-cell mass adaptation, whereas proliferation does not appear to the major event at compensation stage.
- Metformin, notwithstanding to a lesser extent compared with Hfib group, improves glucose tolerance, insulin secretion and alleviated insulin resistance in euglycemic but hyperinsulinemic NRs.

- Metformin activates AMPK and inhibits the hepatic gluconeogenic pathway. Of note, Hfib-fed NRs have a high abundance of hepatic gluconeogenic enzymes.
- Metformin preserves β-cell function and delays the decompensation phase without inducing apoptotic ER stress or altering β-cell mass and proliferation.
- Intervention with Hfib diet, but not metformin, alters the gut microbiota composition. However, plasma active GLP-1shows no change between groups.

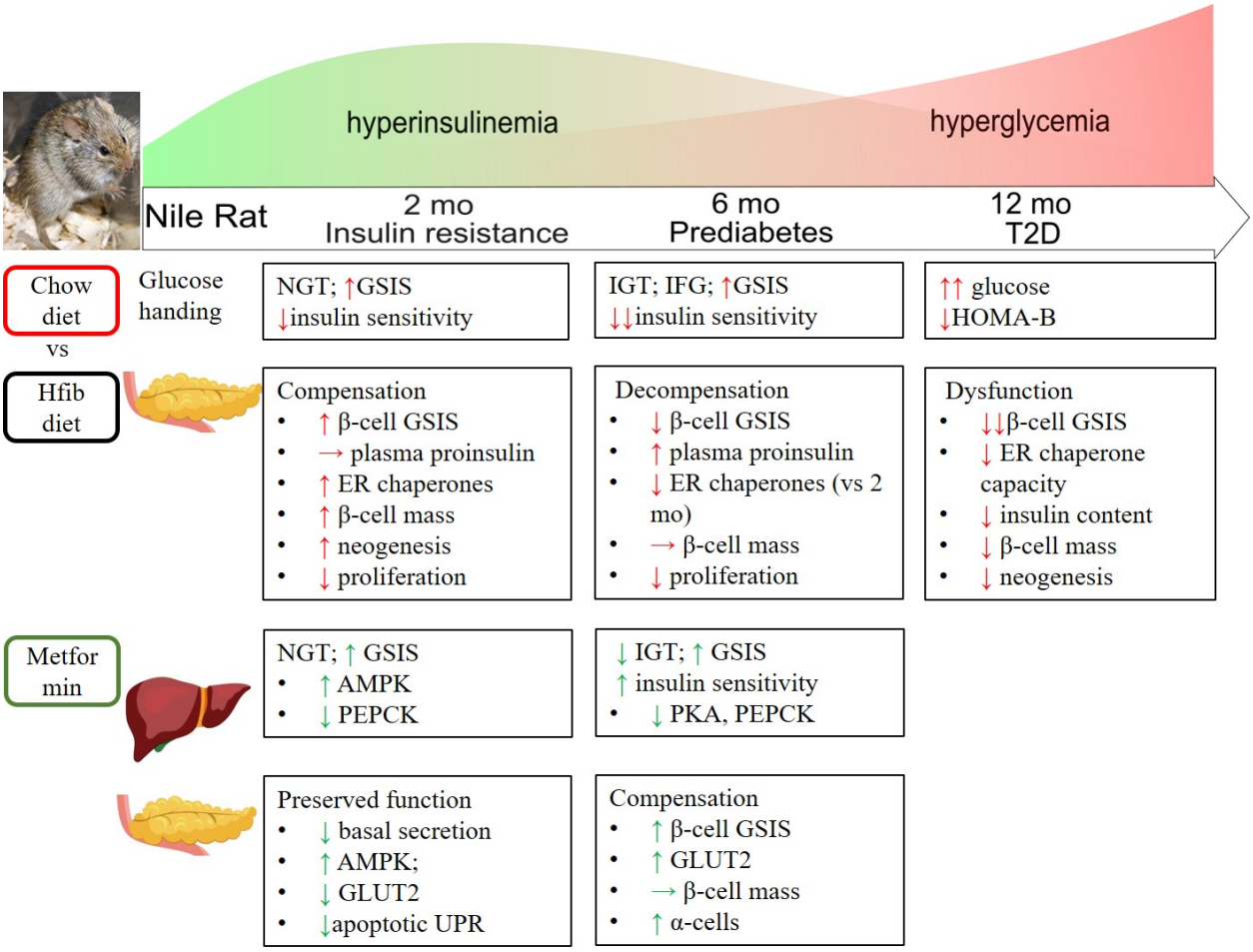

Figure 5-1 Summary of key findings of the current study.

5.2 NR as a model for β-cell compensation and decompensation

Since the NR was suggested as a model for T2D (Chaabo et al. 2010; Noda et al. 2010), it has been used to evaluate diet components and nutrients on T2D development (Bolsinger et al. 2013, 2014, 2017). NR merits attention for similar etiology and disease progression to human T2D (Bolsinger et al. 2013). However, the pathophysiology of this model is less known.

Our previous study showing β-cell mass adaption in Chow-fed NRs before the onset of T2D suggests the possibility of β-cell compensation in early T2D (Yang et al. 2016). Herein, the results of chapter 3 experiments indicate that, in addition to cell mass, β-cell function is compensated by enhancing insulin secretion at the euglycemic hyperinsulinemic stage. The results of tolerance tests revealed that NRs at this stage exhibited impaired insulin sensitivity but NGT which could be due to the 2-fold increase in GSIS that could be attributed to both enhanced β-cell secretion capacity and expanded β-cell mass (Yang et al. 2016). Insulin-resistant NRs with NGT appear to correspond to obese/insulin-resistant but not diabetic subjects in human studies (Butler et al. 2003a; Rahier et al. 2008; Hanley et al. 2010), and allow us to gain insight into the islet function at this stage. Similarly, NRs at 6 months demonstrating IGT and/or IFG with a flat curve of insulin secretion represents the phenotype of human prediabetes. β-cells at 6 months failed to compensate without loss of β-cell mass (Yang et al. 2016). Hence, it is plausible that the sluggish curve of insulin secretion is more related to declining β-cell function than insufficient number of β-cells. This 6-month-old time point is important in the study for illustrating the transition of compensation to decompensation of β-cells. In Chapter 4, the results of animal phenotype and β-cell secretion capacity in Chow NRs are consistent with the pattern observed in Chapter 3, which further validates NR for being a model for β-cell compensation.

5.2.1 ER chaperones in β-cell compensation

Taking advantage of the age-related disease progression in NR, I sought to examine some of the proteins that are related to insulin processing in β-cells at each stage. Plasma proinsulin relative to insulin increased exclusively at 6 months, suggesting a defect in insulin processing by β-cells (Wareham et al. 1999; Pfützner and Forst 2011). Also, the over 10-fold increase in proinsulin production at 6 months is likely due to a surge of insulin biosynthesis driven by increased glucose (Andrali et al. 2008), which could place a great pressure on the ER (Feige and Hendershot 2011). In response to stress, ER chaperones are unregulated to ensure sufficient capacity for protein processing (Eizirik et al. 2008; Scheuner and Kaufman 2008). In NRs, although the abundance of each ER chaperone varied, the overall chaperone capacity in β-cells declined at decompensation and T2D stages, linking failure of ER chaperones and β-cell decompensation (Omikorede et al. 2013; Chan et al. 2013). Also, the positive correlation of PDI with circulating insulin concentration implies a positive role of PDI in insulin secretion as hypothesized by others (Montane et al. 2016). One limitation of the study is that the pancreatic tissue was collected from fasted animals; it could not reflect the ER chaperone capacity upon high glucose challenge, which could be of great importance to β-cell function.

5.2.2 Mechanisms of β-cell mass adaptation

Another key finding reported in Chapter 3 is the unexpected decrease in β-cell proliferation and the increase in neogenesis. A slight increase in β-cell mass was reported in the previous study. Therefore, I initially hypothesized that NRs at the compensation stage would have a higher number of proliferating β-cell cells. However, the β-cell proliferation rate at the

compensation stage was lower than 0.2% and significantly decreased compared with Hfib, a finding which was verified in Chapter 4. Despite the fact that proliferation is one of the primary mechanisms of β-cell expansion in rodent models (Skau et al. 2001; Bock et al. 2003), β-cell replication is very rare in adult human pancreas (Butler et al. 2003a; Hanley et al. 2010), and restricted with aging (Tschen et al. 2009). It is possible that β-cell proliferation occurs before the evident insulin compensation as indicated by the presence of a 50% increase in β-cell area by 2 months of age (Yang et al. 2016).

Besides, Chapter 3 also reported a 5-fold increase in β-cell area in compensating NRs arising from small insulin-positive clusters, which was determined using a surrogate definition of neogenesis (Hanley et al. 2010). The increase in number of these small clusters in the ductal epithelium or abutting the ducts in Chow NRs implies neogenesis could also underly their β-cell mass adaption. Neogenesis has been widely reported in human as a major mechanism of β-cell expansion (Butler et al. 2003a; Meier et al. 2008; Hanley et al. 2010). In future studies, it would be useful to further confirm the identity of the insulin-positive cells by co-labeling with ductal cell markers (Gao et al. 2003; Dadheech et al. 2018).

As summarized in Figure 1-4, β-cell hypertrophy and transdifferentiation can also contribute to β-cells expansion (Meier et al. 2008; Cigliola et al. 2016); however, previous study (Yang et al. 2016) and data in Chapter 3 showed no change in β-cell size or evidence of trans-differentiation at 2 and 6 months. Instead, I observed β-cell dedifferentiation at 12 months, which may be associated with the increased α/β-cell ratio previously observed at that time period (Yang et al. 2016).

5.3 Metformin actions in prediabetic NRs

Evidence from recent studies showing that dietary modification helps prevent or delay T2D in NRs suggests NR as an effective model to study the influence of dietary factors on T2D control (Bolsinger et al. 2013, 2014, 2017). Notwithstanding, how NRs respond to pharmacological approaches to prevent or treat T2D is unknown. Data collected from the DPP revealed that, in addition to lifestyle change, metformin could slow T2D progression by alleviating IGT and normalizing insulin secretion (Knowler et al. 2002; Kitabchi et al. 2005). Therefore, I hypothesized that metformin treatment of NRs during the compensation stage could block the onset of β-cell decompensation and prediabetes. However, results in Chapter 4 show that metformin slightly improved GTT and ITT but did not reduce the systemic insulin secretion, indicating NRs are still insulin resistant. One reason could be related to the dose of metformin. As discussed in Chapter 4, the effect of metformin is dose-dependent (Hirst et al. 2012), and a dose (20 mg/kg) mimicking the clinical use of metformin appears to not fully reverse the insulin resistance. However, in the pilot study to determine an optimal dose, the response of NR to 50 mg/kg was highly heterogeneous and thus was not selected for this trial.

I examined the AMPK signaling pathway as a key regulator of liver metabolism and showed that AMPK activation and downregulated hepatic glucogenic pathways with metformin as expected. Akt, however, exhibited no change in phosphorylation between groups, notwithstanding the elevated insulin concentration. This result reinforces the *in vivo* observation in Chapter 4 that metformin-treated NRs are still insulin resistant albeit with a modestly improved GTT.

One interesting finding is that the healthy Hfib controls exhibited a high abundance of PEPCK and G6Pase in the liver, which implies active hepatic glucose production. When living in

the wild where food is limited or when fed with a low caloric diet like Hfib, active hepatic glucose production could serve as a pro-survival mechanism to allow efficient use of energy, create glucose from non-glucose sources and protect from starvation. Moreover, increased glucogenic enzymes in the Hfib NRs could be driven by a change in insulin, i.e. Hfib diet triggers less insulin secretion, which in turn allows for activation of glucogenic pathways in the liver. The chow diet (which is high in carbohydrate), likely triggers a higher overall insulin concentration, which suppresses glucogenesis in the liver. Obesity, likely driven by greater lipogenesis, may also be a result of the more energy-rich diet driving higher insulin. The dramatic response to the environment and dietary factors is reminiscent of the obesity and insulin-resistance in sand rats, another model for spontaneous T2D (Collier et al. 1997). Although there is a lack of direct evidence, T2D in NR could be a result of the genetic susceptibility to environmental factors (Subramaniam et al. 2018).

5.3.1 Effect of metformin on β-cells

The impact of metformin on β-cell function is controversial (Piro et al. 2012; Lamontagne et al. 2017). The findings regarding β-cell function in Chapter 4 indicate that metformin protects β-cells from dysfunction. Compared to β-cells in Chow NRs, the progression of β-cell dysfunction was delayed with metformin intervention. A noticeable increase in phosphorylated AMPK and decrease in GLUT2 was present in islets with preserved insulin secretion capacity. The evidence so far is not conclusive as discussed in Chapter 4.4, but there is a possibility that the reduced basal insulin secretion seen in β-cell GSIS is associated with decreased glucose sensing and low cellular energy state (Oakhill et al. 2011).

Since I could not repeat the results from studies showing metformin alleviates β-cell function *in vitro*, the protective action of metformin on β-cells may be in part via an indirect mechanism. Therefore, I explored several proposed effects of metformin such as GLP-1 or gut microbiota (Mulherin et al. 2011; Wu et al. 2017); no significant changes were found, indicating the effect of metformin on insulin secretion is not likely via actions on gut microbiota or GLP-1.

5.4 Limitations and future directions

5.4.1 Animal model

A major shortcoming of NRs is that they are feral and not tame like commercial lab rats, which makes them difficult to handle and almost impossible to conduct *in vivo* experiments on without anesthesia. Therefore, for the GTT/ITT/PTT the NRs were anesthetized with isoflurane, which may inhibit insulin secretion (Tanaka et al. 2011). Although negative control animals without glucose injection showed higher but stable blood glucose throughout the GTT, the missing peak of insulin secretion in NRs at 30 minutes of the GTT could be related to isoflurane administration.

Another factor is that as a small colony with a limited number of breeders, our NR colony does undergo inbreeding with some negative consequences, i.e. reduced reproductive ability and colony drift. The insufficient number of animals, especially for NR with significant heterogeneity, could limit statistical power. Introduction of breeding animals from other NR colonies may help to address this issue.

On the other hand, the heterogeneity of NR could help identify risk loci of T2D. Given the assumption that the T2D present in NRs is partially from the interaction of natural genetic

susceptibility to environmental stressors, genotyping of the fast and slow progressors would help identify T2D susceptibility loci, shedding light on the genetic regulation underlying the complex traits of diabetes (Bihoreau et al. 2017).

5.4.2 Experimental design

The glucose-lowering effect of metformin is mainly via reducing glucose output. In this study, PTT was used to assess gluconeogenesis; however, glucose derived from pyruvate cannot reflect the overall glucose output, which consists of gluconeogenesis from other substrates and glycogenolysis. As an alternative, the hyperinsulinemic euglycemic clamp would be more accurate in assessing hepatic glucose output.

In Chapter 4, we observed changes in total GLUT2 expression, which links the improved β-cell function with metformin treatment to glucose sensing. However, it is the GLUT2 located on the plasma membrane that serves as glucose transporter. For this reason, the abundance of membrane GLUT2 should be measured by either immunostaining or immunoblotting of membrane proteins.

For the effect of metformin on GLP-1, active GLP-1 was measured in blood samples collected 4-hour after refeeding. It is worth noting that active GLP-1 is rapidly inactivated after secretion. Therefore, to better assess the postprandial GLP-1 secretion, active GLP-1 should be measured within 2 hours after feeding or during the oral glucose tolerance test (Sukumar et al. 2018).

5.4.3 Mechanism and interpretation

In chapter 3, the results suggest that increased capacity of ER chaperones may help in insulin secretion. It is not conclusive without investigating:

i) the effect of chemical chaperones *in vivo* on systemic insulin secretion;

ii) changes in β-cell chaperone abundance as well as the adaptive UPR upon glucose challenge;

iii) the impact of ER chaperone inhibition on β-cell insulin secretion.

Moreover, it is speculated that impaired insulin processing concomitantly with β-cell decompensation leads to an increase in proinsulin. It is documented that decreased PC1/3 resulted in increased proinsulin in T2D (Zhu et al. 2002; Ozawa et al. 2014), therefore assessment of PC1/3 would provide more insight into the β-cells' ability to process insulin at different T2D stages.

For the mechanisms proposed for β-cell mass adaption, the preliminary results suggest that neogenesis may contribute to β-cell expansion. To further confirm the existence of neogenic cells, co-staining of insulin with ductal cell markers such as cytokeratin or stem cell marker nestin will be necessary (Hanley et al. 2010; Mezza et al. 2014). Although the results of ki67 staining do not support proliferation as a mechanism of β-cell mass adaption, the area of neogenic β-cells decreased after compensation, which suggests a possibility of expansion of new β-cells. Therefore, it is possible that proliferation could occur at or after the compensation stage. In addition, to avoid the influence of tissue processing on ki67 staining, administration of BrdU *in vivo* could be used to assess cell proliferation (Wang et al. 2015).

In chapter 4, I first sought to investigate the response of NR to metformin intervention. Because of the distinct expression pattern of hepatic glucogenic enzymes induced by Chow and

Hfib diet, treating Hfib NRs with metformin will provide more information about the effect of metformin vs diet on glucose control in NR.

Regarding the metformin action on β-cell function, mechanisms of the protective effect are mostly unknown. Based on the evidence in this study, it is suggested that future investigations focus on:

i) β-cell glucose metabolism, including the mitochondrial membrane potential, oxygen consumption, and cellular ATP content (Lamontagne et al. 2009).
ii) The cellular content of reactive oxygen species to determine oxidative stress.
iii) Impact of AMPK activation/ inhibition on β-cell GSIS upon basal and stimulated glucose challenges.
iv) The difference of metformin action on insulin secretion in β-cell at compensation, decompensation, and dysfunctional stages.

5.5 Implications and Conclusions

The studies in this thesis contribute to the understanding of diabetes progression and β-cell function in several ways. Besides demonstrating the natural course of T2D in NRs, I observe a serial change of β-cell function along with the disease progression. The persistent functional compensation before the onset of prediabetes emphasizes the importance of β-cell secretion capacity in diabetes prevention. Also, the correlation of ER chaperone localization with insulin secretion indicates a possible target in the maintenance of β-cell function, which may benefit people at high risk of T2D and reduce the chance of developing T2D due to β-cell exhaustion or decompensation. Moreover, formation of new β-cell clusters seems to be the major mechanism underling β-cell mass adaptation in NRs. Therefore, a thorough understanding of the cellular

basis and the regulation of neogenesis may be of great importance to β-cell mass restoration that could be undertaken in NR. The metformin trial on NRs in the thesis demonstrates an example of evaluating the effect of pharmacological approaches on T2D model that mimics human diabetes traits and also allows insight into the mechanism. Findings in this study indicate that the dose of metformin may be a determining factor of glucose-lowering effect and early treatment of metformin certainly helps in diabetes prevention. Also, long-term exposure of metformin does not further deteriorate β-cell secretion but protects β-cells from decompensation. The mechanism of the protective effect may be related to tight regulation of glucose or lipid metabolism, alleviating secretion abnormalities and exhaustion of β-cells due to glucolipotoxicity.

In summary, findings from this thesis demonstrated a model showing traits of human β-cell compensation and decompensation involving cell function and mass. The enhanced β-cell insulin secretion was correlated with upregulated ER chaperones and co-localization with insulin granules, which decreased with T2D progression. β-cell mass adaption is more associated with the formation of new β-cells rather than proliferation. Evidence showing co-existence of α/β-cell markers at the β-cell dysfunction stage indicates dedifferentiation may be involved in β-cell failure. This T2D progression demonstrated in NRs can be prevented by Hfib diet intervention, or regulated by pharmacological intervention. Early treatment with metformin improves glucose tolerance with downregulated expression of hepatic glucogenic enzymes. Metformin also plays a protective role in β-cell function and delays decompensation in accordance with changes in glucose sensing. The effect is likely elicited indirectly, but not via GLP-1 or gut microbiota. Lastly, metformin does not exert negative effects on β-cell such as pro-apoptotic UPR or suppression of cell proliferation.

Bibliography

Abdul-Ghani, M.A., Tripathy, D., and DeFronzo, R.A. 2006. Contributions of beta-cell dysfunction and insulin resistance to the pathogenesis of impaired glucose tolerance and impaired fasting glucose. Diabetes Care **29**(5): 1130–9. doi:10.2337/diacare.2951130.

Accili, D. 2004. Lilly lecture 2003: the struggle for mastery in insulin action: from triumvirate to republic. Diabetes **53**(7): 1633–42.

Accili, D., and Arden, K.C. 2004. FoxOs at the crossroads of cellular metabolism, differentiation, and transformation. Cell **117**(4): 421–6.

Aguayo-Mazzucato, C., and Bonner-Weir, S. 2018. Pancreatic β Cell Regeneration as a Possible Therapy for Diabetes. Cell Metab. **27**(1): 57–67. doi:10.1016/j.cmet.2017.08.007.

Aleixandre de Artiñano, A., and Miguel Castro, M. 2009. Experimental rat models to study the metabolic syndrome. Br. J. Nutr. **102**(9): 1246–53. doi:10.1017/S0007114509990729.

American Diabetes Association. 2014. Diagnosis and Classification of Diabetes Mellitus. Diabetes Care **37**(Supplement_1): S81–S90. doi:10.2337/dc14-S081.

An, H., and He, L. 2016. Current understanding of metformin effect on the control of hyperglycemia in diabetes. J. Endocrinol. **228**(3): R97–R106. doi:10.1530/JOE-15-0447.

Andrali, S.S., Sampley, M.L., Vanderford, N.L., and Ozcan, S. 2008. Glucose regulation of insulin gene expression in pancreatic beta-cells. Biochem. J. **415**(1): 1–10. doi:10.1042/BJ20081029.

Anello, M., Lupi, R., Spampinato, D., Piro, S., Masini, M., Boggi, U., Del Prato, S., Rabuazzo, A.M., Purrello, F., and Marchetti, P. 2005. Functional and morphological alterations of mitochondria in pancreatic beta cells from type 2 diabetic patients. Diabetologia **48**(2): 282–9. doi:10.1007/s00125-004-1627-9.

Aroda, V.R., Knowler, W.C., Crandall, J.P., Perreault, L., Edelstein, S.L., Jeffries, S.L., Molitch, M.E., Pi-Sunyer, X., Darwin, C., Heckman-Stoddard, B.M., Temprosa, M., Kahn, S.E., Nathan, D.M., and Diabetes Prevention Program Research Group. 2017. Metformin for diabetes prevention: insights gained from the Diabetes Prevention Program/Diabetes Prevention Program Outcomes Study. Diabetologia **60**(9): 1601–1611. doi:10.1007/s00125-017-4361-9.

Bahne, E., Sun, E.W.L., Young, R.L., Hansen, M., Sonne, D.P., Hansen, J.S., Rohde, U., Liou, A.P., Jackson, M.L., de Fontgalland, D., Rabbitt, P., Hollington, P., Sposato, L., Due, S., Wattchow, D.A., Rehfeld, J.F., Holst, J.J., Keating, D.J., Vilsbøll, T., and Knop, F.K. 2018. Metformin-induced glucagon-like peptide-1 secretion contributes to the actions of metformin in type 2 diabetes. JCI insight **3**(23). doi:10.1172/jci.insight.93936.

Bailey, C.J. 1992. Biguanides and NIDDM. Diabetes Care **15**(6): 755–72. doi:10.2337/diacare.15.6.755.

Bailey, C.J., and Turner, R.C. 1996. Metformin. N. Engl. J. Med. **334**(9): 574–9. doi:10.1056/NEJM199602293340906.

Basu, R., Barosa, C., Jones, J., Dube, S., Carter, R., Basu, A., and Rizza, R.A. 2013. Pathogenesis of Prediabetes: Role of the Liver in Isolated Fasting Hyperglycemia and Combined Fasting and Postprandial Hyperglycemia. J. Clin. Endocrinol. Metab. **98**(3): E409–E417. doi:10.1210/jc.2012-3056.

Bauer, P. V, Duca, F.A., Waise, T.M.Z., Rasmussen, B.A., Abraham, M.A., Dranse, H.J., Puri, A., O'Brien, C.A., and Lam, T.K.T. 2018. Metformin Alters Upper Small Intestinal Microbiota that Impact a Glucose-SGLT1-Sensing Glucoregulatory Pathway. Cell Metab. **27**(1): 101-117.e5. doi:10.1016/j.cmet.2017.09.019.

Beagley, J., Guariguata, L., Weil, C., and Motala, A.A. 2014. Global estimates of undiagnosed diabetes in adults. Diabetes Res. Clin. Pract. **103**(2): 150–60. Elsevier Ireland Ltd. doi:10.1016/j.diabres.2013.11.001.

Bernal-Mizrachi, E., Kulkarni, R.N., Scott, D.K., Mauvais-Jarvis, F., Stewart, A.F., and Garcia-Ocaña, A. 2014. Human β-cell proliferation and intracellular signaling part 2: still driving in the dark without a road map. Diabetes **63**(3): 819–31. doi:10.2337/db13-1146.

Bhansali, S., Bhansali, A., and Dhawan, V. 2017a. Favourable metabolic profile sustains mitophagy and prevents metabolic abnormalities in metabolically healthy obese individuals. Diabetol. Metab. Syndr. **9**: 99. doi:10.1186/s13098-017-0298-x.

Bhansali, S., Bhansali, A., Walia, R., Saikia, U.N., and Dhawan, V. 2017b. Alterations in Mitochondrial Oxidative Stress and Mitophagy in Subjects with Prediabetes and Type 2 Diabetes Mellitus. Front. Endocrinol. (Lausanne). **8**: 347. doi:10.3389/fendo.2017.00347.

Bihoreau, M.-T., Dumas, M.-E., Lathrop, M., and Gauguier, D. 2017. Genomic regulation of type 2 diabetes endophenotypes: Contribution from genetic studies in the Goto-Kakizaki rat. Biochimie **143**: 56–65. doi:10.1016/j.biochi.2017.08.012.

Bock, T., Pakkenberg, B., and Buschard, K. 2003. Increased islet volume but unchanged islet number in ob/ob mice. Diabetes **52**(7): 1716–22.

Boland, B.B., Rhodes, C.J., and Grimsby, J.S. 2017. The dynamic plasticity of insulin production in β-cells. Mol. Metab. **6**(9): 958–973. doi:10.1016/j.molmet.2017.04.010.

Bolsinger, J., Landstrom, M., Pronczuk, A., Auerbach, A., and Hayes, K.C. 2017. Low glycemic load diets protect against metabolic syndrome and Type 2 diabetes mellitus in the male Nile rat. J. Nutr. Biochem. **42**: 134–148. doi:10.1016/j.jnutbio.2017.01.007.

Bolsinger, J., Pronczuk, A., and Hayes, K.C. 2013. Dietary carbohydrate dictates development of Type 2 diabetes in the Nile rat. J. Nutr. Biochem. **24**(11): 1945–1952. Elsevier Inc. doi:10.1016/j.jnutbio.2013.06.004.

Bolsinger, J., Pronczuk, A., Sambanthamurthi, R., and Hayes, K.C. 2014. Anti-diabetic effects of palm fruit juice in the Nile rat (Arvicanthis niloticus). J. Nutr. Sci. **3**: e5. doi:10.1017/jns.2014.3.

Bonner-Weir, S., Guo, L., Li, W.-C., Ouziel-Yahalom, L., Lysy, P.A., Weir, G.C., and Sharma, A. 2012. Islet neogenesis: a possible pathway for beta-cell replenishment. Rev. Diabet. Stud. **9**(4): 407–16. doi:10.1900/RDS.2012.9.407.

Bonner-Weir, S., Trent, D.F., and Weir, G.C. 1983. Partial pancreatectomy in the rat and subsequent defect in glucose-induced insulin release. J. Clin. Invest. **71**(6): 1544–53.

Braun, M., Ramracheya, R., Bengtsson, M., Zhang, Q., Karanauskaite, J., Partridge, C., Johnson, P.R., and Rorsman, P. 2008. Voltage-gated ion channels in human pancreatic beta-cells: electrophysiological characterization and role in insulin secretion. Diabetes **57**(6): 1618–28. doi:10.2337/db07-0991.

Braun, M., Ramracheya, R., Johnson, P.R., and Rorsman, P. 2009. Exocytotic properties of human pancreatic beta-cells. Ann. N. Y. Acad. Sci. **1152**: 187–93. doi:10.1111/j.1749-6632.2008.03992.x.

Brewer, J.W. 2014. Regulatory crosstalk within the mammalian unfolded protein response. Cell. Mol. Life Sci. **71**(6): 1067–1079. doi:10.1007/s00018-013-1490-2.

Brown, A.E., and Walker, M. 2016. Genetics of Insulin Resistance and the Metabolic Syndrome. Curr. Cardiol. Rep. **18**(8): 75. doi:10.1007/s11886-016-0755-4.

Buettner, R., Parhofer, K.G., Woenckhaus, M., Wrede, C.E., Kunz-Schughart, L.A., Schölmerich, J., and Bollheimer, L.C. 2006. Defining high-fat-diet rat models: metabolic and molecular effects of different fat types. J. Mol. Endocrinol. **36**(3): 485–501. doi:10.1677/jme.1.01909.

Burke, S.J., Batdorf, H.M., Burk, D.H., Noland, R.C., Eder, A.E., Boulos, M.S., Karlstad, M.D., and Collier, J.J. 2017. db/db Mice Exhibit Features of Human Type 2 Diabetes That Are Not Present in Weight-Matched C57BL/6J Mice Fed a Western Diet. J. Diabetes Res. **2017**: 8503754. doi:10.1155/2017/8503754.

Butler, A.E., Janson, J., Bonner-Weir, S., Ritzel, R., Rizza, R.A., and Butler, P.C. 2003a. Beta-cell deficit and increased beta-cell apoptosis in humans with type 2 diabetes. Diabetes **52**(1): 102–10.

Butler, A.E., Janson, J., Soeller, W.C., and Butler, P.C. 2003b. Increased beta-cell apoptosis prevents adaptive increase in beta-cell mass in mouse model of type 2 diabetes: evidence for role of islet amyloid formation rather than direct action of amyloid. Diabetes **52**(9): 2304–2314. United States.

Cadavez, L., Montane, J., Alcarraz-Vizán, G., Visa, M., Vidal-Fàbrega, L., Servitja, J.-M., and Novials, A. 2014. Chaperones ameliorate beta cell dysfunction associated with human islet amyloid polypeptide overexpression. PLoS One **9**(7): e101797. doi:10.1371/journal.pone.0101797.

Calabuig-Navarro, V., Yamauchi, J., Lee, S., Zhang, T., Liu, Y.-Z., Sadlek, K., Coudriet, G.M., Piganelli, J.D., Jiang, C.-L., Miller, R., Lowe, M., Harashima, H., and Dong, H.H. 2015. Forkhead Box O6 (FoxO6) Depletion Attenuates Hepatic Gluconeogenesis and Protects against Fat-induced Glucose Disorder in Mice. J. Biol. Chem. **290**(25): 15581–94. doi:10.1074/jbc.M115.650994.

Calderari, S., Gangnerau, M.-N., Thibault, M., Meile, M.-J., Kassis, N., Alvarez, C., Portha, B., and Serradas, P. 2007. Defective IGF2 and IGF1R protein production in embryonic pancreas precedes beta cell mass anomaly in the Goto-Kakizaki rat model of type 2

diabetes. Diabetologia **50**(7): 1463–71. doi:10.1007/s00125-007-0676-2.

Camastra, S., Manco, M., Mari, A., Baldi, S., Gastaldelli, A., Greco, A. V, Mingrone, G., and Ferrannini, E. 2005. beta-cell function in morbidly obese subjects during free living: long-term effects of weight loss. Diabetes **54**(8): 2382–9.

Cameron, D.P., Opat, F., and Insch, S. 1974. Studies of immunoreactive insulin secretion in NZO mice in vivo. Diabetologia **10 Suppl**: 649–54.

Chaabo, F., Pronczuk, A., Maslova, E., and Hayes, K. 2010. Nutritional correlates and dynamics of diabetes in the Nile rat (Arvicanthis niloticus): a novel model for diet-induced type 2 diabetes and the metabolic syndrome. Nutr. Metab. (Lond). **7**: 29. doi:10.1186/1743-7075-7-29.

Chambers, E.S., Preston, T., Frost, G., and Morrison, D.J. 2018. Role of Gut Microbiota-Generated Short-Chain Fatty Acids in Metabolic and Cardiovascular Health. Curr. Nutr. Rep. **7**(4): 198–206. doi:10.1007/s13668-018-0248-8.

Chan, C.B. 1993. Glucokinase activity in isolated islets from obese fa/fa Zucker rats. Biochem. J. **295 (Pt 3**: 673–7.

Chan, J.Y., Luzuriaga, J., Bensellam, M., Biden, T.J., and Laybutt, D.R. 2013. Failure of the adaptive unfolded protein response in islets of obese mice is linked with abnormalities in β-cell gene expression and progression to diabetes. Diabetes **62**(5): 1557–68. doi:10.2337/db12-0701.

Chassaing, B., Miles-Brown, J., Pellizzon, M., Ulman, E., Ricci, M., Zhang, L., Patterson, A.D., Vijay-Kumar, M., and Gewirtz, A.T. 2015. Lack of soluble fiber drives diet-induced adiposity in mice. Am. J. Physiol. Gastrointest. Liver Physiol. **309**(7): G528-41. doi:10.1152/ajpgi.00172.2015.

Chen, C., Chmelova, H., Cohrs, C.M., Chouinard, J.A., Jahn, S.R., Stertmann, J., Uphues, I., and Speier, S. 2016. Alterations in β-Cell Calcium Dynamics and Efficacy Outweigh Islet Mass Adaptation in Compensation of Insulin Resistance and Prediabetes Onset. Diabetes **65**(9): 2676–2685. doi:10.2337/db15-1718.

Chen, H., Charlat, O., Tartaglia, L.A., Woolf, E.A., Weng, X., Ellis, S.J., Lakey, N.D., Culpepper, J., Moore, K.J., Breitbart, R.E., Duyk, G.M., Tepper, R.I., and Morgenstern, J.P. 1996. Evidence that the diabetes gene encodes the leptin receptor: identification of a mutation in the leptin receptor gene in db/db mice. Cell **84**(3): 491–5.

Chen, Y., and Brandizzi, F. 2013. IRE1: ER stress sensor and cell fate executor. Trends Cell Biol. **23**(11): 547–55. doi:10.1016/j.tcb.2013.06.005.

Cho, H. 2001. Insulin Resistance and a Diabetes Mellitus-Like Syndrome in Mice Lacking the Protein Kinase Akt2 (PKBbeta). Science (80-.). **292**(5522): 1728–1731. doi:10.1126/science.292.5522.1728.

Cho, N.H., Shaw, J.E., Karuranga, S., Huang, Y., da Rocha Fernandes, J.D., Ohlrogge, A.W., and Malanda, B. 2018. IDF Diabetes Atlas: Global estimates of diabetes prevalence for 2017 and projections for 2045. *In* Diabetes research and clinical practice. doi:10.1016/j.diabres.2018.02.023.

Choi, S.-E., Lee, Y.-J., Jang, H.-J., Lee, K.-W., Kim, Y.-S., Jun, H.-S., Kang, S.S., Chun, J., and Kang, Y. 2008. A chemical chaperone 4-PBA ameliorates palmitate-induced inhibition of glucose-stimulated insulin secretion (GSIS). Arch. Biochem. Biophys. **475**(2): 109–14. doi:10.1016/j.abb.2008.04.015.

Choi, Y.H., Kim, S.G., and Lee, M.G. 2006. Dose-independent pharmacokinetics of metformin in rats: Hepatic and gastrointestinal first-pass effects. J. Pharm. Sci. **95**(11): 2543–52. doi:10.1002/jps.20744.

Cigliola, V., Thorel, F., Chera, S., and Herrera, P.L. 2016. Stress-induced adaptive islet cell identity changes. Diabetes. Obes. Metab. **18 Suppl 1**: 87–96. doi:10.1111/dom.12726.

Collier, G.R., De Silva, A., Sanigorski, A., Walder, K., Yamamoto, A., and Zimmet, P. 1997. Development of obesity and insulin resistance in the Israeli sand rat (Psammomys obesus). Does leptin play a role? Ann. N. Y. Acad. Sci. **827**: 50–63.

Cooper, G.J., Willis, A.C., Clark, A., Turner, R.C., Sim, R.B., and Reid, K.B. 1987. Purification and characterization of a peptide from amyloid-rich pancreases of type 2 diabetic patients. Proc. Natl. Acad. Sci. U. S. A. **84**(23): 8628–32.

Cummings, B.P., Digitale, E.K., Stanhope, K.L., Graham, J.L., Baskin, D.G., Reed, B.J., Sweet, I.R., Griffen, S.C., and Havel, P.J. 2008. Development and characterization of a novel rat model of type 2 diabetes mellitus: the UC Davis type 2 diabetes mellitus UCD-T2DM rat. Am. J. Physiol. Regul. Integr. Comp. Physiol. **295**(6): R1782-93. doi:10.1152/ajpregu.90635.2008.

Dadheech, N., Garrel, D., and Buteau, J. 2018. Evidence of unrestrained beta-cell proliferation and neogenesis in a patient with hyperinsulinemic hypoglycemia after gastric bypass surgery. Islets **10**(6): 213–220. doi:10.1080/19382014.2018.1513748.

Davidson, H.W., Rhodes, C.J., and Hutton, J.C. 1988. Intraorganellar calcium and pH control proinsulin cleavage in the pancreatic beta cell via two distinct site-specific endopeptidases. Nature **333**(6168): 93–6. doi:10.1038/333093a0.

Dean, E.D., Li, M., Prasad, N., Wisniewski, S.N., Von Deylen, A., Spaeth, J., Maddison, L., Botros, A., Sedgeman, L.R., Bozadjieva, N., Ilkayeva, O., Coldren, A., Poffenberger, G., Shostak, A., Semich, M.C., Aamodt, K.I., Phillips, N., Yan, H., Bernal-Mizrachi, E., Corbin, J.D., Vickers, K.C., Levy, S.E., Dai, C., Newgard, C., Gu, W., Stein, R., Chen, W., and Powers, A.C. 2017. Interrupted Glucagon Signaling Reveals Hepatic α Cell Axis and Role for L-Glutamine in α Cell Proliferation. Cell Metab. **25**(6): 1362-1373.e5. doi:10.1016/j.cmet.2017.05.011.

Delghingaro-Augusto, V., Nolan, C.J., Gupta, D., Jetton, T.L., Latour, M.G., Peshavaria, M., Madiraju, S.R.M., Joly, E., Peyot, M.-L., Prentki, M., and Leahy, J. 2009. Islet beta cell failure in the 60% pancreatectomised obese hyperlipidaemic Zucker fatty rat: severe dysfunction with altered glycerolipid metabolism without steatosis or a falling beta cell mass. Diabetologia **52**(6): 1122–1132. Germany. doi:https://dx.doi.org/10.1007/s00125-009-1317-8.

Dentin, R., Hedrick, S., Xie, J., Yates, J., and Montminy, M. 2008. Hepatic glucose sensing via the CREB coactivator CRTC2. Science **319**(5868): 1402–5. doi:10.1126/science.1151363.

Diabetes Prevention Program Research Group. 2015. Long-term effects of lifestyle intervention or metformin on diabetes development and microvascular complications over 15-year follow-up: the Diabetes Prevention Program Outcomes Study. lancet. Diabetes Endocrinol. **3**(11): 866–75. doi:10.1016/S2213-8587(15)00291-0.

Doliba, N.M., Qin, W., Najafi, H., Liu, C., Buettger, C.W., Sotiris, J., Collins, H.W., Li, C., Stanley, C.A., Wilson, D.F., Grimsby, J., Sarabu, R., Naji, A., and Matschinsky, F.M. 2012. Glucokinase activation repairs defective bioenergetics of islets of Langerhans isolated from type 2 diabetics. Am. J. Physiol. Endocrinol. Metab. **302**(1): E87–E102. doi:10.1152/ajpendo.00218.2011.

Donath, M.Y., and Halban, P.A. 2004. Decreased beta-cell mass in diabetes: significance, mechanisms and therapeutic implications. Diabetologia **47**(3): 581–589. doi:10.1007/s00125-004-1336-4.

Dorrell, C., Schug, J., Canaday, P.S., Russ, H.A., Tarlow, B.D., Grompe, M.T., Horton, T., Hebrok, M., Streeter, P.R., Kaestner, K.H., and Grompe, M. 2016. Human islets contain four distinct subtypes of β cells. Nat. Commun. **7**: 11756. doi:10.1038/ncomms11756.

Doyle, M.E., and Egan, J.M. 2007. Mechanisms of action of glucagon-like peptide 1 in the pancreas. Pharmacol. Ther. **113**(3): 546–93. doi:10.1016/j.pharmthera.2006.11.007.

Duca, F.A., Côté, C.D., Rasmussen, B.A., Zadeh-Tahmasebi, M., Rutter, G.A., Filippi, B.M., and Lam, T.K.T. 2015. Metformin activates a duodenal Ampk-dependent pathway to lower hepatic glucose production in rats. Nat. Med. **21**(5): 506–11. doi:10.1038/nm.3787.

Edgar, R.C., Haas, B.J., Clemente, J.C., Quince, C., and Knight, R. 2011. UCHIME improves sensitivity and speed of chimera detection. Bioinformatics **27**(16): 2194–2200. doi:10.1093/bioinformatics/btr381.

Eizirik, D.L., Cardozo, A.K., and Cnop, M. 2008. The role for endoplasmic reticulum stress in diabetes mellitus. Endocr. Rev. **29**(1): 42–61. doi:10.1210/er.2007-0015.

El-Mir, M.Y., Nogueira, V., Fontaine, E., Avéret, N., Rigoulet, M., and Leverve, X. 2000. Dimethylbiguanide inhibits cell respiration via an indirect effect targeted on the respiratory chain complex I. J. Biol. Chem. **275**(1): 223–8.

Ellenbroek, J.H., Tons, H.A., de Graaf, N., Loomans, C.J., Engelse, M.A., Vrolijk, H., Voshol, P.J., Rabelink, T.J., Carlotti, F., and de Koning, E.J. 2013. Topologically heterogeneous beta cell adaptation in response to high-fat diet in mice. PLoS One **8**(2): e56922. United States. doi:https://dx.doi.org/10.1371/journal.pone.0056922.

Ellgaard, L., and Ruddock, L.W. 2005. The human protein disulphide isomerase family: substrate interactions and functional properties. EMBO Rep. **6**(1): 28–32. doi:10.1038/sj.embor.7400311.

Engin, F., Nguyen, T., Yermalovich, A., and Hotamisligil, G.S. 2014. Aberrant islet unfolded protein response in type 2 diabetes. Sci. Rep. **4**: 4054. doi:10.1038/srep04054.

Escribano, O., Guillen, C., Nevado, C., Gomez-Hernandez, A., Kahn, C.R., and Benito, M. 2009. Beta-Cell hyperplasia induced by hepatic insulin resistance: role of a liver-pancreas endocrine axis through insulin receptor A isoform. Diabetes **58**(4): 820–828. United States.

doi:https://dx.doi.org/10.2337/db08-0551.

Feige, M.J., and Hendershot, L.M. 2011. Disulfide bonds in ER protein folding and homeostasis. Curr. Opin. Cell Biol. **23**(2): 167–75. doi:10.1016/j.ceb.2010.10.012.

Ferrannini, E., Gastaldelli, A., and Iozzo, P. 2011. Pathophysiology of prediabetes. Med. Clin. North Am. **95**(2): 327–39, vii–viii. doi:10.1016/j.mcna.2010.11.005.

Ferrannini, E., Muscelli, E., Natali, A., Gabriel, R., Mitrakou, A., Flyvbjerg, A., Golay, A., Hojlund, K., and Relationship between Insulin Sensitivity and Cardiovascular Disease Risk (RISC) Project Investigators. 2007. Association of fasting glucagon and proinsulin concentrations with insulin resistance. Diabetologia **50**(11): 2342–7. doi:10.1007/s00125-007-0806-x.

Festa, A., Williams, K., D'Agostino, R., Wagenknecht, L.E., and Haffner, S.M. 2006. The natural course of beta-cell function in nondiabetic and diabetic individuals: the Insulin Resistance Atherosclerosis Study. Diabetes **55**(4): 1114–20.

Fletcher, B., Gulanick, M., and Lamendola, C. 2002. Risk factors for type 2 diabetes mellitus. J. Cardiovasc. Nurs. **16**(2): 17–23.

Florez, J.C. 2008. Newly identified loci highlight beta cell dysfunction as a key cause of type 2 diabetes: where are the insulin resistance genes? Diabetologia **51**(7): 1100–10. doi:10.1007/s00125-008-1025-9.

Flory, J., and Lipska, K. 2019. Metformin in 2019. JAMA. doi:10.1001/jama.2019.3805.

Foretz, M., Hébrard, S., Leclerc, J., Zarrinpashneh, E., Soty, M., Mithieux, G., Sakamoto, K., Andreelli, F., and Viollet, B. 2010. Metformin inhibits hepatic gluconeogenesis in mice independently of the LKB1/AMPK pathway via a decrease in hepatic energy state. J. Clin. Invest. **120**(7): 2355–69. doi:10.1172/JCI40671.

Forgie, A.J., Gao, Y., Ju, T., Pepin, D.M., Yang, K., Gänzle, M.G., Ozga, J.A., Chan, C.B., and Willing, B.P. 2019. Pea polyphenolics and hydrolysis processing alter microbial community structure and early pathogen colonization in mice. J. Nutr. Biochem. **67**: 101–110. doi:10.1016/j.jnutbio.2019.01.012.

Forslund, K., Hildebrand, F., Nielsen, T., Falony, G., Le Chatelier, E., Sunagawa, S., Prifti, E., Vieira-Silva, S., Gudmundsdottir, V., Pedersen, H.K., Arumugam, M., Kristiansen, K., Voigt, A.Y., Vestergaard, H., Hercog, R., Costea, P.I., Kultima, J.R., Li, J., Jørgensen, T., Levenez, F., Dore, J., MetaHIT consortium, Nielsen, H.B., Brunak, S., Raes, J., Hansen, T., Wang, J., Ehrlich, S.D., Bork, P., and Pedersen, O. 2015. Disentangling type 2 diabetes and metformin treatment signatures in the human gut microbiota. Nature **528**(7581): 262–266. doi:10.1038/nature15766.

Froguel, P., Zouali, H., Vionnet, N., Velho, G., Vaxillaire, M., Sun, F., Lesage, S., Stoffel, M., Takeda, J., and Passa, P. 1993. Familial hyperglycemia due to mutations in glucokinase. Definition of a subtype of diabetes mellitus. N. Engl. J. Med. **328**(10): 697–702. doi:10.1056/NEJM199303113281005.

Fu, A., Eberhard, C.E., and Screaton, R.A. 2013. Role of AMPK in pancreatic beta cell function. Mol. Cell. Endocrinol. **366**(2): 127–34. doi:10.1016/j.mce.2012.06.020.

Fu, A., Ng, A.C.-H., Depatie, C., Wijesekara, N., He, Y., Wang, G.-S., Bardeesy, N., Scott, F.W., Touyz, R.M., Wheeler, M.B., and Screaton, R.A. 2009. Loss of Lkb1 in adult beta cells increases beta cell mass and enhances glucose tolerance in mice. Cell Metab. **10**(4): 285–95. doi:10.1016/j.cmet.2009.08.008.

Gao, R., Ustinov, J., Pulkkinen, M.-A., Lundin, K., Korsgren, O., and Otonkoski, T. 2003. Characterization of endocrine progenitor cells and critical factors for their differentiation in human adult pancreatic cell culture. Diabetes **52**(8): 2007–15.

Gelin, L., Li, J., Corbin, K.L., Jahan, I., and Nunemaker, C.S. 2018. Metformin Inhibits Mouse Islet Insulin Secretion and Alters Intracellular Calcium in a Concentration-Dependent and Duration-Dependent Manner near the Circulating Range. J. Diabetes Res. **2018**: 1–10. doi:10.1155/2018/9163052.

Ghiasi, S.M., Dahlby, T., Hede Andersen, C., Haataja, L., Petersen, S., Omar-Hmeadi, M., Yang, M., Pihl, C., Bresson, S.E., Khilji, M.S., Klindt, K., Cheta, O., Perone, M.J., Tyrberg, B., Prats, C., Barg, S., Tengholm, A., Arvan, P., Mandrup-Poulsen, T., and Marzec, M.T. 2019. Endoplasmic Reticulum Chaperone Glucose-Regulated Protein 94 Is Essential for Proinsulin Handling. Diabetes **68**(4): 747–760. doi:10.2337/db18-0671.

Glaser, B., Kesavan, P., Heyman, M., Davis, E., Cuesta, A., Buchs, A., Stanley, C.A., Thornton, P.S., Permutt, M.A., Matschinsky, F.M., and Herold, K.C. 1998. Familial hyperinsulinism caused by an activating glucokinase mutation. N. Engl. J. Med. **338**(4): 226–30. doi:10.1056/NEJM199801223380404.

Gorasia, D.G., Dudek, N.L., Safavi-Hemami, H., Perez, R.A., Schittenhelm, R.B., Saunders, P.M., Wee, S., Mangum, J.E., Hubbard, M.J., and Purcell, A.W. 2016. A prominent role of PDIA6 in processing of misfolded proinsulin. Biochim. Biophys. Acta **1864**(6): 715–23. doi:10.1016/j.bbapap.2016.03.002.

Granot, Z., Swisa, A., Magenheim, J., Stolovich-Rain, M., Fujimoto, W., Manduchi, E., Miki, T., Lennerz, J.K., Stoeckert, C.J., Meyuhas, O., Seino, S., Permutt, M.A., Piwnica-Worms, H., Bardeesy, N., and Dor, Y. 2009. LKB1 regulates pancreatic beta cell size, polarity, and function. Cell Metab. **10**(4): 296–308. doi:10.1016/j.cmet.2009.08.010.

Graves, T.K., and Hinkle, P.M. 2003. Ca(2+)-induced Ca(2+) release in the pancreatic beta-cell: direct evidence of endoplasmic reticulum Ca(2+) release. Endocrinology **144**(8): 3565–74. doi:10.1210/en.2002-0104.

Gupta, D., Jetton, T.L., LaRock, K., Monga, N., Satish, B., Lausier, J., Peshavaria, M., and Leahy, J.L. 2017. Temporal Characterization of β-cell Adaptive and Maladaptive Mechanisms During Chronic High Fat Feeding in C57BL/6NTac Mice. J. Biol. Chem.: jbc.M117.781047. doi:10.1074/jbc.M117.781047.

Gupta, S., McGrath, B., and Cavener, D.R. 2010. PERK (EIF2AK3) regulates proinsulin trafficking and quality control in the secretory pathway. Diabetes **59**(8): 1937–47. doi:10.2337/db09-1064.

Haataja, L., Snapp, E., Wright, J., Liu, M., Hardy, A.B., Wheeler, M.B., Markwardt, M.L., Rizzo, M., and Arvan, P. 2013. Proinsulin intermolecular interactions during secretory trafficking in pancreatic β cells. J. Biol. Chem. **288**(3): 1896–906.

doi:10.1074/jbc.M112.420018.

Halaas, J.L., Gajiwala, K.S., Maffei, M., Cohen, S.L., Chait, B.T., Rabinowitz, D., Lallone, R.L., Burley, S.K., and Friedman, J.M. 1995. Weight-reducing effects of the plasma protein encoded by the obese gene. Science **269**(5223): 543–6.

Hanley, S.C., Austin, E., Assouline-Thomas, B., Kapeluto, J., Blaichman, J., Moosavi, M., Petropavlovskaia, M., and Rosenberg, L. 2010. Beta-Cell mass dynamics and islet cell plasticity in human type 2 diabetes. Endocrinology **151**(4): 1462–72. doi:10.1210/en.2009-1277.

Harding, H.P., Novoa, I., Zhang, Y., Zeng, H., Wek, R., Schapira, M., and Ron, D. 2000. Regulated translation initiation controls stress-induced gene expression in mammalian cells. Mol. Cell **6**(5): 1099–108.

Harding, H.P., Zhang, Y., and Ron, D. 1999. Protein translation and folding are coupled by an endoplasmic-reticulum-resident kinase. Nature **397**(6716): 271–274. doi:10.1038/16729.

Haze, K., Yoshida, H., Yanagi, H., Yura, T., and Mori, K. 1999. Mammalian transcription factor ATF6 is synthesized as a transmembrane protein and activated by proteolysis in response to endoplasmic reticulum stress. Mol. Biol. Cell **10**(11): 3787–3799. doi:10.1091/mbc.10.11.3787.

He, K., Cunningham, C.N., Manickam, N., Liu, M., Arvan, P., and Tsai, B. 2015. PDI reductase acts on Akita mutant proinsulin to initiate retrotranslocation along the Hrd1/Sel1L-p97 axis. Mol. Biol. Cell **26**(19): 3413–23. doi:10.1091/mbc.E15-01-0034.

He, L., Sabet, A., Djedjos, S., Miller, R., Sun, X., Hussain, M.A., Radovick, S., and Wondisford, F.E. 2009. Metformin and insulin suppress hepatic gluconeogenesis through phosphorylation of CREB binding protein. Cell **137**(4): 635–46. doi:10.1016/j.cell.2009.03.016.

Hegarty, B.D., Turner, N., Cooney, G.J., and Kraegen, E.W. 2009. Insulin resistance and fuel homeostasis: the role of AMP-activated protein kinase. Acta Physiol. **196**(1): 129–145. doi:10.1111/j.1748-1716.2009.01968.x.

Henquin, J.-C., Dufrane, D., Gmyr, V., Kerr-Conte, J., and Nenquin, M. 2017. Pharmacological approach to understanding the control of insulin secretion in human islets. Diabetes. Obes. Metab. **19**(8): 1061–1070. doi:10.1111/dom.12887.

Henquin, J.-C., Dufrane, D., and Nenquin, M. 2006. Nutrient control of insulin secretion in isolated normal human islets. Diabetes **55**(12): 3470–7. doi:10.2337/db06-0868.

Hiddinga, H.J., Sakagashira, S., Ishigame, M., Madde, P., Sanke, T., Nanjo, K., Kudva, Y.C., Lee, J.J., van Deursen, J., and Eberhardt, N.L. 2012. Expression of wild-type and mutant S20G hIAPP in physiologic knock-in mouse models fails to induce islet amyloid formation, but induces mild glucose intolerance. J. Diabetes Investig. **3**(2): 138–47. doi:10.1111/j.2040-1124.2011.00166.x.

Hirst, J.A., Farmer, A.J., Ali, R., Roberts, N.W., and Stevens, R.J. 2012. Quantifying the Effect of Metformin Treatment and Dose on Glycemic Control. Diabetes Care **35**(2): 446–454. doi:10.2337/dc11-1465.

Hollien, J., Lin, J.H., Li, H., Stevens, N., Walter, P., and Weissman, J.S. 2009. Regulated Ire1-dependent decay of messenger RNAs in mammalian cells. J. Cell Biol. **186**(3): 323–331. doi:10.1083/jcb.200903014.

Huang, Q., Bu, S., Yu, Y., Guo, Z., Ghatnekar, G., Bu, M., Yang, L., Lu, B., Feng, Z., Liu, S., and Wang, F. 2007. Diazoxide prevents diabetes through inhibiting pancreatic beta-cells from apoptosis via Bcl-2/Bax rate and p38-beta mitogen-activated protein kinase. Endocrinology **148**(1): 81–91. United States.

Hughey, C.C., Wasserman, D.H., Lee-Young, R.S., and Lantier, L. 2014. Approach to assessing determinants of glucose homeostasis in the conscious mouse. Mamm. Genome **25**(9–10): 522–38. doi:10.1007/s00335-014-9533-z.

Hulman, A., Simmons, R.K., Brunner, E.J., Witte, D.R., Færch, K., Vistisen, D., Ikehara, S., Kivimaki, M., and Tabák, A.G. 2017. Trajectories of glycaemia, insulin sensitivity and insulin secretion in South Asian and white individuals before diagnosis of type 2 diabetes: a longitudinal analysis from the Whitehall II cohort study. Diabetologia **60**(7): 1252–1260. doi:10.1007/s00125-017-4275-6.

Hundal, R.S., Krssak, M., Dufour, S., Laurent, D., Lebon, V., Chandramouli, V., Inzucchi, S.E., Schumann, W.C., Petersen, K.F., Landau, B.R., and Shulman, G.I. 2000. Mechanism by which metformin reduces glucose production in type 2 diabetes. Diabetes **49**(12): 2063–2069. doi:10.2337/diabetes.49.12.2063.

Inagaki, N., Maekawa, T., Sudo, T., Ishii, S., Seino, Y., and Imura, H. 1992. c-Jun represses the human insulin promoter activity that depends on multiple cAMP response elements. Proc. Natl. Acad. Sci. U. S. A. **89**(3): 1045–9.

Iozzo, P., Beck-Nielsen, H., Laakso, M., Smith, U., Yki-Järvinen, H., and Ferrannini, E. 1999. Independent influence of age on basal insulin secretion in nondiabetic humans. European Group for the Study of Insulin Resistance. J. Clin. Endocrinol. Metab. **84**(3): 863–8. doi:10.1210/jcem.84.3.5542.

Itoh, Y., Kawamata, Y., Harada, M., Kobayashi, M., Fujii, R., Fukusumi, S., Ogi, K., Hosoya, M., Tanaka, Y., Uejima, H., Tanaka, H., Maruyama, M., Satoh, R., Okubo, S., Kizawa, H., Komatsu, H., Matsumura, F., Noguchi, Y., Shinohara, T., Hinuma, S., Fujisawa, Y., and Fujino, M. 2003. Free fatty acids regulate insulin secretion from pancreatic beta cells through GPR40. Nature **422**(6928): 173–6. doi:10.1038/nature01478.

Iype, T., Francis, J., Garmey, J.C., Schisler, J.C., Nesher, R., Weir, G.C., Becker, T.C., Newgard, C.B., Griffen, S.C., and Mirmira, R.G. 2005. Mechanism of insulin gene regulation by the pancreatic transcription factor Pdx-1: application of pre-mRNA analysis and chromatin immunoprecipitation to assess formation of functional transcriptional complexes. J. Biol. Chem. **280**(17): 16798–807. doi:10.1074/jbc.M414381200.

Jiang, H., Tong, Y., Yan, D., Jia, S., Ostenson, C.-G., and Chen, Z. 2015. The Soybean Peptide Vglycin Preserves the Diabetic β-cells through Improvement of Proliferation and Inhibition of Apoptosis. Sci. Rep. **5**: 15599. doi:10.1038/srep15599.

Jiang, Y., Huang, W., Wang, J., Xu, Z., He, J., Lin, X., Zhou, Z., and Zhang, J. 2014. Metformin plays a dual role in MIN6 pancreatic β cell function through AMPK-dependent autophagy.

Int. J. Biol. Sci. **10**(3): 268–77. doi:10.7150/ijbs.7929.

Jitrapakdee, S., Wutthisathapornchai, A., Wallace, J.C., and MacDonald, M.J. 2010. Regulation of insulin secretion: role of mitochondrial signalling. Diabetologia **53**(6): 1019–32. doi:10.1007/s00125-010-1685-0.

Jones, H.B., Nugent, D., and Jenkins, R. 2010. Variation in characteristics of islets of Langerhans in insulin-resistant, diabetic and non-diabetic-rat strains. Int. J. Exp. Pathol. **91**(3): 288–301. doi:10.1111/j.1365-2613.2010.00713.x.

Jones, P.M., and Persaud, S.J. 2010. Normal Physiology. Textb. Diabetes, Fourth Ed.

Jorns, A., Tiedge, M., Ziv, E., Shafrir, E., and Lenzen, S. 2002. Gradual loss of pancreatic beta-cell insulin, glucokinase and GLUT2 glucose transporter immunoreactivities during the time course of nutritionally induced type-2 diabetes in Psammomys obesus (sand rat). Virchows Arch. **440**(1): 63–69. Germany.

Kadowaki, T. 2000. Insights into insulin resistance and type 2 diabetes from knockout mouse models. J. Clin. Invest. **106**(4): 459–65. doi:10.1172/JCI10830.

Kahn, S.E. 2003. The relative contributions of insulin resistance and beta-cell dysfunction to the pathophysiology of Type 2 diabetes. Diabetologia **46**(1): 3–19. doi:10.1007/s00125-002-1009-0.

Kaiser, N., Nesher, R., Donath, M.Y., Fraenkel, M., Behar, V., Magnan, C., Ktorza, A., Cerasi, E., and Leibowitz, G. 2005. Psammomys obesus, a model for environment-gene interactions in type 2 diabetes. Diabetes **54 Suppl 2**: S137-44.

Kanda, Y., Shimoda, M., Tawaramoto, K., Hamamoto, S., Tatsumi, F., Kawasaki, F., Hashiramoto, M., Nakashima, K., Matsuki, M., and Kaku, K. 2009. Molecular analysis of db gene-related pancreatic beta cell dysfunction; evidence for a compensatory mechanism inhibiting development of diabetes in the db gene heterozygote. Endocr. J. **56**(8): 997–1008.

Karamanou, M., Protogerou, A., Tsoucalas, G., Androutsos, G., and Poulakou-Rebelakou, E. 2016. Milestones in the history of diabetes mellitus: The main contributors. World J. Diabetes **7**(1): 1–7. doi:10.4239/wjd.v7.i1.1.

Kars, M., Yang, L., Gregor, M.F., Mohammed, B.S., Pietka, T.A., Finck, B.N., Patterson, B.W., Horton, J.D., Mittendorfer, B., Hotamisligil, G.S., and Klein, S. 2010. Tauroursodeoxycholic Acid may improve liver and muscle but not adipose tissue insulin sensitivity in obese men and women. Diabetes **59**(8): 1899–905. doi:10.2337/db10-0308.

Kato, K., Gong, J., Iwama, H., Kitanaka, A., Tani, J., Miyoshi, H., Nomura, K., Mimura, S., Kobayashi, M., Aritomo, Y., Kobara, H., Mori, H., Himoto, T., Okano, K., Suzuki, Y., Murao, K., and Masaki, T. 2012. The Antidiabetic Drug Metformin Inhibits Gastric Cancer Cell Proliferation In Vitro and In Vivo. Mol. Cancer Ther. **11**(3): 549–560. doi:10.1158/1535-7163.MCT-11-0594.

Kawano, K., Hirashima, T., Mori, S., and Natori, T. 1994. OLETF (Otsuka Long-Evans Tokushima Fatty) rat: a new NIDDM rat strain. Diabetes Res. Clin. Pract. **24 Suppl**: S317-20.

Khalkhal, A., Haddar, A., Semiane, N., Mallek, A., Abdelmalek, A., Castex, F., Gross, R., and Dahmani, Y. 2012. Obesity, insulin resistance and diabetes in the sand rat exposed to a hypercaloric diet; possible protective effect for IL1-beta. C. R. Biol. **335**(4): 271–278. France. doi:https://dx.doi.org/10.1016/j.crvi.2012.03.003.

Kim, J.J., Kido, Y., Scherer, P.E., White, M.F., and Accili, D. 2007. Analysis of compensatory beta-cell response in mice with combined mutations of Insr and Irs2. Am. J. Physiol. Endocrinol. Metab. **292**(6): E1694-701. United States.

Kim, M.-H., Jee, J.-H., Park, S., Lee, M.-S., Kim, K.-W., and Lee, M.-K. 2014. Metformin enhances glucagon-like peptide 1 via cooperation between insulin and Wnt signaling. J. Endocrinol. **220**(2): 117–28. doi:10.1530/JOE-13-0381.

King, A.J.F. 2012. The use of animal models in diabetes research. Br. J. Pharmacol. **166**(3): 877–94. doi:10.1111/j.1476-5381.2012.01911.x.

Kitabchi, A.E., Temprosa, M., Knowler, W.C., Kahn, S.E., Fowler, S.E., Haffner, S.M., Andres, R., Saudek, C., Edelstein, S.L., Arakaki, R., Murphy, M.B., Shamoon, H., and Diabetes Prevention Program Research Group. 2005. Role of insulin secretion and sensitivity in the evolution of type 2 diabetes in the diabetes prevention program: effects of lifestyle intervention and metformin. Diabetes **54**(8): 2404–14.

Kluge, R., Scherneck, S., Schürmann, A., and Joost, H.-G. 2012. Pathophysiology and genetics of obesity and diabetes in the New Zealand obese mouse: a model of the human metabolic syndrome. Methods Mol. Biol. **933**: 59–73. doi:10.1007/978-1-62703-068-7_5.

Knowler, W.C., Barrett-Connor, E., Fowler, S.E., Hamman, R.F., Lachin, J.M., Walker, E.A., Nathan, D.M., and Diabetes Prevention Program Research Group. 2002. Reduction in the incidence of type 2 diabetes with lifestyle intervention or metformin. N. Engl. J. Med. **346**(6): 393–403. doi:10.1056/NEJMoa012512.

Knowler, W.C., Fowler, S.E., Hamman, R.F., Christophi, C.A., Hoffman, H.J., Brenneman, A.T., Brown-Friday, J.O., Goldberg, R., Venditti, E., and Nathan, D.M. 2009. 10-year follow-up of diabetes incidence and weight loss in the Diabetes Prevention Program Outcomes Study. Lancet (London, England) **374**(9702): 1677–86. doi:10.1016/S0140-6736(09)61457-4.

Knowler, W.C., Narayan, K.M., Hanson, R.L., Nelson, R.G., Bennett, P.H., Tuomilehto, J., Scherstén, B., and Pettitt, D.J. 1995. Preventing non-insulin-dependent diabetes. Diabetes **44**(5): 483–8.

Koepsell, H., Lips, K., and Volk, C. 2007. Polyspecific organic cation transporters: structure, function, physiological roles, and biopharmaceutical implications. Pharm. Res. **24**(7): 1227–51. doi:10.1007/s11095-007-9254-z.

Koo, S.-H., Flechner, L., Qi, L., Zhang, X., Screaton, R.A., Jeffries, S., Hedrick, S., Xu, W., Boussouar, F., Brindle, P., Takemori, H., and Montminy, M. 2005. The CREB coactivator TORC2 is a key regulator of fasting glucose metabolism. Nature **437**(7062): 1109–11. doi:10.1038/nature03967.

Kruszynska, Y.T., and Olefsky, J.M. 1996. Cellular and molecular mechanisms of non-insulin

dependent diabetes mellitus. J. Investig. Med. **44**(8): 413–28.

de la Cuesta-Zuluaga, J., Mueller, N.T., Corrales-Agudelo, V., Velásquez-Mejía, E.P., Carmona, J.A., Abad, J.M., and Escobar, J.S. 2017. Metformin Is Associated With Higher Relative Abundance of Mucin-Degrading Akkermansia muciniphila and Several Short-Chain Fatty Acid-Producing Microbiota in the Gut. Diabetes Care **40**(1): 54–62. doi:10.2337/dc16-1324.

Lacraz, G., Figeac, F., Movassat, J., Kassis, N., and Portha, B. 2010. Diabetic GK/Par rat beta-cells are spontaneously protected against H2O2-triggered apoptosis. A cAMP-dependent adaptive response. Am. J. Physiol. Endocrinol. Metab. **298**(1): E17-27. United States. doi:https://dx.doi.org/10.1152/ajpendo.90871.2008.

Lamontagne, J., Al-Mass, A., Nolan, C.J., Corkey, B.E., Madiraju, S.R.M., Joly, E., and Prentki, M. 2017. Identification of the signals for glucose-induced insulin secretion in INS1 (832/13) β-cells using metformin-induced metabolic deceleration as a model. J. Biol. Chem. **292**(47): 19458–19468. doi:10.1074/jbc.M117.808105.

Lamontagne, J., Pepin, E., Peyot, M.-L., Joly, E., Ruderman, N.B., Poitout, V., Madiraju, S.R.M., Nolan, C.J., and Prentki, M. 2009. Pioglitazone acutely reduces insulin secretion and causes metabolic deceleration of the pancreatic beta-cell at submaximal glucose concentrations. Endocrinology **150**(8): 3465–74. doi:10.1210/en.2008-1557.

Lange, C., Jeruschke, K., Herberg, L., Leiter, E.H., and Junger, E. 2006. The diabetes-prone NZO/Hl strain. Proliferation capacity of beta cells in hyperinsulinemia and hyperglycemia. Arch. Physiol. Biochem. **112**(1): 49–58. England.

Langelueddecke, C., Jakab, M., Ketterl, N., Lehner, L., Hufnagl, C., Schmidt, S., Geibel, J.P., Fuerst, J., and Ritter, M. 2012. Effect of the AMP-kinase modulators AICAR, metformin and compound C on insulin secretion of INS-1E rat insulinoma cells under standard cell culture conditions. Cell. Physiol. Biochem. **29**(1–2): 75–86. doi:10.1159/000337589.

Lawlor, N., George, J., Bolisetty, M., Kursawe, R., Sun, L., Sivakamasundari, V., Kycia, I., Robson, P., and Stitzel, M.L. 2017. Single-cell transcriptomes identify human islet cell signatures and reveal cell-type-specific expression changes in type 2 diabetes. Genome Res. **27**(2): 208–222. doi:10.1101/gr.212720.116.

Laybutt, D.R., Preston, a M., Akerfeldt, M.C., Kench, J.G., Busch, a K., Biankin, A. V, and Biden, T.J. 2007. Endoplasmic reticulum stress contributes to beta cell apoptosis in type 2 diabetes. Diabetologia **50**(4): 752–763. Germany. doi:10.1007/s00125-006-0590-z.

Leclerc, I., Woltersdorf, W.W., da Silva Xavier, G., Rowe, R.L., Cross, S.E., Korbutt, G.S., Rajotte, R. V, Smith, R., and Rutter, G.A. 2004. Metformin, but not leptin, regulates AMP-activated protein kinase in pancreatic islets: impact on glucose-stimulated insulin secretion. Am. J. Physiol. Endocrinol. Metab. **286**(6): E1023-31. doi:10.1152/ajpendo.00532.2003.

Lee, J., Sugiyama, T., Liu, Y., Wang, J., Gu, X., Lei, J., Markmann, J.F., Miyazaki, S., Miyazaki, J.-I., Szot, G.L., Bottino, R., and Kim, S.K. 2013. Expansion and conversion of human pancreatic ductal cells into insulin-secreting endocrine cells. Elife **2**: e00940. doi:10.7554/eLife.00940.

Lee, Y.-S., Lee, C., Choung, J.-S., Jung, H.-S., and Jun, H.-S. 2018. Glucagon-Like Peptide 1 Increases β-Cell Regeneration by Promoting α- to β-Cell Transdifferentiation. Diabetes **67**(12): 2601–2614. doi:10.2337/db18-0155.

Lentferink, Y.E., van der Aa, M.P., van Mill, E.G.A.H., Knibbe, C.A.J., and van der Vorst, M.M.J. 2018. Long-term metformin treatment in adolescents with obesity and insulin resistance, results of an open label extension study. Nutr. Diabetes **8**(1): 47. doi:10.1038/s41387-018-0057-6.

Lien, F., Berthier, A., Bouchaert, E., Gheeraert, C., Alexandre, J., Porez, G., Prawitt, J., Dehondt, H., Ploton, M., Colin, S., Lucas, A., Patrice, A., Pattou, F., Diemer, H., Van Dorsselaer, A., Rachez, C., Kamilic, J., Groen, A.K., Staels, B., and Lefebvre, P. 2014. Metformin interferes with bile acid homeostasis through AMPK-FXR crosstalk. J. Clin. Invest. **124**(3): 1037–51. doi:10.1172/JCI68815.

Linden, M.A., Lopez, K.T., Fletcher, J.A., Morris, E.M., Meers, G.M., Siddique, S., Laughlin, M.H., Sowers, J.R., Thyfault, J.P., Ibdah, J.A., and Rector, R.S. 2015. Combining metformin therapy with caloric restriction for the management of type 2 diabetes and nonalcoholic fatty liver disease in obese rats. Appl. Physiol. Nutr. Metab. **40**(10): 1038–47. doi:10.1139/apnm-2015-0236.

Liu, Y.Q., Jetton, T.L., and Leahy, J.L. 2002. beta-Cell adaptation to insulin resistance. Increased pyruvate carboxylase and malate-pyruvate shuttle activity in islets of nondiabetic Zucker fatty rats. J. Biol. Chem. **277**(42): 39163–8. doi:10.1074/jbc.M207157200.

Livak, K.J., and Schmittgen, T.D. 2001. Analysis of relative gene expression data using real-time quantitative PCR and the 2(-Delta Delta C(T)) Method. Methods **25**(4): 402–8. doi:10.1006/meth.2001.1262.

Lodish, H.F. 1988. Transport of secretory and membrane glycoproteins from the rough endoplasmic reticulum to the Golgi. A rate-limiting step in protein maturation and secretion. J. Biol. Chem. **263**(5): 2107–10.

Lord, S.R., Cheng, W.-C., Liu, D., Gaude, E., Haider, S., Metcalf, T., Patel, N., Teoh, E.J., Gleeson, F., Bradley, K., Wigfield, S., Zois, C., McGowan, D.R., Ah-See, M.-L., Thompson, A.M., Sharma, A., Bidaut, L., Pollak, M., Roy, P.G., Karpe, F., James, T., English, R., Adams, R.F., Campo, L., Ayers, L., Snell, C., Roxanis, I., Frezza, C., Fenwick, J.D., Buffa, F.M., and Harris, A.L. 2018. Integrated Pharmacodynamic Analysis Identifies Two Metabolic Adaption Pathways to Metformin in Breast Cancer. Cell Metab. **28**(5): 679-688.e4. Elsevier. doi:10.1016/j.cmet.2018.08.021.

Lorenzo, A., Razzaboni, B., Weir, G.C., and Yankner, B.A. 1994. Pancreatic islet cell toxicity of amylin associated with type-2 diabetes mellitus. Nature **368**(6473): 756–60. doi:10.1038/368756a0.

Lupi, R., Del Guerra, S., Tellini, C., Giannarelli, R., Coppelli, A., Lorenzetti, M., Carmellini, M., Mosca, F., Navalesi, R., and Marchetti, P. 1999. The biguanide compound metformin prevents desensitization of human pancreatic islets induced by high glucose. Eur. J. Pharmacol. **364**(2–3): 205–9.

MacDonald, M.J., Longacre, M.J., Langberg, E.-C., Tibell, A., Kendrick, M.A., Fukao, T., and

Ostenson, C.-G. 2009. Decreased levels of metabolic enzymes in pancreatic islets of patients with type 2 diabetes. Diabetologia **52**(6): 1087–91. doi:10.1007/s00125-009-1319-6.

MacDonald, P.E., Joseph, J.W., and Rorsman, P. 2005. Glucose-sensing mechanisms in pancreatic beta-cells. Philos. Trans. R. Soc. Lond. B. Biol. Sci. **360**(1464): 2211–25. doi:10.1098/rstb.2005.1762.

MacDonald, P.E., and Wheeler, M.B. 2003. Voltage-dependent K+ channels in pancreatic beta cells: Role, regulation and potential as therapeutic targets. Diabetologia **46**(8): 1046–1062. doi:10.1007/s00125-003-1159-8.

Madiraju, A.K., Erion, D.M., Rahimi, Y., Zhang, X.-M., Braddock, D.T., Albright, R. a, Prigaro, B.J., Wood, J.L., Bhanot, S., MacDonald, M.J., Jurczak, M.J., Camporez, J.-P., Lee, H.-Y., Cline, G.W., Samuel, V.T., Kibbey, R.G., and Shulman, G.I. 2014. Metformin suppresses gluconeogenesis by inhibiting mitochondrial glycerophosphate dehydrogenase. Nature **510**(7506): 542–6. Nature Publishing Group. doi:10.1038/nature13270.

Maida, A., Lamont, B.J., Cao, X., and Drucker, D.J. 2011. Metformin regulates the incretin receptor axis via a pathway dependent on peroxisome proliferator-activated receptor-α in mice. Diabetologia **54**(2): 339–49. doi:10.1007/s00125-010-1937-z.

Malin, S.K., and Kashyap, S.R. 2014. Effects of metformin on weight loss: potential mechanisms. Curr. Opin. Endocrinol. Diabetes. Obes. **21**(5): 323–9. doi:10.1097/MED.0000000000000095.

Marchetti, P., Bugliani, M., Lupi, R., Marselli, L., Masini, M., Boggi, U., Filipponi, F., Weir, G.C., Eizirik, D.L., and Cnop, M. 2007. The endoplasmic reticulum in pancreatic beta cells of type 2 diabetes patients. Diabetologia **50**(12): 2486–2494. doi:10.1007/s00125-007-0816-8.

Marchetti, P., Del Guerra, S., Marselli, L., Lupi, R., Masini, M., Pollera, M., Bugliani, M., Boggi, U., Vistoli, F., Mosca, F., and Del Prato, S. 2004. Pancreatic islets from type 2 diabetic patients have functional defects and increased apoptosis that are ameliorated by metformin. J. Clin. Endocrinol. Metab. **89**(11): 5535–41. doi:10.1210/jc.2004-0150.

Martin-Montalvo, A., Mercken, E.M., Mitchell, S.J., Palacios, H.H., Mote, P.L., Scheibye-Knudsen, M., Gomes, A.P., Ward, T.M., Minor, R.K., Blouin, M., Schwab, M., Pollak, M., Zhang, Y., Yu, Y., Becker, K.G., Bohr, V.A., Ingram, D.K., Sinclair, D.A., Wolf, N.S., Spindler, S.R., Bernier, M., and de Cabo, R. 2013. Metformin improves healthspan and lifespan in mice. Nat. Commun. **4**: 2192. doi:10.1038/ncomms3192.

Maschio, D.A., Oliveira, R.B., Santos, M.R., Carvalho, C.P.F., Barbosa-Sampaio, H.C.L., and Collares-Buzato, C.B. 2016. Activation of the Wnt/beta-catenin pathway in pancreatic beta cells during the compensatory islet hyperplasia in prediabetic mice. Biochem. Biophys. Res. Commun. **478**(4): 1534–1540. United States. doi:https://dx.doi.org/10.1016/j.bbrc.2016.08.146.

Matveyenko, A. V, and Butler, P.C. 2006. Islet amyloid polypeptide (IAPP) transgenic rodents as models for type 2 diabetes. ILAR J. **47**(3): 225–33.

Matveyenko, A. V, Gurlo, T., Daval, M., Butler, A.E., and Butler, P.C. 2009. Successful versus failed adaptation to high-fat diet-induced insulin resistance: the role of IAPP-induced beta-cell endoplasmic reticulum stress. Diabetes **58**(4): 906–16. doi:10.2337/db08-1464.

McCreight, L.J., Bailey, C.J., and Pearson, E.R. 2016. Metformin and the gastrointestinal tract. Diabetologia **59**(3): 426–435. doi:10.1007/s00125-015-3844-9.

McCulloch, L.J., van de Bunt, M., Braun, M., Frayn, K.N., Clark, A., and Gloyn, A.L. 2011. GLUT2 (SLC2A2) is not the principal glucose transporter in human pancreatic beta cells: implications for understanding genetic association signals at this locus. Mol. Genet. Metab. **104**(4): 648–53. doi:10.1016/j.ymgme.2011.08.026.

McGarry, J.D., Leatherman, G.F., and Foster, D.W. 1978. Carnitine palmitoyltransferase I. The site of inhibition of hepatic fatty acid oxidation by malonyl-CoA. J. Biol. Chem. **253**(12): 4128–36.

Medina-Gomez, G., Gray, S.L., Yetukuri, L., Shimomura, K., Virtue, S., Campbell, M., Curtis, R.K., Jimenez-Linan, M., Blount, M., Yeo, G.S.H., Lopez, M., Seppänen-Laakso, T., Ashcroft, F.M., Oresic, M., and Vidal-Puig, A. 2007. PPAR gamma 2 prevents lipotoxicity by controlling adipose tissue expandability and peripheral lipid metabolism. PLoS Genet. **3**(4): e64. doi:10.1371/journal.pgen.0030064.

Medina-Gomez, G., Yetukuri, L., Velagapudi, V., Campbell, M., Blount, M., Jimenez-Linan, M., Ros, M., Oresic, M., and Vidal-Puig, A. 2009. Adaptation and failure of pancreatic cells in murine models with different degrees of metabolic syndrome. Dis. Model. Mech. **2**(11–12): 582–592. doi:10.1242/dmm.003251.

Meier, J.J., Butler, A.E., Saisho, Y., Monchamp, T., Galasso, R., Bhushan, A., Rizza, R.A., and Butler, P.C. 2008. Beta-cell replication is the primary mechanism subserving the postnatal expansion of beta-cell mass in humans. Diabetes **57**(6): 1584–94. doi:10.2337/db07-1369.

Meier, J.J., Ueberberg, S., Korbas, S., and Schneider, S. 2011. Diminished glucagon suppression after beta-cell reduction is due to impaired alpha-cell function rather than an expansion of alpha-cell mass. Am. J. Physiol. Endocrinol. Metab. **300**(4): E717-23. United States. doi:https://dx.doi.org/10.1152/ajpendo.00315.2010.

Meigs, J.B., Muller, D.C., Nathan, D.M., Blake, D.R., and Andres, R. 2003. The natural history of progression from normal glucose tolerance to type 2 diabetes in the Baltimore Longitudinal Study of Aging. Diabetes **52**(6): 1475–1484. doi:10.2337/diabetes.52.6.1475.

Mezghenna, K., Pomiès, P., Chalançon, A., Castex, F., Leroy, J., Niclauss, N., Nadal, B., Cambier, L., Cazevieille, C., Petit, P., Gomis, R., Berney, T., Gross, R., and Lajoix, A.D. 2011. Increased neuronal nitric oxide synthase dimerisation is involved in rat and human pancreatic beta cell hyperactivity in obesity. Diabetologia **54**(11): 2856–66. doi:10.1007/s00125-011-2264-8.

Mezza, T., Muscogiuri, G., Sorice, G.P., Clemente, G., Hu, J., Pontecorvi, A., Holst, J.J., Giaccari, A., and Kulkarni, R.N. 2014. Insulin resistance alters islet morphology in nondiabetic humans. Diabetes **63**(3): 994–1007. doi:10.2337/db13-1013.

Michael, D.J., Xiong, W., Geng, X., Drain, P., and Chow, R.H. 2007. Human insulin vesicle

dynamics during pulsatile secretion. Diabetes **56**(5): 1277–88. doi:10.2337/db06-0367.

Miller, R.A., Chu, Q., Xie, J., Foretz, M., Viollet, B., and Birnbaum, M.J. 2013. Biguanides suppress hepatic glucagon signalling by decreasing production of cyclic AMP. Nature **494**(7436): 256–60. doi:10.1038/nature11808.

Molina, A.J.A., Wikstrom, J.D., Stiles, L., Las, G., Mohamed, H., Elorza, A., Walzer, G., Twig, G., Katz, S., Corkey, B.E., and Shirihai, O.S. 2009. Mitochondrial networking protects beta-cells from nutrient-induced apoptosis. Diabetes **58**(10): 2303–15. doi:10.2337/db07-1781.

Montane, J., de Pablo, S., Obach, M., Cadavez, L., Castaño, C., Alcarraz-Vizán, G., Visa, M., Rodríguez-Comas, J., Parrizas, M., Servitja, J.M., and Novials, A. 2016. Protein disulfide isomerase ameliorates β-cell dysfunction in pancreatic islets overexpressing human islet amyloid polypeptide. Mol. Cell. Endocrinol. **420**: 57–65. doi:10.1016/j.mce.2015.11.018.

Moore, M.C., Cherrington, A.D., and Wasserman, D.H. 2003. Regulation of hepatic and peripheral glucose disposal. Best Pract. Res. Clin. Endocrinol. Metab. **17**(3): 343–364. doi:10.1016/S1521-690X(03)00036-8.

Movassat, J., Bailbé, D., Lubrano-Berthelier, C., Picarel-Blanchot, F., Bertin, E., Mourot, J., and Portha, B. 2008. Follow-up of GK rats during prediabetes highlights increased insulin action and fat deposition despite low insulin secretion. Am. J. Physiol. Endocrinol. Metab. **294**(1): E168-75. doi:10.1152/ajpendo.00501.2007.

Mulherin, A.J., Oh, A.H., Kim, H., Grieco, A., Lauffer, L.M., and Brubaker, P.L. 2011. Mechanisms underlying metformin-induced secretion of glucagon-like peptide-1 from the intestinal L cell. Endocrinology **152**(12): 4610–9. doi:10.1210/en.2011-1485.

Mykkänen, L., Haffner, S.M., Hales, C.N., Rönnemaa, T., and Laakso, M. 1997. The relation of proinsulin, insulin, and proinsulin-to-insulin ratio to insulin sensitivity and acute insulin response in normoglycemic subjects. Diabetes **46**(12): 1990–5.

Mykkänen, L., Zaccaro, D.J., Hales, C.N., Festa, A., and Haffner, S.M. 1999. The relation of proinsulin and insulin to insulin sensitivity and acute insulin response in subjects with newly diagnosed type II diabetes: the Insulin Resistance Atherosclerosis Study. Diabetologia **42**(9): 1060–6. doi:10.1007/s001250051271.

Nadanaka, S., Okada, T., Yoshida, H., and Mori, K. 2007. Role of disulfide bridges formed in the luminal domain of ATF6 in sensing endoplasmic reticulum stress. Mol. Cell. Biol. **27**(3): 1027–1043. doi:10.1128/MCB.00408-06.

Nathan, D.M., Davidson, M.B., DeFronzo, R.A., Heine, R.J., Henry, R.R., Pratley, R., Zinman, B., and American Diabetes Association. 2007. Impaired fasting glucose and impaired glucose tolerance: implications for care. Diabetes Care **30**(3): 753–9. doi:10.2337/dc07-9920.

Neeland, I.J., Turer, A.T., Ayers, C.R., Powell-Wiley, T.M., Vega, G.L., Farzaneh-Far, R., Grundy, S.M., Khera, A., McGuire, D.K., and de Lemos, J.A. 2012. Dysfunctional adiposity and the risk of prediabetes and type 2 diabetes in obese adults. JAMA **308**(11): 1150–9. doi:10.1001/2012.jama.11132.

Negi, S., Park, S.H., Jetha, A., Aikin, R., Tremblay, M., and Paraskevas, S. 2012. Evidence of

endoplasmic reticulum stress mediating cell death in transplanted human islets. Cell Transplant. **21**(5): 889–900.

Noda, K., Melhorn, M.I., Zandi, S., Frimmel, S., Tayyari, F., Hisatomi, T., Almulki, L., Pronczuk, A., Hayes, K.C., and Hafezi-Moghadam, A. 2010. An animal model of spontaneous metabolic syndrome: Nile grass rat. FASEB J. **24**(7): 2443–53. doi:10.1096/fj.09-152678.

Oakhill, J.S., Steel, R., Chen, Z.-P., Scott, J.W., Ling, N., Tam, S., and Kemp, B.E. 2011. AMPK Is a Direct Adenylate Charge-Regulated Protein Kinase. Science (80-.). **332**(6036): 1433–1435. doi:10.1126/science.1200094.

Ohtsubo, K., Chen, M.Z., Olefsky, J.M., and Marth, J.D. 2011. Pathway to diabetes through attenuation of pancreatic beta cell glycosylation and glucose transport. Nat. Med. **17**(9): 1067–1075. doi:10.1038/nm.2414.

Okada, T., Liew, C.W., Hu, J., Hinault, C., Michael, M.D., Krtzfeldt, J., Yin, C., Holzenberger, M., Stoffel, M., and Kulkarni, R.N. 2007. Insulin receptors in beta-cells are critical for islet compensatory growth response to insulin resistance. Proc. Natl. Acad. Sci. U. S. A. **104**(21): 8977–8982. United States.

Okamoto, H., Hribal, M.L., Lin, H. V, Bennett, W.R., Ward, A., and Accili, D. 2006. Role of the forkhead protein FoxO1 in beta cell compensation to insulin resistance. J. Clin. Invest. **116**(3): 775–782. United States.

Omikorede, O., Qi, C., Gorman, T., Chapman, P., Yu, A., Smith, D.M., and Herbert, T.P. 2013. ER stress in rodent islets of Langerhans is concomitant with obesity and β-cell compensation but not with β-cell dysfunction and diabetes. Nutr. Diabetes **3**(10): e93. England. doi:https://dx.doi.org/10.1038/nutd.2013.35.

Owen, M.R., Doran, E., and Halestrap, A.P. 2000. Evidence that metformin exerts its anti-diabetic effects through inhibition of complex 1 of the mitochondrial respiratory chain. Biochem. J. **348 Pt 3**: 607–14.

Oyadomari, S., Araki, E., and Mori, M. 2002. Endoplasmic reticulum stress-mediated apoptosis in pancreatic β -cells. **7**(4): 335–345.

Ozawa, S., Katsuta, H., Suzuki, K., Takahashi, K., Tanaka, T., Sumitani, Y., Nishida, S., Yoshimoto, K., and Ishida, H. 2014. Estimated proinsulin processing activity of prohormone convertase (PC) 1/3 rather than PC2 is decreased in pancreatic β-cells of type 2 diabetic patients. Endocr. J. **61**(6): 607–14.

Ozcan, U., Yilmaz, E., Ozcan, L., Furuhashi, M., Vaillancourt, E., Smith, R.O., Görgün, C.Z., and Hotamisligil, G.S. 2006. Chemical chaperones reduce ER stress and restore glucose homeostasis in a mouse model of type 2 diabetes. Science **313**(5790): 1137–40. doi:10.1126/science.1128294.

Patanè, G., Piro, S., Rabuazzo, A.M., Anello, M., Vigneri, R., and Purrello, F. 2000. Metformin restores insulin secretion altered by chronic exposure to free fatty acids or high glucose: a direct metformin effect on pancreatic beta-cells. Diabetes **49**(5): 735–40.

Pfützner, A., and Forst, T. 2011. Elevated intact proinsulin levels are indicative of Beta-cell

dysfunction, insulin resistance, and cardiovascular risk: impact of the antidiabetic agent pioglitazone. J. Diabetes Sci. Technol. **5**(3): 784–93. doi:10.1177/193229681100500333.

Pfützner, A., Pfützner, A.H., Larbig, M., and Forst, T. 2004. Role of intact proinsulin in diagnosis and treatment of type 2 diabetes mellitus. Diabetes Technol. Ther. **6**(3): 405–12. doi:10.1089/152091504774198124.

Piro, S., Rabuazzo, A.M., Renis, M., and Purrello, F. 2012. Effects of metformin on oxidative stress, adenine nucleotides balance, and glucose-induced insulin release impaired by chronic free fatty acids exposure in rat pancreatic islets. J. Endocrinol. Invest. **35**(5): 504–10. doi:10.3275/7866.

Plachot, C., Movassat, J., and Portha, B. 2001. Impaired beta-cell regeneration after partial pancreatectomy in the adult Goto-Kakizaki rat, a spontaneous model of type II diabetes. Histochem. Cell Biol. **116**(2): 131–139. Germany.

Portha, B. 2005. Programmed disorders of beta-cell development and function as one cause for type 2 diabetes: The GK rat paradigm. Diabetes. Metab. Res. Rev. **21**(6): 495–504. doi:10.1002/dmrr.566.

Portha, B., Giroix, M.H., Serradas, P., Gangnerau, M.N., Movassat, J., Rajas, F., Bailbe, D., Plachot, C., Mithieux, G., and Marie, J.C. 2001. beta-cell function and viability in the spontaneously diabetic GK rat: information from the GK/Par colony. Diabetes **50 Suppl 1**: S89-93.

Portha, B., Lacraz, G., Kergoat, M., Homo-Delarche, F., Giroix, M.H., Bailbé, D., Gangnerau, M.N., Dolz, M., Tourrel-Cuzin, C., and Movassat, J. 2009. The GK rat beta-cell: A prototype for the diseased human beta-cell in type 2 diabetes. Mol. Cell. Endocrinol. **297**(1–2): 73–85. doi:10.1016/j.mce.2008.06.013.

Prentki, M., and Nolan, C.J. 2006. Islet beta cell failure in type 2 diabetes. J. Clin. Invest. **116**(7): 1802–12. doi:10.1172/JCI29103.

Price, B.D. 1992. Signalling across the endoplasmic reticulum membrane: Potential mechanisms. doi:10.1016/0898-6568(92)90015-Z.

Punthakee, Z., Goldenberg, R., and Katz, P. 2018. Definition, Classification and Diagnosis of Diabetes, Prediabetes and Metabolic Syndrome. Can. J. Diabetes **42**: S10–S15. doi:10.1016/j.jcjd.2017.10.003.

Rahier, J., Guiot, Y., Goebbels, R.M., Sempoux, C., and Henquin, J.C. 2008. Pancreatic beta-cell mass in European subjects with type 2 diabetes. Diabetes. Obes. Metab. **10 Suppl 4**: 32–42. doi:10.1111/j.1463-1326.2008.00969.x.

Rajpal, G., Schuiki, I., Liu, M., Volchuk, A., and Arvan, P. 2012. Action of protein disulfide isomerase on proinsulin exit from endoplasmic reticulum of pancreatic β-cells. J. Biol. Chem. **287**(1): 43–7. doi:10.1074/jbc.C111.279927.

Rankin, M.M., and Kushner, J.A. 2009. Adaptive beta-cell proliferation is severely restricted with advanced age. Diabetes **58**(6): 1365–1372. United States. doi:https://dx.doi.org/10.2337/db08-1198.

Rasheva, V.I., and Domingos, P.M. 2009. Cellular responses to endoplasmic reticulum stress and apoptosis. Apoptosis **14**(8): 996–1007. doi:10.1007/s10495-009-0341-y.

Ravnskjaer, K., Kester, H., Liu, Y., Zhang, X., Lee, D., Yates, J.R., and Montminy, M. 2007. Cooperative interactions between CBP and TORC2 confer selectivity to CREB target gene expression. EMBO J. **26**(12): 2880–9. doi:10.1038/sj.emboj.7601715.

Robertson, R.P., Harmon, J., Tran, P.O.T., and Poitout, V. 2004. Beta-cell glucose toxicity, lipotoxicity, and chronic oxidative stress in type 2 diabetes. Diabetes **53 Suppl 1**: S119-24.

Saltiel, A.R., and Kahn, C.R. 2001. Insulin signalling and the regulation of glucose and lipid metabolism. Nature **414**(6865): 799–806. doi:10.1038/414799a.

Salvalaggio, P.R.O., Deng, S., Ariyan, C.E., Millet, I., Zawalich, W.S., Basadonna, G.P., and Rothstein, D.M. 2002. Islet filtration: a simple and rapid new purification procedure that avoids ficoll and improves islet mass and function. Transplantation **74**(6): 877–9. doi:10.1097/01.TP.0000028781.41729.5B.

Sansbury, F.H., Flanagan, S.E., Houghton, J.A.L., Shuixian Shen, F.L., Al-Senani, A.M.S., Habeb, A.M., Abdullah, M., Kariminejad, A., Ellard, S., and Hattersley, A.T. 2012. SLC2A2 mutations can cause neonatal diabetes, suggesting GLUT2 may have a role in human insulin secretion. Diabetologia **55**(9): 2381–2385. doi:10.1007/s00125-012-2595-0.

Sarparanta, J., García-Macia, M., and Singh, R. 2017. Autophagy and Mitochondria in Obesity and Type 2 Diabetes. Curr. Diabetes Rev. **13**(4): 352–369. doi:10.2174/1573399812666160217122530.

Scharfmann, R., Pechberty, S., Hazhouz, Y., von Bülow, M., Bricout-Neveu, E., Grenier-Godard, M., Guez, F., Rachdi, L., Lohmann, M., Czernichow, P., and Ravassard, P. 2014. Development of a conditionally immortalized human pancreatic β cell line. J. Clin. Invest. **124**(5): 2087–98. doi:10.1172/JCI72674.

Scheuner, D., and Kaufman, R.J. 2008. The unfolded protein response: a pathway that links insulin demand with beta-cell failure and diabetes. Endocr. Rev. **29**(3): 317–33. doi:10.1210/er.2007-0039.

Segerstolpe, Å., Palasantza, A., Eliasson, P., Andersson, E.-M., Andréasson, A.-C., Sun, X., Picelli, S., Sabirsh, A., Clausen, M., Bjursell, M.K., Smith, D.M., Kasper, M., Ämmälä, C., and Sandberg, R. 2016. Single-Cell Transcriptome Profiling of Human Pancreatic Islets in Health and Type 2 Diabetes. Cell Metab. **24**(4): 593–607. doi:10.1016/j.cmet.2016.08.020.

Seino, S., Shibasaki, T., and Minami, K. 2011. Dynamics of insulin secretion and the clinical implications for obesity and diabetes. J. Clin. Invest. **121**(6): 2118–25. doi:10.1172/JCI45680.

Shafrir, E., Ziv, E., and Kalman, R. 2006. Nutritionally induced diabetes in desert rodents as models of type 2 diabetes: Acomys cahirinus (spiny mice) and Psammomys obesus (desert gerbil). ILAR J. **47**(3): 212–24.

Sharma, R.B., O'Donnell, A.C., Stamateris, R.E., Ha, B., McCloskey, K.M., Reynolds, P.R., Arvan, P., and Alonso, L.C. 2015. Insulin demand regulates β cell number via the unfolded protein response. J. Clin. Invest. **125**(10): 3831–46. doi:10.1172/JCI79264.

Shaw, R.J., Lamia, K.A., Vasquez, D., Koo, S.-H., Bardeesy, N., Depinho, R.A., Montminy, M., and Cantley, L.C. 2005. The kinase LKB1 mediates glucose homeostasis in liver and therapeutic effects of metformin. Science **310**(5754): 1642–6. doi:10.1126/science.1120781.

Shen, J., Chen, X., Hendershot, L., and Prywes, R. 2002. ER stress regulation of ATF6 localization by dissociation of BiP/GRP78 binding and unmasking of golgi localization signals. Dev. Cell **3**(1): 99–111. doi:10.1016/S1534-5807(02)00203-4.

Shigeto, M., Ramracheya, R., Tarasov, A.I., Cha, C.Y., Chibalina, M. V, Hastoy, B., Philippaert, K., Reinbothe, T., Rorsman, N., Salehi, A., Sones, W.R., Vergari, E., Weston, C., Gorelik, J., Katsura, M., Nikolaev, V.O., Vennekens, R., Zaccolo, M., Galione, A., Johnson, P.R. V, Kaku, K., Ladds, G., and Rorsman, P. 2015. GLP-1 stimulates insulin secretion by PKC-dependent TRPM4 and TRPM5 activation. J. Clin. Invest. **125**(12): 4714–28. doi:10.1172/JCI81975.

Shirakawa, J., Fernandez, M., Takatani, T., El Ouaamari, A., Jungtrakoon, P., Okawa, E.R., Zhang, W., Yi, P., Doria, A., and Kulkarni, R.N. 2017. Insulin Signaling Regulates the FoxM1/PLK1/CENP-A Pathway to Promote Adaptive Pancreatic β Cell Proliferation. Cell Metab. **25**(4): 868-882.e5. doi:10.1016/j.cmet.2017.02.004.

Shu, L., Zien, K., Gutjahr, G., Oberholzer, J., Pattou, F., Kerr-Conte, J., and Maedler, K. 2012. TCF7L2 promotes beta cell regeneration in human and mouse pancreas. Diabetologia **55**(12): 3296–3307. Germany. doi:https://dx.doi.org/10.1007/s00125-012-2693-z.

da Silva Xavier, G., Leclerc, I., Varadi, A., Tsuboi, T., Moule, S.K., and Rutter, G.A. 2003. Role for AMP-activated protein kinase in glucose-stimulated insulin secretion and preproinsulin gene expression. Biochem. J. **371**(Pt 3): 761–74. doi:10.1042/BJ20021812.

da Silva Xavier, G., Mondragon, A., Mourougavelou, V., Cruciani-Guglielmacci, C., Denom, J., Herrera, P.L., Magnan, C., and Rutter, G.A. 2017. Pancreatic alpha cell-selective deletion of Tcf7l2 impairs glucagon secretion and counter-regulatory responses to hypoglycaemia in mice. Diabetologia **60**(6): 1043–1050. doi:10.1007/s00125-017-4242-2.

Skau, M., Pakkenberg, B., Buschard, K., and Bock, T. 2001. Linear correlation between the total islet mass and the volume-weighted mean islet volume. Diabetes **50**(8): 1763–70.

Smukler, S.R., Arntfield, M.E., Razavi, R., Bikopoulos, G., Karpowicz, P., Seaberg, R., Dai, F., Lee, S., Ahrens, R., Fraser, P.E., Wheeler, M.B., and van der Kooy, D. 2011. The adult mouse and human pancreas contain rare multipotent stem cells that express insulin. Cell Stem Cell **8**(3): 281–93. doi:10.1016/j.stem.2011.01.015.

Sonenberg, N., and Hinnebusch, A.G. 2009. Regulation of Translation Initiation in Eukaryotes: Mechanisms and Biological Targets. doi:10.1016/j.cell.2009.01.042.

Song, I., Patel, O., Himpe, E., Muller, C.J.F., and Bouwens, L. 2015. Beta Cell Mass Restoration in Alloxan-Diabetic Mice Treated with EGF and Gastrin. PLoS One **10**(10): e0140148. United States. doi:https://dx.doi.org/10.1371/journal.pone.0140148.

Song, L., and Fricker, L. 1995. Processing of procarboxypeptidase E into carboxypeptidase E occurs in secretory vesicles. J. Neurochem. **65**(1): 444–53.

Sriburi, R., Jackowski, S., Mori, K., and Brewer, J.W. 2004. XBP1: A link between the unfolded

protein response, lipid biosynthesis, and biogenesis of the endoplasmic reticulum. J. Cell Biol. **167**(1): 35–41. doi:10.1083/jcb.200406136.

Stamateris, R.E., Sharma, R.B., Hollern, D.A., and Alonso, L.C. 2013. Adaptive beta-cell proliferation increases early in high-fat feeding in mice, concurrent with metabolic changes, with induction of islet cyclin D2 expression. Am. J. Physiol. Endocrinol. Metab. **305**(1): E149-59. United States. doi:https://dx.doi.org/10.1152/ajpendo.00040.2013.

Stiles, L., and Shirihai, O.S. 2012. Mitochondrial dynamics and morphology in beta-cells. Best Pract. Res. Clin. Endocrinol. Metab. **26**(6): 725–738. doi:10.1016/j.beem.2012.05.004.

Straub, S.G., James, R.F., Dunne, M.J., and Sharp, G.W. 1998. Glucose activates both K(ATP) channel-dependent and K(ATP) channel-independent signaling pathways in human islets. Diabetes **47**(5): 758–63.

Subramaniam, A., Landstrom, M., Luu, A., and Hayes, K.C. 2018. The nile rat (Arvicanthis niloticus) as a superior carbohydrate-sensitive model for type 2 diabetes mellitus (T2DM). Nutrients **10**(2): 6–14. doi:10.3390/nu10020235.

Sukumar, N., Bagias, C., Goljan, I., Weldeselassie, Y., Gharanei, S., Tan, B.K., Holst, J.J., and Saravanan, P. 2018. Reduced GLP-1 Secretion at 30 Minutes After a 75-g Oral Glucose Load Is Observed in Gestational Diabetes Mellitus: A Prospective Cohort Study. Diabetes **67**(12): 2650–2656. doi:10.2337/db18-0254.

Sun, L., Xie, C., Wang, G., Wu, Y., Wu, Q., Wang, X., Liu, J., Deng, Y., Xia, J., Chen, B., Zhang, S., Yun, C., Lian, G., Zhang, X., Zhang, H., Bisson, W.H., Shi, J., Gao, X., Ge, P., Liu, C., Krausz, K.W., Nichols, R.G., Cai, J., Rimal, B., Patterson, A.D., Wang, X., Gonzalez, F.J., and Jiang, C. 2018. Gut microbiota and intestinal FXR mediate the clinical benefits of metformin. Nat. Med. **24**(12): 1919–1929. doi:10.1038/s41591-018-0222-4.

Szabat, M., Page, M.M., Panzhinskiy, E., Skovsø, S., Mojibian, M., Fernandez-Tajes, J., Bruin, J.E., Bround, M.J., Lee, J.T.C., Xu, E.E., Taghizadeh, F., O'Dwyer, S., van de Bunt, M., Moon, K.-M., Sinha, S., Han, J., Fan, Y., Lynn, F.C., Trucco, M., Borchers, C.H., Foster, L.J., Nislow, C., Kieffer, T.J., and Johnson, J.D. 2016. Reduced Insulin Production Relieves Endoplasmic Reticulum Stress and Induces β Cell Proliferation. Cell Metab. **23**(1): 179–93. doi:10.1016/j.cmet.2015.10.016.

Szendroedi, J., Phielix, E., and Roden, M. 2011. The role of mitochondria in insulin resistance and type 2 diabetes mellitus. Nat. Rev. Endocrinol. **8**(2): 92–103. doi:10.1038/nrendo.2011.138.

Szkudelski, T. 2001. The mechanism of alloxan and streptozotocin action in B cells of the rat pancreas. Physiol. Res. **50**(6): 537–46.

Tabák, A.G., Herder, C., Rathmann, W., Brunner, E.J., and Kivimäki, M. 2012. Prediabetes: a high-risk state for diabetes development. Lancet **379**(9833): 2279–2290. doi:10.1016/S0140-6736(12)60283-9.

Tabák, A.G., Jokela, M., Akbaraly, T.N., Brunner, E.J., Kivimäki, M., and Witte, D.R. 2009. Trajectories of glycaemia, insulin sensitivity, and insulin secretion before diagnosis of type 2 diabetes: an analysis from the Whitehall II study. Lancet (London, England) **373**(9682):

2215–21. doi:10.1016/S0140-6736(09)60619-X.

Tajima, K., Shirakawa, J., Okuyama, T., Kyohara, M., Yamazaki, S., Togashi, Y., and Terauchi, Y. 2017. Effects of metformin on compensatory pancreatic β-cell hyperplasia in mice fed a high-fat diet. Am. J. Physiol. Endocrinol. Metab. **313**(3): E367–E380. doi:10.1152/ajpendo.00447.2016.

Takamoto, I., Kubota, N., Nakaya, K., Kumagai, K., Hashimoto, S., Kubota, T., Inoue, M., Kajiwara, E., Katsuyama, H., Obata, A., Sakurai, Y., Iwamoto, M., Kitamura, T., Ueki, K., and Kadowaki, T. 2014. TCF7L2 in mouse pancreatic beta cells plays a crucial role in glucose homeostasis by regulating beta cell mass. Diabetologia **57**(3): 542–53. doi:10.1007/s00125-013-3131-6.

Talchai, C., Xuan, S., Lin, H. V, Sussel, L., and Accili, D. 2012. Pancreatic β cell dedifferentiation as a mechanism of diabetic β cell failure. Cell **150**(6): 1223–34. doi:10.1016/j.cell.2012.07.029.

Tanaka, K., Kawano, T., Tsutsumi, Y.M., Kinoshita, M., Kakuta, N., Hirose, K., Kimura, M., and Oshita, S. 2011. Differential effects of propofol and isoflurane on glucose utilization and insulin secretion. Life Sci. **88**(1–2): 96–103. doi:10.1016/j.lfs.2010.10.032.

Tang, C., Koulajian, K., Schuiki, I., Zhang, L., Desai, T., Ivovic, A., Wang, P., Robson-Doucette, C., Wheeler, M.B., Minassian, B., Volchuk, A., and Giacca, A. 2012. Glucose-induced beta cell dysfunction in vivo in rats: link between oxidative stress and endoplasmic reticulum stress. Diabetologia **55**(5): 1366–1379. doi:10.1007/s00125-012-2474-8.

Taylor, R., and Holman, R.R. 2015. Normal weight individuals who develop type 2 diabetes: the personal fat threshold. Clin. Sci. (Lond). **128**(7): 405–10. doi:10.1042/CS20140553.

Téllez, N., Vilaseca, M., Martí, Y., Pla, A., and Montanya, E. 2016. β-Cell dedifferentiation, reduced duct cell plasticity, and impaired β-cell mass regeneration in middle-aged rats. Am. J. Physiol. Metab. **311**(3): E554–E563. doi:10.1152/ajpendo.00502.2015.

Thorel, F., Népote, V., Avril, I., Kohno, K., Desgraz, R., Chera, S., and Herrera, P.L. 2010. Conversion of adult pancreatic alpha-cells to beta-cells after extreme beta-cell loss. Nature **464**(7292): 1149–54. doi:10.1038/nature08894.

Thorens, B., Guillam, M.T., Beermann, F., Burcelin, R., and Jaquet, M. 2000. Transgenic reexpression of GLUT1 or GLUT2 in pancreatic beta cells rescues GLUT2-null mice from early death and restores normal glucose-stimulated insulin secretion. J. Biol. Chem. **275**(31): 23751–8. doi:10.1074/jbc.M002908200.

Tourrel, C., Bailbé, D., Meile, M.J., Kergoat, M., and Portha, B. 2001. Glucagon-like peptide-1 and exendin-4 stimulate beta-cell neogenesis in streptozotocin-treated newborn rats resulting in persistently improved glucose homeostasis at adult age. Diabetes **50**(7): 1562–70. doi:10.2337/diabetes.50.7.1562.

Tschen, S.-I., Dhawan, S., Gurlo, T., and Bhushan, A. 2009. Age-dependent decline in beta-cell proliferation restricts the capacity of beta-cell regeneration in mice. Diabetes **58**(6): 1312–20. doi:10.2337/db08-1651.

Tseng, E., Yeh, H.-C., and Maruthur, N.M. 2017. Metformin Use in Prediabetes Among U.S.

Adults, 2005-2012. Diabetes Care **40**(7): 887–893. doi:10.2337/dc16-1509.

Turner, R.C., Cull, C.A., Frighi, V., and Holman, R.R. 1999. Glycemic control with diet, sulfonylurea, metformin, or insulin in patients with type 2 diabetes mellitus: progressive requirement for multiple therapies (UKPDS 49). UK Prospective Diabetes Study (UKPDS) Group. JAMA **281**(21): 2005–12.

Twig, G., Elorza, A., Molina, A.J.A., Mohamed, H., Wikstrom, J.D., Walzer, G., Stiles, L., Haigh, S.E., Katz, S., Las, G., Alroy, J., Wu, M., Py, B.F., Yuan, J., Deeney, J.T., Corkey, B.E., and Shirihai, O.S. 2008. Fission and selective fusion govern mitochondrial segregation and elimination by autophagy. EMBO J. **27**(2): 433–46. doi:10.1038/sj.emboj.7601963.

Uemura, A., Oku, M., Mori, K., and Yoshida, H. 2009. Unconventional splicing of XBP1 mRNA occurs in the cytoplasm during the mammalian unfolded protein response. J. Cell Sci. **122**(Pt 16): 2877–2886. doi:10.1242/jcs.040584.

UKPDS. 1998. Effect of intensive blood-glucose control with metformin on complications in overweight patients with type 2 diabetes (UKPDS 34). UK Prospective Diabetes Study (UKPDS) Group. Lancet (London, England) **352**(9131): 854–65.

De Vos, A., Heimberg, H., Quartier, E., Huypens, P., Bouwens, L., Pipeleers, D., and Schuit, F. 1995. Human and rat beta cells differ in glucose transporter but not in glucokinase gene expression. J. Clin. Invest. **96**(5): 2489–95. doi:10.1172/JCI118308.

Wang, N., Zhang, J., Wu, Y., Liu, J., Liu, L., and Guo, X. 2016. Metformin improves lipid metabolism disorders through reducing the expression of microsomal triglyceride transfer protein in OLETF rats. Diabetes Res. Clin. Pract. **122**: 170–178. doi:10.1016/j.diabres.2016.10.006.

Wang, P., Alvarez-Perez, J.-C., Felsenfeld, D.P., Liu, H., Sivendran, S., Bender, A., Kumar, A., Sanchez, R., Scott, D.K., Garcia-Ocaña, A., and Stewart, A.F. 2015. A high-throughput chemical screen reveals that harmine-mediated inhibition of DYRK1A increases human pancreatic beta cell replication. Nat. Med. **21**(4): 383–388. doi:10.1038/nm.3820.

Wareham, N.J., Byrne, C.D., Williams, R., Day, N.E., and Hales, C.N. 1999. Fasting proinsulin concentrations predict the development of type 2 diabetes. Diabetes Care **22**(2): 262–270. doi:10.2337/diacare.22.2.262.

Weir, G.C., and Bonner-Weir, S. 2004. Five of stages of evolving b-cell dysfunction during progression to diabetes. *In* Diabetes. pp. S16-21. doi:10.2337/diabetes.53.suppl_3.S16.

Weir, G.C., and Bonner-Weir, S. 2013. Islet β cell mass in diabetes and how it relates to function, birth, and death. Ann. N. Y. Acad. Sci. **1281**(1): 92–105. doi:10.1111/nyas.12031.

Weiss, M., Steiner, D.F., and Philipson, L.H. 2000. Insulin Biosynthesis, Secretion, Structure, and Structure-Activity Relationships. *In* Endotext.

Welch, W.J., and Brown, C.R. 1996. Influence of molecular and chemical chaperones on protein folding. Cell Stress Chaperones **1**(2): 109–15.

Weyer, C., Bogardus, C., Mott, D.M., and Pratley, R.E. 1999. The natural history of insulin secretory dysfunction and insulin resistance in the pathogenesis of type 2 diabetes mellitus.

J. Clin. Invest. **104**(6): 787–94. doi:10.1172/JCI7231.

Wild, S., Roglic, G., Green, A., Sicree, R., and King, H. 2004. Global prevalence of diabetes: estimates for the year 2000 and projections for 2030. Diabetes Care **27**(5): 1047–53. doi:10.2337/diacare.27.5.1047.

Wu, H., Esteve, E., Tremaroli, V., Khan, M.T., Caesar, R., Mannerås-Holm, L., Ståhlman, M., Olsson, L.M., Serino, M., Planas-Fèlix, M., Xifra, G., Mercader, J.M., Torrents, D., Burcelin, R., Ricart, W., Perkins, R., Fernàndez-Real, J.M., and Bäckhed, F. 2017. Metformin alters the gut microbiome of individuals with treatment-naive type 2 diabetes, contributing to the therapeutic effects of the drug. Nat. Med. **23**(7): 850–858. doi:10.1038/nm.4345.

Wyett, G., Gibert, Y., Ellis, M., Castillo, H.A., Jan Kaslin, and Aston-Mourney, K. 2018. Metformin, beta-cell development, and novel processes following beta-cell ablation in zebrafish. Endocrine **59**(2): 419–425. doi:10.1007/s12020-017-1502-3.

Xiao, C., Giacca, A., and Lewis, G.F. 2011. Sodium Phenylbutyrate, a Drug With Known Capacity to Reduce Endoplasmic Reticulum Stress, Partially Alleviates Lipid-Induced Insulin Resistance and β-Cell Dysfunction in Humans. Diabetes **60**(3): 918–924. doi:10.2337/db10-1433.

Xin, Y., Gutierrez, G.D., Okamoto, H., Kim, J., Lee, A.-H., Adler, C., Ni, M., Yancopoulos, G.D., Murphy, A.J., and Gromada, J. 2018. Pseudotime Ordering of Single Human β-Cells Reveals States of Insulin Production and Unfolded Protein Response. Diabetes **67**(June): db180365. doi:10.2337/db18-0365.

Xu, X., D'Hoker, J., Stangé, G., Bonné, S., De Leu, N., Xiao, X., Van de Casteele, M., Mellitzer, G., Ling, Z., Pipeleers, D., Bouwens, L., Scharfmann, R., Gradwohl, G., and Heimberg, H. 2008. Beta cells can be generated from endogenous progenitors in injured adult mouse pancreas. Cell **132**(2): 197–207. doi:10.1016/j.cell.2007.12.015.

Yang, K., Gotzmann, J., Kuny, S., Huang, H., Sauve, Y., and Chan, C. 2016. Five stages of progressive beta-cell dysfunction in the laboratory Nile rat model of type 2 diabetes. J. Endocrinol. doi:10.1530/JOE-15-0517.

Ye, L., Robertson, M.A., Hesselson, D., Stainier, D.Y.R., and Anderson, R.M. 2015. Glucagon is essential for alpha cell transdifferentiation and beta cell neogenesis. Development **142**(8): 1407–17. doi:10.1242/dev.117911.

Youle, R.J., and Narendra, D.P. 2011. Mechanisms of mitophagy. Nat. Rev. Mol. Cell Biol. **12**(1): 9–14. doi:10.1038/nrm3028.

Zhang, T., Kim, D.H., Xiao, X., Lee, S., Gong, Z., Muzumdar, R., Calabuig-Navarro, V., Yamauchi, J., Harashima, H., Wang, R., Bottino, R., Alvarez-Perez, J.C., Garcia-Ocana, A., Gittes, G., and Dong, H.H. 2016. FoxO1 Plays an Important Role in Regulating beta-Cell Compensation for Insulin Resistance in Male Mice. Endocrinology **157**(3): 1055–1070. United States. doi:https://dx.doi.org/10.1210/en.2015-1852.

Zhang, Y., Proenca, R., Maffei, M., Barone, M., Leopold, L., and Friedman, J.M. 1994. Positional cloning of the mouse obese gene and its human homologue. Nature **372**(6505):

425–32. doi:10.1038/372425a0.

Zhao, L., Guo, M., Matsuoka, T.-A., Hagman, D.K., Parazzoli, S.D., Poitout, V., and Stein, R. 2005. The islet beta cell-enriched MafA activator is a key regulator of insulin gene transcription. J. Biol. Chem. **280**(12): 11887–94. doi:10.1074/jbc.M409475200.

Zhou, G., Myers, R., Li, Y., Chen, Y., Shen, X., Fenyk-Melody, J., Wu, M., Ventre, J., Doebber, T., Fujii, N., Musi, N., Hirshman, M.F., Goodyear, L.J., and Moller, D.E. 2001. Role of AMP-activated protein kinase in mechanism of metformin action. J. Clin. Invest. **108**(8): 1167–74. doi:10.1172/JCI13505.

Zhu, X., Orci, L., Carroll, R., Norrbom, C., Ravazzola, M., and Steiner, D.F. 2002. Severe block in processing of proinsulin to insulin accompanied by elevation of des-64,65 proinsulin intermediates in islets of mice lacking prohormone convertase 1/3. Proc. Natl. Acad. Sci. U. S. A. **99**(16): 10299–304. doi:10.1073/pnas.162352799.

Zito, E., Chin, K.-T., Blais, J., Harding, H.P., and Ron, D. 2010. ERO1-β, a pancreas-specific disulfide oxidase, promotes insulin biogenesis and glucose homeostasis. J. Cell Biol. **188**(6): 821–832. doi:10.1083/jcb.200911086.

Zou, J., Chassaing, B., Singh, V., Pellizzon, M., Ricci, M., Fythe, M.D., Kumar, M.V., and Gewirtz, A.T. 2018. Fiber-Mediated Nourishment of Gut Microbiota Protects against Diet-Induced Obesity by Restoring IL-22-Mediated Colonic Health. Cell Host Microbe **23**(1): 41-53.e4. doi:10.1016/j.chom.2017.11.003.

Appendices

Appendix A: Applied Physiology, Nutrition and Metabolism manuscript

β-cell compensation concomitant with adaptive ER stress and β-cell neogenesis in a diet-induced type 2 diabetes model

Hui Huang[1], Kaiyuan Yang[2], Rennian Wang [3, 4], Woo Hyun Han[5], Sharee Kuny[5], Paula Horn Zelmanovitz[6], Yves Sauvé[1, 5] and Catherine B Chan[1, 2]

[1] Department of Physiology, University of Alberta, Edmonton, Alberta, T6G 2H7, Canada; [2] Department of Agricultural, Food and Nutritional Science, University of Alberta, Edmonton, Alberta, T6G 2P5, Canada; [3] Children's Health Research Institute, London, Ontario, N6C 2V5, Canada; [4] Department of Physiology and Pharmacology, University of Western Ontario, London, Ontario, N6A 3K7, Canada; [5] Department of Ophthalmology and Visual Sciences, University of Alberta, Edmonton, Alberta, Canada; [6] Department of Psychology, University of Alberta, Edmonton, Alberta T6G 2R3, Canada.

Corresponding author: Catherine B Chan; 6-126B Li Ka Shing Center for Health Research Innovation, University of Alberta, Edmonton, Alberta, T6G2E1, Canada; 1-(780) 492-9964; cbchan@ualberta.ca

Contact information for co-authors:

Hui Huang: hhuang2@ualberta.ca;

Kaiyuan Yang: kaiyuan3@ualberta.ca;

Rennian Wang: rwang@uwo.ca;

Woo Hyun Han: woohyun@ualberta.ca;

Sharee Kuny: skuny@ualberta.ca;

Paula Horn Zelmanovitz: zelmanov@ualberta.ca;

Yves Sauvé: ysauve@ualberta.ca.

ABSTRACT

Insulin-secreting pancreatic β-cells adapt to obesity-related insulin resistance via increases in insulin secretion and β-cell mass. Failed β-cell compensation predicts the onset of type 2 diabetes (T2D). However, the mechanisms of β-cell compensation are not fully understood. Our previous study reported changes in β-cell mass during the progression of T2D in the Nile rat (NR) fed standard chow. In the present study, we measured other β-cell adaptive responses including glucose metabolism and β-cell insulin secretion in NRs at different ages, thus characterizing NR at 2 months as a model of β-cell compensation followed by decompensation at 6 months. We observed increased proinsulin secretion in the transition from compensation to decompensation, indicative of impaired insulin processing. Subsequently, we compared adaptive unfolded protein response (UPR) in β-cells and demonstrated a positive role of ER chaperones in insulin secretion. In addition, the incidence of insulin-positive neogenic but not proliferative cells increased during the compensation phase, suggesting non-proliferative β-cell growth as a mechanism of β-cell mass adaptation. In contrast, decreased neogenesis and β-cell dedifferentiation were observed in β-cell dysfunction. Furthermore, the progression of T2D and pathophysiological changes of β-cells were prevented by increasing fibre content of the diet.

- Our study characterized a novel model for β-cell compensation with adaptive responses in cell function and mass
- The temporal association of adaptive ER chaperones with blood insulin and glucose suggests upregulated chaperone capacity as an adaptive mechanism
- β-cell neogenesis but not proliferation contributes to β-cell mass adaptation

Keywords: type 2 diabetes, animal model, β-cell compensation, ER stress, proliferation, neogenesis

INTRODUCTION

Diabetes is a global public health issue. The adult population affected by diabetes was 425 million worldwide in 2017 and this number is expected to reach 629 million by 2045 (Cho et al. 2018). Over 90% of the diabetic population is diagnosed with type 2 diabetes (T2D), which is a chronic metabolic disorder featuring hyperglycemia resulting from insulin resistance and failure of insulin-producing pancreatic β-cells.

In the natural history of T2D, β-cell adaptation or compensation is a major mechanism in preventing or delaying T2D progression. β-cells are capable of adapting to peripheral insulin resistance, which is associated with obesity and impaired lipid metabolism (Neeland et al. 2012), by producing more insulin (Weyer et al. 1999; Festa et al. 2006). Euglycemia can sometimes be maintained for years until the failure of compensation, leading to an increase in blood glucose and onset of T2D (Tabák et al. 2009; Hulman et al. 2017). Evidence from human studies shows enhanced insulin secretion and expanded β-cell mass in insulin-resistant but not diabetic subjects, suggesting that both β-cell function and mass are involved in β-cell adaptation (Camastra et al. 2005; Rahier et al. 2008; Hanley et al. 2010); however, due to the limited approaches feasible in human research, the cellular mechanisms of human β-cell adaptation are not clear.

Despite animal models being an indispensable tool in T2D research, not all T2D models are appropriate for studying β-cell compensation. For instance, the classic T2D db/db mouse model, which is has a monogenic defect in the leptin receptor, exhibits only a transient adaptation stage followed by early onset of diabetes (Chan et al. 2013). Age, diet and genetic background of the model also affect β-cell phenotype and plasticity observed in the compensation stage (Tschen et al. 2009; Hanley et al. 2010; Burke et al. 2017). To elucidate the molecular basis of β-cell adaptation, a validated animal model that recapitulates human T2D features is required.

Nile rat (NR), *Arvicanthis niloticus*, is a diurnal rodent model of spontaneous T2D. Compared with genetic or chemical-induced models, the NR exhibits a slower progression of T2D when fed a standard chow diet (Chow), which recapitulates human T2D stages from initial hyperinsulinemia through to late-onset

hyperglycemia appearing around 12 months of age (Chaabo et al. 2010; Yang et al. 2016; Subramaniam et al. 2018). This progressive T2D can be prevented in NRs fed on a low-energy, fiber-rich (Hfib) diet (Yang et al. 2016). In Chow-fed NRs, the hyperinsulinemia is sustained for months while maintaining euglycemia (Yang et al. 2016), suggesting β-cell adaptation. In addition, we found that β-cell mass trends upward in Chow-fed NR during the stage of the early hyperinsulinemia (Yang et al. 2016); however, the mild changes observed in β-cell mass are inadequate to explain the dramatic increase in plasma insulin. Therefore, we speculate that, in addition to β-cell mass, β-cell function is enhanced as a mechanism of β-cell compensation in NRs.

Our previous study also suggested that β-cell dysfunction in diabetic NRs at 12 months was associated with compromised insulin processing and endoplasmic reticulum (ER) stress (Yang et al. 2016). ER is a membranous cell organelle consisting of cisternae, where the newly synthesized proinsulin is folded into a three-dimensional structure (Price 1992). Increased insulin demand leads to an overload of proinsulin relative to ER capacity, resulting in unfolded protein accumulation and activation of the ER stress response, also referred to as unfolded protein response (UPR) (Eizirik et al. 2008; Scheuner and Kaufman 2008). Recent evidence has linked early ER stress to β-cell compensation by showing that UPR improves ER capacity, β-cell function and proliferation (Omikorede et al. 2013; Chan et al. 2013; Sharma et al. 2015). Therefore, we then postulated that the adaptive UPR, as part of the mechanism of β-cell adaptation, is associated with changes in β-cell function and mass.

To validate the NR as a model for β-cell compensation, we first sought to evaluate β-cell function in the context of T2D progression *in vivo* and *in vitro*. NRs fed with Hfib diet were used as healthy controls. We then examined the adaptive events occurring in β-cells including colocalization of ER chaperones involved in insulin processing with insulin, cell proliferation, and neogenesis in order to understand the mechanism of β-cell adaptation.

EXPERIMENTAL PROCEDURES

Animals

Male NRs used in this study were from a colony established at the University of Alberta. Original breeder animals were graciously provided by Dr. L. Smale (Michigan State University). Animals were housed at 21°C under a 14-hour light, 10-hour dark cycle. After weaning at 3 weeks, animals were fed with either high energy, low fiber Chow (Prolab® RMH 2000, 5P06, LabDiet, Nutrition Intl., Richmond, IN) or low energy, high fiber Hfib diet (Mazuri® Chinchilla Diet, 5M01, Purina Mills, LLC, St. Louis, MO)(Yang et al. 2016). Rats were fasted for 16 hours with free access to water prior to blood collection and subsequent euthanasia. All animal studies were approved by the University of Alberta Animal Care and Use Committee (Animal use protocol #00000328) and were conducted in accordance with Canadian Council on Animal Care Guidelines.

Glucose and insulin tolerance test

Intraperitoneal glucose tolerance (ipGTT) and insulin tolerance tests (ITT) were performed on animals fasted for 16 h and 4 h, respectively. Due to the feral behavior of NRs, animals were anesthetized with isoflurane (Sigma-Aldrich) during procedures. Glucose and insulin testing involved i.p. injection per kg body weight of 1 g glucose or 1U insulin followed by blood sampling before and 10, 20, 40, 60, 90, 120 minutes after injection. Blood glucose was determined using a CONTOUR NEXT blood glucose monitoring system (Bayer Inc., Mississauga, Canada). Insulin and proinsulin concentrations were determined by ELISA (Crystal Chem Inc. Downers Grove, IL, USA; ALPCO Diagnostics Inc., Salem, NH).

Fasting blood glucose, plasma insulin concentration, and body mass index

Fasting blood glucose (FBG) was measured from a 1-2 μL tail blood sample using a CONTOUR NEXT blood glucose monitoring system. Animals with an FBG of 5.6 mmol/L or higher were considered hyperglycemic as previously established (Yang et al. 2016). The heterogeneity index, introduced as an

indicator of the diversity of FBG phenotype, was calculated by dividing the standard deviation by the mean. Animals were euthanized by Euthanyl injection. Blood and tissue collections were performed as previously described (Yang et al. 2016).

Isolation of pancreatic islets and glucose-stimulated insulin secretion (GSIS)

Pancreatic islets were isolated by collagenase XI digestion (0.5 mg/mL, Sigma, St. Louis, USA) and purified as described (Salvalaggio et al. 2002; Yang et al. 2016). Isolated islets were cultured overnight in Dulbecco's modified Eagle's medium (DMEM) (Gibco, N.Y., USA) supplemented with 8.3 mM glucose and 10% bovine serum. To assess insulin secretion, three isolated islets were incubated in 1 mL of DMEM supplemented with different concentrations of glucose from 2.8-22 mM for 90 minutes and then centrifuged at 1500 rpm for 5 minutes. The supernatant (released insulin) was transferred into new tubes and the pellets were lysed using 1mL of 3% acetic acid. Insulin in the supernatant and the pellet was determined by insulin radioimmunoassay (RIA). Insulin release, when expressed as a percentage, was calculated by dividing released insulin by total insulin content (supernatant + pellet). The stimulation index was calculated as the ratio of insulin release (%) at 16.5 mM versus 2.8 mM glucose. Maximal insulin release and half maximal glucose concentration (EC_{50}) were calculated from a sigmoidal dose-concentration plot using GraphPad Prism version 6.0.

Immunofluorescent microscopy

Pancreatic tissues were fixed with formalin. Sections mounted on glass slides were immunostained for insulin, glucagon, ER proteins, ki67, Pdx1 using species appropriate AlexaFluor or HRP-conjugated secondary antibodies as previously described (Yang et al. 2016). Antibody details and staining conditions are listed in Supplementary Table S1. For ER protein staining, slides were visualized using a Wave FX spinning disk confocal microscope (Quorum Technologies Inc., Guelph, ON, Canada); colocalization and staining intensity were analyzed using Volocity 6.0 (PerkinElmer) as previously described (Yang et al. 2016). For ki67, Pdx1, peroxidase-based staining, images were obtained using a Zeiss Axio Imager Z1 with Axio Vision 4.5 (Carl Zeiss Micro Imaging GmbH, Germany) and quantified with ImageJ (NIH, Bethesda,

MD, USA). In the analysis of β-cell neogenesis, insulin-positive pancreatic duct- or acinar-associated cells or cell clusters that had no more that four cells were classified as "neogenic" β-cells, an accepted surrogate for neogenesis (Okamoto et al. 2006; Hanley et al. 2010). Overall β-cell neogenesis was estimated as the percentage of the neogenic β-cell area to total pancreatic section area.

Semi-quantitative real-time PCR

Total RNA from isolated islets was extracted with TRIzol reagent (Sigma) and cDNA was synthesized with a QuantiTect reverse transcription kit (QIAGEN, Mississauga, ON, Canada) according to the manufacturer's specifications. Real-time PCR was performed using an SYBR green qPCR Mastermix (QIAGEN) and Rotor Gene 6000 Real-time PCR machine (Corbett Research). q-PCR data was analyzed using the delta Ct method (Livak and Schmittgen 2001). Target gene expression was normalized to β-actin. Primers listed in Supplementary Table S2 were designed in regions conserved among mammalian species as described in Supplementary material.

Statistical analyses

For all experiments, data were expressed as the mean ± SEM and statistically analyzed with GraphPad Prism version 6.0. One-way or two-way analysis of variance was used, followed by post-hoc Bonferroni's multiple comparisons if significance was reached. ipGTT and ITT were analyzed using a repeated measures two-way ANOVA. Differences were considered significant at $p<0.05$.

RESULTS

Metabolic characteristics of Nile rats at 2, 6 and 12 months

NRs fed Chow diet display fasting euglycemia at 2 months, moderate increases in glucose at 6 months (FBG heterogeneity index illustrates the phenotypic diversity at this age), and significant hyperglycemia appearing at 12 months (Fig. 1A-B). Fasting blood glucose is changed by diet intervention and Hfib controls maintain stable blood glucose at all ages (overall $p=0.001$, Fig. 1A). NRs in the Chow group display early onset hyperinsulinemia (Fig. 1C). In response to a 50% reduction in whole-body insulin sensitivity (Fig.

1D), β-cell function (HOMA-B) increases (Fig. 1E) during this compensatory stage. Body weight at 6 and 12 months is significantly higher in Chow NRs in comparison with age-matched Hfib controls (Fig. 1F). To better describe this model, data from individual animals are plotted in the five stages proposed for human diabetes based on glucose and insulin concentrations (Fig. 1G)(Weir and Bonner-Weir 2004).

Progression from β-cell compensation to decompensation in NR

To assess β-cell secretory function in NRs, we measured GSIS *in vivo* and *in vitro*. Chow-fed NRs show comparable glucose tolerance compared with Hfib at 2 months (Fig. 2A), with a 2-fold increase in insulin secretion (overall $p< 0.05$, Fig. 2B). Plasma proinsulin relative to insulin, as an indicator of β-cell function (Wareham et al. 1999; Pfützner et al. 2004), does not differ between groups at 2 months (overall $p=0.1$, Fig. 2C). At 6 months, Chow animals present impaired glucose tolerance (overall $p<0.05$, Fig. 2D), with elevated insulin secretion (overall $p<0.05$, Fig. 2E) and proinsulin/insulin ratio (overall $p<0.001$, Fig. 2F) in Chow NRs. Chow-fed animals exhibit impaired insulin tolerance at both 2 and 6 months compared with Hfib (overall $p<0.05$, Fig. 2G and 2H).

In vitro β-cell function was determined by GSIS from intact isolated islets. Although there is no change in the absolute amount of insulin released per islet (Fig. 3A), at 2 months the insulin release relative to total insulin is augmented particularly at lower glucose concentrations (Fig. 3B), indicating enhanced responsiveness to physiological concentrations of glucose of Chow islets . This compensation in Chow-fed NRs fails as the animals age, with a significant reduction in insulin secretion (per islet) at 6 and 12 months (Fig. 3C and 3E) compared to Hfib. The increase in % insulin release in Chow seen at 2 months is diminished at 6 and 12 months (Fig. 3D and 3F). A 50% decrease in half-maximal glucose concentration in 2-month Chow islets (Fig. 3G) indicates a left shift of the glucose response. The stimulation index, another indicator of islet function, is slightly decreased in Chow islets (overall $p<0.05$, Fig. 3H). Total insulin content in islets is markedly reduced with diabetes (12 months, $p< 0.01$, Fig. 3I).

ER chaperones in β-cell compensation versus dysfunction

To investigate the role of impaired insulin processing and adaptive ER stress in T2D NRs, we examined three ER chaperones involved in insulin processing: protein disulfide isomerase (PDI), ER resident protein 44 (ERp44) and ER resident protein 72 (ERp72). Increases in PDI are present in β-cells at 2 and 6 months (Fig. 4A) and demonstrate colocalization with insulin (Fig. 4B). PDI/insulin colocalization coefficient is proportional to circulating fasting insulin concentration (Fig. 4E). ERp44 is also upregulated in Chow animals at 2 and 6 months (Fig. 4A and 4C). ERp72 does not differ between diet groups but significantly declines with age (Fig. 4A and 4D); however, ERp72 colocalization with insulin is inversely related to fasting blood glucose (12 months, $p<0.05$, Fig. 4F).

Critical to adaptive UPR, activating transcription factor -4 and -6 (ATF4, ATF6) and XBP1(X-box binding protein, unspliced and spliced) are involved in stimulating expression of ER chaperones, protein foldase and protein degradation machinery (Scheuner and Kaufman 2008). However, mRNA of transcription factors at 2 months are comparable between groups (Fig. 4G). At 6 months, *Atf4* and *Atf6* show increasing trends between groups ($p=0.06$ and 0.08 for main effect of diet, respectively, Fig. 4G). The spliced (s) and unspliced (u) *Xbp1* demonstrate pronounced increases in the Chow group at 6 months (Fig. 4G).

ER stress can also contribute to β-cell apoptosis and loss of β-cell mass (Eizirik et al. 2008), another feature of human T2D. However, C/EBP homologous protein (CHOP), apoptosis caspase 12 (an ER stress-induced caspase), and caspase 3 (a downstream marker of apoptosis) remain almost undetectable (Supplementary figure S1).

β-cell mass compensation by neogenesis but not proliferation

Previous evidence indicated the occurrence of β-cell mass compensation in Chow NRs (Yang et al. 2016), which has been linked to β-cell proliferation and UPR (Sharma et al. 2015). However, using ki67 as a proliferation marker, the occurrence of $ki67^{+}$/$insulin^{+}$ cells in Chow-fed NRs is very low compared with Hfib (overall $p<0.005$, Fig. 5A and 5B), indicating a mechanism other than cell replication. Surprisingly,

insulin-positive structures meeting the definition for neogenesis (Hanley et al. 2010) demonstrate a marked increase in chow NRs at the compensation stage (2 mo, $p<0.01$, Fig. 6A and 6B), which declined concurrently with onset of β-cell dysfunction (2 mo vs 12 mo, $p<0.01$, Fig. 6A and 6B). Of note, the single β-cells and small β-cell clusters seen in 12-month Chow animals are observed in disrupted islets with α-cells infiltrating the center of the islet (Fig. 6A), which is consistent with the previous result that α/ β-cells ratio increases with diabetes (Sharma et al. 2015).

A growing body of evidence supports that transdifferentiation occurs in the progression of β-cell dysfunction (Mezza et al. 2014; Cigliola et al. 2016). The existence of cells reacting to both insulin and glucagon (Fig. 7A), together with co-occurrence of pancreatic and duodenal homeobox 1 (Pdx1), a β-cell specific transcriptional factor, with glucagon (Fig. 7B), indicate transdifferentiation in NRs. However, whether it is β-cell dedifferentiation or α-cell-to-β-cell compensatory alteration needs more investigation.

DISCUSSION

Weir (Weir and Bonner-Weir 2004) characterized the progression of T2D into multiple stages, in which the compensation stage occurs when insulin secretion increases in the face of insulin resistance and blood glucose is kept within the normal range. Animal studies often indicate the stages of T2D models using plasma insulin as the key marker. However, the insulin trajectory in patients with T2D trends upward even after the diagnosis (Tabák et al. 2009; Hulman et al. 2017). In fact, acute GSIS is suggested to be associated with T2D progression regarding glycemic control (Weir and Bonner-Weir 2004; Festa et al. 2006). Our present result of elevated GSIS during ipGTT confirms that β-cells from chow-fed NRs at 2 months were compensating for decreased insulin sensitivity while the glucose tolerance was well-maintained. In contrast, glucose tolerance in 6-month NRs was impaired albeit with a pronounced rise in insulin secretion. This phenotype fits the features of the decompensation stage (Weir and Bonner-Weir 2004). The diabetic phenotype is prevented by feeding a high-fibre diet after weaning.

Consistent with insulin secretion in vivo, GSIS by isolated islets indicates that Chow β-cells at 2 months were more responsive to glucose than Hfib islets, especially at physiological glucose concentrations (2.8-

5.5 mM). However, responsiveness was diminished at 6 months in spite of the sustained GSIS *in vivo*, which together with elevated plasma proinsulin at 6 months demonstrates a functional change in β-cells during the transition from compensation to decompensation stage (Wareham et al. 1999; Pfützner and Forst 2011). Moreover, both islet insulin content and staining intensity *in situ* (Fig. 3I and Supplementary figure S2) began to decline from 6 months, linking the functional change to decreased insulin synthesis or processing.

To fulfill the increased insulin demand in the context of insulin resistance, β-cells synthesize and process a large amount of proinsulin, which is achieved by a highly active ER (Scheuner and Kaufman 2008). Perturbation in the ER caused by insufficient chaperones can be sensed and corrected by UPR as a protective mechanism of β-cells (Eizirik et al. 2008; Scheuner and Kaufman 2008). In contrast to a recent study showing that UPR is exclusively observed at the decompensation stage (Gupta et al. 2017), our present data suggest adaptive UPR occurs early in the compensation stage. The insulin-colocalized ER resident chaperones showed marked increases in adaptive β-cells (versus Hfib), which then declined concomitant with dysfunction (2 versus 12 months), indicating a positive role of ER chaperones in sustaining β-cell compensation (Omikorede et al. 2013; Chan et al. 2013; Engin et al. 2014; Sharma et al. 2015). Of note, a positive correlation of PDI with circulating insulin concentration was observed in chow-fed NRs. A protective effect of PDI is suggested by a growing number of studies showing PDI overexpression protects β-cell from glucolipotoxicity (Montane et al. 2016), enhances ER-associated degradation (ERAD), and restores insulin production (He et al. 2015; Gorasia et al. 2016). However, no changes were observed regarding transcription factors that are related to ER stress until decompensation at 6 months. A limitation of this study is that nuclear translocation of transcription factors, which could lead to an increase in ER chaperones, could not be directly assessed.

Given that chronic ER stress also induces β-cell apoptosis as part of the pathogenesis of β-cell dysfunction (Negi et al. 2012), the diminished ER chaperones seen at 12 months may imply activation of maladaptive UPR. However, we did not detect any change in CHOP, an apoptotic UPR transcription factor (Rasheva

and Domingos 2009), or caspase 12 (Supplementary figure S1). To better understand ER chaperones and their regulation with diabetes progression, a thorough evaluation of UPR regulators is necessary at different stages.

Our previous study showed an increasing trend in β-cell mass during the compensation stage (Yang et al. 2016), which is another feature of β-cell compensation (Weir and Bonner-Weir 2013). Current evidence favors the concept that β-cells proliferate in response to enhanced glucose metabolism during compensation (Stamateris et al. 2013; Sharma et al. 2015) and UPR is suggested as part of the mechanism (Sharma et al. 2015). However, in our model, we saw a decrease in β-cell proliferation even during the compensation stage when the adaptive UPR was present in β-cells. This is supported by single β-cell sequencing results showing that β-cells are less likely to proliferate under the high workload demanded by insulin biosynthesis (Xin et al. 2018). An inverse relationship of β-cell function and proliferation is demonstrated in immortalized β-cell lines (Scharfmann et al. 2014) and validated in animal models (Szabat et al. 2016). Indeed, β-cell replication is very rare in adult human pancreas (Butler et al. 2003; Hanley et al. 2010), and the proliferation seen in animal models is restricted with aging (Tschen et al. 2009; Gupta et al. 2017).

As an alternative to proliferation, β-cell neogenesis is speculated to be the main event contributing to human β-cell mass adaptation (Butler et al. 2003; Meier et al. 2008; Hanley et al. 2010). Neogenesis is defined as formation of β-cells from progenitor cells (Bonner-Weir et al. 2012). In line with that, we showed a 5-fold increase in β-cell area arising from small insulin-positive clusters using a surrogate definition of neogenesis (Hanley et al. 2010) in compensating NRs, which accounts for over 10% of the total β-cell area reported previously (Yang et al. 2016). The change in number of these small clusters of β-cells induced by diet and age suggests that these are indeed neogenic in origin and not static remnants of embryonic development (Bonner-Weir et al. 2012). Moreover, β-cell dedifferentiation was observed at 12 months, suggesting that in addition to cell growth and death, dedifferentiation is in part related to the disrupted islet structure and failure of β-cell compensation (Talchai et al. 2012).

In summary, we demonstrate a model that recapitulates characteristics of human β-cell compensation to decompensation regarding glucose metabolism, β-cell function and mass (Fig. 7C). The enhanced β-cell insulin secretion was detected at 2 months with a surge of upregulated ER chaperones, which decreased with T2D progression. β-cell mass increased during the compensation stage by nonproliferative means. Our study highlights the temporal relationship of adaptive ER capacity with β-cell function in the transition from compensation to decompensation and changes in islet plasticity that play a role in β-cell mass. Furthermore, the ability to prevent all of the stages of diabetes development in this model by increasing fibre content of the diet provides researchers with the ability to manipulate the stages of compensation and decompensation.

AUTHOR CONTRIBUTIONS

H H performed experiments, analyzed results, and wrote the manuscript. K Y, W H H, S K and R W performed experiments. P H Z analyzed data. All authors revised the manuscript and approved the final version. Y S and C B C provided funding. C B C is the guarantor of this publication and takes full responsibility for the work.

ACKNOWLEDGMENTS

We thank Rachel Bryant and Jillian Schneider for their assistance in performing experiments; Nicole Coursen for preparation of samples; Kunimasa Suzuki for designing qPCR primers.

Parts of this study were presented in abstract form at 19th Canadian Diabetes Association/CSEM Professional Conference, Ottawa, Canada and published as an abstract in a supplement issue of the Canadian Journal of Diabetes, 2016 (40), Issue 5, Supplement, Pages S60–S61.

This work was supported by the Canadian Institutes of Health Research CIHR; MOP 125873) to Y S and C B C. Y S is an AHFMR senior scholar (200800242); H H and K Y are recipients of scholarships from China Scholarship Council.

CONFLICT OF INTEREST

The authors declare that they have no conflict of interest to disclose.

REFERENCES

Bonner-Weir, S., Guo, L., Li, W.-C., Ouziel-Yahalom, L., Lysy, P.A., Weir, G.C., and Sharma, A. 2012. Islet neogenesis: a possible pathway for beta-cell replenishment. Rev. Diabet. Stud. 9(4): 407–16. doi:10.1900/RDS.2012.9.407.

Burke, S.J., Batdorf, H.M., Burk, D.H., Noland, R.C., Eder, A.E., Boulos, M.S., Karlstad, M.D., and Collier, J.J. 2017. db/db Mice Exhibit Features of Human Type 2 Diabetes That Are Not Present in Weight-Matched C57BL/6J Mice Fed a Western Diet. J. Diabetes Res. 2017: 8503754. doi:10.1155/2017/8503754.

Butler, A.E., Janson, J., Bonner-Weir, S., Ritzel, R., Rizza, R.A., and Butler, P.C. 2003. Beta-cell deficit and increased beta-cell apoptosis in humans with type 2 diabetes. Diabetes, 52(1): 102–10.

Camastra, S., Manco, M., Mari, A., Baldi, S., Gastaldelli, A., Greco, A. V, Mingrone, G., and Ferrannini, E. 2005. beta-cell function in morbidly obese subjects during free living: long-term effects of weight loss. Diabetes, 54(8): 2382–9.

Chaabo, F., Pronczuk, A., Maslova, E., and Hayes, K. 2010. Nutritional correlates and dynamics of diabetes in the Nile rat (Arvicanthis niloticus): a novel model for diet-induced type 2 diabetes and the metabolic syndrome. Nutr. Metab. (Lond). 7: 29. doi:10.1186/1743-7075-7-29.

Chan, J.Y., Luzuriaga, J., Bensellam, M., Biden, T.J., and Laybutt, D.R. 2013. Failure of the adaptive unfolded protein response in islets of obese mice is linked with abnormalities in β-cell gene expression and progression to diabetes. Diabetes, 62(5): 1557–68. doi:10.2337/db12-0701.

Cho, N.H., Shaw, J.E., Karuranga, S., Huang, Y., da Rocha Fernandes, J.D., Ohlrogge, A.W., and Malanda, B. 2018. IDF Diabetes Atlas: Global estimates of diabetes prevalence for 2017 and projections for 2045. *In* Diabetes Res. Clin. Pract. doi:10.1016/j.diabres.2018.02.023.

Cigliola, V., Thorel, F., Chera, S., and Herrera, P.L. 2016. Stress-induced adaptive islet cell identity changes. Diabetes. Obes. Metab. 18 Suppl 1: 87–96. doi:10.1111/dom.12726.

Eizirik, D.L., Cardozo, A.K., and Cnop, M. 2008. The role for endoplasmic reticulum stress in diabetes mellitus. Endocr. Rev. 29(1): 42–61. doi:10.1210/er.2007-0015.

Engin, F., Nguyen, T., Yermalovich, A., and Hotamisligil, G.S. 2014. Aberrant islet unfolded protein response in type 2 diabetes. Sci. Rep. 4: 4054. doi:10.1038/srep04054.

Festa, A., Williams, K., D'Agostino, R., Wagenknecht, L.E., and Haffner, S.M. 2006. The natural course of beta-cell function in nondiabetic and diabetic individuals: the Insulin Resistance Atherosclerosis Study. Diabetes 55(4): 1114–20.

Gorasia, D.G., Dudek, N.L., Safavi-Hemami, H., Perez, R.A., Schittenhelm, R.B., Saunders, P.M., Wee, S., Mangum, J.E., Hubbard, M.J., and Purcell, A.W. 2016. A prominent role of PDIA6 in processing of misfolded proinsulin. Biochim. Biophys. Acta, 1864(6): 715–23. doi:10.1016/j.bbapap.2016.03.002.

Gupta, D., Jetton, T.L., LaRock, K., Monga, N., Satish, B., Lausier, J., Peshavaria, M., and Leahy, J.L. 2017. Temporal Characterization of β-cell Adaptive and Maladaptive Mechanisms During Chronic High Fat Feeding in C57BL/6NTac Mice. J. Biol. Chem. 292(30): 12449-12459. doi:10.1074/jbc.M117.781047.

Hanley, S.C., Austin, E., Assouline-Thomas, B., Kapeluto, J., Blaichman, J., Moosavi, M., Petropavlovskaia, M., and Rosenberg, L. 2010. Beta-Cell mass dynamics and islet cell plasticity in human type 2 diabetes. Endocrinology, 151(4): 1462–72. doi:10.1210/en.2009-1277.

He, K., Cunningham, C.N., Manickam, N., Liu, M., Arvan, P., and Tsai, B. 2015. PDI reductase acts on Akita mutant proinsulin to initiate retrotranslocation along the Hrd1/Sel1L-p97 axis. Mol. Biol. Cell, 26(19): 3413–23. doi:10.1091/mbc.E15-01-0034.

Hulman, A., Simmons, R.K., Brunner, E.J., Witte, D.R., Færch, K., Vistisen, D., Ikehara, S., Kivimaki, M., and Tabák, A.G. 2017. Trajectories of glycaemia, insulin sensitivity and insulin secretion in South Asian and white individuals before diagnosis of type 2 diabetes: a longitudinal analysis from the Whitehall II cohort study. Diabetologia, 60(7): 1252–1260. doi:10.1007/s00125-017-4275-6.

Livak, K.J., and Schmittgen, T.D. 2001. Analysis of relative gene expression data using real-time

quantitative PCR and the 2(-Delta Delta C(T)) Method. Methods, 25(4): 402–8. doi:10.1006/meth.2001.1262.

Meier, J.J., Butler, A.E., Saisho, Y., Monchamp, T., Galasso, R., Bhushan, A., Rizza, R.A., and Butler, P.C. 2008. Beta-cell replication is the primary mechanism subserving the postnatal expansion of beta-cell mass in humans. Diabetes, 57(6): 1584–94. doi:10.2337/db07-1369.

Mezza, T., Muscogiuri, G., Sorice, G.P., Clemente, G., Hu, J., Pontecorvi, A., Holst, J.J., Giaccari, A., and Kulkarni, R.N. 2014. Insulin resistance alters islet morphology in nondiabetic humans. Diabetes, 63(3): 994–1007. doi:10.2337/db13-1013.

Montane, J., de Pablo, S., Obach, M., Cadavez, L., Castaño, C., Alcarraz-Vizán, G., Visa, M., Rodríguez-Comas, J., Parrizas, M., Servitja, J.M., and Novials, A. 2016. Protein disulfide isomerase ameliorates β-cell dysfunction in pancreatic islets overexpressing human islet amyloid polypeptide. Mol. Cell. Endocrinol. 420: 57–65. doi:10.1016/j.mce.2015.11.018.

Neeland, I.J., Turer, A.T., Ayers, C.R., Powell-Wiley, T.M., Vega, G.L., Farzaneh-Far, R., Grundy, S.M., Khera, A., McGuire, D.K., and de Lemos, J.A. 2012. Dysfunctional adiposity and the risk of prediabetes and type 2 diabetes in obese adults. JAMA, 308(11): 1150–9. doi:10.1001/2012.jama.11132.

Negi, S., Park, S.H., Jetha, A., Aikin, R., Tremblay, M., and Paraskevas, S. 2012. Evidence of endoplasmic reticulum stress mediating cell death in transplanted human islets. Cell Transplant. 21(5): 889–900.

Okamoto, H., Hribal, M.L., Lin, H. V, Bennett, W.R., Ward, A., and Accili, D. 2006. Role of the forkhead protein FoxO1 in beta cell compensation to insulin resistance. J. Clin. Invest. 116(3): 775–782. United States.

Omikorede, O., Qi, C., Gorman, T., Chapman, P., Yu, A., Smith, D.M., and Herbert, T.P. 2013. ER stress in rodent islets of Langerhans is concomitant with obesity and β-cell compensation but not with β-cell dysfunction and diabetes. Nutr. Diabetes, 3(10): e93. doi:10.1038/nutd.2013.35.

Pfützner, A., and Forst, T. 2011. Elevated intact proinsulin levels are indicative of Beta-cell dysfunction,

insulin resistance, and cardiovascular risk: impact of the antidiabetic agent pioglitazone. J. Diabetes Sci. Technol. 5(3): 784–93. doi:10.1177/193229681100500333.

Pfützner, A., Pfützner, A.H., Larbig, M., and Forst, T. 2004. Role of intact proinsulin in diagnosis and treatment of type 2 diabetes mellitus. Diabetes Technol. Ther. 6(3): 405–12. doi:10.1089/152091504774198124.

Price, B.D. 1992. Signalling across the endoplasmic reticulum membrane: Potential mechanisms. Cell Signal, 4(5): 465-70. doi:10.1016/0898-6568(92)90015-Z.

Rahier, J., Guiot, Y., Goebbels, R.M., Sempoux, C., and Henquin, J.C. 2008. Pancreatic beta-cell mass in European subjects with type 2 diabetes. Diabetes. Obes. Metab. 10 Suppl 4: 32–42. doi:10.1111/j.1463-1326.2008.00969.x.

Rasheva, V.I., and Domingos, P.M. 2009. Cellular responses to endoplasmic reticulum stress and apoptosis. Apoptosis, 14(8): 996–1007. doi:10.1007/s10495-009-0341-y.

Salvalaggio, P.R.O., Deng, S., Ariyan, C.E., Millet, I., Zawalich, W.S., Basadonna, G.P., and Rothstein, D.M. 2002. Islet filtration: a simple and rapid new purification procedure that avoids ficoll and improves islet mass and function. Transplantation, 74(6): 877–9. doi:10.1097/01.TP.0000028781.41729.5B.

Scharfmann, R., Pechberty, S., Hazhouz, Y., von Bülow, M., Bricout-Neveu, E., Grenier-Godard, M., Guez, F., Rachdi, L., Lohmann, M., Czernichow, P., and Ravassard, P. 2014. Development of a conditionally immortalized human pancreatic β cell line. J. Clin. Invest. 124(5): 2087–98. doi:10.1172/JCI72674.

Scheuner, D., and Kaufman, R.J. 2008. The unfolded protein response: a pathway that links insulin demand with beta-cell failure and diabetes. Endocr. Rev. 29(3): 317–33. doi:10.1210/er.2007-0039.

Sharma, R.B., O'Donnell, A.C., Stamateris, R.E., Ha, B., McCloskey, K.M., Reynolds, P.R., Arvan, P., and Alonso, L.C. 2015. Insulin demand regulates β cell number via the unfolded protein response. J. Clin. Invest. 125(10): 3831–46. doi:10.1172/JCI79264.

Stamateris, R.E., Sharma, R.B., Hollern, D.A., and Alonso, L.C. 2013. Adaptive beta-cell proliferation

increases early in high-fat feeding in mice, concurrent with metabolic changes, with induction of islet cyclin D2 expression. Am. J. Physiol. Endocrinol. Metab. 305(1): E149-59. doi:10.1152/ajpendo.00040.2013.

Subramaniam, A., Landstrom, M., Luu, A., and Hayes, K.C. 2018. The nile rat (Arvicanthis niloticus) as a superior carbohydrate-sensitive model for type 2 diabetes mellitus (T2DM). Nutrients, 10(2): 6–14. doi:10.3390/nu10020235.

Szabat, M., Page, M.M., Panzhinskiy, E., Skovsø, S., Mojibian, M., Fernandez-Tajes, J., Bruin, J.E., Bround, M.J., Lee, J.T.C., Xu, E.E., Taghizadeh, F., O'Dwyer, S., van de Bunt, M., Moon, K.-M., Sinha, S., Han, J., Fan, Y., Lynn, F.C., Trucco, M., Borchers, C.H., Foster, L.J., Nislow, C., Kieffer, T.J., and Johnson, J.D. 2016. Reduced Insulin Production Relieves Endoplasmic Reticulum Stress and Induces β Cell Proliferation. Cell Metab. 23(1): 179–93. doi:10.1016/j.cmet.2015.10.016.

Tabák, A.G., Jokela, M., Akbaraly, T.N., Brunner, E.J., Kivimäki, M., and Witte, D.R. 2009. Trajectories of glycaemia, insulin sensitivity, and insulin secretion before diagnosis of type 2 diabetes: an analysis from the Whitehall II study. Lancet, 373(9682): 2215–21. doi:10.1016/S0140-6736(09)60619-X.

Talchai, C., Xuan, S., Lin, H. V, Sussel, L., and Accili, D. 2012. Pancreatic β cell dedifferentiation as a mechanism of diabetic β cell failure. Cell, 150(6): 1223–34. doi:10.1016/j.cell.2012.07.029.

Tschen, S.-I., Dhawan, S., Gurlo, T., and Bhushan, A. 2009. Age-dependent decline in beta-cell proliferation restricts the capacity of beta-cell regeneration in mice. Diabetes, 58(6): 1312–20. doi:10.2337/db08-1651.

Wareham, N.J., Byrne, C.D., Williams, R., Day, N.E., and Hales, C.N. 1999. Fasting proinsulin concentrations predict the development of type 2 diabetes. Diabetes Care, 22(2): 262–270. doi:10.2337/diacare.22.2.262.

Weir, G.C., and Bonner-Weir, S. 2004. Five of stages of evolving b-cell dysfunction during progression to diabetes. Diabetes, 53 Suppl 3: S16-21. doi:10.2337/diabetes.53.suppl_3.S16.

Weir, G.C., and Bonner-Weir, S. 2013. Islet β cell mass in diabetes and how it relates to function, birth,

and death. Ann. N. Y. Acad. Sci. 1281(1): 92–105. doi:10.1111/nyas.12031.

Weyer, C., Bogardus, C., Mott, D.M., and Pratley, R.E. 1999. The natural history of insulin secretory dysfunction and insulin resistance in the pathogenesis of type 2 diabetes mellitus. J. Clin. Invest. 104(6): 787–94. doi:10.1172/JCI7231.

Xin, Y., Gutierrez, G.D., Okamoto, H., Kim, J., Lee, A.-H., Adler, C., Ni, M., Yancopoulos, G.D., Murphy, A.J., and Gromada, J. 2018. Pseudotime Ordering of Single Human β-Cells Reveals States of Insulin Production and Unfolded Protein Response. Diabetes, 67(June): db180365. doi:10.2337/db18-0365.

Yang, K., Gotzmann, J., Kuny, S., Huang, H., Sauve, Y., and Chan, C. 2016. Five stages of progressive beta-cell dysfunction in the laboratory Nile rat model of type 2 diabetes. J. Endocrinol. doi:10.1530/JOE-15-0517.

FIGURES

Figure 1

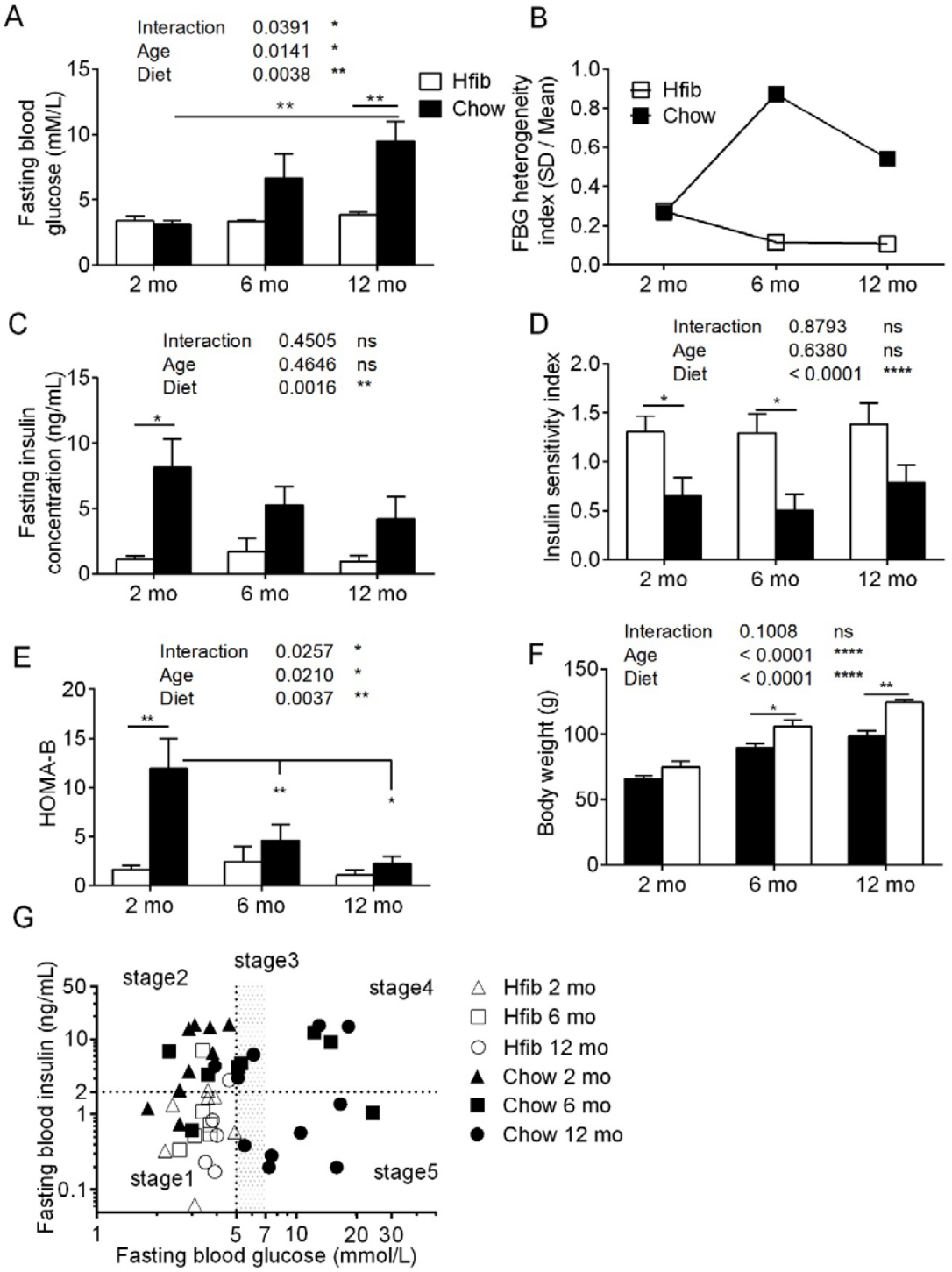

Figure 2

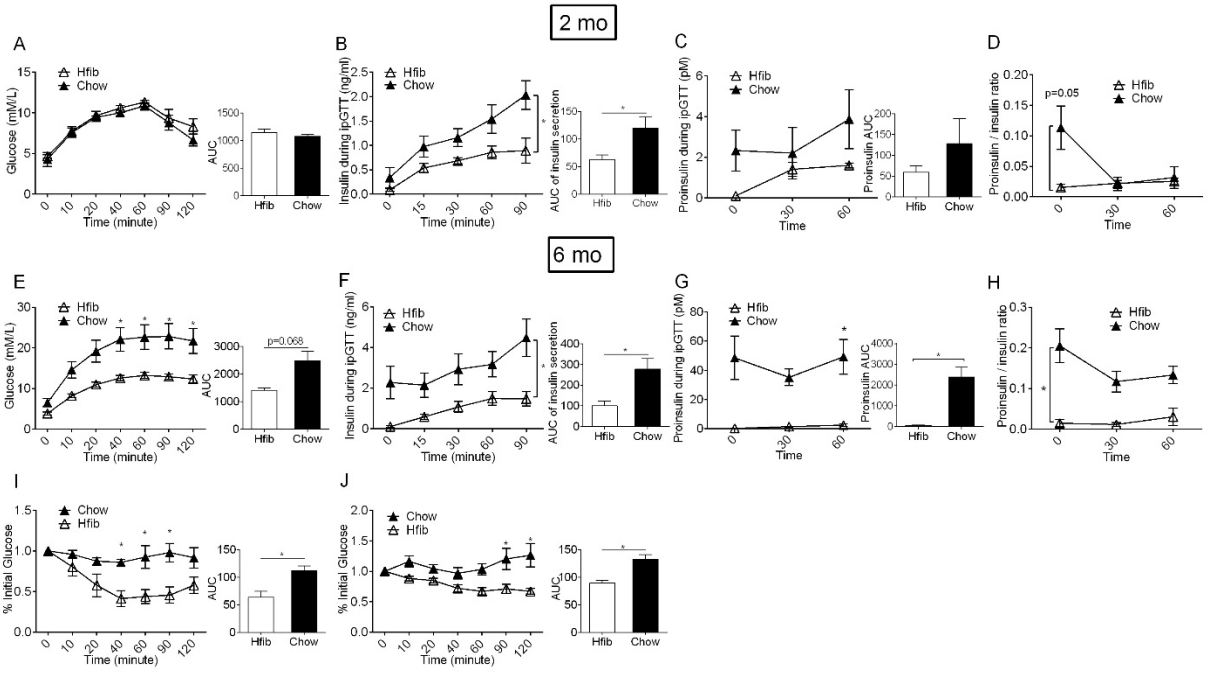
2 mo
6 mo
A
B
C
D
E
F
G
H
I
J
Hfib
Chow
Glucose (mM/L)
Time (minute)
AUC
Insulin during ipGTT (ng/ml)
AUC of insulin secretion
Proinsulin during ipGTT (pM)
Proinsulin AUC
Time
Proinsulin / insulin ratio
p=0.05
p=0.068
% Initial Glucose

Figure 3

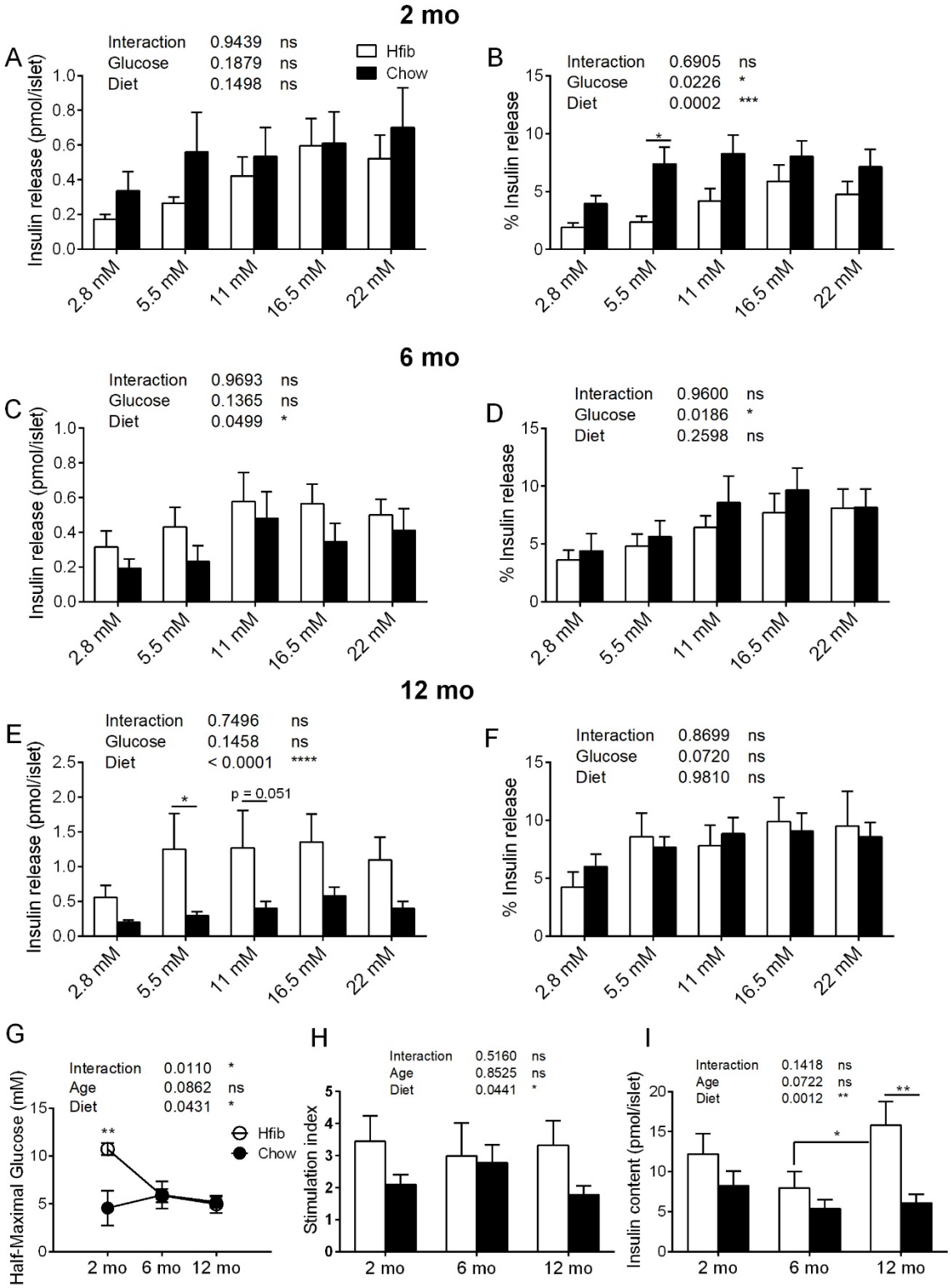
2 mo
A
Interaction 0.9439 ns
Glucose 0.1879 ns
Diet 0.1498 ns
Hfib
Chow
Insulin release (pmol/islet)
B
Interaction 0.6905 ns
Glucose 0.0226 *
Diet 0.0002 ***
% Insulin release
6 mo
C
Interaction 0.9693 ns
Glucose 0.1365 ns
Diet 0.0499 *
Insulin release (pmol/islet)
D
Interaction 0.9600 ns
Glucose 0.0186 *
Diet 0.2598 ns
% Insulin release
12 mo
E
Interaction 0.7496 ns
Glucose 0.1458 ns
Diet < 0.0001 ****
p = 0.051
Insulin release (pmol/islet)
F
Interaction 0.8699 ns
Glucose 0.0720 ns
Diet 0.9810 ns
% Insulin release
2.8 mM
5.5 mM
11 mM
16.5 mM
22 mM
G
Interaction 0.0110 *
Age 0.0862 ns
Diet 0.0431 *
Hfib
Chow
Half-Maximal Glucose (mM)
2 mo
6 mo
12 mo
H
Interaction 0.5160 ns
Age 0.8525 ns
Diet 0.0441 *
Stimulation index
I
Interaction 0.1418 ns
Age 0.0722 ns
Diet 0.0012 **
Insulin content (pmol/islet)

Figure 4

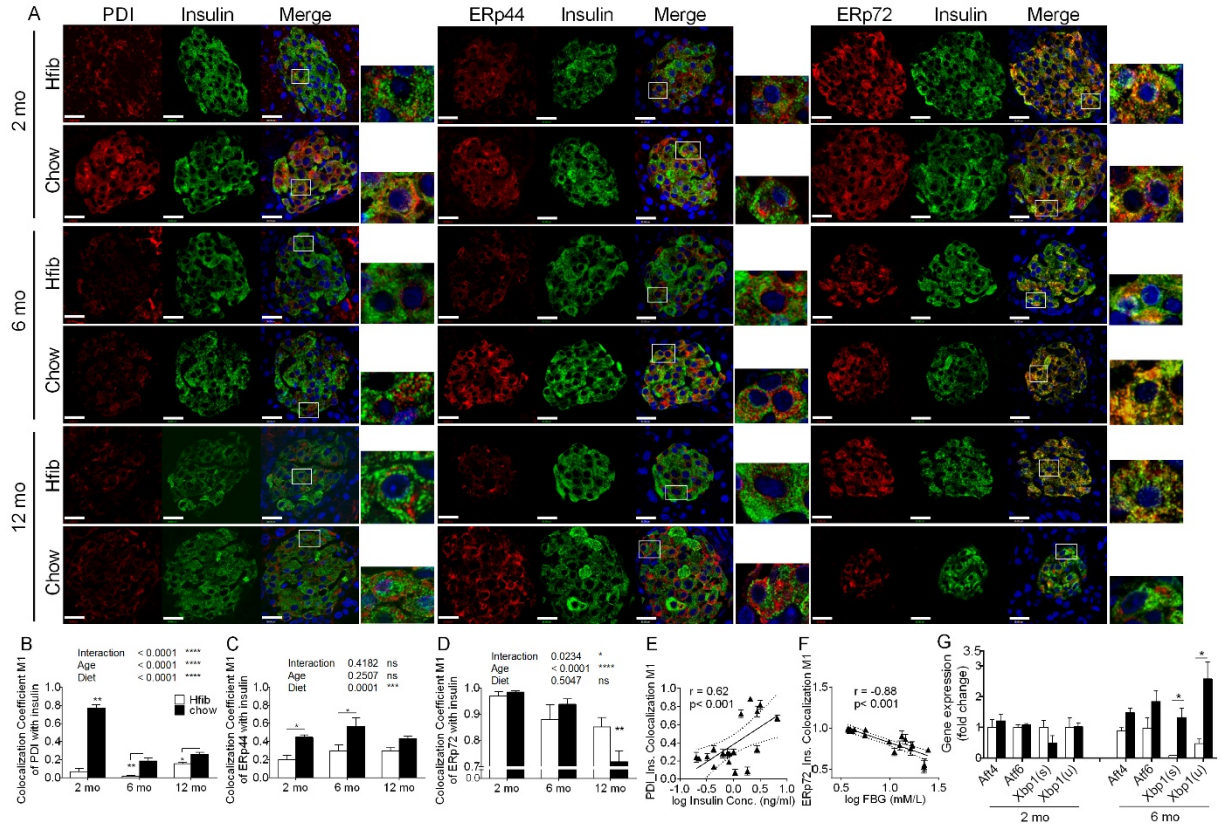
A
PDI
Insulin
Merge
ERp44
ERp72
2 mo
6 mo
12 mo
Hfib
Chow
B
Colocalization Coefficient M1 of PDI with insulin
Interaction < 0.0001 ****
Age < 0.0001 ****
Diet < 0.0001 ****
Hfib
chow
C
Colocalization Coefficient M1 of ERp44 with insulin
Interaction 0.4182 ns
Age 0.2507 ns
Diet 0.0001 ***
D
Colocalization Coefficient M1 of ERp72 with insulin
Interaction 0.0234 *
Age < 0.0001 ****
Diet 0.5047 ns
E
PDI Ins. Colocalization M1
r = 0.62
p< 0.001
log Insulin Conc. (ng/ml)
F
ERp72 Ins. Colocalization M1
r = -0.88
p< 0.001
log FBG (mM/L)
G
Gene expression (fold change)
Aft4
Atf6
Xbp1(s)
Xbp1(u)
2 mo
6 mo

Figure 5

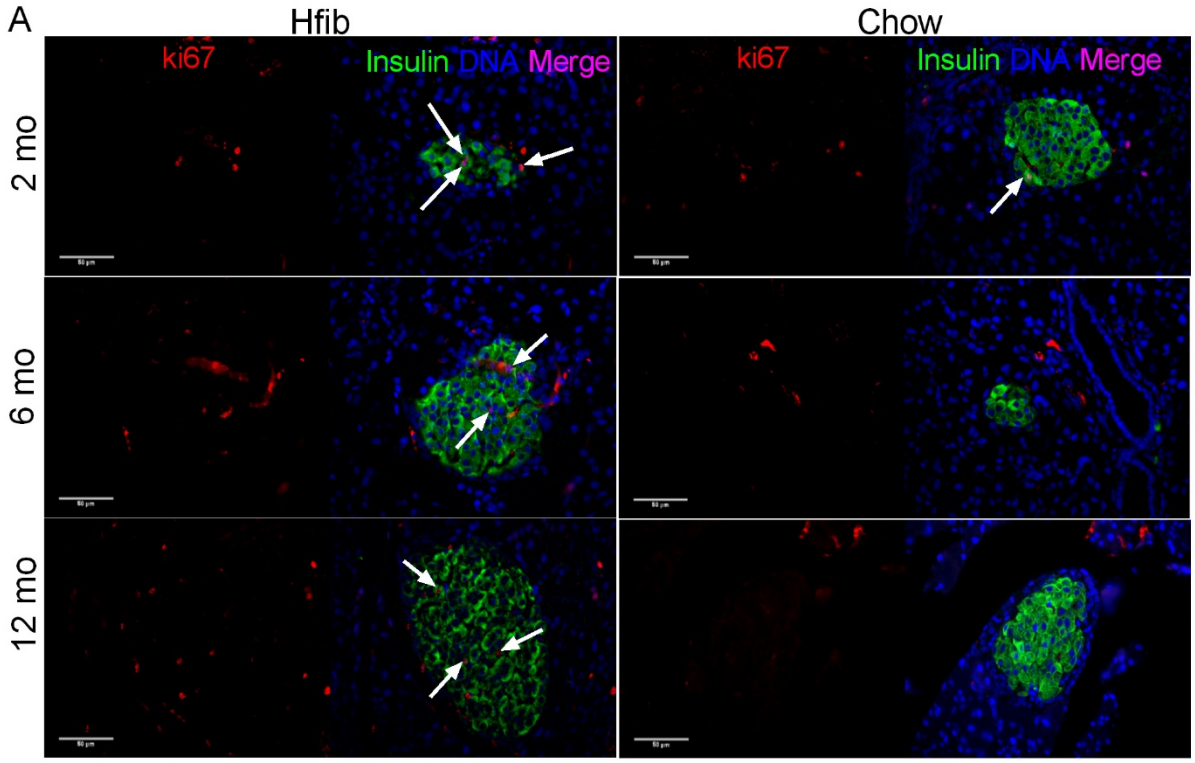
A
Hfib
Chow
ki67
Insulin DNA Merge
2 mo
6 mo
12 mo

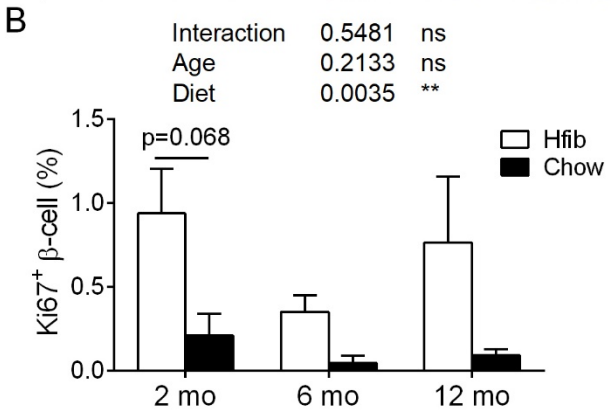
B
Interaction 0.5481 ns
Age 0.2133 ns
Diet 0.0035 **
p=0.068
Hfib
Chow
Ki67+ β-cell (%)
1.5
1.0
0.5
0.0
2 mo
6 mo
12 mo

Figure 6

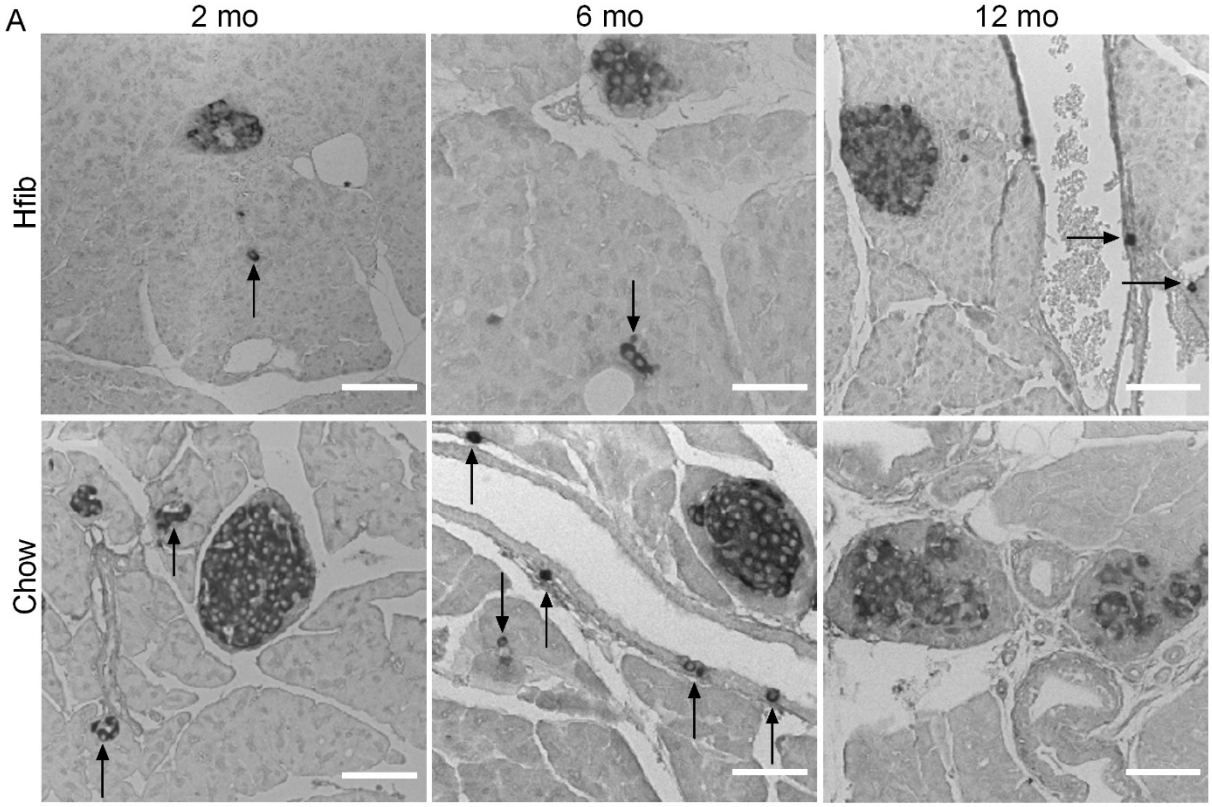
A
2 mo
6 mo
12 mo
Hfib
Chow

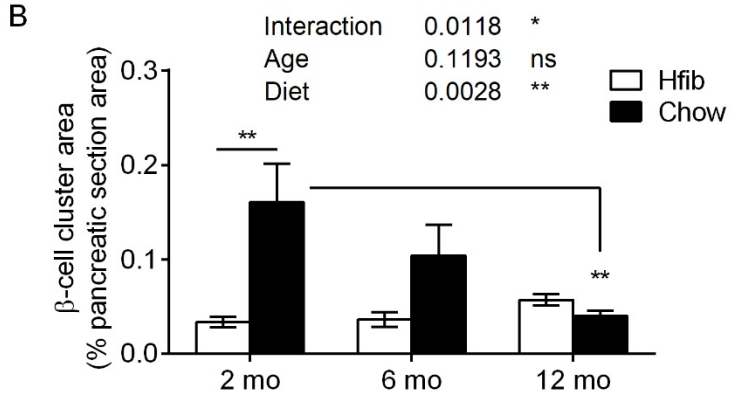
B
Interaction 0.0118 *
Age 0.1193 ns
Diet 0.0028 **
Hfib
Chow
β-cell cluster area
(% pancreatic section area)
0.3
0.2
0.1
0.0
**
**
2 mo
6 mo
12 mo

Figure 7

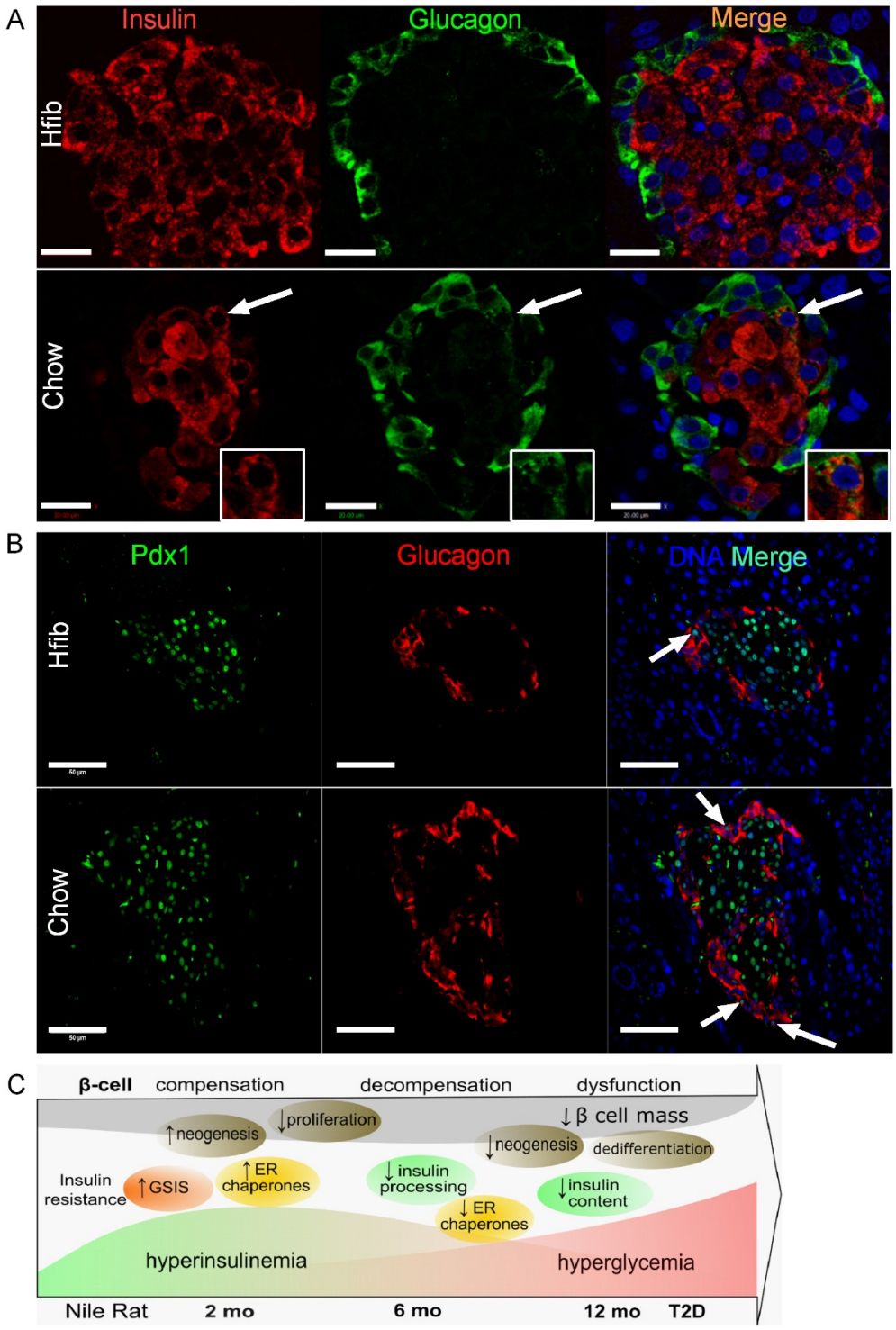
A
Insulin
Glucagon
Merge
Hfib
Chow
B
Pdx1
Glucagon
DNA Merge
Hfib
Chow
C
β-cell
compensation
decompensation
dysfunction
↓β cell mass
↑neogenesis
↓proliferation
↓neogenesis
dedifferentiation
Insulin resistance
↑GSIS
↑ER chaperones
↓insulin processing
↓insulin content
↓ER chaperones
hyperinsulinemia
hyperglycemia
Nile Rat
2 mo
6 mo
12 mo
T2D

FIGURE LEGENDS

Fig.1 Fasting blood glucose and insulin of NR at different T2D stages.

A: Fasting blood glucose; B: Heterogeneity index of FBG; C: Fasting plasma insulin; D: Insulin sensitivity index; E: β-cell function index (HOMA-B); F: Body weight; G: Five stages of type 2 diabetes development in NRs; stage 1=Normal, stage 2=Compensation, stage 3=Decompensation, stage 4= Dysfunction/onset of T2D, stage 5= Overt T2D. Data are presented as mean ± SEM. n= 9, 8 and 12 in Chow group at 2, 6 and 12 months, respectively; n= 7 in all Hfib groups. * $p<0.05$ using Bonferroni's multiple comparison test following 2-way ANOVA.

Fig. 2 *In vivo* assessment of glucose homeostasis and β-cell function.

A, D: Blood glucose during ipGTT at 2 (A) and 6 (D) months; B and E: Insulin secretion during ipGTT at 2 (B) and 6 (E) months; C and F: Proinsulin relative to insulin concentration at 2 (C) and 6 (F) months; G and H: Percentage change in blood glucose during ITT at 2 (G) and 6 (H) months. Data are presented as mean ± SEM. n=4, 11 in Chow group at 2 and 6 months, respectively; n= 4-7 in Hfib groups. *$p<0.05$, **$p<0.01$ using Bonferroni's multiple comparison tests following 2-way ANOVA.

Fig. 3 *In vitro* islet secretory function analysis.

A, C and D: Absolute insulin secreted per islet in GSIS at 2 (A), 6 (C) and 12 (D) months; B, D and F: Glucose-stimulated insulin secretion (GSIS) as percentage of total insulin content; G: Half-maximal glucose (EC_{50}); H: Stimulation index; I: Islet insulin content. Data are presented as mean ± SEM. n=9, 8 and 12 in Chow group at 2, 6 and 12 months, respectively; n= 7 in all Hfib groups. *$p<0.05$, **$p<0.01$ using Bonferroni's multiple comparison tests following 2-way ANOVA.

Fig. 4 Diet and age-related effects on ER chaperones in β-cells.

A: Representative images of ER chaperones in islets from 2-12 months; B-D: Colocalization of PDI (B),

ERp44 (C) and ERp72 (D) with insulin in β-cells; E: Positive correlation of PDI and blood insulin concentration with dotted lines representing 95% confidence intervals; F: Negative correlation of ERp72 and fasting blood glucose; G: mRNA expression UPR transcription factors. Data are presented as means ± SEM. n=5, 6 and 8 in Chow group at 2, 6 and 12 months, respectively; n=4, 4 and 8 in Hfib group at 2, 6 and 12months. *$p<0.05$ using Bonferroni's multiple comparison tests following 2-way ANOVA. Scale bar = 20μm.

Fig. 5 β-cell proliferation.

A: Representative images of ki67-positive staining in β-cells; B: Quantification of β-cell proliferation as percentage of all beta-cells. Data are presented as mean ± SEM. n=4 in ki67 staining. The analysis was Bonferroni's multiple comparison tests following 2-way ANOVA. Scale bar= 50μm.

Fig. 6 Estimate of β-cell neogenesis.

A: Representative images of neogenetic β-cell clusters; B: Quantification of neogenic β-cell area. Data are presented as mean ± SEM. n=4-6. The analysis was Bonferroni's multiple comparison tests following 2-way ANOVA. Scale bar= 80μm.

Fig. 7 Evidence of dedifferentiation at the late stage of diabetes.

A: Co-occurrence of insulin$^+$/ glucagon$^+$ in islet at 12 months; B: Pdx1$^+$ /Glucagon$^+$ cell at 12 months; C: Summary of events occurring in type 2 diabetes development of NR. Scale bar (A)= 20μm Scale bar (B)= 50μm.

Appendix B: Data extraction table for the animal model review in Chapter 1.3

Table 1. Obesity monogenic T2D Model

Authors	Aims/Purpose of study	Strain	Diabetes-induced by	Metabolic phenotype	β-cell compensation function	β-cell compensation mass	Main findings	Additional findings
Medina-Gomez et al. 2007	Investigate the mechanism of β-cell adaptation in diabetes-resistant ob/ob mice	C57BL/6J	homozygous *Lep* $^{ob/ob}$ mutation	IR; ↑ plasma insulin; euglycemia at 14 wks	↑GSIS	↑β-cell area	Lack of PPARγ2 induced severe dyslipidemia and β-cell dysfunction, associated with ↓proliferation, ↑oxidative stress, ↑ macrophage infiltration	No difference in β-cell function and mass between *db/db* and POKO mice at 4 wks
			homozygous *Lep* $^{ob/ob}$ mutation × PPARγ2$^{-/-}$	IR; impaired lipid metabolism; hyperglycemia at 14 wks	↓GSIS	↓β-cell area		
Chan et al. 2013	Investigate UPR gene expression in diabetes-prone db/db mice and diabetes-resistant ob/ob mice	C57BL/6J	homozygous *Lep* $^{ob/ob}$ mutation	↑plasma insulin, obesity and IGT at 6 wks	↑GSIS presented at 6 but not 16 wks		Sustained adaptive UPR was critical in β-cell compensation; Chemical chaperones partially restored β-cell function	C57BL/6J strain showed strong adaptative response to IR regardless of *ob/ob* or *db/db* mutation
		C57BL/KsJ	homozygous *Lepr* $^{db/db}$ mutation	↑plasma insulin, obesity, IGT at 6 wks; ↑blood glucose at 16 wks	↑GSIS at 6 wks then ↓ at 16 wks			
Engin et al. 2014	Examine ER stress markers (ATF6, XBP1, p-eIF2α) in β-cells at different stages of T2D	Human	Gene × Diet interaction	Obesity; duration of T2D from 0.25 to 20 years			Failure of UPR in β-cell was associated with onset of hyperglycemia in both animal models	P-eIF1α responded differently in diabetes between mouse
		C57BL/6J	High fat feeding	Obesity; ↑glucose; ↑ insulin after 13 wks of HFD	↑plasma insulin			

		C57BL/6 J	homozygous *Lep* $^{ob/ob}$ mutation	↑insulin after 4 wks; transient ↑glucose at 8 wks			and human; transient increase in UPR after 1 week of HFD	models and human
Kanda et al. 2009	Investigate the molecular mechanism of *Lepr*^{db} mutation associated with β-cell failure	C57BL/ KsJ	heterozygous *Lepr* $^{db/m}$ mutation × HFD	euglycemia at 8,12 wks	↑plasma insulin; ↑GSIS	↑ β-cell/ islet ratio	db/m: resistant to HFD- induced IGT due to β-cell compensation; db/db: ↓differentiation/ proliferation; ↑apoptosis/ ER stress/ oxidative stress	Upregulation of Ins1/2, bcl-2 and ERK1 was associated with ↑ β-cell function in db/m mice
			homozygous *Lepr* $^{db/db}$ mutation	↑TG; ↑NEFA; ↑plasma insulin; hyperglycemia at 8, 12 wks	↓GSIS; ↓ insulin content	↓β-cell/ islet;↑β-cell mass		
Burke et al. 2017	Compare diet-induced and genetic mouse models in recapitulating human T2D features	C57BL/ KsJ	heterozygous *Lepr* $^{db/m}$ mutation	→fat mass, insulin and glycemia at 14 wks	↑ plasma insulin		db/db mice exhibited feature of human T2D with ↑ β-cell area and loss of β-cell identity; HFD mice didn't show hyperglycemia and β-cell dedifferentiation	Expression of G6Pase was upregulated in only db/db mice
			homozygous *Lepr* $^{db/db}$ mutation	↑fat mass; ↑glucagon; ↑blood glucose at 7 wks	↑ plasma insulin	↑ β-cell area		
Jones et al. 2010	Assess metabolic characteristics and islet morphology in obese and diabetic rats	Obese Zucker fatty (ZF) rat	homozygous *Lepr* ^{fa} mutation	↑ plasma insulin at 6, 14 wks	↑islet size at 14 wks	↑islet size	Obese ZF rats showed hyperinsulinemia with islet hyperplasia; whereas ZDF rats exhibited insulin deficiency and β-cell loss	No change in β-cell proliferation or neogenesis between models other than an age-related reduction
		Zucker diabetic fatty (ZDF) rat	Selective inbreeding of diabetic *Lepr* $^{fa/fa}$ rat	Obesity; ↑insulin at 6 wks; ↓insulin at 14 wks	↑↓ plasma insulin	↓ β-cell / islet ratio; ↓ β-cell number		

Omikorede et al. 2013	Study the relationship between ER stress and β-cell dysfunction in T2D	Obese Zucker fatty rat	homozygous *Lepr*$^{fa/fa}$ mutation	Obesity; ↑ insulin; normal glucose	↑Ins 2 expression		Adaptive UPR and β-cell function gene were upregulated in ZF and fZDF rats, which were downregulated in fZDF+HFD rats	CHOP was not correlated with the development of β-cell dysfunction
		Female Zucker diabetic fatty (fZDF) rat	Selective inbreeding of *Lepr*$^{fa/fa}$ rat	Obesity; ↑ insulin; mild ↑HbA1c	↑Ins 2 expression			
			Lepr$^{fa/fa}$ × HFD	Obesity; ↓insulin; ↑↑HbA1c	↓Ins 2 expression			

Table 2. Transgenic Model

Authors	Aims/Purpose of study	Strain	Diabetes induced by	Metabolic phenotype	β-cell compensation function	β-cell compensation mass	Main findings	Additional findings
Butler et al. 2003	Study the mechanism for the deficit in β-cell mass in T2D in obese (A^{vy}/A) hIAPP transgenic model	C57Bl/6	hIAPP knock-in × A^{vy}/A mutation-induced obesity	hIAPP- A^{vy}/A: ↑glucose at 10wks, ↑insulin at 25 wks		→ β-cell mass	Induction of hIAPP failed in β-cell mass expansion with profound ↑ apoptosis, albeit with ↑ β-cell neogenesis and replication rate	The ↑frequency of β-cell apoptosis occurred before development of amyloid deposits.
				A^{vy}/A: obesity; ↑insulin; normal glucose at 10-40 wks		↑↑β-cell mass		
Matveyenko et al. 2009	Investigate hIAPP in β-cell adaptation to diet-induced T2D	Sprague-Dawley rats	hIAPP knock-in × HFD	hIAPP-HFD: ↑body weight; ↑glucose; IR; ↑hepatic output	→GSIS	→ β-cell mass	β-cell failed to compensate in function or mass in hIAPP insulin-resistant rats, due to ER stress-related apoptosis	hIAPP induced ER stress-related apoptosis without HFD
				HFD: ↑body weight; normal glucose; IR	↑GSIS	↑↑β-cell mass		

Hiddinga et al. 2012	Determine the pathogenetic role of hIAPP in β-cell from hIAPPknock-in mice	C57Bl/6J	hIAPP knock-in × HFD	hIAPP-HFD: ↑body weight; mild ↑glucose; IGT	↓insulin	→ β-cell mass	hIAPP induction deteriorated glucose intolerance in vivo and lack of compensatory insulin secretion independently of amyloid deposits	hIAPP induction didn't change metabolic phenotype of animals on chow diet
				HFD: ↑body weight; normal glucose; IGT	↑insulin	→ β-cell mass		
Kim et al. 2007	Study IR and Irs2 mutation in β-cell compensation	129/sv × C57BL/6J	$IR^{+/-}$ × $Irs2^{-/-}$	↓body weight; ↓fat mass; ↑leptin and adiponectin; IGT; normal fasting glucose	↑ plasma insulin	↓β-cell mass	IR-Irs2 mutation resulted in compensatory hyperinsulinemia even with declined β-cell mass	
Okada et al. 2007	Study β-cell compensation in the liver-specific insulin receptor and IGF knockout mice	129/sv × C57BL/6J× DBA/2	(liver) $IR^{-/-}$	IGT; IR; normal glucose	↑ plasma insulin; ↑GSIS	↑β-cell mass	liver-specific $IR^{-/-}$ exerted ↑insulin secretion and ↑proliferation; loss of β-cell compensation in $\beta IR^{-/-}$ mice is related to Foxo1	β-cell specific $IR^{-/-}$ failed to induce β-cell compensation in function and mass
			(β-cell) $IR^{-/-}$	Mild IGT	→ plasma insulin	↓β-cell mass (on chow and HFD)		
Escribano et al. 2009	Study the role liver-pancreas endocrine axis in β-cell compensation to insulin resistance	C57BL/6	Inducible (liver) $IR^{-/-}$	IGT; IR; ↑plasma insulin; hyperglycemia at 12 months	Dose-dependent ↑insulin	Dose-dependent ↑β-cell mass	Liver $IR^{-/}$ induced β-cell hyperplasia by ↑hepatic IGT and ↑ insulin receptor A related proliferation	
Okamoto et al. 2006	Determine the effect of FoxO1 mutation in	129/sv	(Muscle) $IR^{-/-}$	normal glucose	↑ plasma insulin	↑β-cell mass	FoxO1 mutation prevented ↑β-cell mass in insulin-	

	insulin-resistant β-cell/liver-specific $IR^{-/-}$ mice	× C57BL/6 J× FVB	(Muscle) $IR^{-/-}$ × (liver/ β-cell) $FoxO1^{S253A}$	↑↑ blood glucose	↑ plasma insulin	→β-cell mass	resistant model by ↓ proliferation not neogenesis	
Zhang et al. 2015	Investigate the role of FoxO1 in β-cell compensation	C57Bl/6J	FoxO1 knock-in	↑glucose tolerance;	↑GSIS		FoxO1 induction facilitated β-cell compensation by ↑ cell mass; ↑ β-cell function gene; ↑antioxidative function	FoxO1 was involved under both physiological and pathophysiological conditions
			FoxO1 knock-in × HFD	↑body weight; ↑fat mass; alleviated IGT but not ITT	↑↑GSIS	↑β-cell mass		

Table 3. Experimentally Induced Model

Authors	Aims/Purpose of study	Strain	Diabetes induced by	Metabolic phenotype	β-cell compensation		Main findings	Additional findings
					function	mass		
Ellenbroek et al. 2013	Study the heterogeneity of β-cell compensation to insulin resistance induced by HFD feeding	C57BL/6 J (8 wks)	HFD (6 wks)	↑body weight; ↑caloric intake; IGT with ↑insulin; IR	↑GSIS	↑β-cell area; → β-cell mass	β-cells in the splenic region showed phenomenal adaptation related to cell function and area, compared to the islet in duodenal/ gastric regions	β-cell adaptation in islets from different regions was comparable in islet graft
Stamateris et al. 2013	Study the initiator and identity of β-cell adaptation in response to short-term HFD	C57BL/6 J (10-12 wks)	HFD (1 wk)	↑body weight; IGT; ↑caloric intake; ↑testicular fat pad; ↑fed glucose/insulin	↓GSIS (→β-cell identity)	↑β-cell area; ↑β-cell mass	1-week HFD was able to trigger ↑β-cell via ↑proliferation	

Maschio et al. 2016	Investigate Wnt/β-catenin signaling in β-cell adaptative proliferation in mice fed on HFD	C57BL/6/JUnib (4-5 months)	HFD (30 or 60 days)	↑fed (not fasted) glucose/insulin after 30d HFD; ↑fasted and fed glucose/insulin; IGT after 60d HFD		↑β-cell volume at 60d	↑β-cell proliferation in HFD-mice was correlated with ↑β-catenin/ cyclin D1&2/c-Myc	30d-HFD was not able to induce β-cell proliferation
Gupta et al. 2017	Characterize β-cell adaptation and the cellular mechanism in long-term HFD-feeding mice	C57BL/6NTac (6 wks)	HFD (16 wks)	↑body weight/fed glucose/insulin/IGT with ↑insulin (1-16wks); impaired ITT at 11 wks	↑GSIS (2 wks); ↓GSIS (16 wks)	↑β-cell mass (4-16 wks)	β-cell adaptation duo to overnutrition is mediated by ↑PPARγ and downstream differentiation genes and ER stress	↑β-cell mass was correlated with ↑ small islets
Tschen et al. 2009	Investigate the capacity of β-cell proliferation in response to HFD, exendin-4 and HFD-STZ	C57BL/6J at 6 wks	HFD for 8 wks; or exendin-4 (10 nmol/kg) for 7 days; or a single dose of STZ (90 mg/kg) injection	IGT, IR after HFD; hyperglycemia 7 days after STZ injection		↑ β-cell mass over HFD, exendin-4	Old mice failed in β-cell mass adaptation with a limited capacity of proliferation upon overnutrition; exendin-4 or STZ-induced β-cell ablation	
		C57BL/6J at 7-8 months		IGT, IR and hyperglycemia after HFD; hyperglycemia 7 days after STZ injection		→ β-cell mass over HFD, exendin-4		
Meier et al. 2011	Investigate change in α-cell function and mass related to hyperglucagonemia in T2D mice	CD-1 mouse (6 wks)	STZ (40 mg/kg body wt on 5 consecutive days)	↑glucose (14 d); IGT with ↓insulin and ↑glucagon (28d)		↓β-cell mass (70%); →α-cell mass	Hyperglucagonemia in STZ-mice was more related to altered α-cell function than α-cell expansion	Insulin treatment failed to restore suppression of glucagon

Shu et al. 2012	Study the role of TCF7L2 in β-cell replication and neogenesis	C57BL/6 J (6 wks)	HF/sucrose diet for 16 wks followed by a dose of STZ (90 mg/kg)	IGT at 8wks after HF/sucrose diet; ↑fasting and fed glucose 4 d after STZ injection		↑β-cell mass; 50% ↓β-cell mass after STZ	↑TCF7L2 was correlated with ↑β-cell replication and neogenesis in HFD/STZ or exendin-4 mice and human islets	Old mice failed in of β-cell mass adaptation upon overnutrition with ↓Tcf7l2
Jiang et al. 2015	Study the effect of polypeptide-vglycin on β-cell replenishment in diabetes	C57BL/6 (2 months)	HFD for 12 wks followed by multiple doses of STZ (25 mg/kg)	↑fed glucose; IGT		↓β-cell area	Long-term vlycin treatment restored β-cell mass and ↑insulin sensitivity by exerting Gsk3 β/Glut4 and Akt/Erk signaling	Glucose was restored in HFD-STZ mice 5 months after STZ injections
Song et al. 2015	Examine the effect of EGF and gastrin on β-cell replenishment in alloxan-induced diabetes using genetic lineage tracing model	RIP-CreER/R26-LacZ) mice	Alloxan (70mg/kg)	↑↑glucose 3 days after injection		↓β-cell mass; ↓β-cell number	EGF and gastrin-induced β-cell regeneration via ↑proliferation, ↑neogenesis and re-differentiation	EGF and gastrin prevented macrophage infiltration in islets
Delghingaro-Augusto et al. 2009	Characterize β-cell dysfunction in Zucker fatty rat subjected to pancreatectomy	Zucker lean (f*a*/+) rat	60% Px	No change in metabolic features 3 wks after Px	→GSIS	→β-cell mass	60% Px in ZF vs lean rats failed to induce β-cell mass restoration or functional compensation, despite ↑proliferation/regeneration	Islets from Px rats showed ↓insulin content; impaired insulin biosynthesis; glucose/lipid metabolism
		Zucker fatty (*fa/fa*) rat (6 wks)		↑blood glucose; ↓insulin; ↑TG	↓GSIS	→β-cell mass;		

Rankin et al. 2009	Investigate β-cell proliferation potential at old age	B6129SF 1/J (2 and 8-19 months)	50% Px	No change in metabolic features 2 wks after Px			Basal and Px/ STZ/exendin-4 - induced β-cell proliferation decreased with age (2 vs 8-19 months);	Px-induced acinar proliferation was well maintained at all age
Téllez et al. 2016	Investigate the β-cell regeneration capacity of mid-age rats	Wistar rat (1 and 12 months)	90% Px	Hyperglycemia in 50% 12-mon Px-rats 14d after Px		↑β-cell area, →β-cell mass	90% Px in mid-age rat induced ↑pancreas weight, ↑acinar cell mass, ↑cell dedifferentiation, but not β-cell mass albeit with ↑proliferation and cell size	β-cell mass was restored in young rats 14 days after Px; Gastrin had no effect on pancreas restoration

Table 4. Polygenic Model

Authors	Aims/Purpose of study	Strain	Diabetes induced by	Metabolic phenotype	β-cell compensation function	β-cell compensation mass	Main findings	Additional findings
Plachot et al. 2001	Investigate the β-cell replication potential in GK rats	GK rat	Selective inbreeding from IGT Wistar rats × 90% Px	↓body weight; ↑blood glucose	↓ plasma insulin	↓ β-cell mass	GK showed ↓ β-cell regeneration potential after 90% Px compared with wildtype Wister rats.	
Lacraz et al. 2010	Study the mechanism for β-cell being protected from oxidative stress induced-apoptosis in GK/par rats	GK rat	Selective breeding from IGT Wistar rats	Transient prediabetes from birth to weaning; Adult rats: ↓insulin; IGT; hyperglycemia	↓GSIS	↓ β-cell mass; ↓ β-cell/islet ratio	Increased oxidative stress was correlated with the onset of diabetes; adult β-cells were resistant to H_2O_2-induced apoptosis in a cAMP-dependent manner	

Lange et al. 2006	Compare the proliferation capacity of β-cell from NZO/H1 mice with prediabetes or diabetes	NZO mouse	Selective inbreeding from agouti mice	Obesity; ↑insulin with normal blood glucose; ↑blood glucose with insulin deficiency	↑ plasma insulin	↑ β-cell mass	↑β-cell proliferation in euglycemic mice was correlated with ↑plasma insulin	
Huang et al. 2007	Investigate the effect of diazoxide on preventing β-cell from apoptosis in OLETF rats	OLETF rat	Selective inbreeding from Long-Evans rats	Obesity; early ↑insulin; IGT at 8 wks; ↑blood glucose at 24 wks	↑ plasma insulin (16 wks)	↑ β-cell mass (16 wks)	Diazoxide prevented the onset of T2D in OLETF rats by ↑insulin secretion and ↓β-cell apoptosis via ↑MAPK/Bcl-2/Bax	
Cummings et al. 2008	Characterize UCD-T2DM rats as a model of human T2D	UCD-T2DM rat	Obese Sprague - Dawley rat × lean Zucker diabetic fatty rat	Early ↑insulin and normal glucose at 4 months; ↑FFA; ↑glucagon; ↓insulin and ↑blood glucose at 6/ 9 months(F/M)	↑ plasma insulin (prediabetes)	↑islet volume and content (prediabetes)	Both male and female rats developed progressive hyperglycemia due to failure of insulin compensation	
Jörns et al. 2002	Study the hyperinsulinemia and hyperglycemia during disease development in sand rats	Sand rat	Chow with high-energy diet (2.93 kcal/g)	↑insulin, normal glucose after 1 week of HED; hyperglycemia after 3 wks of HED	↑insulin		Sand rats developed hyperglycemia 3 wks after HED with ↑insulin but abnormal islet structure and ↓GCK/↓ GLUT2	50% rats exhibited hyperglycemia after 1 week of HED
Khalkhal et al. 2012	Investigate effects of IL-1β and IFN-γ on GSIS in lean and obese sand rats	Sand rat	Chow diet (3.25 kcal/g)	Obesity; ↑TG; ↑cholesterol; ↑insulin, normal glucose (50% non-diabetic);	↑GSIS (obese) ↓GSIS (diabetic)		β-cell compensated to insulin resistance in obese sand rats; IL-1β exerted acute GSIS of	IFN-γ didn't affect β-cell

				↑glucose (50% diabetic)			β-cell from obese but not lean sand rats	function in sand rats
Yang et al. 2016	Characterize β-cell dysfunction during T2D progression in Nile rats	Nile rat	Chow diet	Obesity; ↑insulin (2 months); hyperglycemia (12 months)	↓GSIS (12 months)	↓ β-cell area (12 months)	Nile rat exhibited progressive β-cell dysfunction with disrupted islet structure and ER stress	